Role of interneuron-oligodendrocyte precursor cell communication in the somatosensory cortex : common embryonic origin and death

Domiziana Ortolani

Université de Paris

École doctorale **Bio Sorbonne Paris Cité 562**

Laboratoire: Institut de Psychiatrie et Neurosciences de Paris

Team : Interactions between neurons and oligodendroglia in myelination and myelin repair U1266

Role of interneuron-oligodendrocyte precursor cell communication in the somatosensory cortex: common embryonic origin and death

Par Domiziana Ortolani

Thèse de doctorat de Neurobiology

Dirigée par Maria Cecilia Angulo
Présentée et soutenue publiquement le 09/10/2020

Devant un jury composé de:

Pr. Micaela Galante	Universitè Paris Saclay	Examinatrice
Dr. Alberto Bacci	UPMC	Le rapporteur
Dr. Jean Marie Mangin	UPMC	Le rapporteur
Pr. Mehrnaz Jafarian-Tehrani	Université de Paris	Président du jury
Dr. Maria Cecilia Angulo	Université de Paris	Examinatrice

Rôle de la communication entre les interneurones et les cellules précurseurs d'oligodendrocytes dans le cortex somatosensoriel: origine embryonnaire commune et mort cellulaire

Les cellules précurseurs d'oligodendrocytes (CPOs) génèrent des oligodendrocytes (OL), les cellules gliales responsables de la production de myéline dans le SNC. Au cours des 15 dernières années, il a été montré l'existence d'entrées synaptiques fonctionnelles entre les neurones et les CPOs dans le cerveau, mais le rôle de ces synapses particulières est encore peu compris. Néanmoins, ces synapses pourraient être impliquées dans les mécanismes contrôlant l'oligodendrogénèse, et donc la myélinisation cérébrale. Des études antérieures de l'équipe ont montré que les CPOs du cortex somatosensoriel reçoivent des entrées synaptiques transitoires en provenance des interneurones GABAergiques au moment de la différentiation massive des CPOs en oligodendrocytes. Ces résultats montrent que les CPOs sont des partenaires privilégiés des interneurones lors du développement postnatal et suggèrent que l'activité de ces neurones pourrait contrôler la fonction des CPOs pendant la période critique de leur différenciation en oligodendrocytes. Pendant ma thèse, je me suis intéressée à l'impact de cette relation étroite entre les interneurones corticaux et les CPOs au cours du développement. En utilisant différentes approches dans deux projets différents, mon objectif était de comprendre comment les interneurones modifient la fonction des CPOs et la formation des circuits neuronaux.

Dans mon premier projet, nous avons évalué si l'activité in vivo des interneurones corticaux GABAergiques modifie la prolifération et la différentiation des CPOs au pic de

connectivité interneurones-CPOs, c'est-à-dire au jour postnatal 10 (PN10). Pour ce faire, nous avons utilisé deux lignées transgéniques différentes pour exprimer le canal sensible à la lumière Channelrhodopsin-2 (ChR2) soit dans les interneurones exprimant la parvalbumine (PV), soit dans les interneurones en provenance de l'eminence ganglionnaire médiane (EGM) embryonnaire. Tout d'abord, nous avons montré que la souris PV^{Cre};ChR2-YFP n'était pas adaptée pour la stimulation des interneurones PV chez le souriceau car la ChR2 n'est pas exprimée dans ces interneurones à la deuxième semaine postnatale. En revanche, nous avons démontré que la souris $Nkx2.1^{Cre}$;ChR2-YFP constitue un très bon outil pour ce type de stimulation car l'expression précoce du facteur de transcription Nkx2.1 assure l'expression efficace de la ChR2 au cours du développement postnatale. Nous nous sommes donc focalisés dans l'étude de cette deuxième lignée et avons développé une approche efficace pour la stimulation optogénétique chez le souriceau. En premier lieu, nous avons évalué notre capacité à générer des potentiel d'action dans les interneurones exprimant la ChR2 sur des tranches aigües du cortex somatosensoriel avec une stimulation lumineuse. Parmi les protocoles testés, un train de stimulation à 10 Hz s'est révélé le plus efficace pour évoquer directement et de manière fidèle des potentiels d'action dans les interneurones $ChR2^{+}$. Ensuite, nous avons mis en place une chirurgie permettant d'implanter une mini-fibre optique dans le cerveau du souriceau pour effectuer des stimulations in vivo. La stimulation à 10 Hz combinée à des enregistrements de champs ont montré également que la stimulation était efficace chez l'animal éveillé. Enfin, nous avons analyser l'effet de l'activation des interneurones ChR2 in vivo sur les cellules de la lignée oligodendrocytaire grâce à des immunomarquages. La photoactivation des interneurones n'a pas révélé des

changements dans la densité des CPOs ou de leur prolifération. Ceci suggère que les interneurones ne régulent pas ce processus dans les CPOs à P10.

Dans le deuxième projet, nous avons analysé les interactions entre les interneurones GABAergiques corticaux et les CPOs ayant une même origine embryonnaire et issus de l'EGM et de la zone préoptique (ZPO). Notamment, nous avons étudié leur connectivité, leur organisation spatiale et leur mort cellulaire programmée pour évaluer l'impact fonctionnel de leur origine embryonnaire commune sur, d'une part, le fonctionnement des circuits inhibiteurs et, d'autre part, l'homéostasie des cellules de la lignée oligodendrocytaire. Par le biais d'enregistrements électrophysiologiques, notamment des doubles enregistrements, et d'immunomarquages sur plusieurs lignées transgéniques, nous avons mis en évidence une interaction postnatale complexe entre les interneurones et les CPOs provenant de la même origine. En effet, ces cellules ont tendance à former des groupes anatomiquement distincts qui montrent une connectivité synaptique significativement plus élevée que celle entre interneurones et CPOs d'origine embryonnaire différent. Par ailleurs, l'inactivation génétique du gènes pro-apoptotique BAX dans les cellules dérivées du EGM/ZPO a révélé une perte de la connectivité préférentielle entre ces deux types cellulaires. Ceci a lieu malgré une augmentation importante de l'inhibition neuronale dans les circiuits ce qui montre que les interneurones empêchés de mourir sont toujours fonctionnels dans les circuits matures. La perte de la connectivité préférentielle entre les cellules de même origine qui sont forcées de survivre suggère donc que les synapses interneurones-CPO pourraient être impliquées dans la survie des CPO. Nos résultats ont montré également que prévenir génétiquement la mort cellulaire des interneurones et des CPOs du même origine induit une augmentation de la densité oligodendrogliale provenant d'autres source embryonnaire. Ces résultats révèlent

un nouveau rôle de la mort cellulaire programmée au cours du développement cortical dans le contrôle du nombre d'oligodendroglie grâce à un mécanisme cellulaire non autonome. En conclusion, des évidences dans la littérature et les données de cette thèse montrent que la communication entre les interneurones GABAergique et les cellules de la lignée oligodendrocytaire pourrait jouer un rôle majeur dans la construction et la modulation des réseaux neuronaux corticaux.

Glossary

5HT3aR	5-hydroxytryptamine 3a receptor
AEA	Anterior Entopenducular Area
AIS	Axonal Initial Segment
AMPARs	α-amino-3-hydroxy-5-methyl-4-isoxazolepropionic acid receptors
Arch	Archaerhodopsin
Bak	Bcl2 antagonist/killer 1
Bax	Bcl2- associated X
BDNF	Brain-derived neurotrophic factor
BH	Bcl2 homology domain
BoNT/A	Botulinum neurotoxin type A
Ca^{2+}	Calcium
Casp	Caspase
CB	Calbindin
CCK	Cholecystokinin
CGE	Caudal Ganglionic Emincence
Chodl	Chondrolectin
ChR2	Channelrhodopsin 2
C_m	Membrane capacitance
CNS	Central Nervous System
CNTF	Ciliary neurotrophic factor
CPTs	Cortical plate transient neurons
CR	Calretinin
CRs	Cajal-Retzius cells
DREADDs	Designer receptor Exclusively Activated by Designer Drugs
DRGs	Dorsal Root Ganglion neurons
EDU	5-ethynyl-2'-deoxyuridine
EM	Electron microscopy
EPSCs	Excitatory postsynaptic currents
ER	Endoplasmic reticulum

ERK	Extracellular signal-Regulated Kinase
FBI	Feedback Inhibition
FFI	Feedforward Inhibition
FGF1	Fibroblast growth factor 1
FirstOPCs	First wave of OPCs
FS	Fast-Spiking
FSI	Fast-spiking interneuron
GABA	Gamma-Aminobutyric acid (GABA)
$GABA_BR$	$GABA_B$ receptor
GABARs	GABA receptors
GABAzine	SR 95531
GATs	GABA transporters
HDACs	Histone deacetylases
IAPs	Apoptosis inhibitor proteins
IK^+	K^+ currents
IL-6	Interleukin 6
IN	Interneuron
INa^+	Na^+ currents
IP3	1,4,5-trisphosphate
IPSPs	Inhibitory Postsynaptic Potentials
K^+	Potassium
KCC2	K^+, Cl^- transporter 2
LFPs	local field potentials
LIF	Leukemia inhibitory factor
L-VGCC	L-type voltage-gated calcium channels
MBP	Myelin basic protein
mEPSCs	Miniature excitatory postsynaptic currents EPSCs
MGE	Medial Ganglionic Emincence
mGLURs	Metabotropic Glutamate Receptors
miR	micro-RNA
MOM	Mitochondrial outer membrane
MOMP	Mitochondrial outer membrane permeabilization

MyRF	Myelin gene regulatory factor
MZ	Marginal Zone
Na^+	Sodium
NFAT	Nuclear factor of activated T cells
NFSIs	Non-fast-spiking interneurons
NG2	Nerve/Glial antigens 1 and 2
NGF	Nerve Growth Factor
NKCC1	Na^+ ,K^+, $2Cl^-$ transporter 1
NMDA-R	N-methyl-D-aspartate receptor
NOS	Nitric Oxide Synthase
NpHR	Halorhodopsin
NPY	Neuropeptide Y
Nrg3	Neuregulin 3
NT-3	Neurotrophin-3
OLs	Oligodendrocyte
OPC	Oligodendrocyte Precursor Cells
PCD	Programmed Cell Death
PDGF	Platelet-derived growth factor
PDGFRα	Platelet-derived growth factor receptor
PFC	Prefrontal cortex
PI3K	Phosphoinositide 3-Kinase
PKC	Protein Kinase C
PLC	Phospholipase C
PLP	Proteolipid protein
PN	Pyramidal or Projecting Neuron
POA	Preoptic Area
POH	Preoptic-Hypothalamic
POM	Posterior medial nucleus
PP	Preplate
PSP	Postsynaptic Potential
PV	Parvalbumin
RG	Radial glia

RGPCs	Radial Glia Progenitor Cells
R_{in}	Input resistance
scRNA-seq	Single-cell RNA sequencing
Shh	Sonic Hedgehog
SPs	Subplate Neurons
SST	Somatostatin
SWI/SNF	Switch/Sucrose Non-Fermentable
T_C	Cell-cycle time
Tent	Tetanus toxin
TFEB	Transcription factor EB
TTX	Tetrodotoxin
VGAT	Vesicular GABA transporter
VGCCs	Voltage-Gated Ca^{2+} Channels
VIP	Vasoactive Intestinal Peptide
VPM	Ventral Posterior Medial nucleus
VZ	Ventricular Zone
τ_m	Membrane time constant

Introduction

1. CEREBRAL CORTEX

The first description of the cerebral cortex is dated back on XX century when Brodmann identified 52 different regions based on cytoarchitectonic criteria named “cortical area” (**Figure 1**).

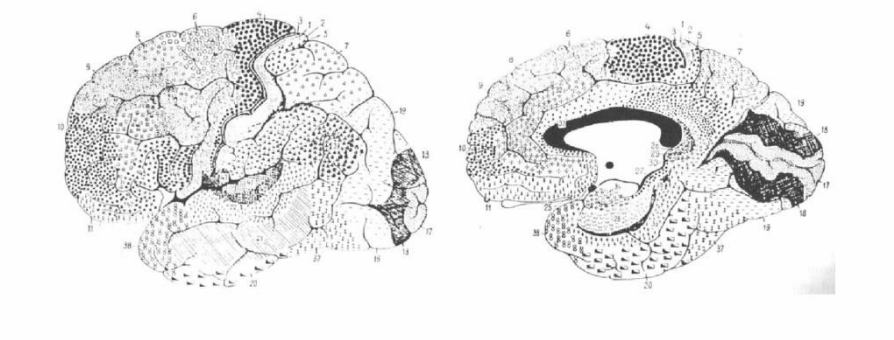

Figure 1. Brodmann's classification of the cortex. Each number is assigned to a different areas for a total of 52 different regions (Adapted from Strotzer, 2009)

This anatomic subdivision was later confirmed from Penfield studies which provided a functional map of the human cortex based on electrical brain stimulation in conscious patients (Mazzola et al., 2012). The map is designed as a “little man” or Penfield’s Homunculus (Arminjon, 2009) (**Figure 2**).

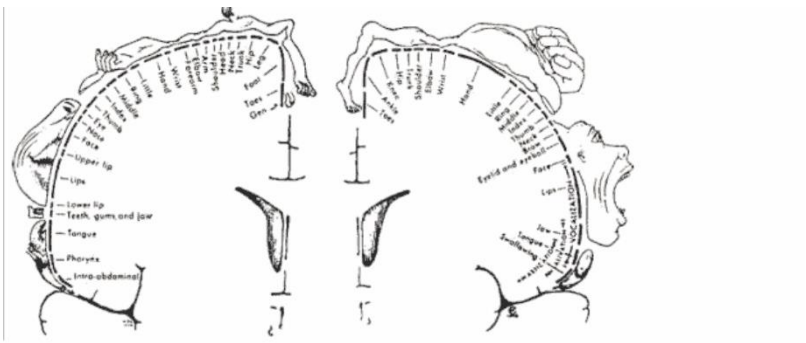

Figure 2. Penfield's Homunculus. Functional map of the human cortex dedicated to sensory and motor processing. On the left side is rapresemted the sensory homunculus while on the right the cortical motor homunculus. (Adapted from Arminjon, 2009).

Starting from this initial evidences, more recent studies improved our understanding of the somatotopic arrangement of the cortex and its cellular organization, topic we are going to extensively describe in the following paragraphs.

1.1 Cerebral cortex and its general organization

1.1.1 Generalities

The cerebral cortex is a complex organ, responsible for the higher cognitive functions including memory, perception, attention and motor planning. The cortex is the most external part of the brain composed by two hemispheres which communication allows for the synchronization and the integration of sensory, motor and cognitive informations. The cerebral cortex can be anatomically divided into neocortex (or isocortex) and allocortex, which includes structures like the hippocampus and the olfactory cortex. The neocortex is an evolutionary acquisition of mammals, mainly organized in six distinct anatomical layers, characterized by different cell populations and density (Maricich et al., 2001). These differences in the cytoarchitecture have been used to define different anatomical areas, often related with different cortical functions. Indeed, the cerebral cortex is tangentially organized in different functional areas according to the integration of different inputs. It is therefore possible to identify a visual, somatosensory, auditive, motor and cognitive cortex. These different regions are composed by a huge diversity of neuronal types organized, as we said before, in six distinct layers, bound together by short-range connections, forming cortical columns (~ 200–600 mm of diameter). It has been long discussed the presence of all the six layers in the motor cortex, long defined lacking layer IV (LIV). Recently, Yamawaki et al. (2014) described a rudmentary functional LIV in mouse motor cortex with properties and connections similar to LIV in sensory areas.

In the cortex, it is possible to identify two major groups of neurons present in a plethora of different subtypes: the excitatory Pyramidal or Projecting Neurons (PNs) and the Interneurons (INs). These neurons can be distinguished by their morphology, molecular or electrophysiological properties and their laminar position settled in the different cortical columns. Another classification is based on the different kind of connections. PNs connectivity can be divided in two distinct groups: the corticocortical conncetions, characterized by local cortical circuits, and the corticofugal, sending their projections from the cortex to the other

brain regions. Corticocortical connections are subdivided into Commissural and Associative projections. The Commissural PNs project to the contralateral hemisphere allowing the synchronization and integration of bilateral information while the Associative PNs connect cortical areas localized in the same hemisphere. Another kind of connections are the one directed to the thalamus and classified as coritcofugal corticothalamic projections. The neurons localized in the superficial layers (L II-III-IV) mainly form corticocortical connections. Differently than superficial layers, deep layer neurons (L V-VI) project to subcortical targets, usually forming corticofugal connections (Lodato et al., 2015; Petersen, 2019).

This classification is a schematic representation of the cortex projections and it is restricted to PNs. Regarding neurons releasing gamma-aminobutyric acid (GABA), most of them retain their axon in their respective layer, column or area. For this feature, they are called short-axoned, or INs. Afferences and efferences together build the complex cytoarchitecture of the functionally distinct cortical regions. For example, somatosensory cortex LIV is the main target of sensorial thalamic inputs and, as a consequence, it appears more developed compared to the motor cortex. In the other hand, LV in the motor cortex is more represented, sending projections to subcortical regions. This complex organization starts early during the embryonic development and continue in the postnatal period, where the experience plays a crucial role in refining the cortical neuronal circuit assembly (Alfanoa and Studer, 2013; Crawley et al., 1997). In the understanding of cerebral cortex organization and functions, it is crucial to follow the sequential steps that bring to a correct assembly of this complex organ.

1.1.2 The somatosensory cortex

Their first description of cortical columns is dated back in 1957 when Mountcastle observed this particular organization in the cat somatosensory cortex. Since then, columns have been considered the modular building block composing the cerebral cortex architecture (Horton and Adams, 2005). The cortical columns are easy to visualize in the barrel cortex of rodent somatosensory cortex, which represents an important model system for its good accessibility, well characterized structure and network.

Mouse whiskers or vibrissae are typically characterized by a somatotopic map within LIV of the primary somatosensory (S1) cortex (**Figure 3A**). Each whisker is associated with a specific structure named “barrel”, a columnar organization appearing in tangential sections as “rings”

composed by cell bodies with a central region poorly occupied by somata (**Figure 3B**). In coronal sections, LIV can be described as columns separated from one to another by a region with few cells called septum (Petersen, 2007). This particular cytoarchitecture of LIV was first time observed in formalin-fixed, Nissl-stained and Cox-fixed, Golgi-Nissl-stained sections cut coronally and tangentially to the pia. It was easy to distinguish in these stains the cilindrical structures of 100–400 µm in diameter, and perpendicular to the pia. The synaptic pathway from a single whisker to its associated barrel is well described from Petersen (2007) (**Figure 3A**). The whisker deflection induces the opening of mechanogated ion channels followed by a depolarization which can trigger action potential in the neurons of the trigeminal nerve. These sensory neurons send excitatory synaptic inputs in the trigeminal nuclei of the brainstem. Trigeminothalamic neurons have also a specific organization in "barrelettes", each receiving inputs from a single whisker (Veinante and Deschenes, 1999). Ventral posterior medial (VPM) nucleus of the thalamus receives the sensory information from the principal trigeminal neurons, finally projecting to the primary somatosensory neocortex in LIV (**Figure 9A**), formed by the somatosensory "barrel" map, almost organized as whiskers on the mouse snout (Woolsey and Van der Loos, 1970).

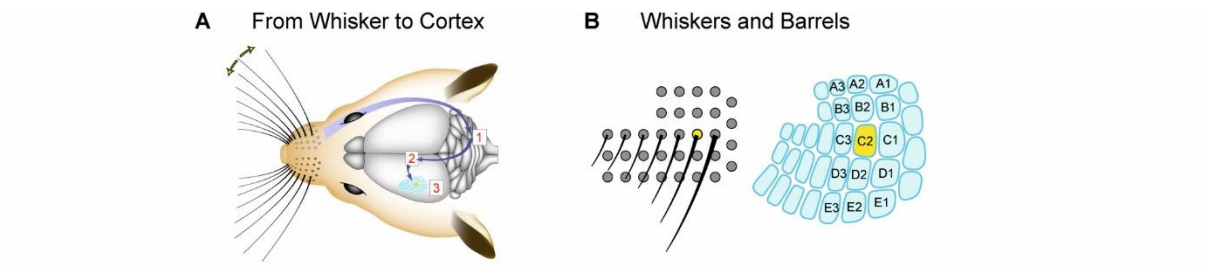

Figure 3. Synaptic Pathways from whisker to the Barrel Cortex. A. Deflection of a whisker evokes APs in the trigeminal nerve (in blue), which releases glutamate at a first synapse in the brain stem (1). The brain stem neurons send sensory information to the thalamus (2), where a second glutamatergic synapse excites thalamocortical neurons projecting to the primary somatosensory barrel cortex (3) B. The layout of whisker follicles (left, only C- row whiskers shown) and its somatotypical barrel field in layer 4 of the primary somatosensory cortex (right). The standard nomenclature for both whiskers and barrels consists of the rows A–E and the arcs 1, 2, 3, etc. As an example, C2 whisker follicle and the C2 barrel are highlighted in yellow. (Adapted from Petersen, 2007)

1.2 Cerebral cortex development

During the development, all the structures of central nervous system (CNS) are generated by stem cells localized in the border of the brain ventricles. These progenitors follow different pathways giving rise to three types of progenitor cells: the radial glia (RG), the neuroepithelial cells and the basal progenitors (Gotz and Huttner, 2005). The radial glia undergoes an asymmetrical division which maintains the RG pool and generates either a postmitotic neuron or a basal progenitor. These basal progenitors are also involved in neuron generation after a small number of symmetric divisions. All this process is called neurogenesis and is followed by the neuronal migration, dendrites and axons formation and synaptogenesis. After neurogenesis, the stem cells involved in neuron generation also participate to glial cells formation (astrocytes and oligodendrocyte) through a process called gliogenesis. A crucial step for a correct cortical development is the regulation of specific cell densities to ensure a correct function of neuronal circuits. A conserved strategy to maintain cell numbers is based on the programmed cell death (PCD) of cells. In the nervous system, PCD is also a mechanism of quality control that removes aberrant cells and refines neuronal circuits (Haydar et al., 1999). It has been demonstrated in the peripheral nervous system (PNS) that neurons compete for target-derived survival factors available in limited amounts. This theory has been named “trophic theory states” which leads to the elimination of up to 50% of neurons (Oppenheim, 1991; Yamaguchi and Miura, 2015). Differently from the PNS where this theory is widely supported, in the CNS, it remains to be controversial.

1.2.1 Corticogenesis generalities

The cerebral cortex develops from the pallium, the most dorsal region of the telencephalon. The neocortex is organized in distinct layers and their formation involved two different migrations: radial and tangential migration.

In particular, glutamatergic neurons derive from the pallial ventricular zone (VZ) and their progenitors reach the final position through a radial migration. On the contrary, GABAergic INs and oligodendroglial cells are produced by progenitors localized in the subpallium, reaching the cortex through a tangential migration (Anderson et al., 1997). The cortical layer formation by radial migration starts around days 11-18 during the embryonic development

(E11-E18) and is mediated by the radial glia progenitor cells (RGPCs) placed as a scaffold to direct neurons to their final position. The first neuronal cells produced during the cortical development are Cajal-Retzius cells (CRs) and subplate neurons (SPs) that migrate from the VZ to populate the first postmitotic neuronal layer known as preplate (PP). PP formation is followed by a second migration wave that splits the PP in two different layers, the superficial marginal zone (MZ) which is the final position for CRs, and the deeper SP. In between E14-E18, we observe consequential migration waves of post-mitotic neurons from the VZ that travel across the SP to form the sequential layers of the cortical plate (**Figure 4**). It has been shown from studies which date cell birth deteremined through thymidine tritiated injection that the corticogenesis is an "inside-out" process. In this process, neurons born early in the development settle in the deepest layers while the later born neurons are localized in the superficial layers (Gupta et al., 2002).

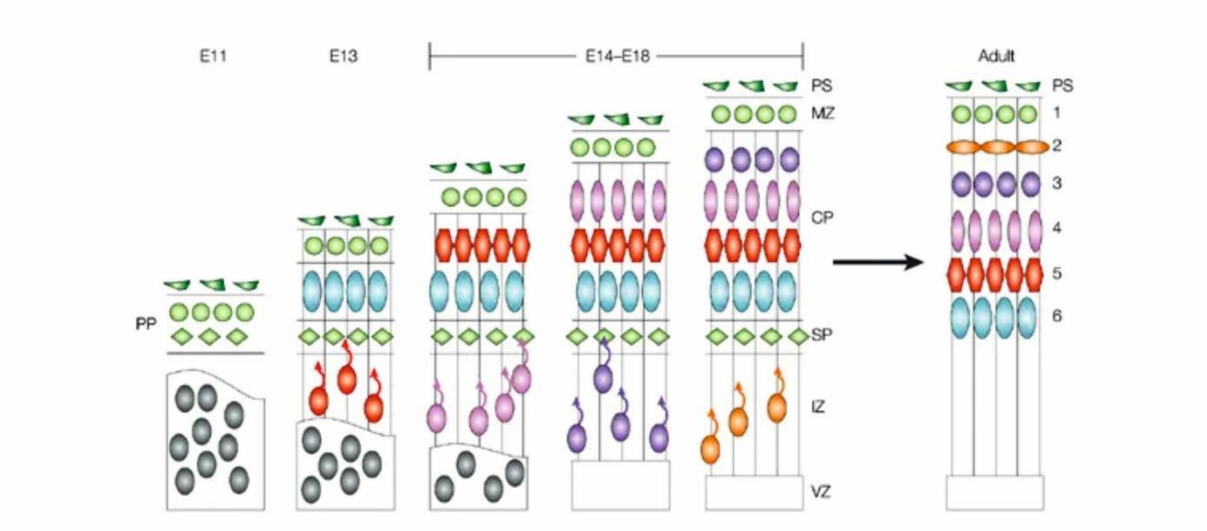

Figure 4. Neocortical-layer formation. Neocortical organization into six distinct neuronal layers. Key developmental stages. At E11, the preplate (PP) is established by a postmitotic wave of neurons that has migrated from the ventricular zone (VZ) to the PIAL SURFACE (PS). By E13, a second postmitotic neuronal wave has migrated through the intermediate zone (IZ) and split the PP into the marginal zone (MZ) and subplate (SP), creating the cortical plate (CP). During E14–E18, subsequent waves of neurons expand the CP in an inside-out fashion, as each wave of neurons passes its predecessors to settle underneath the MZ. In adulthood, the SP degenerates, leaving behind a six-layered neocortex. (Adapted from Gupta, 2002)

Differently from glutamatergic neurons, GABAergic cortical INs derive from segregated subpallial regions: the ganglionic emincences, medial (MGE) and caudal (CGE), and the preoptic regions, including the preoptic area (POA) and the adiacent preoptic-hypothalamic

border domain (POH) (**Figure 5**; Flames et al., 2007). These different regions give rise to different subpopulation of INs characterized by the expression of different molecular markers, morphology and electrophysiological properties (Lim et al., 2018).

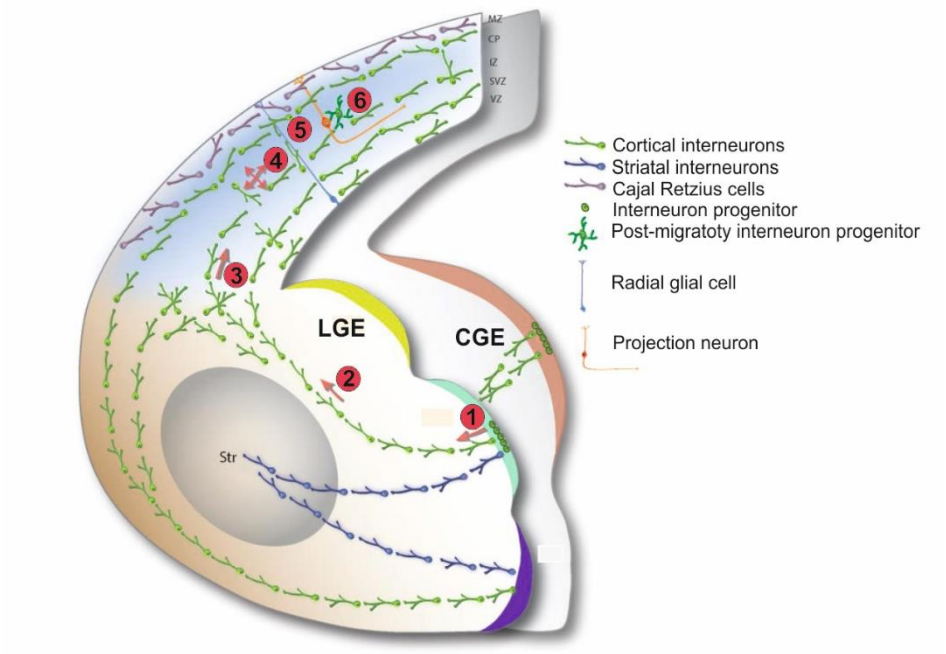

Figure 5. Patterns of interneuron migration in the developing telencephalon.
Schematic representation of rostral and caudal hemi-section through the mouse telencephalon at mid-embryonic (E15) stage. The numbers (from 1 to 6) indicate the major « decision-making » steps involved in the migration of cortical interneurons derived from the subpallium. Interneurons derived from MGE are in green, POA in purple, or CGE represent in orange, move out from the proliferative zones and initiate their migration towards the developing neocortex and striatum. Cortical interneurons travel around the developing striatum, transit across the cortico-subpallial boundary, and course tangentially into the cortex, whereas striatal interneurons ventrolaterally migrate into the developing striatum. Once reached the neocortex, interneurons undergo to local migration to finally settle in specific areal and laminar locations within the emerging CP, prior to forming functional synaptic contacts with appropriate projection neuron partners. (Adapted from Guo and Anton, 2014)

INs move from subpallial regions to the cortex through a tangential migration (**Figure 5**; Wonders and Anderson, 2006). In the cortex, beside neurons, we can identify three main classes of glial cells: astrocytes, oligodendrocytes (OLs) and microglia. Astrocytes and OLs are generated from the same progenitors as for neurons. Once the neurogenesis is finished, there is a developmental switch where progenitors become gliogenic. Microglia has a different embryonic origin, deriving from a wave of early hematopoiesis in the yolk sac. As already

shown for GABAergic INs, cortical oligodendrocyte precursor cells (OPCs) derives from embryonic subpallial regions.

1.2.2 Interneuron origin and classification

INs are generated from progenitor cells in the embryonic subpallium, telencephalon ventral region that are subdivided into several progenitor domains expressing specific transcription factors (Flames et al., 2007, Hansen et al. 2013). Among them, we identify MGE, CGE, the preoptic regions and finally the septum (**Figure 5**). Most of cortical INs derives from progenitors settled in the MGE, CGE and POA (Gelman and Marin, 2010). The origin and development of cortical IN diversity involve a series of crucial fine-tuned events protracted for a long-range of time (**Figure 5**). This period between the IN birth and the specification of their mature features has led to diverging models on the mechanisms responsible to generate IN diversity (Wamsley and Fishell, 2017). One model proposes that IN differentiation in distinct subclasses occurs at the level of progenitors or shortly after becoming postmitotic, but before their migration. Thus, their specification would depend on transcription factors which restrict their potential to generate only certain classes of INs. On the contrary, the "competing model" proposes that IN identity is established when they reach their final position, relatively late in development, after receiving signals from the surrounding environment. It has been shown that the expression of some genes encoding the transcription factors Dlx1, Dlx2, Ascl1, Gsx1 and Gsx2 is crucial for the specification of all GABAergic neurons in the subpallium (Wang et al., 2013; Long et al., 2009). Then, the emergence of the IN diversity from this region is linked to the spatial and temporal specification of progenitor cells by the expression of additional transcription factors which restrict their potential to generate just specific subclasses of GABAergic INs.

The most accepted IN classification recognizes three major classes (**Figure 6**). The first is characterized by the expression of the Ca^{2+}-binding protein paravalbumin (PV), the second one by the peptide hormone somatostatin (SST) and finally, the third, express the serotonin 5-hydroxytryptamine 3a receptor (5HT3aR). These three specific markers are not overlapping (Lee et al., 2010; Rudy et al., 2011). Others, like calbindin (CB), calretinin (CR), cholecystokinin (CCK), reelin, nitric oxide synthase (NOS) and the neuropeptide Y (NPY) are co-expressed in the different subclasses (**Figure 6** ; Xu et al., 2006; Tremblay et al., 2016).

Recent studies focused their attention on the molecular mechanisms involved in the generation of cortical IN diversity, identifying details on the genetic cascade involved in MGE-derived IN specification. It has been shown that the generation of these INs involves regulatory networks of two parallel genes. The first is started by the expression of Dlx1 and Dlx2 which promotes the specification of GABAergic lineage by repressing Olig2 (transcription factor required for OL specification) and induce the expression of genes encoding enzymes for GABA synthesis (Petryniak et al., 2007; Pla et al., 2018). Dlx1 and Dlx2 also induce the expression of Dlx5 and Dlx6, which are in turn important for the migration and differentiation of cortical INs (Pla et al., 2017; Wang et al., 2010).

Interestingly, these two genes are crucial for the specification and integration, specifically of MGE-derived INs in developing cortex network, promoting their dendrites and axons formation (Pla et al., 2017). A parallel gene regulatory pathway is initiated by the homeobox transcription factor Nkx2-1 essential for the specification of IN subclass composed by PV and SST MGE-derived INs. Nkx2-1 induces Lhx6 expression, transcription factor critical for the maturation of cortical GABAergic INs derived from the MGE (Liodis et al., 2007; Vogt et al., 2014). Indeed, MGE and POA progenitors are characterized by the early expression of Nkx2-1, which confers them unique properties and regional identity (Butt et al., 2005-2008). Moreover, it has been shown that the MGE can be divided in three different regions, dorsal, intermediate and ventrocaudal, characterized by the expression of different molecular markers: Nkx6-2 in the first and the ETS transcription factor Etv1 in the other two domains. Experiments of fate mapping revealed that SST^+ cells are preferentially generated from the dorsal part whereas PV^+ are abundantly produced from the ventrocaudal domain (Inan et al., 2012; Fogarty et al., 2007); the intermediate domain produces both. From these evidences, we can recognize the influence of progenitor spatial organization on the future specification of cortical INs (Torigoe et al., 2016). Differently from MGE and POA progenitors, cortical CGE derived INs are specified by the expression of many molecular markers, among them Nr2f2 transcription factor (Kanatani et al., 2008). Finally, cells deriving from the POH, most caudal progenitors in the preoptic region, do not express Nkx2-1, showing more similarities with the CGE (Flames et al., 2007). In particular, the preoptic region, including POA and POH, displays molecular similarities with the MGE and CGE, respectively. It has been shown that POA progenitors also express the transcription factors Dbx1 giving rise to a small but highly diverse cortical IN subclasses (Pierani et al., 2001). These different crucial regulatory genes for IN

specification, besides the differences in morphological and electrophysiological properties observed in mature GABAergic INs, point out the complexity to define an unequivocal classification.

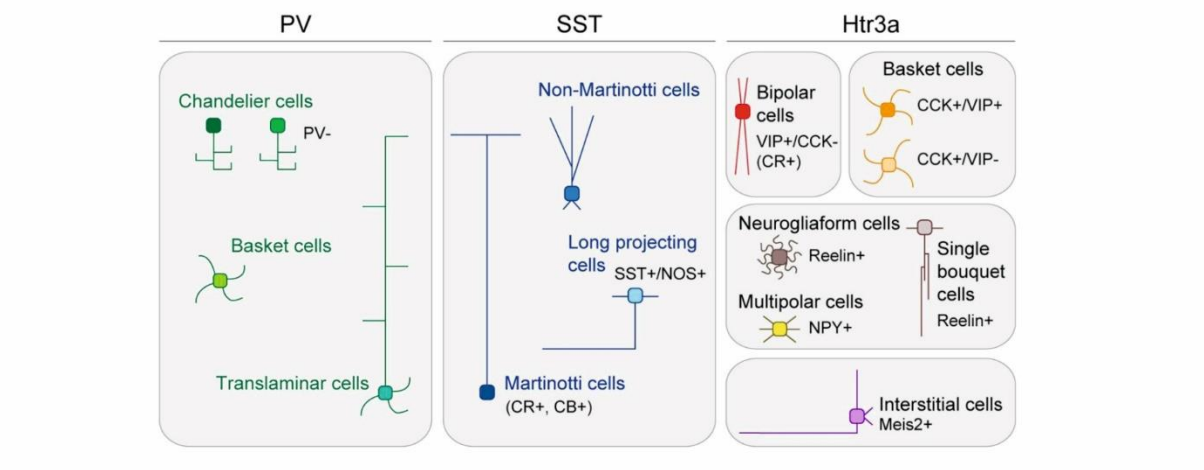

Figure 6. Diversity of GABAergic neurons in the neocortex. Schemas showing the main subclasses of cortical interneurons in the mouse neocortex. The most recognized classfication identify three large classes based on the expression of PV, SST and 5Htr3a. A small fraction of PV+ basket cells also express SST. (Adapted from Lim et al., 2018)

PV INs are the most abundant (~40%) and extensively described cortical INs, commonly divided in three major subclasses, all characterized by a fast-spiking (FS) firing profile (Kawaguchi et al., 1987). They include the chandelier and the basket cells, most abundant and homogeneously distributed INs in the neocortex, and the translaminar INs, relatively rare and mostly localized in layer LV – LVI (**Figure 6**; Lim et al., 2018). Chandelier cells, also defined axo-axonic cells, mainly project to the Axonal Initial Segment of PNs (AIS) and are localized at the border between LI and LII and in LVI (**Figure 7**). The basket cells, the most represented type of INs in the neocortex, form synapses on the soma and proximal dendrites of PNs cells and other INs (**Figure 7**). They are heterogeneously distributed across all the cortical regions and specifically localized through LII to LVI in the neocortex. The second class of INs expressing SST, represents a more heterogeneous group in which it is possible to identify two main subtypes according to their morphology: Martinotti and non-Martinotti cells. One characteristic that differentiate Martinotti cells from non-Martinotti cells is their axonal plexus formed in LI and the expression of the overlapping marker CR (**Figure 6**). The firing patterns of Martinotti cells are relatively heterogeneous but they are often involved in disynaptic inhibition (Nigro et al., 2018; Silberberg and Markram, 2007). Additionally, non-Martinotti cells differentiate from Martinotti cells for their lower resting potential and a higher firing

frequency. Martinotti cells are mostly localized in LII, LIII and LV while SST non-Martinotti cells are found throughout LII to LVI and particularly abundant in LIV, where they are mostly connected with PV basket cells (**Figure 7**; Nigro et al., 2018; Xu et al., 2006; Ma et al., 2006; Xu et al., 2013). In addition to these two subclasses, SST expressing INs include a small population of long-range GABAergic projecting neurons, mostly localized in deep layers and projecting to other regions of the neocortex (**Figure 6**). They have adapting and irregular spiking firing properties, frequently co-expressing NOS, chondrolectin (Chodl) and NPY (He et al., 2016).

Finally, the third class is represented by 5HT3aR INs, far more diverse group than PV and SST. They are separated in two groups, the INs expressing vasoactive intestinal peptide (VIP) and the one that do not (**Figure6**). The most characteristic VIP INs have a bipolar morphology with axons oriented to the most superficial layers. They have an adapting firing properties and preferentially target SST and PV INs, mediating disinhibition (**Figure 7**; Pronneke et al., 2015 ; Jiang et al., 2015). VIP INs are mostly found in LII and LIII, and co-express CR. On the contrary, multipolar VIP INs are basket cells co-expressing CCK. Non-VIP can be mainly subdivided in neurogliaform and CCK-expressing INs. Neurogliaform cells represent the 90% of LI INs (**Figure6**). They preferentially contact dendrites eliciting slow long-lasting Inhibitory Postsynaptic Potentials (IPSPs), favoring $GABA_B$ receptor ($GABA_BR$) activation (**Figure 7**). Finally, non-VIP CCK INs provide a somatic inhibition through an asynchronous release (**Figure 7**; Tremblay et al., 2016).

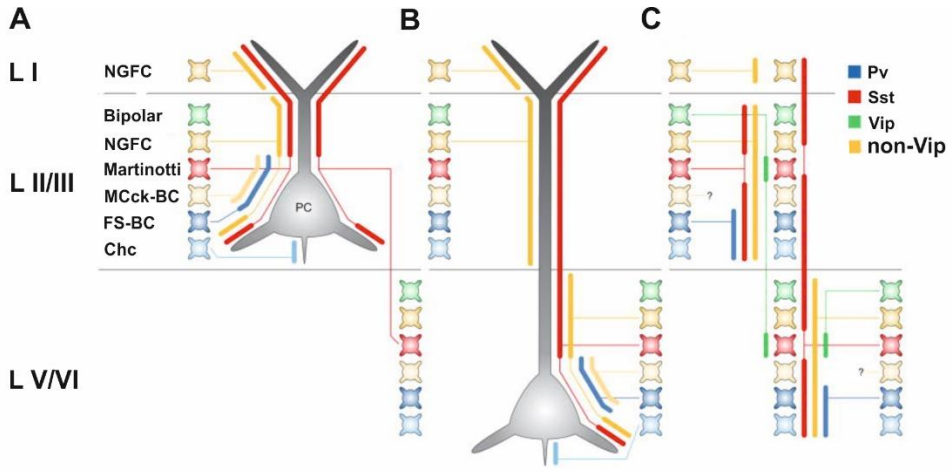

Figure 7. Cell-specific connectivity and subcellular domains targeted by interneuron subtypes.
A. Rapresentation of LII/III interneurons connectivity to pyramidal cells. SST Martinotti cells in red and non-Vip 5HT3aR neurogliaform cells in dark yellow are two major IN subtypes targeting dendrites. Both LII/III and LV Martinotti cells have been shown to connect to LII/III PCs (Jiang et al., 2015; Kapfer et al., 2007). The perisomatic region and proximal dendrites are targeted by Cck basket cells (light yellow) and PV fast-spiking basket cells (dark blue). The axon initial segment is contacted by PV chandelier cells (light blue). B. Interneuron connectivity with pyramidal cells settled in layer V/VI. LII/III Martinotti cells only poorly contact infragranular PCs thus among Martinotti cells only those in infragranular layers target LV PCs. In contrast, LI, LII/III and LV/VI NGFCs contact PC dendrites. Perisomatic and axonal contacts are provided by infragranular basket and chandelier cells. C Connectivity among INs. NGFCs target all interneuron subtypes and thus their connectivity is solely restricted by the extent of their axonal arbor. Martinotti cells contact all IN subtypes except other Sst INs. Cck basket cells is assumed to receive inputs from both Martinotti cells and NGFCs. PV basket cells are known to strongly connect to other PV cells. Vip bipolar cells are selective for other interneurons, particularly Sst INs. LII/III bipolar Vip INs can contact both LII/III and LV Sst INs. While the connectivity of infragranular Vip cells has not been investigated, it is assumed to show similar cell type selectivity than supragranular Vip INs and be restricted to deep layers given that their axons do not ascend to supragranular. (Adapted from Tremblay et al., 2016)

The incredible diversity of INs described above, their different connectivity and their particular distribution in different layers reflects the many various roles they assume in neuronal networks. It has been observed that IN final identity can be recognized only when they are integrated into neuronal circuits. This observation is corroborated from studies which demonstrated that activity dependent interactions with the cortical microenvironment are crucial to determine the final IN identity (Wamsley and Fishell, 2017). It has been widely shown that during cortical development GABAergic INs undergo many changes in their both morphological and neurochemical profiles. After their specification, INs migrate from their subpallial regions to translocate to the cortex and start their integration into neuronal circuits, crucial event to finally acquire their mature neurochemical and morpho-physiological attributes (Du et al., 1996; Martini et al., 2009). Several evidences suggested that PN activity has an important role in IN allocation, distribution and connectivity. For example, recent studies have shown that INs are driven in their final laminar distribution by PN signals like the neuregulin 3 (Nrg3) (Bartolini et al., 2017). In addition, it has been reported that INs interact with specific classes PNs anticipating the formation of specific excitatory and inhibitory connections in the developing cerebral cortex. In particular, they showed that excitatory projection neurons can modulate afferent inputs by local PV INs, modulating the wiring of cortical microcircuits (Ye et al., 2015). Moreover, it has been shown that some IN motifs are present all over the time during cortical development while some are transient, described mainly in the deep and superficial layers of the barrel cortex (Petersen, 2007). Regarding their intrinsic electrophysiological properties and excitability, it was showed that neocortical INs display a lower threshold for action potential generation than PNs at early postnatal stages which confers them a higher probability to be recruited at the early phases of network

synchronization (Rheims et al., 2008). Whole-cell recordings *in vitro* performed in dentate gyrus basket cells showed that, in association with morphological changes, as the growth membrane surface area, intrinsic passive membrane properties are also altered. For example, the membrane capacitance (C_m) increases during the development while the input resistance decline (R_{in}). Moreover, it has also been observed an acceleration in the membrane time constant (τ_m) during IN maturation (Doischer et al., 2008). Similar alterations in passive membrane properties have been found in the neocortex (Daw et al., 2007; Rheims et al., 2008). The propagation of Postsynaptic Potentials (PSPs) in dendrites and soma is strongly dependent on the structure of the dendrites and the passive membrane properties. Shorter and less complex dendrites result in a lower C_m. Moreover, τ_m measure in young basket cells is two times longer than in mature ones (∼20 ms at PN 6-10 vs. ∼10 ms at PN 18-25) and R_{in} is significantly higher (∼380 MΩ P6-10 vs. ∼80 MΩ at PN 18-25). Altogether, these data suggest a higher R_m in young neurons (Doischer et al., 2008). These differences observed in membrane passive properties have as a consequence larger peak amplitudes and slower time courses of PSPs recorded in young neurons compared to mature cells. All these evidences suggest that young INs, compared to mature, display a different integration for PSPs, favoring spatial and temporal summation of synaptic inputs. On the other hand, mature INs with long dendrites, fast τ_m and low R_m support, instead, coincidence detection. Regarding the axonal changes, young INs undergo substantial postnatal growth, increasing the connectivity with their target cells and altering active properties (Du et al., 1996; Doischer et al., 2008; Sauer & Bartos, 2010). Whole-cell recordings of bascket cells revealed an increase in the peak amplitude and a decline in the half-duration of single action potentials (Doischer et al., 2008). Furthermore, mature fast-spiking INs of the barrel cortex discharge at higher frequency in response to membrane depolarization (Daw et al., 2007). The developmental up-regulation of fast delayed-rectifier K^+ channels for example (Du et al., 1996; Rudy and McBain, 2001; Tansey et al., 2002), is concordant with the maturation of INs from slow to fast discharging units. In summary, during the development, INs undergo morphological, passive and active membrane properties changes, favouring a slow signalling in the young until they acquire mature properties which contribute to a rapid signalling in the mature neuronal network. The complexity in INs specification and their morphological and electrophysiological changes during the development is a fine-tuned process to ensure a proper maturation.

Indeed, defects in GABAergic INs maturation results in drastic malfunctions of the mature circuitry, which has as a consequence the manifestation in neurological disease.

1.2.2.1 Interneurons in the network

INs can interact forming different kind of synaptic contacts, named chemical and electrical synapses. Electrical synapses allow for the ion exchange from neighbor neurons through a structure called gap-junctions, specialized intercellular connections formed by connexins, hemi-channels located in pre and post junctional cell membranes (Bennet and Zukin, 2004). Gap junctions are mostly found in PV INs, modulating their activity by synchronizing action potential firing (Hatch et al., 2017). It has been shown that this type of communication occurs mostly between INs of the same subclass in the cortex (Galarreta and Hestrin, 1999; Gibson et al., 1999).

The integration of INs in neuronal networks follows few stereotypical patterns of connection (Lim et al., 2018). There is no a general IN connectivity rules but some recurrent patterns can be identified. For example, thalamocortical inputs to LIV preferentially form synaptic contacts with some specific INs, and intracortical axons of corticothalamic neurons settled in LVI preferentially target inhibitory over excitatory neurons (Xu et al., 2013; Bortone et al., 2014). All the different subclasses of INs form three main "archetype circuit motifs": the feedforward inhibition (FFI), feedback inhibition (FBI), and disinhibition (**Figure 8**). The FFI inhibition is described like an excitatory input contacting INs which then synapse onto principal cells. Therefore, the afferent excitatory input provides a disynaptic inhibition to principal cells through INs . (**Figure 8A**).

The more studied FFI is in the somatosensory (barrel) cortex, involving PV basket cell INs receiving excitatory thalamic input from the VPM and connected with the neighboring spiny neurons (Sun, Huguenard and Prince, 2006). Differently from the feedforward, in FBI, the source of the excitatory inputs comes directly from the cell innervated by the IN creating like a closed loop (**Figure 8B**). This kind of circuit allows for the fine control of the balance between excitation and inhibition in local circuits. Finally, the disinhibition occurs when an IN inhibits another IN removing the second IN inhibition on a PN (**Figure 8C**). It has been shown in some studies that this kind of inhibition is provided mostly by 5HT3aR INs (Tremblay et al., 2016).

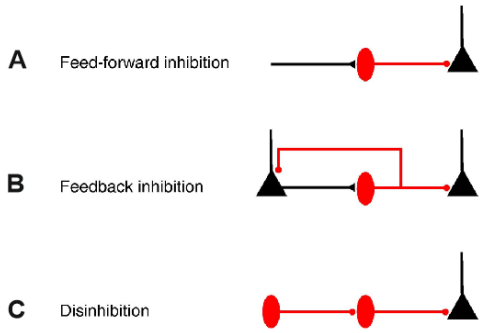

Figure 8. Inhibitory circuit motifs. Three main motifs involving GABAergic interneurons represented in red, exist ubiquitously in the cortex. A. Feed-forward inhibition B. Feedback inhibition C. Disinhibition. (Adapted from Feldmeyer et al., 2017)

1.2.2.2 Barrel cortex circuits

The somatosensory cortex receives multiple inputs to a single column. In particular, we can identify two main sensory inputs: one from VPM and one from posterior medial nucleus (POM), both examples of thalamocortical projections (**Figure 9A**). Another example of somatosensory cortex connection is represented from the outputs coming from multiple layers into a column, with some of them projecting to neighboring barrels in order to integrate information across the whisker somatotopic map.

One of the main targets of thalamocortical axons are the spiny stellates cells in LIV, excitatory neurons highly interconnected to each other in order to amplify the received thalamic excitatory input (**Figure 9A**). Moreover, these cells contact PNs settled in all cortical layers which integrate the input in between different columns to finally send the outputs in other brain regions (Vitali and Jabaudon, 2014). Not only LIV but also LVA and LVIB neurons receive thalamic inputs and, in turn, send their axons to many cortical and sub-cortical structures (**Figure 9A**). In this panorama, GABAergic interneuronal networks play a crucial role to ensure a correct function of sensory input integration. INs can be classified as trans-columnar and trans-laminar looking at their axonal projection pattern. The thalamocortical afferents, coming from the VPM, contact different types of INs, which in turn synapse onto excitatory neurons in the same or other cortical layers mediating different inhibitory patterns. Fast-spiking INs (FSIs) are the main target of thalamocortical afferents and represent the major source of rapid intracortical inhibition in LIV (Gibson et al., 1999). Indeed, LIV basket FSIs, showing dense axonal arborizations locally restricted to the home barrel, target the perisomatic

compartments of excitatory cells, causing a robust thalamocortical feed-forward inhibition. The chandelier cells, instead, form axo-axonic contacts, controlling the action potential output of PNs mostly localized in upper LII-III and LVb and VI (Somogyi et al., 1977; Taniguchi et al., 2013). LIV SST INs are also innervated by thalamocortical afferents, but their response to thalamic stimulation is considerably weaker than that of LIV PV FS (Cruikshank et al., 2010). PV INs are involved in the thalamocortical FFI, receiving excitatory inputs from the VPM and sending projection to spiny stellate cells, which receive thalamic afferents too. LV PV INs are highly interconnected between them but also receive strong inhibition from SST cells. A recent study described a translaminar inhibition in which axons of excitatory LIV stellate cells form synapses with LVb PV FS, which, in turn, drive inhibition in LVb PNs. SST Martinotti cells receive facilitating excitatory synaptic input from nearby PNs, ensuring a frequency-dependent disynaptic inhibition on PNs dendrites. In the barrel cortex, VIP INs play a role in disinhibition by contacting both PV and SST INs (Naka and Adesnik, 2016).

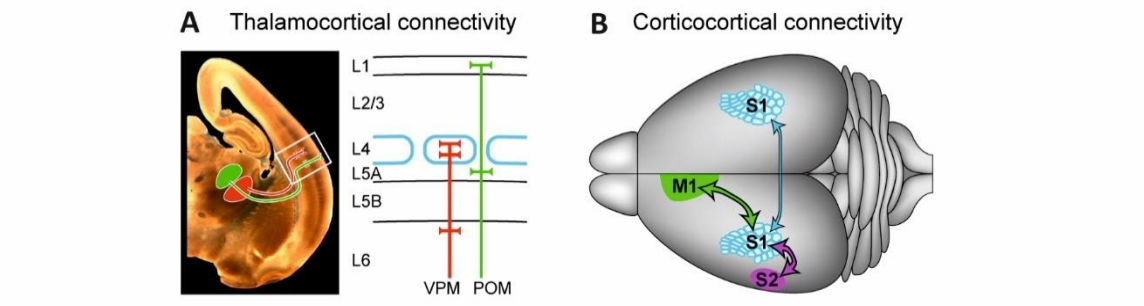

Figure 9. Thalamocortical pathways for signaling whisker-related sensory information to the barrel cortex. Neurons in the ventral posterior medial (VPM) nucleus (labeled red, left) are glutamatergic. Signal information relating to a deflections of a single whisker. The axons of VPM neurons terminate predominantly in individual layer 4 barrels, with a minor innervation in upper layer 6 (right). (Adapted from Petersen, 2007)

1.2.3 OPC origin: three distinct developmental waves

Historically, in the mammalian CNS the astrocytes, OLs and microglia were classified as glial cells. Later, studies identified another major glial cell population characterized by the expression of the proteoglycan NG2 (nerve/glial antigens 1 and 2) distributed throughout the grey and white matter. To reflect their multi-processed morphology and lineal relationship to OLs, this cell population has also been called polydendrocytes, parenchymal cells expressing the NG2 (Nishiyama, Watanabe, Yang and Bu, 2002). It is now widely accepted that the polydendrocytes or NG2 cells are OPCs that generate OLs in the developing and mature CNS.

In the forebrain OL lineage is generated from Olig2^{+} cells settled in the subpallium (Nery et al., 2001; Tekki-Kessaris et al., 2001). Olig2 is expressed in both, neuronal and OL lineage cells, thus OL lineage specification occurs later, in the germinal zone, to become committed to NG2 cells. During the development Olig2 expression is sustained promoting the expression of the transcription factor Sox10, restricted to OL lineage cells, representing the first step in OPC specification. Sox10 is known to promote the expression of platelet-derived growth factor (PDGF) receptor (PDGFRα), crucial for OPC survival and proliferation (Nishiyama et al., 2009). NG2 expression starts slightly later than PDGFRα expression, around E17 (Nishiyama et al., 1996).

OPC generation starts from the subpallium while a fraction derives from the cortex at postnatal stages (Kessaris et al., 2006). It has been shown through experiments of fate mapping that OPCs are generated in three different sequential waves expressing specific markers and coming from different embryonic regions. The first wave derives from the ventral MGE and anterior entopenducular area (AEA) at E11.5 - E12.5, the second wave originate from LGE/CGE at E15.5, and the last wave develops at birth in the cortex (Kessaris et al., 2006). Each wave is characterized by the expression of specific transcription factors like the Nkx2-1, expressed from progenitors of the first wave, the Gsh2 from the second and finally, Emx1 from the third (**Figure 10**). Once generated, OPCs coming from different regions start their migration to their final positions. It was recently demonstrated that OPC migration during development is mediated by vasculature, which act as physical support. OPCs migration through the parenchyma is favored by endothelium-OPC interactions, which depends on the Wnt pathway activation and the chemokine receptor CXCR4 (Tsai et al., 2016). Once OPCs in the cortex, their primary function is to generate myelinating OLs, not only during postnatal development, but also during adulthood. The existence of three distinct waves in OPCs development raised the question about the possibility to generate different population of OLs. Recently, it has been shown that the OL progenitors expressing the transcription factor Nkx2.1 are completely eliminated after the birth and replaced by other populations with any alteration, suggesting a redundant role with the other following OPCs waves (Kessaris et al., 2006). Studies conducted by Richardson's group observed that the ablation of a specific OPC wave is compensated by the others, corroborating the idea that the three different waves are or can become functionally equivalent (Kessaris et al., 2006). Recently, it has been shown from single-cell RNA sequencing (scRNA-seq) that adult OLs can be classified in six different mature OL states,

suggesting a functional heterogeneity (Marques et al., 2016). Thus, Marques et al. (2018) specifically investigated the different OPC waves to understand whether they could differentiate into different OL populations. They analyzed the transcriptional profile of cell expressing PDGFRα/GFP^{+} at different developmental stages, specifically at E13.5, E17.5 and PN 7. The scRNA-seq identified that the heterogeneity observed in the embryonic OPCs was slightly smoothed out during the development, suggesting a transcriptional convergence of OPCs arising from different germinal zones (Marques et al., 2018). These evidences suggested that the different previously identified populations of OLs may not be related with intrinsic OPC properties, but likely related with the local environment.

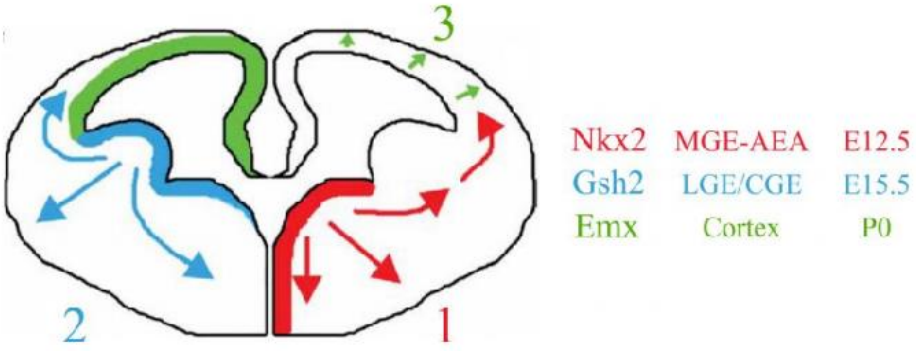

Figure 10. Forebrain OPCs are born in three sequential waves. 1) *Nkx2.1*-expressing progenitors starting at E12.5, 2) *Gsh2*-expressing LGE/CGE progenitors starting at E15.5 3) *Emx1*-expressing cortical precursors starting around birth. (Adapted from Kessaris et al., 2006)

1.2.4 Cell death

1.2.4.1 Generalities

During cortical development, one of the conserved strategies described to ensure a correct number and normal function of cellular components of the nervous system is based on overproduction followed by a selective elimination of cells during specific developmental stages (Oppenheim, 1991). In the PNS, it was demonstrated that overproduced cells compete for a limited amount of trophic factors (Oppenheim 1989) that are produced by synaptic targets or other contacting cells (neuronal or glia). In the developing CNS, neuronal activity and neurotransmitter inputs seem to play a more significant role than trophic factors in promoting neuronal survival.

Transient cell populations, like CRs or RG, have also been identified as signaling centers or scaffolds that release molecules responsible for a correct organization of the cerebral cortex (Kiecker and Lumsedn, 2012). This process of developmental death is known as PCD, essential for proper embryonic and postnatal development (Glucksmann, 1951, Jacobson et al., 1997). Recent progress in modern experimental techniques allowed us to address the mechanisms and the biological function of this developmental process (**Figure 11**).

The word apoptosis also defined as “not accidental cell death”, was given in 1972 (Kerr et al., 1972). This process was first clearly observed in genetic studies on C.Elegans that identified many molecular determinants involved in this mechanism (Ellis et al. 1991). It has been later shown that cells can undergo death following three different mechanisms: apoptosis, necrosis and autophagy (Galluzzi et al., 2018). The apoptosis is the major form of PCD in the developing nervous system, mechanism for quantitative matching, sculpting, and deleting anatomical structures, in order to regulate cell number, eliminate defective cells and finally ensure a correct assembly of neuronal circuits (**Figure 11**).

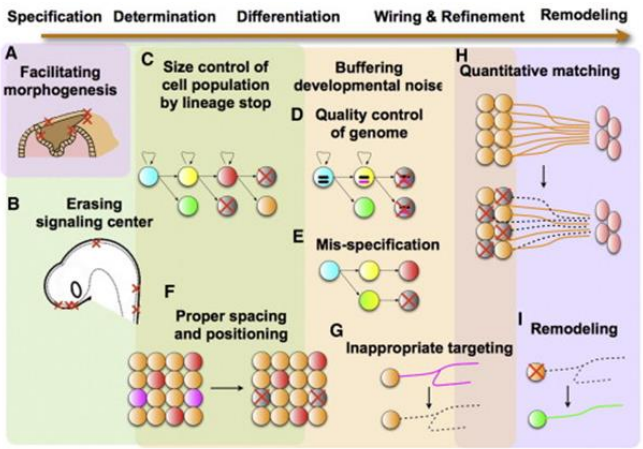

Figure 11. Roles of PCD during Nervous System Development. Schematic representation of functions of cell death during neural development. The « X » in red indicates cells that undergo PCD. (Adapted from Yamaguchi and Miura, 2015).

We can identify two different types of apoptosis, extrinsic or intrinsic, defined depending from the microenvironment perturbation source. Intrinsic apoptosis is initiated by a variety of microenvironmental perturbations like growth factors or mitotic defects while the extrinsic is mostly driven by extracellular signals and mediated by plasma membrane receptors (Galluzzi et al., 2018). However, the cellular mechanisms involved in these two processes culminate with the activation of a family of cysteine proteases known as caspases. In the intrinsic

pathway, we have an irreversible permeabilization of the mitochondrial outer membrane (MOM) with a consequent release in the cytosol from the intermembrane space of antagonists for apoptosis inhibitor proteins (IAPs), such as Smac/Diablo and the cytocrome C (Kale et al., 2012, Saelens et al., 2014). Nowadays, it is well known that PCD is mediated by an evolutionarily conserved signaling pathway that involves the pro-apoptotic BCL2 family, identified by a conserved Bcl2 homology (BH) domain (Kvansakul et al., 2015). Among the proapoptotic proteins, the Bcl2- associated X protein (Bax) and the Bcl2 antagonist/killer 1 (Bak) are the only BCL2 family members characterized in mammalian cells which oligomerize in the MOM forming pores. It has been recently shown that Bax can form rings that perforate the MOM with its consequent permeabilization (MOMP) (**Figure 12**). The cytocrome c and Smac/Diablo release has as a consequence the formation of a protein complex known as the apoptosome, which is responsible for caspase 9 (Casp9) activation (Li et al., 1997). This complex then catalyzes the activation of the so-called executioner caspases Casp3 and Casp7, which are the last step in the process responsible for the destruction of the cell in both types of apoptosis (Julien & Wells 2017).

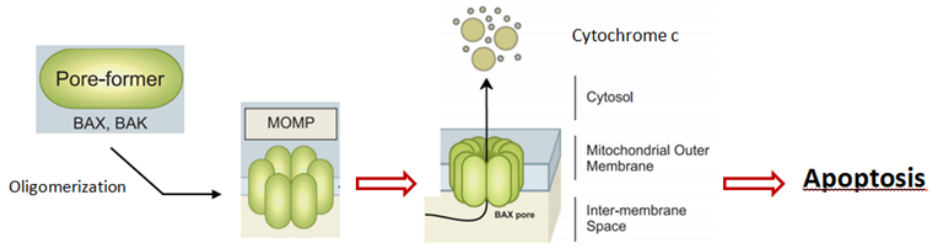

Figure 12. Mitochondrial outer membrane permeabilization (MOMP) mediated by BAX BAK oligomerization and following release of Cytochrome c, the apoptosis mediator. (Adapted Frm Kale et al., 2017)

Differently from the intrinsic apoptosis, the external apoptosis is started from different pathways activated by two different receptors. The first, called death receptor, is triggered by specific ligands while the second, known as dependence receptor, is activated only when the levels of ligands drop down a specific threshold. Among the dependence receptors, which are particularly abundant in the developing nervous system, we can list neurotrophin receptors TrkA and TrkC, which bind to nerve growth factor (NGF) and neurotrophin-3 (NT-3), respectively (Dekkers et al., 2013), the netrin 1 receptors (DCC, Unc5A, Unc5B, Unc5C, and Unc5D) and the sonic hedgehog (Shh) receptor Ptch1 (Goldschneider & Mehlen 2010). The

neurotrophin receptor $p75^{NTR}$ can also interact with TrkA and TrkC and act as a death receptor when directly activated by proneurotrophins (Dekkers et al., 2013, Nykjaer et al., 2005). The pathways involved in the extrinsic apoptosis generally culminate with the activation of Casp8 to ultimately converge, as well as for instrinsic apoptosis, with the executioner caspases Casp3 and Casp7.

The PCD occurs in two distinct developmental stages: during the embryonic period, with the elimination of progenitors and early born cells, and after birth during the circuit assembly. It has been estimated that a range from 20% to 70% of cell progenitors die during cortical embryonic development (Blashke et al., 1996; Thomaidou et al., 1997). The first cell death event has been observed around E10.5 in the pallium while, in the subpallium, death is not such a frequent event during the embryonic stage. Differently from the already described mechanism depending from Bax/Bak effectors, the embryonic cell death follows a different mechanism, more linked to cell cycle checkpoints (Pilaz et al., 2016). Post-natal cell death mainly occurs during the two first weeks in the mouse and, as demonstrated by studies based on simple cell counting and TUNEL assay (Ferrer et al., 1990; Finlay & Slattery 1983), it is a process affecting around the 25-35 % of cortical cells. Even if different cell populations undergo PCD, this evolutionary conserved process has different roles according to the cells fated to die. It is most likely used to refine the final cell number or, as a quality control, it aims to eliminate misplaced or abnormally wired neurons (**Figure 11;** Clarke 1992). In some cases, the elimination of entire population occurs as a mechanism that could remove unnecessary signals for the circuit assembly and maturation (Fogarty and Bergmann 2015). The mechanisms regulating the PCD in different cell populations of the CNS have been widely studied. It has been demonstrated that it occurs in glutamatergic and GABAergic neurons, eliminated by around 30-40 % (Southwell et al., 2012; Verney et al., 2000), while in large scale in other cell populations, like the CRs, the SPs, the cortical plate transient neurons (CPTs) and the first wave of OPCs (firstOPCs), almost completely eliminated after the birth. These early-born neuronal populations, since massively disappear up to the 90% after birth, are defined as “transient” because they are transiently present in the developing cortex (Price et al., 1997; Causeret, Coppola and Pierani, 2018).

In the neocortex It has been recently demonstrated that just the ~30 % of Glutamatergic PNs die and it occurs early in the postnatal development, in between PN 2 and PN 5 (Wong et al. 2018). CRs, the first-born cortical neurons settled in LI undergo extensive cell death (94-97 %)

between PN 4 and PN 10 (Chowdhury et al. 2010; Ledonne et al., 2016). SPs, essential for the correct assembly of thalamocortical connections, disappear completely during the early postnatal development (Hoerder-Suabedissen and Molnar, 2015). CPTs, glutamatergic neurons present during embryonic development, crucial in the radial growth of the neocortex in a non-cell autonomous manner, massively die during the first postnatal weeks. In addition, microglial cells are dramatically eliminated by the 50% between the third and the sixth postnatal week (Nikodemova et al 2015).

Interestingly, it has been observed a strong correlation between neuronal activity and apoptosis rate. Neuronal activity manipulation, either pharmacologically or by electrical stimulation, has an impact on the level of apoptosis in different cell populations. For example, it has been shown that survival of PNs is tightly connected with neuronal activity. Cell survival pathways are usually mediated by L-type voltage-gated calcium channels (L-VGCC) and N-methyl-D-aspartate receptor (NMDAR) activated by electrical activity with a consequent intracellular calcium (Ca^{2+}) increase, messenger translated into pro-survival or pro-death signal. Early studies in culture showed that, using antagonist of voltage-dependent sodium (Na^{+}) channels, widely decreases PNs survival (Ruijter et al. 1991). This observation was later replicated *in vivo*, where injection of tetrodotoxin (TTX) to PN 2 rats induced an increase in the number of cortical apoptotic neurons (Murase et al., 2011). On the contrary, increasing the spontaneous firing rate modifying the extracellular potassium (K^{+}) concentration reduces the cortical cell death in rat and mouse cell cultures (Ghosh et al., 1994; Golbs et al., 2011). It has been shown that Ca^{2+} increase, resulting from a neuronal activity increase, triggers the activation of three different pro-survival pathways: the Phosphoinositide 3-Kinase (PI3K)/Akt pathway, the Protein Kinase C/Extracellular signal-Regulated Kinase (PKC/ERK) pathway and the Ca^{2+}/calmodulin pathway. Specifically, the PI3K activates the serine/threonine kinase Akt which directly phosphorylates and inactivates pro-apoptotic members of the Bcl-2 family members, caspases or Forkhead transcription factors (Brunet et al., 1999), thereby inhibiting cell death. Recent study conducted on PNs showed that the deletion of the two apoptotic factors Bax and Bak increases PN number (~ 12%) compared to the control mice (Wong et al., 2018). This evidence reinforces previous evidences cited above which observed a correlation between the Ca^{2+} increase mediated by neuronal activity as mediator of BCl2 pro-apoptotic factors inhibition. The Bax/Bak dependent death of PNs occurs in a different proportion comparing the different cortical regions and also between different layers of the same cortical

area (Blanquie et al., 2017). In contrast with the glutamatergic PNs, neuronal activity is a crucial signal that triggers CRs death (Blanqui et al. 2017). The different behavior observed in CRs is probably due to their low resting potential and the high expression level of the Na^+ ,K^+, $2Cl^-$ transporter 1 (NKCC1) transporter compared (Achilles et al. 2007) to the low level of K^+, Cl^- transporter 2 (KCC2) (Pozas et al. 2008). The chloride inward transporter NKCC1 is highly expressed in CRs which mantain the depolarizing effect of GABA due to the High Cl^- in the CR intracellular space. This NKCC1-dependent GABA action increases $p75^{NTR}$ expression in CRs which induces their death during early cortical development. These *in vitro* observations were later confirmed *in vivo* where the genetic deletaion of NKCC1 in mice induces a higher survival rate of CRs compared to control animals. In addition, as for PNs, it has been observed that CRs are rescued by the targeted elimination of pro-apoptotic Bax (Ledonne et al., 2016). The mechanisms involved in SPs elimination remain unclear. Recent study shown that SPs do not die but are passively dispersed into LVIb or adjacent white matter of the neocortex (Duque et al., 2016 ; Kostovic & Rakic 1980 ; Marx et al., 2017), contraddicting the classical assumption that SPs gradually disappear during early postnatal development (Price et al., 1997). Nowadays, it still unknown whether at least a fraction of SPs undergo PCD and wether the mechanisms are similar to the one alredy described for PNs.

1.2.4.2 Interneuron cell death

As already described for PNs, GABAergic IN cell death is a Bax/Bak dependent process that has a peak in the first two postnatal weeks. The portion of GABAergic INs that undergoes PCD is from 30% to 40% and it occurs later in the development compared to PNs (Southwell et al. 2012). Southwell et al., (2012) characterized the developmental cell death of cortical INs quantifying the expression of the apoptotic marker, cleaved caspase-3, marker for cellular apoptosis (**Figure 13**). They performed experiments in different conditions, *in vitro* and *in vivo,* quantifying the cleaved caspase-3 expression during the development from PN 1 to PN 15. They observed a peak in cell death *in vivo* around PN 7-11, and a declined towards zero by PN 15, evidence confirmed later *in vitro* where the 66% of cell death occurred between PN 11 and PN 15 (**Figure 13**). Southwell et al. (2012) demonstrated that, as for PNs, IN PCD is Bax/Bak dependent. They compared IN cell death between GAD67-GFP mouse with $Bax^{-/-}$;GAD67-GFP mutant, observing between PN 5 and PN 120, any decrease in cortical IN population in Bax KO

(**Figure 13**). Interestingly, they also demonstrated that Bax-dependent cell death uniformly occurred across the different subclasse of cortical INs observing similar proportions of GAD67-GFP neurons labeled by PV, SST, NPY, and calretinin in both wild type and Bax mutant mice. Moreover, to corroborate their findings, they also quantified IN PCD observed in a series of transplantation experiments. First, they transplanted IN progenitors coming from the MGE into postnatal neocortex and observed that transplanted IN death occurs at the same cellular age of endogenous INs, around PN 7-11. These data suggested that IN cell death is regulated by their proper intrinsic maturation state. To test if IN death was depending by a competition for extrinsic survival signals, they transplanted INs lacking TrkB, a neurotrophin receptor primarily expressed in the CNS. Interestingly, they observed similar rates of cell death providing a strong evidence that INs regulate their own numbers without influence from external simuli. Thus, they hypothesized that INs compete with endogenous neurons to survive. Therefore, they transplanted DsRed-expressing IN precursors into GAD67-GFP mice and observed an equal number of endogenous INs in both recipient and control hemispheres, suggesting a competition between endogenous and transplanted INs. Interestingly, recent studies observed that GABAergic IN survival, as well as PNs, is positively influenced by neuronal activity. In particular, a recent study performed *in vivo* investigated the molecular mechanisms involved in cortical IN survival mediated by PN activity (Wong et al 2018). They focused their attention on the serine-threonine kinase Akt, critical mediator of neuronal survival, and its antagonist, the phosphatase and tensin homolog PTEN. Interestingly, PTEN levels are very heterogeneous among MGE/POA INs and transiently elevated in INs in deep and superficial layers of S1 during the peak of IN cell death. In order to understand whether levels of PTEN during this period were correlated with IN cell death they injected PTEN inhibitor bpV(pic) at PN 7 and PN 8 in wild type mice observing that PTEN inhibition increased the density of MGE INs compared to control mice. Interestingly, when PTEN inhibitor injection was outside the range of time of IN PCD they observed no significant changes in PV and SST IN density compared to controls. These data revealed that PTEN is most likely required cell-autonomously for IN apoptosis during the normal period of IN cell death. Then, to test if PN activity has an impact on IN survival regulating the expression of PTEN levels they performed Designer receptor Exclusively Activated by Designer Drugs (DREADDs) experiments to increase the activation of PNs between PN 5 and PN 8. Then, they quantified PTEN levels in cortical INs at PN 8 observing a significant decreased in GABAergic INs as a consequence of PN activation.

All these evidences demonstrated that PN activity exerts a positive effect on IN survival in a cell-autonomously way (Wong et al 2018).

Moreover, it has been shown that Nkx2-1 INs receive a prominent but transient translaminar PN synaptic inputs during a crucial period in cortical development, suggesting the excitatory activity as a leading signal for GABAergic IN survival and integration in the network (Anastasiades et al. 2016). This communication and influence of PNs on IN survival and integration could be a mechanism to ensure a correct balance between excitatory and inhibitory neurons in the cerebral cortex.

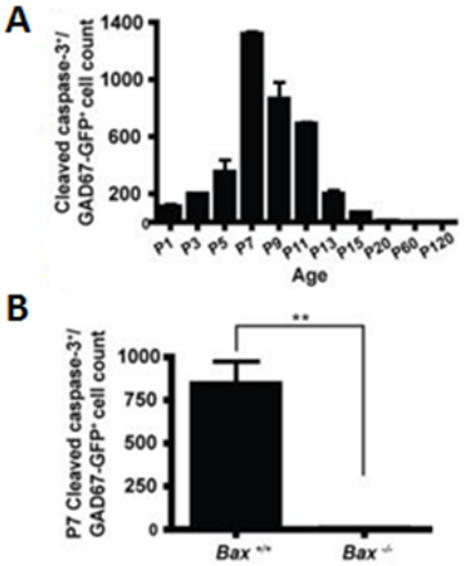

Figure 13. *Bax*-dependent PCD eliminates 40% of developing interneurons from the postnatal mouse neocortex. A. Temporal profile of cleaved caspase-3 expression in the neocortex of GAD67-GFP mice. Cleaved caspase-3 expression has a peak at P7, and decrease to nearly undetectable levels by P15. B. Cleaved caspase-3 expression detected in control and *Bax*$^{-/-}$ mice. (Adapted from Southwell et al., 2012)

1.2.4.3 Oligodendroglia cell death

Among the glial cells, just a small portion of astrocytes seems to undergo PCD while oligodendroglial and microglial cells are widely adjusted during cortical development.

The control of OPC number is a crucial step and has to be tightly regulated to ensure a correct number of OLs and myelination. Different models have been described about the regulation of OPC survival and death. One of the most recognized is based on the competition for survival factors during development (Barres et al., 1992). Experiments of genetic tracing revealed that cortical OPCs are generated and eliminated with specific spatio-temporal patterns, identifying three sequential waves in OPC productions (Kessaris et al., 2006). The first OPCs are almost completely eliminated at PN 10, when the OL production and myelination process have not started yet, and are mainly OPCs generated from the MGE and POA (Trapp et al., 1997, Kessaris et al., 2006) (**Figure 14**).

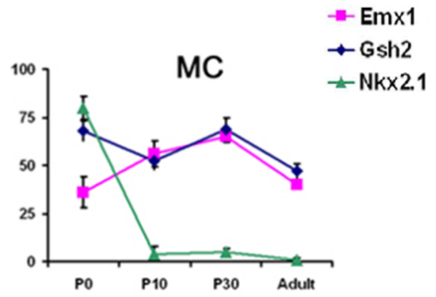

Figure 14. The embryonic Nkx2.1-derived OL lineage is rapidly eliminated during postnatal life. The proportional contributions of the three different populations (Emx1, Gsh2, Nkx2.1) of $Sox10^+$ OL lineage cells are presented as percentage of the total number of $Sox10^+$ cells in the examined regions (here rapresented the motor cortex). OLs/OLPs derived from Nkx2.1-expressing precursors are largely eliminated between birth and adulthood from most regions examined. (Adapted from Kessaris et al., 2006)

Moreover, Kessaris et al., (2006) showed that the first wave is replaced by OPCs produced in the second and third waves, suggesting that this cell population may play redundant functions since they are replaced with no drastic alterations. They also showed that the first wave of OPCs was rescued by the ablation of the two following one, corroborating the hypothesis of the competition for survival factors and suggesting firstOPCs as less performing than the others.

PDGFRα is one of the most mitogeneic factors, known to be involved also in promoting OPC survival. In addition, the OPC expression of Glutamate, GABA and ATP receptors (Bergles et al., 2000; Lin and Bergles, 2004; Hamilton et al., 2010) make OPCs sensitive to neurotransmitter release. Indeed, recent studies performed in organotipic cortical slice showed that endogenous GABA increase OPC cell death (Hamilton et al., 2017).

In addition to OPCs, OL also undergo PCD (Sun et al., 2018). A recent study showed that OL cell death is mediated by a Bax/Bak pathway (**Figure 15**). In particular, they showed that the transcription factor EB (TFEB) is highly expressed by differentiating OL, acting cell-autonomously through PUMA, pro-apoptotic factor which bind the anti-apoptotic Bcl-2 family members to induce Bax/Bak activation (**Figure 15**) with following mitochondrial dysfunction, caspase activation and finally OL PCD (Sun et al., 2018). Indeed, TFEB cKO exhibited an increase in OL number and ectopic myelination (**Figure 15**).

I will extensively describe oligodendroglia homeostasis in the following chapter.

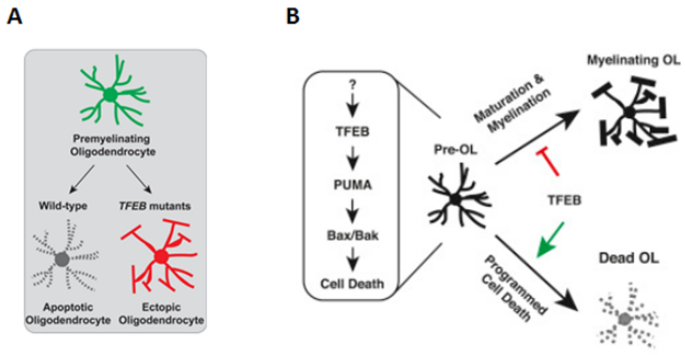

Figure 15. A. Transcription factor EB (TFEB) is highly expressed by differentiating oligodendrocytes (in green) and its genetic deletion causes precocious and ectopic myelination due to ectopic pre-OL survival during development in many parts of the murine brain. B. The TFEB-PUMA-Bax-Bak axis controls the location and timing of CNS myelination promoting PCD of a subset of premyelinating oligodendrocytes, allowing for the selective elimination of OL in normally unmyelinated brain regions. (Adapted from Sun et al., 2018)

2. OLIGODENDROGLIA

2.1 OPCs, historical background

Neuroglia description began far in the XIX century, when Rudolf Virchow, on 1846 published glia description as a connective tissue in the brain, spinal cord and higher sensory nerves which was impacting nervous elements (Somjen, 1988). During this period studies where based on simple observations using rudimental microscopes and draws to represent just the cell morphology with any functional related aspect. In this panorama, anatomists started to release description of different kind of cells like Theodor Schwann introducing the term "white substance" as myelin description (1839) or Henri Dutrochet, illustrating two major types of cells in the mollusk brain, later identified as neurons and glial cells (1824). Virchow was the first to use the term "neuroglia" or "Nervenkitt" in 1856, but the first detailed description of a glial cell type was given by Heinrich Müller in 1851.

Camillo Golgi in 1870 refined the description of glial cells provided by Müller using the "black reaction" (potassium dichromate and osmic acid fixation, followed by silver nitrate impregnation) technique which allows to randomly stain entirely neurons and glial cells with their processes. Finally, in 1889-1921, with the development of more sophisticated staining technique, was possible to differentiate glial cells in different population characterized by different morphology and properties: the stellate glia named Astrocytes, the OLs identified and named in 1921 by Pío del Río-Hortega who also identified the microglia (1919) (Andriezen, 1893; Fan and Agid, 2018).

In 1928, Del Río Hortega identified four subclasses of OLs, according to their morphology and location. He also identified the "dwarf astrocytes", a cell type sharing the size and shape of soma with OLs, but differing for their shorter extensions dichotomized at acute angles. This is considered one of the first descriptions of OPCs (Perez-Cerda et al., 2015). The "dwarf astrocytes", nowadays named as OPCs, showed intermediate properties between neuronal and glial cells, expressing Na^+ currents (INa^+) as neurons, but not discharging action potentials and expressing K^+ currents (IK^+) present in other glial cell types. These OL subclasses have been named in many different ways such as NG2 cells for the two associated antigens defined as nerve/glial (NG) antigens 1 and 2 (Wilson, 1981) or OPCs.

2.2 Oligodendroglia homeostasis

2.2.1 OPC proliferation

OPCs are the most abundant proliferating progenitors in the postnatal CNS. These cells remain proliferative throughout their lifespan, during development, in the adult and in response to myelin injury (Bergles and Richardson, 2015 ; Clarke et al., 2012; Kang et al., 2010; Ortiz et al., 2019). Differently from perinatal OPCs that generate OLs and astrocytes *in vivo* (Masahira et al., 2006; Zhu et al. 2008; Suzuki et al., 2017), postnatal OPCs generate only OLs, except in the piriform cortex in which it has been reported they also produce some neurons (Rivers et al., 2008 ; Guo et al., 2010). Despite their feature of being proliferating cells throughout their lifespan, it has been observed in the corpus callosum that the duration of their cell-cycle time (T_C) changes during development with a decrease with age, ∼3 days at PN 21 and ∼10 days at PN 60 (Young et al., 2013). Moreover, it has been shown a change in OPC proliferation rate according to different brain regions: OPCs in white matter have a higher proliferation and differentiation rate compared to those settled in the grey matter (Hughes et al., 2013; Moshrefi-Ravasdjani et al., 2017; Dimou et al., 2008). OPC proliferation rate can also change in the same region, according to environmental signals as a substantial turnover or as a consequence of an injury. These evidences point out an incredible heterogeneity. The control of OPC number is a crucial step and has to be tightly regulated to ensure a correct number of OLs and cortex myelination. There are different models described in literature about the regulation of OPC proliferation and survival. One example proposed is that OPC proliferation and survival is regulated by release of factors from neighboring cells. First, studies performed *in vitro* identified different proteins acting as survival factors: insulin like IGF-1 and IGF-2, neurotrophins (NT-3), ciliary neurotrophic factor (CNTF), leukemia inhibitory factor (LIF), interleukin 6 (IL-6) and finally, the PDGF (Barres et al., 1992). *In vivo* studies conducted specifically on IGF-I corroborate the in vitro evidences identifying IGF-1 and IGF-2 as stimulating survival and proliferation of oligodendrocyte progenitors (Barres et al., 1992 ; Beck et al., 1995)

PDGFα is the most characterized mitogenic and survival factor in OPCs, produced by astrocytes and neurons, which binds the PDGFRα on OPC surface (Noble et al., 1988; Richardson et al., 1988). It has been shown that PDGFα level, acting through different pathways, has an impact on both OPC proliferation and survival while inhibits their differentiation (Barres et al., 1993; Baron et al., 2005; Fernandez et al., 2000). Barres et al. (1992) showed that increasing PDGFα in the developing optic nerve decreases normal OL death by up to 90%. Another example

recently identified is the Fractalkine secreted from MGE-derived INs, which has been described to promote proliferation and differentiation of OPCs in culture and *in vivo* (Voronova et al., 2017).

It has also been shown that the activation of AKT1-mtor pathway in cerebellar granule induces the expression of secreted proteins like brain-derived neurotrophic factor (BDNF), Activin-A and fibroblast growth factor 1 (FGF1), having a role in promoting OPC proliferation and myelination (Goebbels et al., 2017). A second mechanism modulating proliferation and differentiation is mediated by neuronal activity as I will describe below, in the last paragraph of this chapter. A third mechanism is based on the overproduction of OPCs and then, the adjustment of their cell number during development by apoptosis as described above.

2.2.2 OPCs differentiation

In the CNS, once OPCs migrate and reach their final position, differentiation process starts and proceeds in a caudal to rostral gradient (Brody et al., 1987). OPCs are proliferating progenitors in the CNS producing myelinating OLs during development and also in the adulthood. First, irreversible "choice" in OPC development is whether to start the process of differentiation and become mature OLs or remain OPCs, increasing and maintaining the OPC pool in the adult brain. This decision depends on many different intrinsic factors, but it is also influenced by the environment, like their localization in grey or white matter or neuronal activity. OPCs undergo a series of steps before their differentiation into premyelinating and finally myelinating OLs. This extended proccess, which involves both activation of genes to promote differentiation and repression of genes that prevent differentiation, must be regulated in time and space.

Among the intrinsic factors that regulate OL development chromatin remodeling is a key process, occurring in two major ways, in order to modulate gene expression. Firstly, covalent modifications of histones such as deacetylation or acetylation to silence or activate genes, respectively. Secondly, ATP-dependent remodeling mediated by Switch/Sucrose Non-Fermentable (SWI/SNF) enzymes, such as Smarca4/Brg1, that modify the position of nucleosomes, increasing the accessibility of specific genes (He and Lu, 2013; Jacob, Lebrun-Julien, Suter, 2011). Casaccia and colleagues first established that histone deacetylation plays important roles for oligodendrocyte lineage progression (Marin-Husstege et al., 2002).

Regarding the extrinsic factors regulating OPC differentiation, Shh acts as a signal inducing histone deacetylation by histone deacetylases (HDACs) in order to repress the expression of genes that normally block OPC differentiation, allowing differentiation to proceed. Once the block is relieved, OL-specific transcription factors (Olig1 and Olig2) initiate the process of differentiation by binding enhancers of OL-specific genes and recruiting the SWI/SNF chromatin remodeling protein Smarca4/Brg1 (He and Lu, 2013 ; Jacob, Lebrun-Julien, Suter, 2011). Thus, Smarca4/Brg1 make transcription factors and other genes accessible, which may be required for OL differentiation.

In addition to Shh signal, it has been shown that OPCs start to differentiate when extracellular differentiation inhibitors are downregulated by the expression of microRNAs that prevent their transcription (Dugas et al., 2010; Zhao et al., 2010). For example, Dugas et al., (2010) identified some micro-RNA (miR) like miR-219, which directly repress the expression of PDGFRα, mitogenic factor known to induce OPC proliferation and survival and inhibiting their differentiation. In literature have been described many extracellular signals promoting or inhibiting OPC differentiation and among them we can list signaling molecules, growth factors, cytokines, neurotransmitters and metabolic signals (Wheeler and Fuss, 2016). As we already described in the previous paragraph, a crucial growth factor for OPCs development is PDGFα, a mitogen factor able to suppress the differentiation of cultured OPCs (Barres et al., 1993). Even though its inhibition effects on OPC differentiation is well known, the PDGFα downstream targets remained unclear for long time. Nowadays, it came out a study which identified Gab1 as a crucial regulator of OPC differentiation (Zhou et al.; 2020). This downstream target is downregulated by PDGFα stimulation and upregulated during OPC differentiation. Moreover, its specific ablation by conditional knockout mice induces a significant decrease of the 47% in OL density (positive to Olig2 and CC1, the latest mature OL marker) compared with control mice (Zhou et al., 2020).

In addition, as already described for OPC proliferation, it has been observed in experiments of transplantation that their differentiation rate change according to OPC localization: OPCs in white matter were more efficient progenitors than OPCs in the grey matter (Viganò et al., 2013). In addition, experiments of pulse-chase labeling with 5-ethynyl-2'-deoxyuridine (EDU, marker of cells in S phase of the cell cycle) using *PLPDsRed* mice after EDU injection, showed that the time spent by OPCs to differentiate in mature OL is ~ 3 days at PN 8 in both cortex and corpus callosum (Hill et al., 2014). This range of time increase with age (8 days observed

at PN 21). Moreover, another experiment showed that sensory deprivation reduces the survival of divided OPCs engaged in the process of differentiation (Hill et al., 2014). All these evidences suggest that OPCs start to be sensitive to micro-environmental signals which act in a specific period. Finally, regarding neuronal activity, it is now recognized that axons provide synaptic and extrasynaptic inputs to OPCs through numerous factors that converge, modulating the Ca^{2+} intracellular concentration. However, whether or how Ca^{2+} actually affects OPC and OL biology is relatively unclear. Interestingly, a study in our team performed in the somatosensory barrel cortex identified a peak of synaptic connectivity between PV INs and OPCs followed by a period of massive OPC differentiation during the second postnatal week (Orduz et al., 2015). Even though this evidence suggests this connectivity as promoting oligodendrogenesis, a later study in the team did not reveal any effect of impairing OPC GABAergic synaptic activity on OPC differentiation (Balia et al., 2017). Moreover, during OPC differentiation into OLs, it occurs a loss of synaptic transmission mediated by α-amino-3-hydroxy-5-methyl-4-isoxazolepropionic acid receptors (AMPARs) and a switch of $GABA_A$Rs signaling from synaptic to extrasynaptic (De Biase et al., 2010; Kukley et al., 2010; Vélez-Fort et al., 2010). Even if these evidences demonstrated that synaptic activity does not affect OPC differentiation like an on-off mechanism, there are many evidences in literature that neuronal activity has an important role in promoting oligodendrogenesis, probably through another kind of communication. For example a recent study observed an increase in the density of proliferating OPCs and mature OLs after chronic pharmacogenetics stimulation in both corpus callosum and somatosensory cortex neurons (Mitew et al*.,* 2018).

Another big question is whether neuronal activity could induce specifically OL production, enhancing OPC differentiation without prior cell division. A recent study seemed to support the hypothesis of a possible specific effect of neuronal activity on the differentiation process. It has been shown that mice performing a complex motor learning task (complex wheel running) rapidly increased the generation of pre-myelinating ($Enpp6^+$) OLs and only a small proportion of OPC differentiation was directly preceded by proliferation (McKenzie et al., 2014). Recently, Hughes and colleagues performed longitudinal two-photon *in vivo* imaging in the forelimb-region of motor cortex throughout learning and rehearsal of a skilled to study the effects of learning on the rate of oligodendrogenesis and remodeling of pre-existing myelin sheaths in healthy mice. The study revealed that learning transiently suppressed oligodendrogenesis but subsequently increased OL generation, OPC differentiation, and

retraction of pre-existing myelin sheaths (Bacmeister et al., 2020). Interestingly early studies conducted by Zonouzi et al. (2011) showed that AMPARs expressed in immature OPCs have a major permeability compared to OPCs in differentiation, corroborating the hypothesis of Ca^{2+} as responsible for the choice between proliferation and differentiation of OPCs. Nowadays, it is clear that regulation of intracellular Ca^{2+} affects many aspects of OPC development, involved in key stages of OPCs, OL formation and function. There are many candidate regulators of intracellular Ca^{2+} in OPCs, particularly in response to synaptic input from axons (Bergles et al. 2000, Gallo et al. 2008, Kukley et al. 2007, Mangin & Gallo 2011, Ziskin et al. 2007). In addition, OPCs express many ion channels that constitute possible sources of intracellular Ca^{2+} increase such as Voltage-Gated Ca^{2+} Channels (VGCCs), NMDARs, metabotropic Glutamate Receptors (mGLURs), GABA receptors (GABARs), Purinergic Receptors, Muscarinic Acetylcholine Receptors. Although it remains relatively unclear how changes in intracellular Ca^{2+} regulate key aspects of OPC and OL biology, insights are now beginning to emerge. Regarding OPC differentiation into OLs, it has been shown that Ca^{2+} signaling regulates the expression of the nuclear factor of activated T cells (NFAT), a target of Sox10, crucial to initiate OPC maturation in OLs (Bergles & Richardson 2015; Weider et al. 2018). In addition, it has been shown, in a model of demyelination after cuprizone treatment, that proliferating OPCs localized in demyelinated areas expressed high levels of Cav1.2 channels, suggesting that L-type Ca^{2+} entry might play a fundamental role in driving differentiation and/or regulating survival of newly generated OLs after demyelination (Paez et al. 2009).

In conclusion, all these studies on OPC proliferation and differentiation into mature OL reflect the complexity of these processes and their regulation. They bring into play a series of linked cellular transformation involving different pathways and mechanism from early development and throughout adult life.

2.2.3 OL lineage in myelination

The first definition of “myelin” was introduced by Virchow in 1858, and Penfield later identified the generation of myelin sheaths as one of the main role of mature OLs. Myelin

sheaths ensure the electrical isolation of axons allowing for the salutatory conduction of action potentials, which are propagated between nodes of Ranvier, increasing in the conduction velocity and metabolic efficiency (Nave, 2010). The nodes of Ranvier are axon segments enriched in Na^+ channels which allow the rapid propagation of action potentials from one node to another. In response to both intrinsic molecular cues and extracellular signals, OPCs are able to leave their mitotic stage and differentiate into myelin-producing OLs. It has long been well recognized that much of the regulation of OL behavior is intrinsic, involving mechanisms such as an internal "clock" that limits the number of OPC cell divisions, as observed in cell cultures lacking neurons (Temple et al., 1986). Regarding the extrinsic signals, we recognize axonal surface ligands, secreted molecules, and axonal activity. Many OL-specific or regulated genes crucial in regulating the myelination process has been identified through wide-based gene expression analysis such as DNA microarray. For example the myelin gene regulatory factor (MyRF) is expressed in the CNS only by postmitotic OLs at the end of the differentiation process. It has been shown that conditional inactivation of MyRF in the OL lineage blocks the process of differentiation at an early premyelinating stage, suggesting that this factor is crucial for the expression of myelin genes and the initiation of the myelination process (Cahoy et al., 2008). This was corroborated in later studies which forced expression of MyRF in OPCs, observing as a consequence a precocious expression of myelin proteins (Emery et al., 2009). The deficits seen after MyRF inactivation were similar to those observed after blocking Sox10 or Olig1 activity, suggesting a cooperation between the different transcription factors, each of them with a specific roles in OL differentiation and myelin gene expression. These findings demonstrate that the transition from an OPC into a myelinating OL requires the induction of promyelination factors, such as MyRF, in addition to the down-regulation of inhibitory factors that block OPC differentiation. Interestingly, although the role of neuronal activity in myelination is now widely recognized, it has been demonstrated that, once OPC differentiation ends, the initiation of the process does not require dynamic axonal signaling in culture. Indeed, a study *in vitro* demonstrated the ability of OLs to myelinate synthetic nanofibers over a diameter threshold of ~300 nm, suggesting that the diameter is an intrinsic signal which acts together with extrinsic factors to promote myelination (Lee et al., 2012).

Once OPC differentiation reaches the last steps, mature OLs undergo several morphological changes (process extension, lamellipodia formation) which allow OL to produce up to ~ 50

different myelinating processes (Hildebrand et al., 1993). Extrinsic factors, such as secreted molecules and neuronal activity, are crucial in this process as they act as important signals to drive mature OLs in axon selection and ensheathment. The roles of neuronal activity in driving the late stages of myelination such as the initiation of myelination and axonal ensheathment by myelin membranes have been demonstrated both *in vitro* and *in vivo*. In particular, recent studies have demonstrated that enhancing neuronal activity increases both OL production and OPC differentiation during development and adulthood (Gibson et al., 2014; Mitew et al., 2018). One of the first evidence for neuronal activity as a modulator of myelination process was provide by Demerens et al. (1996). They show that blocking axonal activity with TTX significantly reduced the formation of myelinated axonal segments. It has been suggested that a released axonal factor is able to instruct nearby OL processes to modulate the ensheathment. This idea is supported by a study demonstrating that active unmyelinated axons secrete neurotransmitters and neurotrophic factors extrasynaptically (Kukley, Capetillo-Zarate, Dietrich, 2007) which interact with pre-myelinating OLs expressing a huge diversity of receptors (Káradóttir and Attwell, 2007). A recent study conducted in zebrafish demonstrated that blocking synaptic vesicle release through tetanus toxin (Tent), impairs CNS myelination by reducing the number of myelin sheaths made by individual OLs during their short period of formation. They also found that stimulating neuronal activity increases myelin sheath formation by individual OLs (Mensch et al., 2015). Again in zebrafish, using *in vivo* time-lapse microscopy, it has been observed that the use of TTX to block neuronal activity was not preventing the myelin sheaths formation, but was just reducing the new formed myelinated axons (Hines et al., 2015). Interestingly, they also observed that neuronal activity was able to stabilize wrapping sheaths, observing a major stability in the active ones. All these evidences demonstrate that axon selection is biased by electrical activity**,** which also contributes to the maintenance of nascent sheaths (Hines et al. 2015).

It has been well described the existence of diverse forms of axo-glial communication alternative to synaptic transmission that could have an impact on mature OLs and myelination. Wake et al. (2015), in collaboration with our team, focused their attention on axon-glia communication to understand the mechanism controlling the OL preferential choice for active axons. They treated first half of Dorsal Root Ganglion neurons (DRGs) co-coltured with OPCs with Botulinum neurotoxin type A (BoNT/A), a blocker of vesicular release able to inhibit neurotransmitter release, for at least 4 weeks. Then, they introduced DRG neurons in the co-

colture with no treatment. The following quantification of the number of myelinated axons showed that, given a choice, OLs preferentially myelinated axons able to release vesicles. Moreover, they also demonstrated that axo-glia communication was mediated by non-synaptic contacts, observing Ca^{2+} transients evoked by the activation of extrasynaptic receptors for ATP and glutamate in OPCs lacking synaptic currents (Wake et al., 2015). Later, an *in vivo* study confirmed the bias choice of newly formed OLs for active axons (Mitew et al., 2018). Interestingly, recent studies performed *in vivo* focused their attention on the effect of Ca^{2+} activity observed in OLs on myelin formation. The aim was to understand whether different frequencies and amplitudes of Ca^{2+} events could impact axonal ensheathment. Baraban et al. (2018) confirmed these hypothesis by showing that both the increase in Ca^{2+} transient duration and amplitude were translated in a retraction, first of the sheaths and finally of the processes. Another study *in vivo* focused on the effect of Ca^{2+} activity on myelin and showed that myelin elongation was triggered by a specific level of Ca^{2+}, in between a minimum and a maximum value, limits beyond which they observed the opposite effect with a retraction of myelin sheaths (Krasnow et al., 2018; Batterfeld et al., 2019). All these evidences identify Ca^{2+} signaling as an intracellular pathway deeply involved in myelin biogenesis and modulating different steps in myelin formation (axon selection, sheet elongation and stability).

It has also been showed that the experience in young and adult mice can modify myelin strcutures. For example, social isolation of young adult mice results in myelin thinning in the prefrontal cortex, an important region for social function (Liu et al., 2012; Makinodan et al.,2012). Using a model of young adult mice forced in social isolation for 8 weeks, they then measured myelin thickness in electron microscopy (EM) images observing thinner myelin sheaths in isolated mice prefrontal cortex (PFC) compared to the controls (Liu et al., 2012). Notably, they demonstrated that the thinner myelin observed in isolated mice was associated with an immature nuclear chromatin present in myelinating OLs with a lower proportion of nuclear heterochromatin. As we already mentioned, histone deacetylation is required for OL differentiation and chromatin compaction, whereas high levels of histone acetylation are associated with impaired myelination and euchromatic nuclei. Together, these evidences suggest that myelin plasticity in the adult brain is influenced by prolonged social isolation which impairs OL differentiation and myelin formation through changes in nuclear heterochromatin. Another study showed that neuronal activity was regulating

oligodendrogenesis not only in juvenile but also in adult mice promoting oligodendrogenesis and improving motor sckills (Gibson et al., 2014). An important set of experiments conducted in Richardson lab has provided the first evidence that adaptive oligodendrogenesis contributes to learning task performances (McKenzie et al. 2014). Training mice to perform a complex motor task was found to induce OPC proliferation and oligodendrogenesis as we already mentioned before (McKenzie et al. 2014). Similar results were obtained through the optogenetic stimulation of neurons in the premotor cortex of adult mice, a cortical region involved in motor planning (Gibson et al., 2014). New OL production is necessary for acquisition of the complex motor task (Gibson et al., 2014; Xiao et al., 2016). These experiments illustrate a role for activity-regulated oligodendrogenesis in motor learning and underline the possible role that activity-regulated changes in myelin-forming cells could play in learning, indicating that ongoing myelination regulates aspects of learning in the adult CNS. Together, these data demonstrate that myelination is a fine-tuned process, tightly dependent on intrinsic factors, molecule release, neuronal activity and experience. Therefore, alterations in the network could impact this balance and lead to pathological conditions of the CNS.

2.3 Neuronal activity in OPC homeostasis

Nowadays several studies have significantly advanced our understanding, identifying important roles for neuronal activity in controlling oligodendroglial cell homeostasis and their capacity of producing myelin in both developing and mature CNS. It has been extensively described that OPCs are sensitive to neurotransmitter release, expressing different synaptic and extrasynaptic receptors such as ionotropic receptors for glutamate, GABA and ATP, all of them with a depolarizing effect (Bergles et al., 2000; Lin and Bergles, 2004; Hamilton et al., 2010) (**Figure 16**).

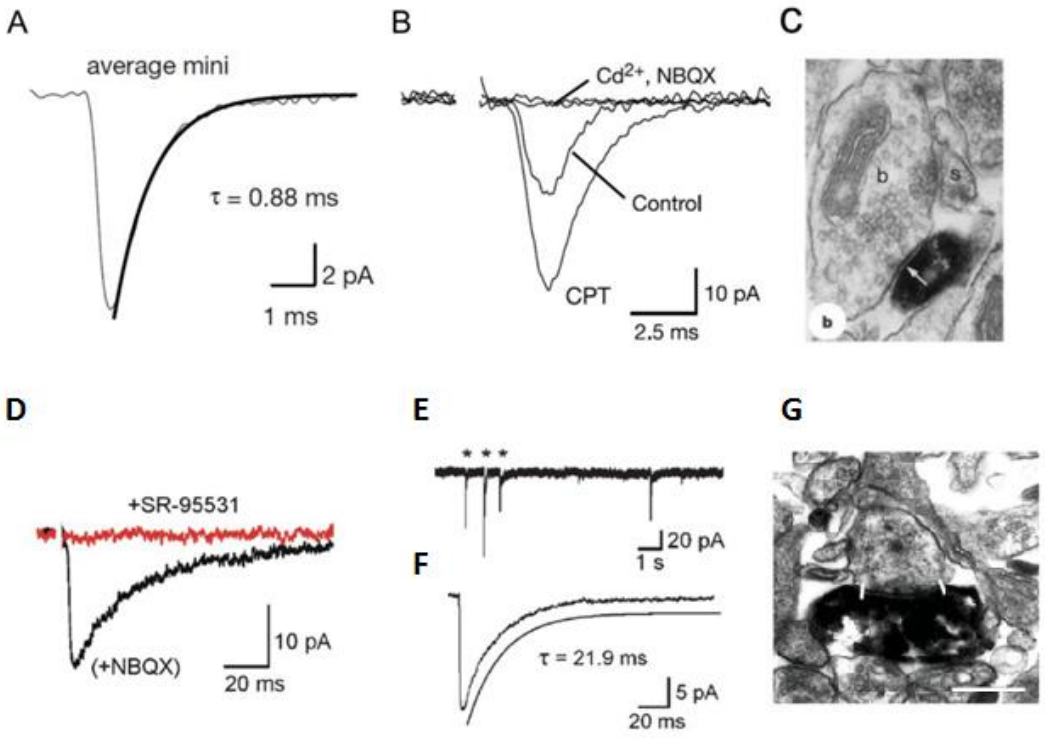

Figure 16. Glutamatergic and GABAergic synapses into hippocampal OPCs
A. Average of miniature synaptic events, triggered by pardaxin, a neurotoxin that enhances the frequency of vesicular release. The resulting current was fitted with a single exponential function. B. Plot of peak amplitudes of evoked responses in control and after 8-cyclopentyltheophylline (CPT, 1 mM) application. These responses were blocked by cadmium Cd2+ (CdCl2, 30 mM) or NBQX (5 mM). C. Electron micrograph of a neuron-OPC synaptic contact. In black, sections of a process (peroxidase reaction) from a physiologically identified, biocytin labelled OPC receiving a synapse (arrow) from a bouton (b) that also contacts a dendritic spine D. Stimulation of stratum radiatum afferences triggering an inward current in presence of NBQX. The current is blocked by SR95531 (gabazine), so GABAAR mediated E. Spontaneous inward currents in the presence of TTX (1 µM) and NBQX (5 µM). F. Average of miniature synaptic events obtained in the presence of TTX, NBQX and the secretagogue ruthenium red. G. Electron micrograph of a putative GABAergic synaptic junction. The postsynaptic terminal with pleomorphic vesicles, containing probably GABA, contacts an OPC (black, peroxidase reaction). Scale bar, 0.4 µm. (Adapted from Bergles et al., 2000 and Lin and Bergles, 2004).

In addition, OPCs can interact with signaling molecules secreted as a consequence of neuronal activity. Neurotransmitter release converges through different mechanisms that regulates OPCs and OLs intracellular Ca^{2+}, an ion well known to be involved in cell proliferation and exerting a pro-survival effect. It is thus a central candidate mediator of activity-driven oligodendroglia homeostasis.

OPCs express both Ca^{2+}-permeable and impermeable AMPARs. Glutamate release can increase OPC intracellular Ca^{2+} in two different ways: directly, through Ca^{2+}-permeable AMPARs, and indirectly through VGCCs expressed by OPC plasma membrane, activated after AMPAR-mediated Na^{+} influx depolarization (Fulton et al. 2010, Haberlandt et al. 2011). OPCs and OLs also express NMDARs, with several studies indicating that glutamate can activate

NMDAR-mediated Ca^{2+} influx in both OPCs and mature OLs (Karadottir & Attwell 2007; Karadottir et al., 2005). In particular, it has been recently shown from Spitzer et colleagues (2019) that a NMDAR-mediated current may be restricted to non-proliferative OPCs in a quiescent state, just before their differentiation into OLs. In addition to ionotropic glutamate receptors, OPCs highly express mGluRs. These receptors activates phospholipase C (PLC) and inositol 1,4,5-trisphosphate (IP3) production and thus drives Ca^{2+} efflux from the endoplasmic reticulum (ER), a major mechanism by which the intracellular levels of $Ca^{2+}$are regulated. Additionally, mGluRs are also known to increase the expression of Ca^{2+}-permeable AMPARs in OPCs (Zonouzi et al. 2011). On the contrary, mGluRs are found in a lesser extent in mature OLs (Luyt et al. 2003, 2006).

Regarding GABA, this neurotransmitter acts by binding two different types of receptors: the ionotropic $GABA_A$ and $GABA_C$ receptors and the metabotropic $GABA_B$ receptors. OPCs express $GABA_A$Rs (Von Blankenfeld et al. 1991, Williamson et al. 1998) and, in contrast to its inhibitory effect on mature neurons, GABA has a depolarizing effect on OPCs since the Cl^- reversal potential of OPCs is approximately −40 mV (Lin & Bergles 2003). This depolarization may also activate VGCCs causing a subsequent OPC intracellular Ca^{2+} increase (Haberlandt et al. 2011, Tanaka et al. 2009, Vélez-Fort et al. 2010). How $GABA_B$ affects OPCs or OLs *in vivo* is still unknown.

ATP is released in an activity-driven manner from axons (Hamilton et al. 2010). Hamilton et al. (2010), through Ca^{2+} imaging in the isolated optic nerves, demonstrated that ATP can induce Ca^{2+} influx in OPCs by the activation of either P2X7 receptors which are ligand-gated, non-selective Ca^{2+} channels, or P2Y1 receptors, metabotropic receptors linked to G protein activation and IP3-dependent Ca^{2+} release from internal stores (Hamilton et al. 2010). In addition, OPCs express VGCCs, inducing a Ca^{2+} influx. There are evidence for an expression of different isoforms such as L-type (Cav1.2, 1.3) and T-type (Cav3.1, 3.2) VGCCs (Haberlandt et al. 2011, Zhang et al. 2014), highly expressed in OPCs, but rapidly downregulated as these progenitors differentiate into OLs (Larson et al., 2015; Zhang et al., 2014).

All these evidences suggest that neuronal activity can regulate cortical oligodendrogenesis through many different paths which converge in intracellular Ca^{2+} increases (Goebbels et al., 2017; Karadottir and Kuo, 2018; Maldonado et al., 2013). Several recent studies confirmed early studies performed by Barres and Raff (1993), observing that neuronal activity manipulation have an impact on oligodendroglia proliferation and differentiation in

multiple CNS regions during the development (Mangin et al., 2012; Gibson et al., 2014; Mitew et al. 2018). Regarding glutamate effect on OPC proliferation, Gallo et al. (1996) demonstrated that activating glutamatergic signaling via AMPA/kainate receptors inhibits OPC proliferation in culture. Next, an *ex vivo* study in organotypic cerebellar slice cultures goes in the same direction (Fannon et al. 2015). Similarly, early sensory deprivation of mouse barrel cortex by whisker removal results in a decrease of glutamate release, increasing the proliferation of $NG2^+$ OPCs at PN 6. This suggests that glutamatergic signaling from thalamocortical axons acts to inhibit proliferation *in vivo* (Mangin et al. 2012). On the contrary, it has been observed that electrical and optogenetic stimulation of PNs in rat and mouse motor and premotor cortex induces OPC proliferation respectively in the cerebrospinal tract and in the premotor pathway (Li et al., 2010; Gibson et al., 2014). In addition, as I already discussed before, Barres and Raff (1993) observed that OPC division was largely promote by axon activity in the optic nerve. All these data cited above are confusing but the experiments are not specifically targeting AMPAR-mediated synaptic activity on OPCs. They probably, involved indirect effects mediated by neurons. Furthermore, recent studies focused their attention on the effect of AMPAR subunit manipulation of OPCs on proliferation. For example, Chen et al. (2018) modified the properties of GluA2 subunit in OPC AMPAR in the corpus callosum during the second and the third postnatal week, a crucial period for OPC proliferation and differentiation. In particular, they performed three different manipulations: the replacement in the GluA2(R583Q)-GFP subunit (Ca^{2+}-permeable) of an arginine(R)583 with glutamine(Q) (Hume et al., 1991), to create exclusively Ca^{2+}-permeable AMPARs; expression of the GluA2(R583E)-GFP subunit (pore-dead), the reduction of the number of functional GluA2-containing AMPARs by replacing arginine(R)583 with glutamic acid(E) (Dingledine et al., 1992, Shi et al., 2001) and, finally, the overexpression of the cytoplasmic C-terminal (GluA2(813-862)) of GluA2 (C-tail), which mediates trafficking of receptors to the membrane and interactions with other proteins within the AMPAR complex (Henley, 2003). The two first manipulations of AMPARs in OPCs induced a large increase in EDU^+ OPCs and reduced the differentiation of OPCs into OLs. In contrast, the expression of the C-tail did not alter OPC proliferation but had a negative effect on the differentiation, decreasing the number of OLs (Chen et al., 2018). This effect could be due to the increase in AMPAR Ca^{2+} permeability. The entry of this ion indeed induces a continue cycling of immature OPCs as already described from precedent studies (Zonouzi et al., 2011). However, another recent study based on conditional knockout of different AMPAR

subunits in OPCs demonstrated that the synaptic activity of glutamate on OPCs and early OLs have an impact on survival and myelination but does not affect OPC proliferation (Kougioumtzidou et al., 2017). In particular, they observed that the double KO for the GluA 2/3 and the triple KO for GluA 2/3/4 subunits have a negative impact on pre-myelinating OL but not on OPCs, reducing the OL accumulation with a consequent decrease in myelination. These data, resulting from the subunit elimination from the onset of mouse development, are contradictory compared with the manipulation of AMPAR signaling in OPCs performed by Chen and colleagues (Chen et al., 2018).

ATP is another described potent regulator of survival, proliferation, and differentiation of oligodendroglial population. It has been shown to stimulate astrocyte proliferation and differentiation, contributing to the process of reactive astrogliosis. Moreover, ATP has been recently described to induce proliferation of neural stem cells. Recent studies investigated the effect of ATP and ADP in purified OPC cultures demonstrating a marginal change in proliferation (14 ± 0.9% and 12 ± 0.6% increase over control cultures, respectively) and a significant increase of cells expressing galactocerebroside (O1), a marker of differentiated OLs (80% compared to the controls) (Agresti et al., 2005).

As for glutamate, the role of GABA on OPC proliferation is no clear and still under intense investigation. A recent study based on OPC γ2-$GABA_AR$ deletion, subunit crucial for the synaptic signaling between PV INs and OPCs (Balia et al., 2015; Orduz et al., 2015), brought more evidences about the effect of GABA on OPC development. In the somatosensory cortex, there is a high synaptic IN-OPC connectivity during the second postnatal week (Orduz et al., 2015; Vélez-Fort et al., 2010), followed by a critical period for OPC proliferation and differentiation (Hill et al., 2014; Orduz et al., 2015). Balia et al. (2017) examined the impact of γ2-$GABA_AR$ inactivation on OPC development, observing no changes in cell densities at PN 10 and PN 13. These results suggested that γ2-$GABA_AR$ deletion, postsynaptic subunit, does not affect oligodendroglia proliferation and differentiation (Balia et al., 2017). On the contrary, recent studies demonstrated that endogenous GABA, acting through $GABA_AR$, suppresses OPC proliferation, reduces the number of mature OLs and increases cell death (Hamilton et al., 2017). In particular, they observed that the application of SR 95531 (GABAzine), $GABA_AR$ antagonist, on organotypic brain slices of mice expressing GFP in OL lineage induces an increase of OPCs (~48%) and mature OL (~73%). Interestingly, GABAzine application increases not only the proliferation but also the survival of OPCs, suggesting that GABA endogenous

release promotes cell death. In addition, they also focused their attention on the effect of GABA on myelination. They observed that the application of GABAzine induced a 42±19% increase of fluorescence of the myelin basic protein (MBP), suggesting that GABA is a negative modulator of myelin formation. On the contrary endogenous GABA release was able to increase the internode length (Hamilton et al., 2017). However, in another experimental paradigm it has been observed that, decreasing $GABA_AR$ activity increases OPC proliferation and reduces OL differentiation (Zonouzi et al. 2015). They investigated whether manipulation of GABAergic transmission *in vivo* could alter the proliferation and differentiation of NG2-cells.

All these studies point out the complexity and the several mechanisms through which neuronal activity can impact and modulate oligodendroglia homeostasis. It is this thus of crucial importance proceed step by step in the study of a so complex mechanism, using different approaches and manipulations to finally aquire more knowledges on the regulation of oligodendroglia homeostasis by neuronal activity.

3 IN – OPCs COMMUNICATION: Common embryonic origin, life and death

3.1 GABA signaling in OPC

3.1.1 Synaptic and Extrasynaptic $GABA_AR$ in OPCs

It is now well recognized the presence of a huge diversity of ionotropic and metabotropic GABA receptors expressed in oligodendroglia (**Figure 17**). A first evidence of $GABA_AR$ expression is dated back on 1984 when wholecell patch clamp recordings identified a depolarizing GABA current in cultured OLs (Gilbert, Kettenmann and Schachner, 1984). Differently from neurons, in which the effect of GABA during postnatal development, in OPCs the neurotransmitter has always a depolarizing effect with a chloride reversal potential of OPCs is approximately −40 mV (Lin & Bergles, 2004; Zonouzi et al., 2015). Some years later, Von Blankenfeld demonstrated (1991) that the amplitude of GABA-evoked current was 10 fold bigger in OPCs than in OLs, suggesting a decrease in the expression with the differentiation, resulting in a lower density of GABARs in OLs (**Figure 17**) (Von Blankenfeld et al., 1991).

The first evidence of GABAergic synaptic input on OPCs was demonstrated from Lin and Bergles in 2004 (**Figure 16**), observing a $GABA_AR$ mediated synaptic currents in hippocampal OPCs. Today, the presence of $GABA_ARs$ is confirmed in many CNS regions such as the hippocampus, neocortex, and cerebellum as the existence of synaptic inputs between GABAergic neurons and OPCs (Tanaka et al., 2009; Velez-Fort et al., 2012; Maldonado & Angulo, 2015). It has been recently shown that synaptic contacts are transient, lost during postnatal development in the somatosensory cortex and cerebellum (Vélez-Fort et al., 2010; Zonouzi et al., 2015) (**Figure 17**). Despite the loss of synaptic transmission during development, it is possible to observe an extrasynaptic response mediated by GABA spillover from nearby INs (Vélez-Fort et al., 2010; Balia et al., 2015). In order to characterize the subunit composition in OPCs $GABA_ARs$, studies in our team performed experiments of single cell RT-PCR combined with pharmacology. Interestingly, a huge diversity in subunit composition was identified in OPCs.

$GABA_ARs$ have a heteropentameric structure composed by the association of 19 subunits (α1–6, β1–3, γ1–3, δ, ε, θ, π, and ρ1–3.). The molecular heterogeneity of $GABA_AR$ composition mediate two distinct forms of inhibitory transmission, synaptic or extrasynaptic which mediate phasic and tonic inhibition, respectively. Receptors containing γ2 subunit in

association with α1, α2 or α3, mostly mediate phasic synaptic inhibition, while the subunits α4, α5 or α6 are predominantly or exclusively found in extrasynaptic receptors, more likely mediating tonic inhibition. The different association in subunits is also related with receptor localization and pharmacology. In the CNS, $GABA_A$Rs are mostly formed by the association of αβγ subunits with a stoichiometry of two α, two β, and one γ subunits. Synaptic $GABA_A$Rs of OPCs in the somatosensory cortex contain mainly α1, α5, and γ2 subunits, although they may also contain γ1 and γ3 (Balia et al., 2015). Interestingly, Balia et al., (2015) found a transient expression of γ2 subunits in OPCs, that was high during the second postnatal week and then undergo a downregulation, followed by a switch from synaptic to extrasynaptic GABAergic transmission (Balia et al., 2015; Passlick & al. 2013). Indeed, γ2 subunit is found just in few exptrasynaptic $GABA_A$Rs. In mature OLs, functional genomic analyses showed a high expression of α1, α3, and γ1, along with low levels of γ2 subunits (Cahoy et al., 2008; Zhang et al., 2014; Arellano et al., 2015). All these evidences support a reorganization of $GABA_A$Rs expression and communication in OL lineage that might depend on the different functions of these cells at different developmental stages. Oligodendroglia expresses also the metabotropic $GABA_B$Rs that promote OPC migration *in vitro* and, as demonstrated for $GABA_A$Rs, they are downregulated during the OPC differentiation (Luyt et al. 2007). The effect of $GABA_B$Rs on OPCs or OLs *in vivo* remains to be demonstrated.

It is clear that GABARs play an important role in OPC and OL biology, but the way in which GABAR signals are transduced into functions is poorly understood. In addition, the composition and expression of GABAR changes at different developmental stages, suggesting different roles in oligodendroglia according to specific maturation stages. Therefore, deciphering the stage and context-specific roles of GABA and the downstream signaling pathways in regulating the OL lineage remains an important challenge in the field.

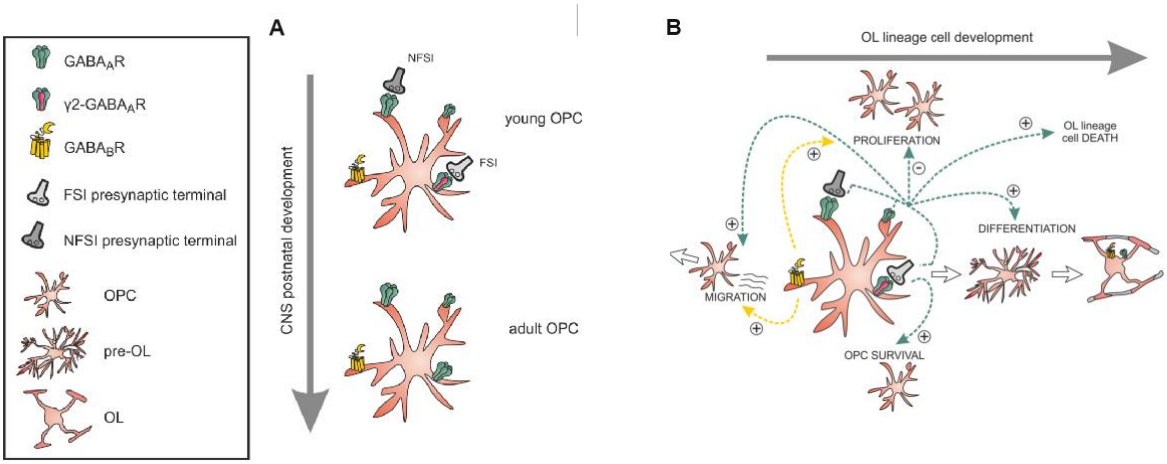

Figure 17. Roles of GABA signaling in neuronal-oligodendroglia communication. A. Changes of GABA receptor expression during CNS development. GABAergic synaptic communication and OPCs is mediated by distinct types of GABAARs. The subunit composition of GABAARs change according to the identity of the presynaptic interneuron. Only two types of presynaptic interneurons have been identified so far: fast-spiking PV interneurons (FSI) and non-fast spiking interneurons (NFSI). These GABAergic synapses are present at early postnatal stages, with a decrease in the expression during development. A switch from a synaptic to an extrasynaptic communication occurs in concomitance with the loss of γ2 subunits. B. Different roles of GABA signaling. Open arrows show the lineage progression from OPCs to myelinating OLs. Dash arrows indicate a controversial role or a role that needs to be confirmed. In most cases, it is not possible to discriminate whether GABAAR-mediated roles are synaptic or extrasynaptic. (Adapted from Habermacher, Angulo and Benamer, 2019)

3.1.2 Synaptic and Extrasynaptic GABAergic transmission of OPCs

Presynaptic GABA release in the synaptic cleft induces first the activation of synaptic receptor. Then, neuronal and glial GABA transporters (GATs) rapidly remove the excess of GABA, allowing the restoration of conditions for another transmission event. However, different signalling mechanisms mediated by neurotransmitters over this classic framework has been described. For example, GABA can diffuse in the extracellular compartment and activates receptors just outside the synaptic cleft (within 100–200 nm). The different mechanisms could involve peri-and/or presynaptic receptors and extrasynaptic receptors, as, for example, metabotropic receptors which can be expressed peri- and postsynaptically (Baude et al 1993, Mateos et al 2000). When a prolonged neuronal activity occurs, GABA reaches high concentrations diffusing to significant distances (of the order of 0.5 µm) before activating its target. This phenomenon is named 'spillover'. Since the EC_{50} of extrasynaptic receptors is lower compared to the synaptic ones, their activation in presence of lower concentrations of GABA neurotransmitter is possible. The “typical” spillover, in which neurotransmitter release from the presynaptic terminal diffuses to activate receptors at neighbouring synapses of the

same type and extrasynaptic receptors on the pre- or postsynaptic cell, is defined as intersynaptic spillover (DiGregorio et al., 2002). The heterosynaptic spillover, instead, involves spillover to neighboring cells that are neither pre- nor postsynaptic to the neurotransmitter synaptic source.

The classic volume transmission involves neuromodulators released from specialised axonal varicosities. The neuromodulators then diffuse over relatively large distances (of the order of 1 µm through the extracellular space), activating uniformly-distributed high-affinity receptors (Fuxe and Agnati, 1991). This type of communciation has been observed in glial cells, but not specifically in OLs (Angulo et al., 2008). This small amount of GABA observed in spillover events, from nanomolar to few micromolar, is able to sustain the activation of extrasynaptic $GABA_A$Rs that result in a continuous opened conductance. This specific mode of extrasynaptic $GABA_A$Rs activation is called tonic inhibition (Farrant and Nusser, 2005). Tonic inhibition can be considered to be a mixture of intersynaptic spillover (because of its partially-synaptic source) and volume transmission (because of its regional characteristics and possibly non-synaptic source). Finally another kind of communication, known as ectopic release , is mediated by vesicles directly fused with the plasma membrane outside synaptic zones (Kukley et al., 2007 ; Ziskin et al., 2007 ; Matsui and Jahr, 2003). It liberates neurotransmitter directly on opposite sufficient receptor densities to elicit detectable miniature excitatory postsynaptic currents EPSCs (mEPSCs).

In Oligodendroglial cells, it has been observed the presence of both, synaptic and extrasynaptic transmission, usually related with a specific developmental stage (Lin & Bergles, 2004). Our team identified a transient synaptic connectivity mediated by receptors containing the γ2 subunit (Vélez-Fort et al., 2010; Balia et al., 2015). In particular, Vélez-Fort et al., observed synaptic currents, characterized by their fast rise time, recorded in OPCs during the first days after birth (PN 3-PN 14). They repeated the same experiment in the fourth PN week, and observed a strong decrease in synaptic activity. Finally, to test whether this decrease was depending on a loss in synaptic contacts, they analyzed the miniature events after the application of Na^+ channel blocker TTX, AMPA/kainate antagonist NBQX, and the NMDA antagonist D-AP-5. Miniature synaptic events were detected in the second postnatal week while they almost completely disappeared at the fourth postnatal week. All these evidences showed a strong reduction of GABAergic synaptic activity after the second postnatal week.

In another study conducted by Mangin and colleagues (2008), it was observed that close OPCs and INs were more likely to exhibit synchronized EPSCs compared with INs separated by >200 µm. The finding that OPCs are sensing patterns of activity arising in closely associated neurons suggests that OPCs cell function is finely regulated by the local network.

3.2 Interneuron-OPC communication: effects on OPC function

3.2.1 Interneuron-OPC connectivity

Regarding the identity of the GABAergic neurons synaptically connected to OPCs, many questions have to be solved to understand the impact of IN-OPC communication in the development and stability of cortical networks (Lin and Bergles, 2004; Kukley et al., 2008; Mangin et al., 2008). Tanaka et al., (2009) were the first to reported putative synaptic contacts between PV INs and OPCs by immunostaining. They colabeled GABAergic synapse markers, vesicular GABA transporter (VGAT) and gephyrin, with PV, to identify contacts between PV GABAergic INs and OPCs. This potential connectivity was confirmed by study in our team using paired recordings, which allowed us to identify a preferential and functional PV INs and OPC connectivity in the somatosensory cortex (Orduz et al., 2015). Interestingly, the postsynaptic receptors of these synapses comprised γ2 subunits (Orduz et al., 2015). On the contrary, same experiments using paired recordings showed a poor connectivity between non-fast-spiking interneurons (NFSIs) and OPCs, and these synapses lack $GABA_A$Rs with γ2 subunits. We already described the common embryonic origin for cortical INs derived from the MGE and POA (PV and SST) and the firstOPCs from the first wave (Flames et al., 2007; Kessaris et al., 2006). It would thus be possible that this common origin and their preferential connectivity have a crucial role in the inhibitory networks during cortical development. Indeed, a close relationship between MGE-derived INs and OPCs is already known since these INs secrete fractalkine and other factors that promote cortical OPC differentiation (Voronova et al., 2017).

3.2.2 IN-OPC communication in OPC functions

OPCs are the only non-neuronal cell population in the CNS that form bona fide synapses with neurons, including GABAergic INs. The most fascinating question that is still unsolved is the functional role of the synaptic connectivity between GABAergic INs and OPCs. The consequences of $GABA_AR$ activation on OPC development and function have been extensively studied but the results are still controversial.

My team recently explored the function of these synapses by genetically silencing γ2-$GABA_AR$ in OPCs during that critical period of cortical oligodendrogenesis. No changes in cell densities were found at PN 10 and PN 13. These results suggested that γ2 deletion, a crucial subunit for synaptic transmission, does not affect oligodendroglia proliferation and differentiation (Balia et al., 2017). We can conclude that at least γ2-$GABA_AR$-mediated synapses do not play a role in these processes during development. However, other studies demonstrated that endogenous GABA, acting through $GABA_AR$, suppresses OPC proliferation, reduces the number of mature OLs and increases cell death (Hamilton et al., 2017). In addition, they observed that GABA was a negative modulator of myelin formation while increasing the internode length (Hamilton et al., 2017). A precedent study performed in a perinatal hypoxia condition showed that the loss of synaptic activity in OPCs was correlated with an increase in OPC proliferation and a delay in the differentiation and myelination (Zonouzi et al., 2015). In particular, the intraperitoneal injection of the GABA antagonist bicuculline increased by three-fold the number of proliferating OPCs and reduced by half the number of mature OLs. They also tested the opposite condition, increasing the GABA availability by administrating of GAT-1 inhibitors and, as expected, they observed an increase in the number of mature OLs in both conditions, normoxic and hypoxic animals. The authors concluded that $GABA_AR$-mediated depolarization induces the maturation of OPCs *in vivo*. They reproduced and confirmed the progression from OPCs into mature OLs by the specific deletion of the NKCC1. In this model, they observed impairment in OPCs differentiation, as they previously revealed during hypoxia, suggesting that GABAergic synapses inhibit proliferation and promote OPC differentiation (Zonouzi et al., 2015). However, none of these two last studies directly targeted the synapses and thus they do not constitute a direct proof of the implication of GABAergic synapses in the dynamics of OPC proliferation and differentiation. Nevertheless, they strongly reveal an intimate relationship between these two cell populations.

Finally, Tong et al. (2009) proposed that $GABA_A$Rs activation is involved in OPC migration via the activation of Na^+/Ca^{2+} exchangers type 1 rather than in OPC proliferation. However, this result has not been confirmed yet *in vivo*. Regarding the myelination process, the role of GABARs is still not well understood. Stedehouder et al. (2018) performed chemogenetic experiments in order to specific stimulate a subset of PV INs. They observed that their activation modified the morphology and myelination of PV^+ axons without any change in OL cell density and total myelin, suggesting a potential role for GABA in the modulation of PV^+ axons myelination. We could hypothesize a role in this process for PV IN-OPC synapses, known to be mediated by γ2-$GABA_A$Rs (Benamer et al., 2020).

All these evidences support the idea that INs and OPCs are close partners during cortical development. This restricted transient synaptic connectivity between GABAergic INs and OPCs, characterized by a sophisticated spatial organization, occurs in a specific temporal window of massive PCD of both cortical INs and OPCs. Moreover, this period seems to be of crucial importance for cortical oligodendrogenesis, since followed by a massive differentiation of OPCs into OLs one week later. The convergence in the embryonic origin of INs and firstOPC, their death and their highly regulated transient IN-OPC connectivity suggests possible interactions between these two cell types that might participate to cortical construction. In my work, we rescued ~40% of embryonically related MGE- and POA-derived INs and firstOPCs committed to die by genetically imparing PCD. Our idea was to analyse the impact of the disruption of this tightly regulated balance on cortical networks and oligodendroglia development.

3.2.3 Interneuron myelination

Many studies on myelin focused their attention on long-range projection neurons because of its function to speed up the conduction of action potentials. For example, it has been shown that PN myelination followed precise patterns, having distinct profiles of distribution, proper of each cortical layer (Tomassy et al., 2014). In particular, layer II/III PNs display an intermittent pattern of myelination (Tomassy et al., 2014). However, myelination of short-range GABAergic basket cells was also early revealed by EM studies showing that local axons collaterals of inhibitory neurons can also be myelinated (Fairén et al. 1977; De Felipe et al., 1986; Somogyi and Soltész, 1986). Nevertheless, compared to PNs, which have been

extensively investigated, little is known about GABAergic IN myelination. A recent study based on array tomography showed that a large fraction of myelinated axons in the cortex contains neurotransmitter GABA. In addition, immunostaining revealed that they were PV^+ neurons (Micheva et al., 2016; Stedehouder et al., 2017). Moreover, Micheva et al. (2016) observed a particular myelin protein composition in GABA containing axons. Comparing PLP and MBP proteins in segments of the same thickness, they found that GABA myelinated axons had 20% higher MBP immunofluorescence compared to the excitatory ones, while PLP had no significant changes. Inhibitory neurons, particularly PV INs, are indeed involved in many local microcircuits and fine-tune and modulate cortical networks by using FFI and FBI as we previously described. The continue investigation of PV IN myelination patterns and its functional consequence is therefore of crucial importance in the understanding of cortical network behavior. As previously described for excitatory neurons, also PV IN myelination is tightly enhanced by neuronal activity. Stedehouder et al. (2018) used cell specific DREADD to selectively activate PV INs and consequently analyze cell myelin structure of these neurons. They observed that the stimulation was able to induce an increase of the ~ 50% in axonal length with a proportional increase in myelination (Stedehouder et al., 2018). In this study, the authors demonstrated a novel form of activity-dependent myelination mediated by axonal morphological plasticity of PV INs. It has been thought that IN myelination and plasticity ensure the integrity of precisely timed action potentials and support their local synchronization, necessary in the generation of high-frequency oscillations. Indeed PV INs have implication in gamma oscillation, rhythmic fluctuations in local field potentials (LFPs) (~25–100 Hz) involved in higher-order brain functions like selective attention and operational memory (Colgin et al., 2009; Colgin and Moser, 2010). It has been shown that PV INs, through their phasic synaptic inhibition of large PNs, are essential for the production of synchronized network oscillations. Given this critical PV IN role in mediating gamma oscillations, their myelination could be of crucial importance by playing a role in firing synchronization and metabolic support. Indeed, the impairment of gamma oscillations mediated by PV INs is known to be involved in many cognitive disorder (Mably and Colgin, 2018). Moreover, recent studies identified global myelination abnormalities in schizophrenia patients. It has been shown from diffusion tensor imaging studies that drug naïve patients had defects in myelination from the first psychotic episodes (Mandl et al., 2013) and later during the disease development. With the increase of studies focused on PV IN myelination and the implication

of these neurons in gamma oscillations, it has been proposed a a potential contribution of PV IN myelination defects in schizophrenia etiology (Stedehouder and Kushner 2017). Myelin disruption could indeed impair action potential fidelity, cause energy deficits during high demanding cognitive activities or induce the occurrence of ectopic action potentials. In turn, these defects would disrupt inhibitory network function, having an impact on long range thalamocortical and cortico-striatal circuits involved in schizophrenia.

3.3 Embrionically related partners

As we already described before, the majority of INs arise from the MGE and POA (60% and the 10%, respectively) around E10.5 from progenitors expressing the transcription factor Nkx2.1. The MGE give rise to INs expressing PV and SST, two non-overlapping markers that identifies distinct IN populations with particular electrophysiological properties and morphological profiles (Lim et al., 2018). The POA, instead, covers a very heterogeneous population including mainly PV, SST and reelin cells (Gelman et al., 2009). Fate mapping and migration studies revealed that MGE progenitors move from the subpallium and reach the cortex through a tangential migration (Wamsley and Fishell, 2017).

Regarding OPC embryonic development, cre-lox fate mapping studies in mice showed that OPCs are generated in three different sequential waves. Interestingly, the first wave of OPCs is generated around the E12.5 from progenitors settled, as well as for the majority of INs, in the MGE and the POA, expressing respectively Nkx2.1 and Dbx1 transcription factors (Kessaris et al., 2006; Gelman et al., 2011). Moreover, OPCs reach their final position following the same migratory routes of INs, from the subpallium to the dorsal pallium around E14.5. All these evidences identify a common embryonic origin for MGE- and POA-derived INs and firstOPCs, suggesting a cross talk and a specific relationship between these two cell populations. In line with this hypothesis, experiment of lineage tracing showed that progenitors expressing NG2 and Olig2, specific markers for oligodendroglia lineage, generate INs in deep layers of the dorsal cerebral cortex (Tsoa et al., 2014). Besides this common embryonic origin, INs coming from the MGE and POA and OPCs maintain close relationships during the first postnatal days and throughout cortical development. For instance, it has been shown that INs release paracrine factors promoting proliferation and differentiation of OPCs (Voronova et al., 2017). One of the main features of OPCs is that they are the only non-neuronal cell type in the CNS

receiving functional synaptic inputs from neurons (Lin et al., 2004). Moreover, a transient peak of synaptic connectivity between GABAergic INs and OPCs of the somatosensory cortex has been described at PN 10, an age preceded by PCD and followed by massive OL differentiation (Kessaris et al., 2006, Orduz et al., 2015, Southwell et al., 2012). The team also recently demonstrated that INs preferentially interact with OPCs, forming highly organized synaptic networks (Orduz et al., 2015). Another interesting aspect is the postnatal PCD involving both populations (Southwell et al., 2012; Kessaris et al., 2006). The firstOPCs are mostly completely eliminated from the cortex at PN 10 and replaced by the other waves, while a small portion survives in other CNS regions (Minocha et al., 2015; Marques et al., 2018). Furthermore, the genetic ablation of firstOPCs is simply replaced from the following waves with no drastic alterations in network myelination (Kessaris et al., 2006). This compensation could be explained by the OPC tendency to homeostatically maintain their cell number and to display different transcriptional profiles that converge towards one during postnatal development (Marques et al., 2018). Concerning INs, 40% of these neurons is also eliminated during the first two postnatal weeks (Southwell et al., 2012). In fact, the relationship between INs and OPCs implicates other subpopulations. The second wave of OPCs that arises later in embryonic development (E14.5) partially overlaps with the other major (30%) IN subclass expressing 5HT3Ra since both cell types are born in the CGE from progenitors expressing Gsh2 (LGE only for OPCs). All these evidences, describing the convergence in the embryonic origin between INs and OPCs coming from ventral regions, their death and their highly regulated transient IN-OPC connectivity, suggests possible interactions between these two cell types that might participate to cortical construction. Therefore, based on all these evidences, my work assessed the potential properties and functions of IN-OPC interactions, focusing our attention on the firstOPCs and INs coming from the same embryonic regions.

Methods & Results

Article I

A. Objective

OPCs generate OLs, the glial cells responsible for producing myelin in the CNS. In the last 20 years, it has been demonstrated the existence of functional synaptic inputs between neurons and OPCs throughout the brain, but the role of these neuron-glia synapses remain elusive. These synapses could be implicated in the mechanisms controlling oligodendrogenesis, and thus myelination in the brain. Recently, a study in our team identified that OPCs receive a transient but prominent synaptic input from GABAergic INs during early postnatal development, which correlates with the onset of cortical oligodendrogenesis (Vélez-Fort et al., 2010; Orduz et al., 2015). Moreover, Orduz et al. (2015) showed that two distinct types of presynaptic INs contact OPCs: PV-expressing FSIs are highly connected with OPCs while PV-negative NFSIs are proportionally less connected. Although a following study in the team demonstrated that the genetic ablation of γ2 subunit in OPC $GABA_A$Rs, which mediate INs and OPC synaptic transmission, was not affecting oligodendrogenesis (Balia et al., 2017), Orduz data indicate the existence of a close relationship between INs and OPCs during the first two postnatal weeks, a critical period for cortical circuit construction. Nowadays, it is well recognized that INs and OPCs can communicate through synaptic and extrasynaptic transmission, expressing $GABA_A$Rs, and also by release of factors. IN activity may thus affect OPC functions through different pathways (Maldonado and Angulo, 2015; Passlick et al., 2013; Voronova et al., 2017). Based on these evidences, our aim was to investigate GABAergic OPC interactions, particularly in the somatosensory barrel cortex, a well characterized region known to be highly myelinated in the adult.

In this first project, we used an optogenetic approach to set up an efficient protocol of photostimulation to selectively activate cortical GABAergic INs *in vivo* at PN 10, i.e. at the peak of IN-OPC connectivity. In particular, we targeted specific IN subpopulations by using two Cre transgenic mouse lines where Channelrhodopsin 2 (ChR2) expression was driven by two different promoters, PV and Nkx2.1, Ca^{2+}-binding albumin protein and transcription factor expressed earlier in cortical development respectively. Finally, we studied the effects of photoactivation on OPC proliferation. Our main goal was to identify whether GABAergic INs are crucial in regulating non-neuronal functions during cortical development as oligodendrogenesis.

We addressed the following specific aims:

1) To evaluate the expression of the light-sensitive protein ChR2 in INs of two distinct transgenic mice during the second postnatal week in acute brain slices
2) To evaluate the parameters for an efficient photostimulation of ChR2-expressing INs in different transgenic lines in acute brain slices and *in vivo*
3) To analyze the effect of *in vivo* photoactivation of INs on OPC proliferation

In summary, the question of how neuronal activity control OPC development is far from being answered and a causal link between interneuronal activity, GABAergic synapses and OPC dynamics is missing.

B. Methodology

1) Optogenetic stimulation

Optogenetics is a technique to modulate or track cell activity by photostimulation introducing light-sensitive proteins through genetic manipulation. Proteins like ChR, halorhodopsin (NpHR), and archaerhodopsin (Arch) are used to activate or silence neuronal activity. Genetically encoded sensors for ions or membrane voltage are instead used to monitor neuronal activity. « The effector in this system is light that has the advantage to operate with high spatial and temporal resolution at multiple wavelengths and locations » (Duebel et al., 2015).

One of the first steps in the development of the optogenetics as potential tool for research investigation was the discovery of the bacteriorhodopsin, a rhodopsin-like protein from *Halobacterium halobium* membrane that pumps protons after photostimulation (Oesterhelt, Stoeckenius, 1971). Later, other members of the opsin family like the halorhodopsin (Sugiyama and Mukohata, 1984) and ChR (Nagel et al., 2002) were identified. In particular, we used in our study a member of ChRs, the family of blue light-

activated non-specific cation channels discovered in the algae species *Chlamydomonas reinhardtii* (Nagel et al., 2002) (**Figure 18**). The first described ChR was ChR1 whereas ChR2 was later characterized from the same organism. ChRs are composed by 7 transmembrane domain proteins and are the only known channels directly gated by light. Advances in the technique have introduced additional ChR variants such as ChR2/H134R, ChR2/E123T(ChETA), VChR1, VChR2, ChR2/C128X/D156A, ChD, ChEF and ChIEF each with unique features and limitations (Lin, 2011). Since its discovery, ChR2 has been used in research as a tool to selectively depolarise membranes of excitable cells upon photostimulation. ChR2, differently from the proton-selective ion channel ChR1, is a non-specific light-sensitive ion channel, allowing for the transport of univalent and divalent cations, with the following relative permeability: $H^+ > Na^+ > K^+ > Ca^{2+} > Mg^{2+}$ (**Figure 18A**). ChR1 was the first ChR characterised *ex vivo* (Nagel et al., 2002) but its low conductance at pH7 compared to the later discovered ChR2 made it less interesting as a scientific tool. From the molecular point of view, a blue light photostimulation induces a switch in the configuration of opsin forming the channel pore (from trans to cis) (**Figure 18B**). This modification causes the disruption of interactions among residues with following opening of the channel. The membrane depolarization induced by cation influx can trigger action potentials in neurons (**Figure 18A**).

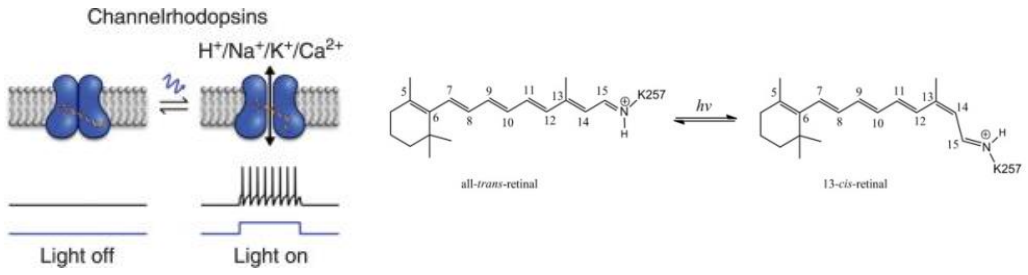

Figure 18 . A. Channelrhodopsins (blue, on the left) depolarize cells and can trigger action potentials in neurons upon illumination with blue light. B. Photoreceptor activation is mediated by the isomerization of 11-*cis* retinal to all-*trans* rétinal upon photosstimulation. (Adapted from Boyden, 2011)

Differently from voltage-gated Na^+ and K^+ channels, the opening and closing kinetics of ChR2 are slow. The more accepted model identifies a photocycle characterized by two open states (O1–O2) and two non-conductive "D" sub-states, with a slow recovery in between of 10-20 s after a dark period (Stehfest and Hegemann, 2010). This slow recovery has as result a limit in the stimulation frequency, since the ChR2 cannot follow with fidelity light pulses triggered at high frequencies. For its depolarizing effect, ChR2 has been extensively used in neuroscience as a tool to specifically activate neuronal circuits without strong perturbation of the cell structure and physiology. Usually the channel is genetically fused with YFP, as in our experimental model, to allow and easy detection of cells expressing the protein.

2) Transgenic Cre-Lox mice used in our study

In our study, we wanted to selectively activate GABAergic INs *in vivo* at PN 10 in order to increase their activity and evaluate the effects of this increase on OPC proliferation. Most of GABAergic INs (70%) and the firstOPCs derive from progenitors which express Nkx2.1 early in the development. We thus used the Nkx2.1-Cre transgenic line, expressing the *cre* recombinase under the control of the Nkx2.1 promoter (Xu et al., 2008). The sequence of Nkx2.1 was modified by replacing the first 15 bp of the exon 2 with the *cre* coding sequence in order to express this enzyme in the Nkx2.1-expressing precursors of INs. Thus, this line may be useful for generating conditional mutations in both INs and oligondroglia cells derived from these progenitors.

We also used a second transgenic line, $Pvalb^{tm1(cre)Arbr}$ (PV^{Cre}), where the endogenous PV promoter was directing the *cre* recombinase expression in PV-expressing cells (Hippenmeyer et al., 2005). We used this line to specifically drive the expression of the ChR2 in PV^+ FSIs, highly connected

with OPCs during the peak of synaptic connectivity observed at PN 10 (Orduz et al., 2015).

Finally, to obtain the specific expression of the ChR2 in cortical INs, we crossed these two lines with ChR2(H134R)-YFP$^{lox/lox}$. « ChR2(H134R)-YFP$^{lox/lox}$ transgenic line has a *loxP*-flanked STOP cassette which prevents transcription of the downstream ChR2(H134R)-YFP fusion gene » (Jax laboratories). When bred to *cre* recombinase expressing lines, the resulting offspring express the light-gated cationic channel activated by illumination with blue light (450-490 nm), allowing for the rapid *ex vivo*/*in vivo* activation of the cells of our interest. The ChR2(H134R)-YFP expression mediated by Cre recombinase was easy detectable by the YFP fluorescence, fused with the channel.

We analyzed two different mouse lines expressing ChR2 in different subsets of cortical GABAergic INs in order to determine to which extend these lines could be used to photostimulate INs at PN 10 *in vivo.* We found that PV^{Cre}/ChR2-YFP$^{lox/lox}$ mice were not suitable for developmental studies since ChR2 was poorly expressed in PV INs during the second postnatal week. On the contrary, we showed that Nkx2.1^{Cre}/ChR2-YFP$^{lox/+}$ mice represent a good tool to activate two major types of INs (PV and SST) at PN 10 because the early expression of the transcription factor ensures an efficient expression of the light sensitive protein at early postnatal development.

C. Main Results

1) <u>Functional ChR2 Expression in Cortical GABAergic Interneurons of Cre-Lox Transgenic Mice in Brain Slices</u>

We first observed in PV^{Cre}:ChR2-YFP$^{lox/lox}$ mice a low expression at PN 10 of ChR2 (YFP^{+} cells) compared to later stages (PN 20-26), result corroborated by electrophysiological experiments. On the contrary, Nkx2.1^{Cre}:ChR2-YFP$^{lox/+}$ mice showed a sufficient YFP^{+} expression in INs at PN 10-12, although lower compared to later stages. We also demonstrated a

functional expression of ChR2 at PN 10 in Nkx2.1^{Cre}:ChR2-YFP$^{lox/+}$ line since recording YFP^{+} cells upon photostimulation we observed a response with action potential discharges to light-pulse trains. The INs response showed a progressive decrease when increasing the stimulation frequency from 20 to 50 Hz.

2) Light-Evoked Local Field Potentials in Acute Slices and *in vivo* in Nkx2.1^{Cre}:ChR2-YFP$^{lox/+}$ Mice

To assess our ability to generate action potentials in ChR2-expressing INs, we first tested whether 10 Hz light stimulation was able to elicit LFPs in acute cortical slices. We observed light-evoked high fidelity LFP responses in cortical L II to VI. The responses were less sensitive to the glutamatergic and GABAergic receptor antagonists (APV, NBQX and Gabazine) than TTX, Na^{+} channel blocker. These data indicate that light-evoked LFPs were mainly generated from action potentials by ChR2-expressing INs.

We also demonstrated that a 3h stimulation protocol adapted fromexperiments in slices and primary used by Ortiz et al. (2019) in another study of the team were able to induce a response in Nkx2.1^{Cre}:ChR2-YFP$^{lox/+}$ mice *in vivo* at PN 10.

3) Effect of *in vivo* Interneuron Activation on the Oligodendroglia Population

We demonstrated that the interneuron photoactivation does not affect the density of proliferating OPCs after a 3 h stimulation protocol, quantifying in both controls and photostimulated mice the total population of EdU^{+} cells, which target proliferating cells, and the EdU^{+}/Olig2^{+}/CC1^{-} OPCs. This suggests a limited effect of IN activity on OPC proliferation at PN 10.

frontiers in Cellular Neuroscience

TECHNOLOGY REPORT
published: 06 December 2018
doi: 10.3389/fncel.2018.00477

In vivo Optogenetic Approach to Study Neuron-Oligodendroglia Interactions in Mouse Pups

Domiziana Ortolani[1,2†], Blandine Manot-Saillet[1,2†], David Orduz[2], Fernando C. Ortiz[2,3] and Maria Cecilia Angulo[1,2*]*

[1] *INSERM U894, Institute of Psychiatry and Neuroscience of Paris, Paris, France,* [2] *INSERM U1128, Paris, France,* [3] *mechanisms of Myelin Formation and Repair Lab, Instituto de Ciencias Biomédicas, Facultad de Ciencias de la Salud, Universidad Autónoma de Chile, Santiago, Chile*

Optogenetic and pharmacogenetic techniques have been effective to analyze the role of neuronal activity in controlling oligodendroglia lineage cells in behaving juvenile and adult mice. This kind of studies is also of high interest during early postnatal (PN) development since important changes in oligodendroglia dynamics occur during the first two PN weeks. Yet, neuronal manipulation is difficult to implement at an early age because high-level, specific protein expression is less reliable in neonatal mice. Here, we describe a protocol allowing for an optogenetic stimulation of neurons in awake mouse pups with the purpose of investigating the effect of neuronal activity on oligodendroglia dynamics during early PN stages. Since GABAergic interneurons contact oligodendrocyte precursor cells (OPCs) through *bona fide* synapses and maintain a close relationship with these progenitors during cortical development, we used this relevant example of neuron-oligodendroglia interaction to implement a proof-of-principle optogenetic approach. First, we tested Nkx2.1-Cre and Parvalbumin (PV)-Cre lines to drive the expression of the photosensitive ion channel channelrhodopsin-2 (ChR2) in subpopulations of interneurons at different developmental stages. By using patch-clamp recordings and photostimulation of ChR2-positive interneurons in acute somatosensory cortical slices, we analyzed the level of functional expression of ChR2 in these neurons. We found that ChR2 expression was insufficient in PV-Cre mouse at PN day 10 (PN10) and that this channel needs to be expressed from embryonic stages (as in the Nkx2.1-Cre line) to allow for a reliable photoactivation in mouse pups. Then, we implemented a stereotaxic surgery to place a mini-optic fiber at the cortical surface in order to photostimulate ChR2-positive interneurons at PN10. *In vivo* field potentials were recorded in Layer V to verify that photostimulation reaches deep cortical layers. Finally, we analyzed the effect of the photostimulation on the layer V oligodendroglia population by conventional immunostainings. Neither the total density nor a proliferative fraction of OPCs were affected by increasing interneuron activity *in vivo*, complementing previous findings showing the lack of effect of GABAergic synaptic activity on OPC proliferation. The methodology described here should provide a framework for future investigation of the role of early cellular interactions during PN brain maturation.

Keywords: optogenetics, GABAergic interneuron, oligodendrocyte precursor cell, developing brain, somatosensory cortex, proliferation

OPEN ACCESS

Edited by:
Dirk Feldmeyer, Forschungszentrum Jülich, Helmholtz-Gemeinschaft Deutscher Forschungszentren (HZ), Germany

Reviewed by:
Markus Rothermel, RWTH Aachen University, Germany
Elias Leiva-Salcedo, University of Santiago, Chile

***Correspondence:**
Fernando C. Ortiz
fernando.ortiz@uautonoma.cl
Maria Cecilia Angulo
maria-cecilia.angulo@parisdescartes.fr

† Co-first authors

Received: *10 September 2018*
Accepted: *22 November 2018*
Published: *06 December 2018*

Citation:
Ortolani D, Manot-Saillet B, Orduz D, Ortiz FC and Angulo MC (2018) In vivo Optogenetic Approach to Study Neuron-Oligodendroglia Interactions in Mouse Pups. Front. Cell. Neurosci. 12:477. doi: 10.3389/fncel.2018.00477

INTRODUCTION

The advent of optogenetics (Boyden et al., 2005) and pharmacogenetics (Conklin et al., 2008; Dong et al., 2010) have allowed for a big progress revealing detailed mechanisms behind intercellular communication (Aston-Jones and Deisseroth, 2013; Adamantidis et al., 2015; Chen et al., 2018). Optogenetics is based on the expression of photosensitive protein-channels in specific cell types, making possible to activate or inhibit particular components of a given circuit by using light (Boyden et al., 2005; Han and Boyden, 2007; Aston-Jones and Deisseroth, 2013). Typically, the activation of a targeted neuron is achieved by photoactivation of a channel-rhodopsin 2 (ChR2) variant. The ChR2 is a cationic channel which activation leads to the depolarization of the cell membrane (Ernst et al., 2008). If the light-induced rise in the membrane potential reaches the activation threshold of intrinsic depolarizing ion channels expressed by the cell (i.e., voltage-dependent sodium or calcium channels), an action potential is triggered (Zhang et al., 2006, 2007; Ernst et al., 2008). By this mechanism, the generation of action potentials of targeted neurons can be controlled with high spatiotemporal precision.

While optogenetic techniques have largely contributed to our current understanding of neuronal network function in the mature central nervous system (CNS), their use to investigate the developing brain has been poor and only recent efforts have started to be done in this direction (Bitzenhofer et al., 2017a,b). A significant limitation when studying developing circuits is to reach enough levels of ChR2 expression on cell membranes in order to induce efficient responses by photostimulation. Given the variable protein expression during developmental stages, the heterologous expression of light-sensitive channels driven by endogenous cell promoters in the neonatal brain is not reliable enough (see Bitzenhofer et al., 2017a). In addition, *in vivo* brain photostimulation usually requires the placement of a ferrule or mini-optic fiber that is fixed on the cranial bone (Gradinaru et al., 2009; Yizhar et al., 2011), a procedure more difficult to apply on the soft skull of mouse pups. This issue has probably precluded the use of optogenetics to study developing circuits, privileging pharmacogenetics (Wong et al., 2018), a versatile but less precise technique in time and space.

During early postnatal (PN) development, neurons form transient circuits before establishing mature networks (Anastasiades et al., 2016). Interestingly, oligodendrocyte precursor cells (OPCs), the major source of myelinating oligodendrocytes in the CNS, receive a transient synaptic input from GABAergic interneurons during early PN development (Vélez-Fort et al., 2010; Zonouzi et al., 2015). Indeed, OPCs are the only non-neuronal cells synaptically contacted by neurons in the CNS (Bergles et al., 2000). In the somatosensory (barrel) cortex, the interneuron-OPC connectivity reaches a peak at PN10, 1 day prior to oligodendrocyte (OL) differentiation, and then declines progressively to disappear during the fourth PN week (Vélez-Fort et al., 2010; Balia et al., 2015; Orduz et al., 2015). Although the genetic inactivation of a specific interneuron-OPC synapse does not impair the proliferation and differentiation of OPCs at early PN stages (Balia et al., 2017), these data indicate the existence of a close relationship between interneurons and OPCs during a critical period for cortical circuit construction. Interneuron activity may thus affect OPC function through different synaptic and extrasynaptic mechanisms in the immature neocortex (Maldonado and Angulo, 2015). Indeed, in addition to interneuron-OPC synaptic interactions, OPCs express extrasynaptic $GABA_A$ receptors (Passlick et al., 2013; Balia et al., 2015). Moreover, interneurons directly communicate with OPCs in the developing brain by secreting over 50 paracrine factors such as fractalkine that promote OPC differentiation (Voronova et al., 2017).

In this article, we describe an experimental protocol to activate cortical GABAergic interneurons *in vivo* by using optogenetics in mouse pups and analyze the effect of interneuron activity in OPC dynamics. We tested Nkx2.1-Cre and Parvalbumin (PV)-Cre lines to drive the expression of ChR2 in subpopulations of interneurons. We analyzed the functional expression of this photosensitive channel by combining patch-clamp recordings with photostimulation in acute somatosensory cortical slices. We found that ChR2 expression was insufficient in the PV-Cre mouse line at PN10, while the Nkx2.1-driven expression allowed for a reliable photoactivation in the developing cortex. Next, we developed a stereotaxic surgery to place a mini-optic fiber at the cortical surface to photostimulate ChR2-positive interneurons at PN10 in awake mouse pups. Finally, we analyzed the effect of interneuron photoactivation on the oligodendroglia population by conventional immunostainings. Our approach should provide a methodological tool to study the function of different neuron-oligodendroglia interactions in the early PN brain.

MATERIALS AND METHODS

Transgenic Mice

All experiments followed European Union and institutional guidelines for the care and use of laboratory animals and were approved by French committees for animal care of the University Paris Descartes and the Ministry of National Education and Research (N°CEEA34.MCA.070.12). For experiments, we used transgenic Nkx2.1-$Cre^{(+/-)}$:ChR2 (H134R)-$YFP^{(lox/+)}$ and PV-$Cre^{(+/-)}$:ChR2 (H134R)-$YFP^{(lox/lox)}$ mice from PN8 to PN26 obtained after crossing from Nkx2.1-Cre (Kessaris et al., 2006), PV-Cre (JAX n°008069) and ChR2-lox (JAX n°012569).

Electrophysiology and Photostimulation in Acute Slices

Acute parasagittal slices (300 μm) of the barrel cortex were obtained with an angle of 10° to the sagittal plane using a vibratome (Microm HM650V) as previously described (Vélez-Fort et al., 2010; Orduz et al., 2015). Slices were prepared in an ice-cold solution containing (in mM): 215 sucrose, 2.5 KCl, 1.25 NaH_2PO_4, 26 $NaHCO_3$, 20 glucose, 5 pyruvate, 1 $CaCl_2$, and 7 $MgCl_2$ (95% O_2, 5% CO_2) and incubated for 30 min at 33°C in an extracellular solution containing (in mM): 126 NaCl, 2.5 KCl, 1.25 NaH2PO4, 20 glucose, 5 pyruvate, 2 $CaCl_2$ and 1 $MgCl_2$ (95% O_2, 5% CO_2). For recordings, slices were transferred to a recording

chamber perfused with the same extracellular solution at 2–3 ml/min. An Olympus BX51 microscope equipped with a 40× fluorescent water-immersion objective, a Q-imaging camera and a CoolLed pE-2 fluorescent system (Scientifica, United Kingdom) allowed us to visualize the YFP fluorescent protein of ChR2-expressing interneurons in acute slices. Layer V ChR2-expressing interneurons were recorded at RT in whole-cell configuration with pipettes having a resistance of 3–5 MΩ and containing an intracellular solution with (in mM): 130 KGlu, 0.1 EGTA, 0.5 $CaCl_2$, 2 $MgCl_2$, 10 HEPES, 2 Na_2-ATP, 0.2 Na-GTP and 10 Na_2-phosphocreatine (pH≈7.3; 300 mOsm). Photostimulation of ChR2-expressing interneurons was obtained with an optic fiber (200 μm, NA = 0.66; Prizmatix Ltd., Israel) placed on layer V of the slice close to the patched cell and connected to a LED source delivering 460 nm wavelength light pulses (UHP-Mic-LED-460, Prizmatix Ltd., Israel). Local field potentials (LFPs) were recorded with a recording pipette filled with extracellular solution and located in layer V close to the optic fiber.

Whole-cell recordings were obtained using Multiclamp 700B, filtered at 3 kHz and digitized at 20 kHz. Digitized data were analyzed off-line using pClamp10.6 (Molecular Devices, United States) and Neuromatic package within IGOR Pro 6.0 environment (Wavemetrics, United States). The identity of interneurons was first assessed by analyzing the firing properties of neurons recorded in current-clamp mode as previously described (Orduz et al., 2015). Briefly, we used a depolarizing pulse of 800 ms to measure the instantaneous discharge frequency ($F_{initial}$), the frequency at 200 ms (F_{200}), the frequency at the end of the pulse ($F_{final,}$) and the total frequency (F_{total}). We calculated both early and late accommodations. The membrane input resistance R_m of neurons was calculated from a −200 pA hyperpolarized 800 ms step. The spike threshold, the first and second action potential amplitudes, and their corresponding durations were extracted from a 200 pA depolarizing pulse of 80 ms to calculate the amplitude reduction and duration increase. The amplitude of the after-hyperpolarization (AHP) was calculated as the difference between the threshold and the peak of the fast hyperpolarization.

Train pulses of light were used to elicit action potentials in ChR2-expressing interneurons (10 ms, 1 mW per pulse). Light trains of 10, 20, 30, and 50 Hz during 30 s were applied to define the optimal frequency inducing an effective activation of patched ChR2-expressing interneurons. For each frequency, we calculated the number of spikes (N_s) with respect to the number of light pulses (N_{LP}) and determined the percentage of success as $[N_s/N_{LP}] \times 100$. LFPs were elicited by stimulating with light trains (10 Hz, 2 s). In a set of experiments, the extracellular solution contained: 50 μM (2R)-amino-5-phosphonovaleric acid (APV, ref: HB0225, Hellobio); 10 μM 2,3-dihydroxy-6-nitro-7-sulfamoyl-benzo[f]quinoxaline (NBQX, ref: ab120046, abcam) and 10 μM Gabazine (SR 95531, ref: ab120042, Abcam). Tetrodotoxin (TTX, ref: HB1035, Hellobio) was applied at a final concentration of 1 μM.

Surgery and *in vivo* Photostimulation

Animals (PN10-11) were deeply anesthetized with ketamine/xylazine (0.1/0.01 mg/g, IP) and fixed in a stereotaxic frame adapted to mouse pups (Kopf Instruments, United States). The skin above the skull was disinfected and incised. In these young mice, the bone structure is not sufficiently transparent to let in the light into the cortex, and too soft to support the weight of the implant containing the mini-optic fiber. Thus, the skull was artificially stiffened with a double layer of glue before a hole was stereotaxically drilled above the barrel cortex area. For the adherence of the glue on the skull, the conjunctive tissue was first removed by a very local drop of HCl solution (1 mM). Caution was taken to apply this solution on a very restricted area to avoid any contact with the mouse skin or other tissues. Once cleaned, the skull was artificially stiffened with a double layer of glue (SuperGlue, Gel, ethyl-2-cyanoacrylate). The first layer was obtained by gently spreading out a first drop on the bone above the somatosensory cortex. After 10 min, a

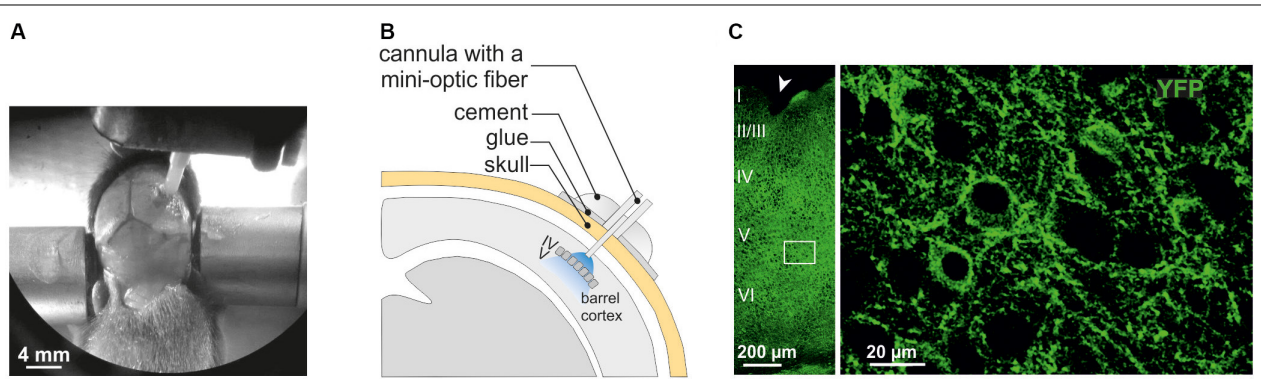

FIGURE 1 | Surgery for *in vivo* optogenetic stimulation of interneurons of the somatosensory cortex in mouse pups. **(A)** An anesthetized PN10 mouse holding the implant and fixed in a stereotaxic apparatus is shown. Before to place the mini-optic fiber the skull is covered with two layers of glue. In this example, the skin of the animal was more widely incised for visibility on the picture. **(B)** Scheme of the mini-optic fiber implanted at the surface of the somatosensory barrel cortex. **(C)** Confocal images of ChR2-expressing interneurons in layers from I to VI (left; low magnification) and in layer V (right; high magnification of the white square in the left) of the barrel cortex of a $Nkx2.1^{Cre}$:ChR2-$YFP^{Lox/+}$ mouse at PN10. ChR2 expression driven by the Nkx2.1 promoter is detected by the YFP reporter (green). The arrowhead indicates a small lesion induced when removing the optic fiber of the pup after perfusion. It allows us to precisely locate the place of the mini-optic fiber.

second layer of glue was similarly applied in the same region. Then, we waited around 20 min to ensure that the glue was completely dry before drilling the hole. Finally, the cannula accommodating the mini-optic fiber was implanted according to the following coordinates: 2.7 mm lateral to midline, 3.7 mm posterior to Bregma, and 0.1 mm depth from brain surface with an angle of 10° (**Figures 1A,B**; cannula: 1.25 mm; fiber: 200 μm diameter, NA = 0.66; Prizmatix Ltd., Israel). Some animals were implanted using an optrode containing a mini-optic fiber and a fine-wire recording electrode (Ni/Ag) of 50 μm diameter reaching layer V. In this case, a pin connector was fixed to the skull at the back of the brain to be used as a ground. Finally, the optogenetic implant was fixed to the skull with dental cement (Unifast Trad ivory 339104) and the skin was sutured around the implant (Mersilene®, EH7147H, Ethicon). Mice were recovered from anesthesia in an environment at 37°C before the photostimulation experiment. Once the animal was completely awake, the mini-optic fiber was connected to a 460 nm ultra-high power LED source through two optic fiber patch cords (UHP-mic-LED-460; Prizmatix Ltd., Israel). The first patch cord (200 μm diameter, NA 0.66) was connected from the mini-optic fiber to a rotary joint that spins freely, and the second (1000 μm, NA 0.66) was connected from the rotary joint to the optogenetics-LED optogenetics-LED source. This latter was connected to a current controller that in turn was commanded by a pulser device that creates programmable TTL pulses from a software (Prizmatix Pulser/Pulser PC Software, Prizmatix Ltd., Israel). Mice were photostimulated according to a 3 h protocol composed by 36 light trains of 30 s delivered at 10 Hz [10 ms on/90 ms off pulses; ∼3–4 mW per pulse, a power estimated from measurements in continuous wave (CW) mode] and separated by a resting period of 4.5 min. Considering that our duty cycle is 10%, we estimated that the total energy applied during a 30 s photostimulation train is equivalent to 9–12 mJ. Prior to the surgery, the power at the tip of each mini-optic fiber was systematically measured with an optical power meter (PM100D coupled with sensor S120C, Thorlabs, United States) by connecting it to the LED system operating in CW mode (maximum output power at the 200 μm mini-optic fiber tip: ∼4.5 mW). Once the surgery was completed, we set the values in the current controller to deliver the proper power at the tip of the fiber during the photostimulation. For LFP recordings, the recording electrode was connected to the headstage of a Multiclamp 700B amplifier through a 50 μm diameter Ni/Ag wire, and the ground of the mouse connected to the ground of the amplifier. Finally, the animal was placed inside a small ($\sim 20 \times 20 \times 20\ cm^3$) custom-made Faraday cage and light trains of 10 Hz were elicited to evoke LFPs in current-clamp ($I = 0$) voltage follower mode.

Immunostainings, EdU Proliferation Assay and Countings

Fifteen minutes prior to photostimulation, intraperitoneal EdU injections were performed to labeled cells in the S phase of the cell cycle (10 mM EdU solution in PBS at 50 mg/kg; ref. C10340, ThermoFisher Scientific, United States). 1 h after the end of the photostimulation, mice were perfused with phosphate buffer saline (PBS) followed by 0.15 M phosphate buffer (PB) containing 4% paraformaldehyde (PFA, Electron Microscopy Sciences, United States), pH 7.4. Brains were then left in PFA for 2 h at 4°C before washing and storing them in PBS at 4°C. The day of immunostainings, coronal vibratome slices (100 μm) were prepared in PBS at 4°C and permeabilized with 1% Triton and 4% Normal Goat Serum (NGS) during 2 h at RT under agitation. Then, slices were first incubated at 4°C under gently agitation for 3 nights with rabbit anti-Olig2 (1:400, ref. AB9610, Merck-Millipore) and mouse anti-CC1 (1:100, ref. OP80, Calbiochem) diluted in 0.2% Triton X-100 and 2% NGS and revealed for 2 h at RT with secondary antibodies coupled to Alexa-405 and Alexa-633, respectively (1:500, ThermoFisher Scientific). EdU was revealed for 2 h at RT after immunostainings by using the Clik-iT EdU Alexa-555 (C10638, ThermoFisher Scientific). Between each incubation step and at the end of the protocol, slices were rinsed 3 times in PBS for 10 min under genlty agitation.

Confocal images (0.75 μm z-step) were acquired using a 63X oil objective (NA = 1.4) with a LSM 710 confocal microscope (Zeiss) and processed using NIH ImageJ[1] as described (Balia et al., 2017). Cell densities were obtained by counting $Olig2^+$, $CC1^+$, and EdU^+ cells with the ROI manager tool (ImageJ) and by dividing the number of cells by the volume, as previously described (Balia et al., 2017).

Statistics

All data were expressed in mean ± SEM. A level of $p < 0.05$ was used to designate significant differences. Two group comparisons were performed using the non-parametric Mann–Whitney Test. Multiple comparisons were done with the non-parametric Kruskal–Wallis Test followed by a Dunn's multiple comparison test. Statistics and plotting were performed using GraphPad Prism 5.00 (GraphPad Software Inc., United States).

RESULTS

Functional ChR2 Expression in Cortical GABAergic Interneurons of Cre-Lox Transgenic Mice in Brain Slices

Three major cortical GABAergic interneuron subtypes can be defined according to the expression of three different markers: PV-, somatostatin (SST)-, and ionotropic serotonin receptor 5HT3a (5HT3aR) (Rudy et al., 2011). PV and SST interneurons constitute about 70% of the total population whereas 5HT3aR interneurons about 30% (Rudy et al., 2011). Cortical GABAergic interneurons are mainly born in the medial and caudal ganglionic eminences (MGE and CGE, respectively). The MGE is the site of origin of 60% of the cortical interneurons, mostly PV- and SST-interneurons (Marín, 2013; Wamsley and Fishell, 2017), while the CGE is the second source producing approximatively 30% of interneurons (Anderson et al., 2001; Nery et al., 2002). More recently, Gelman et al. (2011) also demonstrated that the

[1] http://imagej.nih.gov/ij

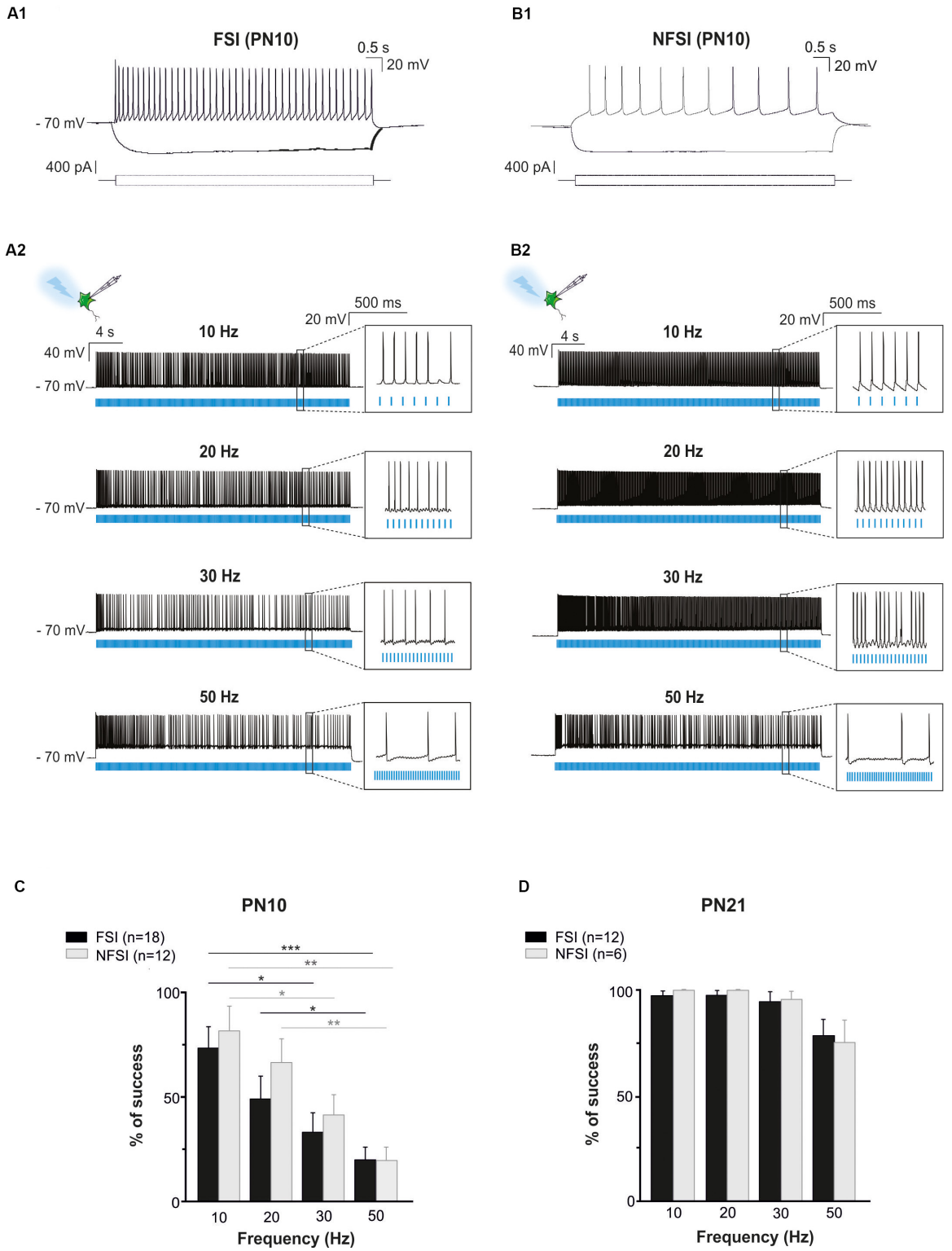

FIGURE 2 | Photoactivation of ChR2-expressing FSI and NFSI in PN10 Nkx2.1^{Cre}:ChR2-YFP$^{Lox/+}$ mouse pups in brain slices. **(A1,B1)** Current-clamp recordings of a FSI **(A1)** and a NFSI **(B1)** expressing ChR2 in cortical layer V at PN10. Note the differences of firing properties between the two cells in response to 800 ms depolarizing and hyperpolarizing steps (bottom square pulses). **(A2,B2)** The same FSI **(A2)** and NFSI **(B2)** were photostimulated (blue bars) with 10 ms light pulses during 30 s at different frequencies. **(C,D)** Average percentage of success to elicit action potentials with light trains at different photostimulation frequencies for FSI (black) and NFSI (gray) at PN10 **(C)** and PN21 **(D)**. *$p < 0.05$; **$p < 0.01$; and ***$p < 0.001$ for comparisons across each interneuron subtype, Kruskal–Wallis Test followed by a Dunn's *post hoc* Test; not significant differences ($p > 0.05$) between FSI and NFSI for each frequency are not indicated; Mann–Whitney test.

TABLE 1 | Electrophysiological properties of FSI and NFSI at PN10 in Nkx2.1^{Cre}:ChR2-YFP$^{Lox/+}$ mice.

Parameter PN 10	FSI(*n* = 18)	NFSI (*n* = 12)	*p*-value	Comparison
F_{total} (Hz)	30.94 ± 2.84	31.67 ± 2.43	NS	–
$F_{initial}$ (Hz)	**94.65 ± 8.43**	**131.20 ± 13.41**	**<0.05**	**FSI < NFSI**
F_{200} (Hz)	63.86 ± 5.13	68.06 ± 5.50	NS	–
F_{final} (Hz)	59.56 ± 5.66	54.01 ± 4.84	NS	–
Early accommodation (%)	**30.64 ± 2.03**	**44.87 ± 3.74**	**<0.01**	**FSI < NFSI**
Late accommodation (%)	**5.11 ± 1.55**	**11.12 ± 1.79**	**<0.05**	**FSI < NFSI**
Threshold (mV)	−39.86 ± 2.48	−35.88 ± 1.89	NS	–
First spike amplitude (mV)	74.23 ± 1.89	78.71 ± 1.60	NS	–
Second spike amplitude (mV)	73.30 ± 1.80	74.48 ± 1.62	NS	–
Spike amplitude reduction (%)	**1.02 ± 0.25**	**5.10 ± 0.91**	**<0.0001**	**FSI < NFSI**
First spike duration (ms)	1.32 ± 0.08	1.49 ± 0.16	NS	–
Second spike duration (ms)	**1.42 ± 0.08**	**1.89 ± 0.22**	**<0.05**	**FSI < NFSI**
Spike duration increase (%)	**7.84 ± 0.71**	**26.00 ± 2.62**	**<0.0001**	**FSI < NFSI**
AHP (mV)	**−11.07 ± 1.21**	**−5.63 ± 0.76**	**<0.01**	**FSI > NFSI**
AHP width (ms)	**30.17 ± 14.49**	**9.38 ± 1.96**	**<0.05**	**FSI > NFSI**
Rm(MΩ)	203.07 ± 16.62	206.74 ± 46.89	NS	

F_{total}, total frequency; $F_{initial}$, instantaneous discharge frequency; F_{200}, frequency at 200 ms; F_{final}, frequency at the end of the pulse; AHP, after-hyperpolarization; R_m, membrane input resistance. Statistical differences are in Bold.

embryonic preoptic area (POA) is a third source and suggested that this region contributes with approximately 10% of all GABAergic interneurons in the murine cerebral cortex. POA-derived progenitors give rise to PV, SST, and Reelin-expressing interneurons (Marín, 2013).

The specification of cortical interneurons in each generating area depends on a transcriptional network that regulates interneuron development. Among transcription factors important for interneuron specification, Nkx2.1 is specifically expressed in MGE- and POA-derived progenitors that generate 70% of cortical interneurons. These progenitors mainly generate both PV and SST interneurons with those in the POA producing more heterogeneous neuron subtypes (Marín, 2013; Wamsley and Fishell, 2017). Interestingly, the earliest wave of OPCs is also generated from Nkx2.1-expressing progenitors settled in the MGE and POA (Kessaris et al., 2006). Nevertheless, most of the Nkx2.1-derived precursors giving rise to oligodendroglia are eliminated by PN10 and thus should not significantly interfere to the ChR2 targeting of Nkx2.1-derived interneurons from this PN stage (Kessaris et al., 2006).

In the present study, we used Nkx2.1^{Cre}:ChR2-YFP$^{Lox/+}$ mice to drive the PN ChR2 expression in MGE- and POA-derived interneurons from embryonic stages (from ∼E11.5 which corresponds to the peak of interneuron production; Anderson et al., 2001). At PN10-12, YFP$^+$ interneurons were easily detected in the Nkx2.1^{Cre}:ChR2-YFP$^{Lox/+}$ mouse line in all cortical layers (**Figure 1C**). We focused on layer V since our previous studies in interneuron-OPC interactions were performed in this layer (**Figure 1C**; Vélez-Fort et al., 2010; Balia et al., 2015, 2017; Orduz et al., 2015). We first examined the electrophysiological properties of YFP$^+$ cells in layer V by using patch-clamp recordings in acute slices of the barrel cortex (**Figures 2A1,B1** and **Table 1**). As expected from Nkx2.1-derived interneurons at this age, recorded YFP$^+$ cells could be distinguished as fast-spiking interneurons (FSI; **Figure 2A1**) and non-fast-spiking interneurons (NFSI; **Figure 2B1**) by their characteristic action potential discharges in response to current injections (Daw et al., 2007; Orduz et al., 2015). FSI were mainly distinguished from NFSI by their pronounced AHP and a restricted spike duration increase and amplitude reduction during action potential discharges (**Table 1**; see Orduz et al., 2015). Other analyzed parameters such as the initial frequency, second spike duration and early and late accommodations were also different between the two groups (**Table 1**; see section "Materials and Methods").

To test whether ChR2 was functionally expressed at PN10 in Nkx2.1^{Cre}:ChR2-YFP$^{Lox/+}$ mice, we photostimulated recorded YFP$^+$ interneurons using an optic fiber placed in Layer V. Independently of the interneuron identity, all tested YFP$^+$ cells responded with action potential discharges to light-pulse trains (**Figures 2A2,B2**). While the success rate of the response during a 30 s-train delivered at 10 Hz was very high for both FSI and NFSI, a progressive decrease in the capacity of neurons to follow the stimulation train was observed when increasing the frequency from 20 to 50 Hz (**Figures 2A2,B2,C**). No significant differences were observed between FSI and NFSI for each tested frequency, indicating that it is not possible to set up specific parameters to exclusively activate either FSI or NFSI (**Figure 2C**).

Two main reasons could explain the decreased response of YFP$^+$ interneurons at higher frequency photostimulation trains: (1) a limited intrinsic capacity of immature interneurons to sustain high frequency discharges during long trains, and (2) a lower level of expression of ChR2 at PN10. To assess the first possibility, we mimicked the light train protocol with current pulse injections at 50 Hz for 30 s (**Figures 3A1,A2**). All recorded FSI and NFSI responded faithfully with action potentials to each current pulse injection, while the success rate during train photostimulation remains low at this early

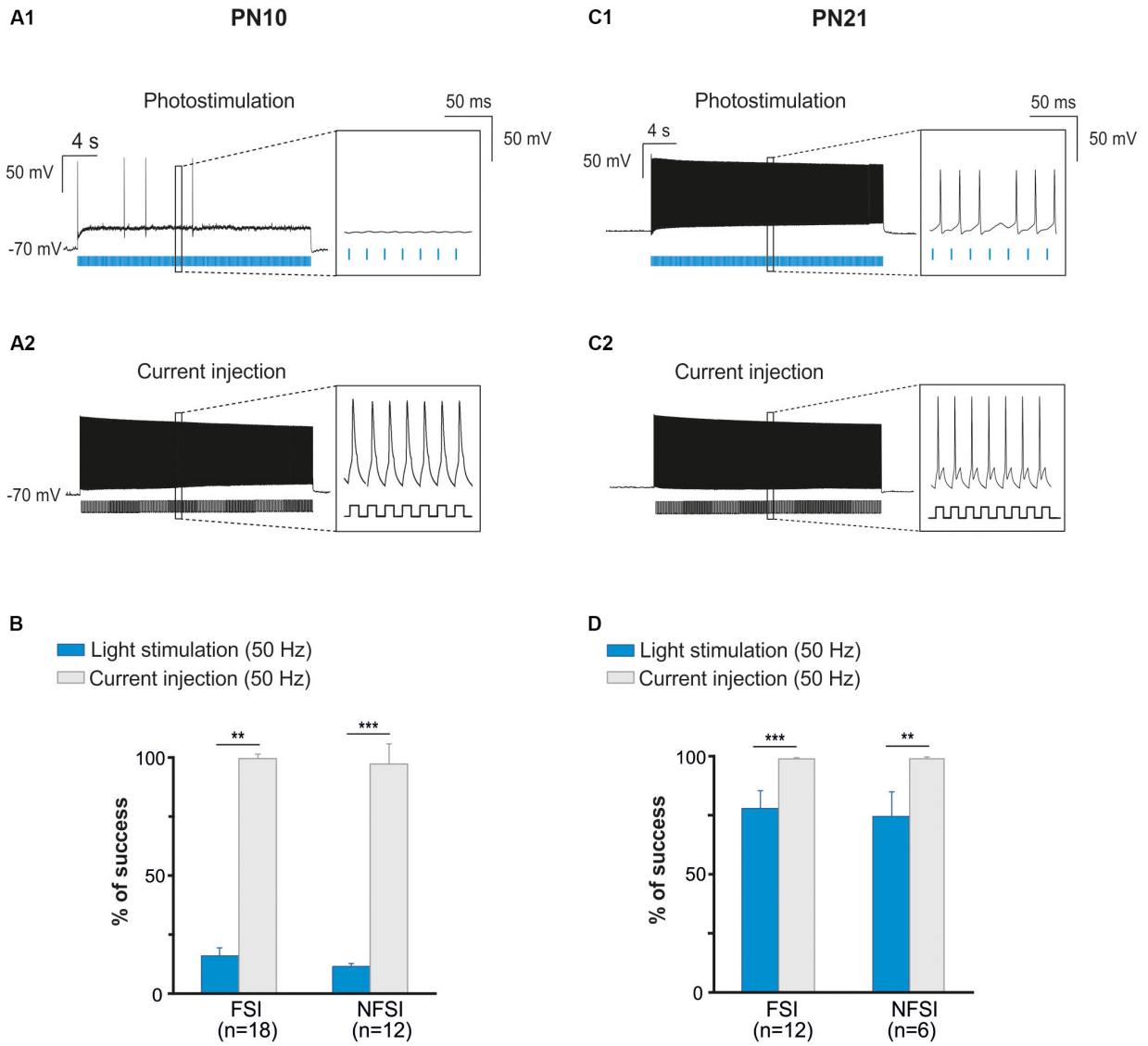

FIGURE 3 | The fail of response at high frequency photostimulation in brain slices at PN10 is not due to interneuron immature membrane properties. **(A)** An identified ChR2-expressing interneuron recorded in current-clamp mode during a 50 Hz photostimulation protocol **(A1)** in a brain slice at P10. Note the numerous failures (inset) in response to blue light pulses (blue bars). The same neuron stimulated with current injections (400 pA, 10 ms; **(A2)**) at 50 Hz showed virtually no failures (inset). **(B)** Comparison between the percentage of success of photostimulation versus current stimulation at 50 Hz for FSI and NFSI in mice at PN10. **(C)** An identified ChR2-expressing interneuron recorded in current-clamp mode during a 50 Hz photostimulation protocol **(C1)** in a brain slice at PN21. Note the increased number of APs (inset) triggered by photoactivation (blue bars) compared with the interneuron at PN10 **(A1)**. The same neuron stimulated with current injections (400 pA, 10 ms; **C2**) at 50 Hz showed virtually no failures (insets). **(D)** Comparison between the percentage of success of photostimulation versus current stimulation at 50 Hz for FSI and NFSI in mice at PN21. $^{**}p < 0.01$ and $^{***}p < 0.001$, Mann–Whitney Test.

PN stage (**Figures 3A,B**). Therefore, the intrinsic properties of interneurons in younger mice are not responsible for a low success rate during higher frequency trains. To test for the level of expression of ChR2 during development, we performed the same experiments at PN19-22, i.e., during the third PN week (**Supplementary Figure 1** and **Table 2**). Although we observed a maturation of the electrophysiological properties of interneurons during the second and third PN weeks (**Tables 1**, **2**; Pangratz-Fuehrer and Hestrin, 2011), FSI were still distinguished from NFSI by the presence of a more pronounced AHP and small variations of the duration and amplitude spikes (**Supplementary Figures 1A1,B1** and **Table 2**). Other parameters such as early accommodation and input resistance were significantly different between FSI and NFSI at a later developmental stage (**Table 2**). After recording the electrophysiological profile, we photostimulated the patched YFP^{+} interneuron using trains of photostimulation at 10, 20, 30, and 50 Hz (**Supplementary Figures 1A2,B2**). At PN19-22, the success rates for both FSI and NFSI were close to 100% for trains at 10, 20, and 30 Hz and dropped to around 80% at 50 Hz (**Figure 2D** and **Supplementary**

TABLE 2 | Electrophysiological properties of FSI and NFSI at PN21 in Nkx2.1^{Cre}:ChR2-YFP$^{Lox/+}$ mice.

Parameter PN 21	FSI (*n* = 18)	NFSI (*n* = 8)	*p*-value	Comparison
F_{totAl} (Hz)	64.5 ± 6.42	64.38 ± 8.37	NS	–
$F_{initial}$ (Hz)	185.7 ± 22.46	243.1 ± 24.14	NS	–
F_{200} (Hz)	132.9 ± 11.81	131.8 ± 20.54	NS	–
F_{final} (Hz)	126.5 ± 13.36	116 ± 16.79	NS	–
Early accommodation (%)	**21.99 ± 4.01**	**45.78 ± 6.61**	**<0.01**	**FS < NFS**
Late accommodation (%)	5.2 ± 1.93	6.49 ± 2.28	NS	–
Threshold (mV)	−44.26 ± 1.25	−44.59 ± 0.92	NS	–
First spike amplitude (mV)	77.84 ± 1.7	81.82 ± 1.57	NS	–
Second spike amplitude (mV)	76.23 ± 1.6	76.65 ± 1.6	NS	–
Spike amplitude reduction (%)	**2.0 ± 0.3**	**6.05 ± 3.68**	**<0.01**	**FS < NFS**
First spike duration (ms)	0.6 ± 0.04	0.77 ± 0.12	NS	–
Second spike duration (ms)	0.62 ± 0.04	0.87 ± 0.14	NS	–
Spike duration increase (%)	**3.47 ± 0.41**	**11.96 ± 1.98**	**<0.0001**	**FS < FS**
AHP (mV)	**−18.63 ± 0.93**	**−11.16 ± 1.73**	**<0.01**	**FS > NFS**
AHP width (ms)	**5.4 ± 0.77**	**2.29 ± 0.21**	**<0.05**	**FS > NFS**
Rm(MΩ)	**185.9 ± 14.55**	**242.8 ± 18.62**	**<0.05**	**FS < NFS**

F_{total}, total frequency; $F_{initial}$, instantaneous discharge frequency; F_{200}, frequency at 200 ms; F_{final}, frequency at the end of the pulse; AHP, after hyperpolarization; R_m, membrane input resistance. Statistical differences are in Bold.

Figures 1A2,B2), as expected from the limited capacity of ChR2 to follow high frequency trains (Lin et al., 2009). Indeed, current injections mimicking photostimulation at 50 Hz in PN19-22 mice caused a significantly higher success rate of ∼100% in FSI and NFSI (**Figures 3C,D**). Altogether, these results indicate that a lower level of ChR2 expression in the second PN week compared to 10 days later is probably at the origin of the decrease of the success rate with respect to the photostimulation frequency at PN10.

Since PV-expressing FSI are highly connected to OPCs in the second PN week (Orduz et al., 2015), we also aimed at specifically photostimulating these interneurons in PV^{Cre}:ChR2-YFP$^{Lox/Lox}$ mice during this period. However, YFP$^+$ interneurons were never detected in acute slices under the epifluorescence microscope and were very rarely observed under the confocal microscope at PN10 (**Figure 4A**). The scarcity of ChR2 expression in this mouse line at early PN stages was concomitant to the lack of response of FSI, recognized from their intrinsic electrophysiological properties, to a 10 Hz-photostimulation train at this age (n = 2, **Figures 4B1,B2**). Since this line has been extensively used in the adult (Cardin et al., 2010), we examined later developmental PN stages. Compared to PN10, immunostainings revealed an extensive co-labeling of PV and YFP in cell bodies and branches at PN20 and PN26 (**Figure 4A**). At PN19-22, 5 out of 7 neurons emitted at least one action potential in response to light train stimulation at 10 Hz (**Figure 4B2**) and one cell responded faithfully to each train pulse. In average, the success rate of discharge at 10 Hz was 14.62 ± 14.23% (**Figure 4C**). However, FSI rarely responded to higher frequency light trains at this age (**Figure 4C**). All recorded YFP$^+$ neurons at PN26 responded faithfully with action potentials to each pulse of the light train stimulation at 10 Hz (success rate: 100%, n = 7, **Figures 4B1,C2**). Nevertheless, the success rate of YFP$^+$ FSI progressively decreased at 20, 30, and 50 Hz-photostimulation trains (**Figure 4**). Therefore, there is an increased functional expression of ChR2 from PN10 to PN26 in PV^{Cre}:ChR2-YFP$^{Lox/Lox}$ mice. Considering that in Nkx2.1^{Cre}:ChR2-YFP$^{Lox/+}$ at PN21 the success rate of FSI is still high at 50 Hz (**Figure 2C**), a maximum level of ChR2 expression is probably not attained in PV^{Cre}:ChR2-YFP$^{Lox/Lox}$ mice in the fourth PN week.

In summary, contrary to a late PN expression of ChR2 in PV^{Cre}:ChR2-YFP$^{Lox/Lox}$ mice, ChR2 is already expressed in Nkx2.1^{Cre}:ChR2-YFP$^{Lox/+}$ mice at PN10, the age corresponding to the peak of synaptic connectivity between interneurons and OPCs in the somatosensory cortex (Orduz et al., 2015). Indeed, all recorded YFP$^+$ interneurons responded to photostimulation trains at this developmental stage, although the success rate during a long train of 30 s significantly decreases at frequencies higher than 30 Hz. The most suitable light train frequencies to obtain a maximum and reliable number of action potentials during 30 s in Nkx2.1^{Cre}:ChR2-YFP$^{Lox/+}$ mice were between 10 and 20 Hz. Since FSI and NFSI fire at lower frequency rates in pups than in adults (**Tables 1**, **2**), 10 Hz constitutes a good compromise to efficiently activate around 80% of interneurons during long light trains (30 s; **Figure 2C**).

Light-Evoked Local Field Potentials in Acute Slices and *in vivo* in Nkx2.1^{Cre}:ChR2-YFP$^{Lox/+}$ Mice

Neocortical GABAergic interneurons are inhibitory cells and constitute a minority of cortical neurons (10–20% in rodents; Rudy et al., 2011). For these two reasons, our observation of a single photoactivated interneuron does not necessarily ensure that light stimulation through the optic fiber will induce the activation of an interneuron population. To assess our ability to generate action potentials in a large number of ChR2-expressing interneurons, we first examined whether

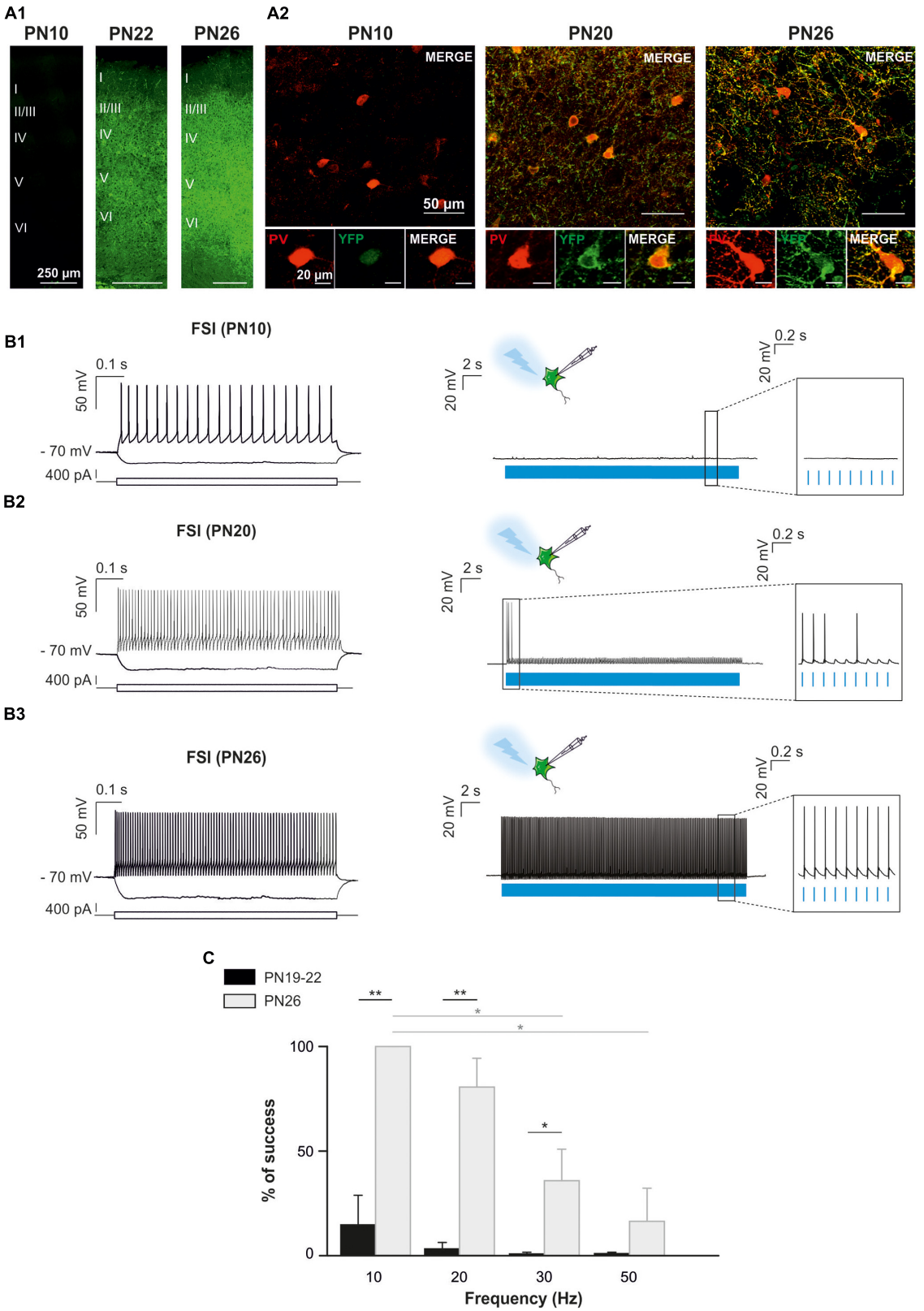

FIGURE 4 | Optogenetic stimulation of FSI in PV^{Cre}:ChR2-$YFP^{Lox/Lox}$ mice during postnatal cortical development in brain slices. **(A)** Confocal images of cortical interneurons expressing ChR2 (YFP, green) and PV protein (red) at low (left) and high (right) magnifications at PN10, PN20 and PN26 mice. Note the faintly cytoplasmatic expression of YFP at PN10 compared to a brighter and more extensive membrane expression at later ages. **(B)** Current-clamp recordings of a layer V

(Continued)

FIGURE 4 | Continued
ChR2-expressing FSI **(B1)** at PN10. Depolarizing and hyperpolarizing steps are indicated (bottom square pulses). No action potentials were evoked by a 10 Hz photostimulation train (blue pulses) in this neuron (**B1** right, inset), but the photoactivation-induced response increased during development (**B2,B3**, right). Note that photoactivation (blue pulses) of a layer V ChR2- expressing FSI at PN26 evoked action potentials in response to every light pulse (B3 right, inset). **(C)** Average percentage of success to elicit action potentials with light trains delivered from 10 to 50 Hz at PN19-22 and PN26 in the PV^{Cre}:ChR2-$YFP^{Lox/Lox}$ mice. $^{*}p < 0.05$; $^{**}p < 0.01$, Kruskal–Wallis Test followed by a Dunn's *post hoc* Test; not significant differences ($p > 0.05$) between FSI and NFSI for each frequency are not indicated.

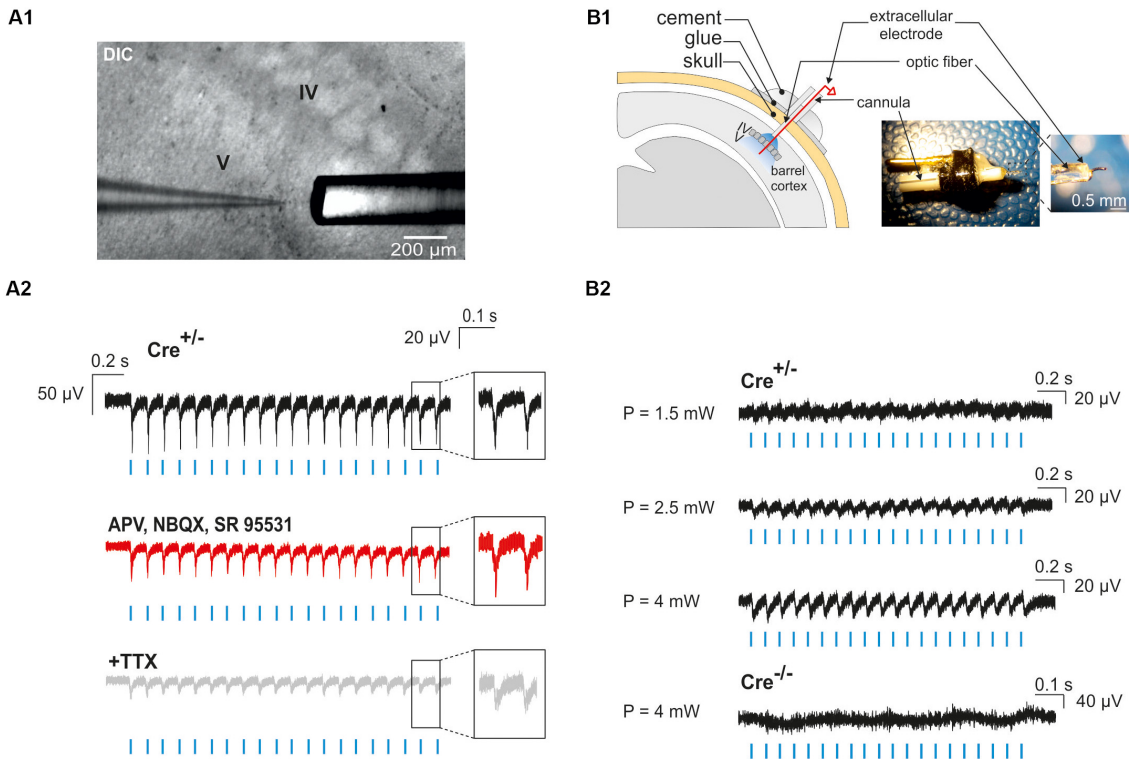

FIGURE 5 | Photo-evoked LFPs in PN10 mouse pups in brain slices and *in vivo*. **(A)** Extracellular recordings were performed in the cortical layer V of brain slices during photostimulation with an optic fiber located just above the recording site **(A1)**. LFPs evoked by photostimulation (**A2**, blue lines) were faithfully reproduced in response to every light pulse (black trace, inset) in ChR2-expressing transgenic mice ($Cre^{+/-}$). Recording of the same slice during bath application of glutamatergic and GABAergic antagonists (50 µM APV, 10 µM NBQX, 10 µM SR95531; **A2** red trace) and TTX (1 µM, **A2** gray trace) are shown. DIC: Differential interference contrast image. **(B)** *In vivo* extracellular recordings of cortical layer V were performed by the placement of a custom-made optrode containing a mini-optic fiber and a 50 µm Ni/Ag wire **(B1)**. *In vivo* LFPs were successfully evoked by photostimulation (**B2**, blue lines) above 1.5 mW of light power in a ChR2-expressing transgenic mouse ($Cre^{+/-}$). The reported powers from 1.5 to 4 mW correspond to the power per pulse estimated from measurements in continuous wave (CW) mode. No responses were evoked in a $Cre^{-/-}$ control mouse.

photostimulation elicited LFPs in acute cortical slices. We found that a 10 Hz photostimulation train induced LFPs with great fidelity in cortical layers II to VI (n = 2 slices in 2 animals, not shown), but since most of interneuron-OPC interactions in pups have been described in layer V (Vélez-Fort et al., 2010; Balia et al., 2015, 2017; Orduz et al., 2015), we analyzed in more detail the effect of interneuron activation in this layer (**Figures 5A1,A2**; n = 5 slices in 2 animals). These LFPs were less sensitive to the glutamatergic and GABAergic receptor antagonists APV, NBQX, and SR95531 than to the Na^{+}-channel blocker tetrodotoxin (TTX) that abolishes action potential generation [**Figures 5A1,A2**; amplitude reduction of the first LFP: 4.32 ± 0.86% (n = 5) and 48.39 ± 12.1% (n = 3), respectively]. It is noteworthy that a TTX-insensitive component also persisted in all tested slices (**Figure 5A2**). It probably corresponded to the LFP generated by the current directly flowing through ChR2 channels in interneurons. These data indicate that recorded light-evoked LFPs upon 10 Hz photostimulation trains resulted from the direct generation of action potentials by multiple nearby ChR2-expressing interneurons instead of postsynaptic potentials (the latter could have been generated by inhibitory postsynaptic potentials or by disinhibition of inhibitory circuits resulting in increased excitatory postsynaptic potentials).

To analyze the effect of photostimulation *in vivo*, we performed a surgery at PN10 to implant an optrode including an optic fiber placed at the surface of the cortex. Since light poorly penetrates into scattering tissue, we tested whether neuronal responses were evoked by light in layer V by using a wire electrode to record light-evoked LFPs in this layer at a frequency

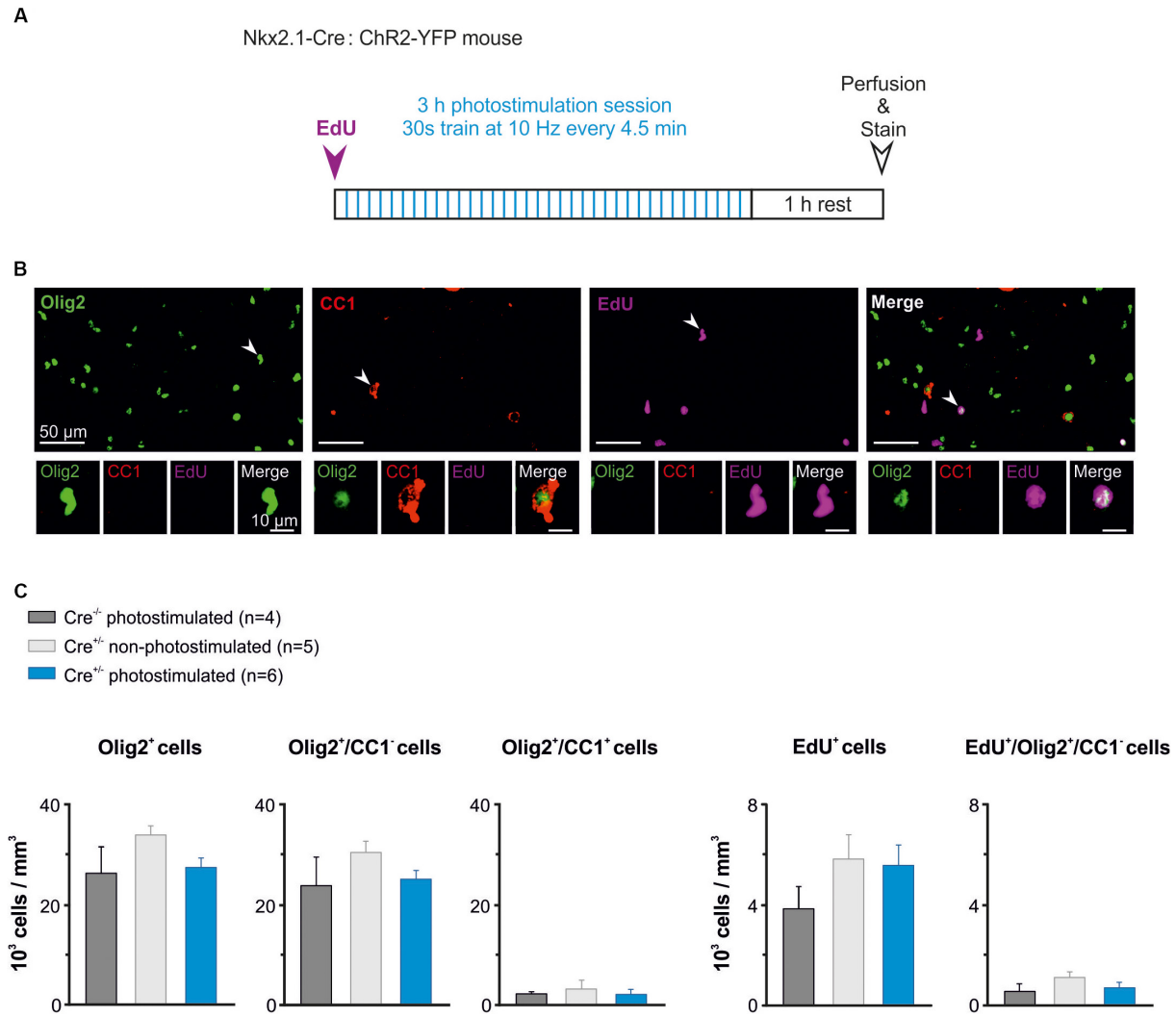

FIGURE 6 | The *in vivo* photoactivation of layer V cortical interneurons at P10 does not modify oligodendroglia density. **(A)** Experimental design for a photostimulation protocol. Mice were injected with EdU (50 mg/kg) and then photostimulated during 3 h. **(B)** Olig2 (green), CC1 (red) and EdU (magenta) cells stained after the photostimulation session. An Olig2^{+}/CC1 $^{-}$OPC is indicated in the first panel (arrowhead, insets). Only few Olig2^{+}/CC1^{+} OLs were found at this age (arrowhead in second panel, insets). Note that not all EdU-stained cells were Olig2^{+} cells (arrowheads in the last two panels). **(C)** Density of total oligodendroglia (lig2^{+}), OPCs (Olig2^{+}/CC1^{-}), differentiated OLs (Olig2^{+}/CC1^{+}), total proliferative cells (EdU^{+}), and proliferative OPCs (Edu^{+}/Olig2^{+}/CC1^{-}) in the three tested conditions. No significant differences were found for any comparison ($p > 0.05$, Kruskal–Wallis Test followed by a Dunn's *post hoc* Test).

of 10 or 20 Hz (**Figure 5B1**). To firmly maintain the optrode on the mouse skull, it was necessary to artificially harden the bone with a layer of glue before drilling (see section "Materials and Methods"). Once the animal was awake after surgery, it was placed in a chamber where the mini-optic fiber was connected to a 460 nm LED source through an optic fiber patch cord in order to record light-evoked LFPs (**Figure 5B2**; 4 Cre$^{(+/-)}$ mice and 3 Cre$^{(-/-)}$ mice). Photostimulation trains elicited weak responses when the power was set at 1.5 mW per pulse at the tip of the optrode (**Figure 5B2**). However, light-evoked LFPs increased for each light pulse at 2.5 and 4 mW (**Figure 5B2**). These responses were absent in Cre$^{(-/-)}$ animals of the same littermates, used here as a control group (**Figure 5B2**).

Our results demonstrate that Nkx2.1^{Cre}:ChR2-YFP$^{Lox/+}$ mice can be used to activate a population of ChR2-expressing interneurons as early as PN10. We established the best conditions for whole-cell and LFP recordings in brain slices and set up the conditions to ensure layer V interneuron activation *in vivo*.

Effect of *in vivo* Interneuron Activation on the Oligodendroglia Population

It was recently showed that photoactivation of layer V glutamatergic neurons has a rapid effect on increasing the proliferation rate of OPCs in juvenile mice (Gibson et al., 2014). Here, we analyzed whether the activity of GABAergic interneurons also influence OPC proliferation at PN10-11, when

the synaptic connectivity between interneurons and OPCs is maximal in the somatosensory cortex (Orduz et al., 2015). We photostimulated awake pups to trigger a response of layer V ChR2-expressing interneurons using ∼3–4 mW per pulse (**Figure 5B2**). In these set of experiments, the wire electrode was not present on the implant (**Figure 1B**). Based on our previous characterization in slices, we chose 10 Hz as frequency for *in vivo* photostimulation. However, since 10 Hz represents a relatively low stimulation frequency for cortical interneurons that discharge at higher rates even in the immature mice (**Table 1**), we opted to multiply the number of stimulation trains. The photostimulation protocol lasted 3 h and comprised 36 stimulation trains of 30 s at 10 Hz (**Figure 6A**). Before the photostimulation session, we intraperitoneally injected 50 mg/kg of EdU, a thymidine analog that integrates the genome during the S phase of the cell cycle (**Figure 6A**). After the photostimulation session, we waited 1 h before perfusing the animal and removing the implant (**Figure 6A**). Then, immunostainings were performed to simultaneously identify all OL lineage cells (Olig2) and mature OLs (CC1), while EdU was revealed to detect proliferating cells. We considered $Olig2^+/CC1^-$ cells as OPCs and $Olig2^+/CC1^+$ cells as differentiated OLs (**Figure 6B**). We compared the effect of the photostimulation within three different experimental groups: 1) $Cre^{(-/-)}$ ChR2-non-expressing photostimulated mice ($n = 4$); 2) $Cre^{(+/-)}$ ChR2-expressing non-photostimulated mice ($n = 5$); and 3) $Cre^{(+/-)}$ ChR2-expressing photostimulated mice ($n = 6$). The two first groups were considered as controls.

The region carrying the implant was recognized under the confocal microscope by the presence of a small lesion in upper layers of the cortex (**Figure 1C**). To ensure that we analyzed the photostimulated area, only the slices showing a small lesion were further imaged at high resolution in order to perform cell countings in layer V (1 to 3 slices per mice). Cell countings did not reveal any significant difference in the total density of $Olig2^+$ cells, $Olig2^+/CC1^-$ OPCs or differentiated $Olig2^+/CC1^+$ OLs (**Figure 6C**, left). As expected for this early developmental age, most $Olig2^+$ cells were OPCs in all conditions (**Figure 6C**, left). Moreover, we found that controls and photostimulated mice did not display any significant change in the total population of EdU^+ cells or in the population of $EdU^+/Olig2^+/CC1^-$ OPCs (**Figure 6C**, Right). It is noteworthy that no $EdU^+/Olig2^+/CC1^+$ OLs were observed in our samples, suggesting more symmetric than asymmetric divisions of OPCs at PN10-11. In conclusion, we did not observe any difference in the density of proliferating OPCs after a 3 h stimulation protocol, suggesting a limited effect of interneuron activity on OPC proliferation at this age. This result supports and complements our previous findings showing that the GABAergic synaptic activity of OPCs does not play a role in oligodendrogenesis (Balia et al., 2017).

DISCUSSION

Here, we describe an experimental procedure to activate cortical GABAergic interneurons of PN10 mouse pups by using an optogenetic approach. We first determined that Nkx2.1-driven ChR2-expression allowed for a reproducible activation of cortical layer V GABAergic interneurons at PN10, whereas ChR2 was insufficiently expressed in the PV-Cre mouse at the same age. Combining photostimulation with both whole cell patch-clamp recordings in brain slices and *in vivo* extracellular recordings, we determined a suitable photostimulation protocol to ensure a reliable photoactivation of targeted cells. We also provide an experimental procedure to place a mini-optic fiber in the neonatal mouse brain in order to photoactivate interneurons in deep cortical layers of awake pups. Finally, we analyzed the effect of a particular neuronal photoactivation protocol on the oligodendroglia population in the neonatal neocortex.

Optogenetic studies have been proved to largely contribute to our current understanding of mature nervous system circuitry. However, only recent efforts have allowed for the implementation of this technique in the neonatal brain (Bitzenhofer et al., 2017a,b; Ahlbeck et al., 2018). Indeed, one of the major prerequisite for a selective and reliable optogenetic stimulation is to attain a sufficient level of opsin expression in targeted cells. This is more difficult to achieve in mouse pups due to the low or variable protein expression during early PN stages. In line with this, we found that the functional ChR2 expression of FSI in PV-Cre:ChR2-$YFP^{flox/flox}$ mice was largely insufficient at PN10, preventing the emission of action potentials in these interneurons. PV, the major marker of FSI, starts to be expressed during the first PN week, but reaches high levels late during neocortical development. At PN10, PV mRNA expression revealed a moderate labeled of mRNA-positive cells in layer V of the somatosensory cortex compared to PN16 (De Lecea et al., 1995). A developmental increased pattern of PV expression was also observed in our immunostainings in concomitance with an increased ChR2 expression (**Figure 4**). Therefore, the PV-Cre transgenic mouse line is not appropriate for inducing a sufficient ChR2 expression driven by the PV promoter at PN10. Contrary to the late expression of ChR2 in PV-Cre:ChR2-$YFP^{flox/flox}$ mice, this channel is more expressed at this age in Nkx2.1-Cre:ChR2-$YFP^{flox/+}$ mice (**Figure 1C**). An efficient ChR2 expression was expected in this mouse line since Nkx2.1 is expressed in interneuron progenitors at early embryonic stages (Marín, 2013; Wamsley and Fishell, 2017). In addition, fate-mapping approaches used to track the development of Nkx2.1-derived interneurons exhibited the distribution of these neurons in the mouse somatosensory barrel cortex already in the first PN week (Butt et al., 2005). The choice of Cre transgenic mouse lines is therefore crucial for inducing a sufficient ChR2 expression early in PN development.

Another key aspect of an optogenetic approach is to ensure a reliable and consistent readout of action potential discharges triggered by photostimulation. This is particularly important considering recent reports indicating that, depending on the neuronal subtype and light stimulation parameters (i.e., pulse duration), photoactivation of ChR2 might silence instead of increasing neuronal activity (Lin et al., 2013; Herman et al., 2014). This undesirable effect is explained by a light-induced depolarization block that results from an overactivation of ChR2 and its subsequent exaggerated cation influx, leading to

an insufficient repolarization (Lin et al., 2013; Herman et al., 2014). Importantly, Herman et al. (2014) reported that cortical interneurons were 2 to 4 times more susceptible to ChR2-dependent silencing than excitatory neuronal subtypes. Although the light pulse duration was the major responsible for the observed depolarization block in this study (Herman et al., 2014), a high frequency photoactivation can also be a triggering mechanism (Grossman et al., 2011). A first characterization of the response of ChR2-expressing neurons to photostimulation in brain slices is an important step, sometimes neglected, to define a pertinent protocol for *in vivo* experiments, even when behavioral tests are conducted.

In the present report, we determined that 10 ms light pulses delivered at 10–20 Hz reliably trigger action potential discharges during 30 s in ChR2-expressing interneurons of Nkx2.1-Cre:ChR2-YFP$^{flox/+}$ mice at PN10. Interestingly, action potentials were triggered with high fidelity in these same cells at frequencies of 50 Hz upon depolarizing current injections. These results indicate that the inability of interneurons to respond to light stimuli is not due to their immature intrinsic membrane properties at this age, but likely to ChR2 expression levels and channel gated properties. Indeed, the opening and closing kinetics of ChR2 are slower than those of voltage-gated Na^+ and K^+ channels. Photocycle models for ChR2 describe two open states (O1–O2) and at least two non-conductive "D" sub-states characterized by a slow recovery –from 10 s to more than 20 s– after a dark period (Ernst et al., 2008; Stehfest and Hegemann, 2010; Grossman et al., 2011; Saita et al., 2018). This requirement of a long-lasting dark period to recruit ChR2 activation upon a new light stimulus partially explains the limited neuronal response to high frequency photostimulation (Ernst et al., 2008; Grossman et al., 2011). In addition, due to the O1-to-O2 turnover, short inter-pulse intervals preclude the proper ChR2 closing (Grossman et al., 2011; Saita et al., 2018). In this line, Grossman et al. (2011) found that in response to 50 Hz photostimulation trains applied to ChR2-transfected hippocampal neurons, only 63% of the responsive ChR2 were closed in the inter-pulse interval compared to 99% at 10 Hz, preventing membrane repolarization and leading to the depolarization block of these neurons (Grossman et al., 2011). Nevertheless, since not all the channels are activated upon a single photostimulation, a strong level of protein expression can partially compensate for ChR2 slow kinetics. Indeed, we observed that photostimulation of FSI delivered at 50 Hz in PV-Cre:ChR2-YFP$^{flox/flox}$ mice in the fourth PN week was less efficient than that of FSI in Nkx2.1-Cre:ChR2-YFP$^{flox/+}$ mice in the third PN week (∼15 vs. 75%, respectively).

Neuron-OPC communication has been extensively studied in both gray and white matters (Maldonado et al., 2011; Maldonado and Angulo, 2015). Interestingly, GABAergic synaptic contacts are established on OPCs early in the PN neocortex, reaching a peak at PN10 (Vélez-Fort et al., 2010; Balia et al., 2015; Orduz et al., 2015). In addition, interneurons are known to act in a paracrine manner by releasing fractalkine to promote OPC development in the immature neocortex (Voronova et al., 2017). Finally, Stedehouder et al. (2018) recently demonstrated that PV interneuron myelination by oligodendrocytes is an activity-dependent process, as shown for other neuronal cell types (Hines et al., 2015; Mensch et al., 2015; Wake et al., 2015). All these data indicate a close relationship between GABAergic interneurons and oligodendroglia during PN development, and suggest a role of the activity of these neurons in regulating oligodendroglia function. After determining the parameters for interneuron photoactivation *in vivo* at PN10, we examined the effect of an increased interneuron activity on OPC proliferation at this critical developmental stage for OPC development in the somatosensory cortex (Hill et al., 2014; Balia et al., 2017). We found that the activity of GABAergic interneurons did not change either OPC proliferation or the number of OPCs and OLs in response to a 3 h photostimulation session. This result is in line with our previous report showing no changes in OPC proliferation after the genetic inactivation of interneuron-OPC synapses at the same age (Balia et al., 2017). However, a previous study had shown that 30 min photoactivation of cortical glutamatergic neurons had a rapid effect on the proliferation of these progenitors in juvenile mice (Gibson et al., 2014). It is therefore possible that the activity of glutamatergic and GABAergic neurons in the neocortex play different roles in OPC function. Alternatively, other stimulation paradigms for interneuron activation, closer to their higher firing frequency, need to be tested. Indeed, OPCs might respond in a different manner to different stimulation paradigms (Nagy et al., 2017). To test this possibility, however, other variants of ChR2 would be probably more appropriate such as the form E123T/T159C that has a success rate higher than 80% at 60 Hz (Berndt et al., 2011), or the ChETA variant that allows for a stimulation up to 200 Hz (Gunaydin et al., 2010).

CONCLUSION

In conclusion, this report provides a step-by-step description of an experimental protocol for the optogenetic interrogation of a neuron-oligodendroglia interaction in mouse pups. This methodology could be useful for instance to analyze whether neuronal activity promotes oligodendroglia migration by inspecting the cell density in different cortical layers after *in vivo* stimulation or to search for activity-dependent interneuron-OPC synaptic plasticity by performing electrophysiology in brain slices or immunostainings of synaptic compartments at the end of the *in vivo* protocol. It can also be adapted to other optogenetic tools and cellular interactions of the developing brain to get new insights on the role of glial cells *in vivo* during neuronal circuit formation and maturation.

AUTHOR CONTRIBUTIONS

The two co-first authors conducted optogenetic and electrophysiological experiments in brain slices and *in vivo* and performed data analysis. DO participated in initial experiments of the project. All authors wrote the manuscript. FCO and MCA designed experiments and supervised the project.

FUNDING

This work was supported by Fondation pour la Recherche Médicale («Equipe FRM DEQ20150331681»), Agence Nationale de la Recherche (ANR-14-CE13-0023-02), Fondation ARSEP and subaward agreement from the university of Connecticut with funds provided by the grant N°RG-1612-26501 from National Multiple Sclerosis Society (NMSS). FO was recipient of FRM and ARSEP post-doctoral fellowships and is supported by the Chilean National Fund for Scientific and Technological Development (FONDECYT, INICIACION #11160616). MCA is a CNRS investigator.

ACKNOWLEDGMENTS

We thank M. Omnes for genotyping, the NeuroImag (IPNP) and SCM Imaging Platforms (Paris Descartes University) and A. Pierani (IPNP) for providing us the Nkx2.1-Cre line.

SUPPLEMENTARY MATERIAL

The Supplementary Material for this article can be found online at: https://www.frontiersin.org/articles/10.3389/fncel.2018.00477/full#supplementary-material

REFERENCES

Adamantidis, A., Arber, S., Bains, J. S., Bamberg, E., Bonci, A., Buzsáki, G., et al. (2015). Optogenetics: 10 years after ChR2 in neurons –views from the community. *Nat. Neurosci.* 18, 1202–1212. doi: 10.1038/nn.4106

Ahlbeck, J., Song, L., Chini, M., Bitzenhofer, S. H., and Hanganu-Opatz, I. L. (2018). Glutamatergic drive along the septo-temporal axis of hippocampus boosts prelimbic oscillations in the neonatal mouse. *eLife* 7:e33158. doi: 10.7554/eLife.33158

Anastasiades, P. G., Marques-Smith, A., Lyngholm, D., Lickiss, T., Raffiq, S., Kätzel, D., et al. (2016). GABAergic interneurons form transient layer-specific circuits in early postnatal neocortex. *Nat. Commun.* 7:10584. doi: 10.1038/ncomms10584

Anderson, S. A., Marín, O., Horn, C., Jennings, K., and Rubenstein, J. L. (2001). Distinct cortical migrations from the medial and lateral ganglionic eminences. *Development* 128, 353–363.

Aston-Jones, G., and Deisseroth, K. (2013). Recent advances in optogenetics and pharmacogenetics. *Brain Res.* 1511, 1–5. doi: 10.1016/j.brainres.2013.01.026

Balia, M., Benamer, N., and Angulo, M. C. (2017). A specific GABAergic synapse onto oligodendrocyte precursors does not regulate cortical oligodendrogenesis. *Glia* 65, 1821–1832. doi: 10.1002/glia.23197

Balia, M., Vélez-Fort, M., Passlick, S., Schäfer, C., Audinat, E., Steinhäuser, C., et al. (2015). Postnatal down-regulation of the GABAA receptor γ2 subunit in neocortical NG2 cells accompanies synaptic-to-extrasynaptic switch in the GABAergic transmission mode. *Cereb. Cortex* 25, 1114–1123. doi: 10.1093/cercor/bht309

Bergles, D. E., Roberts, J. D., Somogyi, P., and Jahr, C. E. (2000). Glutamatergic synapses on oligodendrocyte precursor cells in the hippocampus. *Nature* 405, 187–191. doi: 10.1038/35012083

Berndt, A., Schoenenberger, P., Mattis, J., Tye, K. M., Deisseroth, K., Hegemann, P., et al. (2011). High-efficiency channelrhodopsins for fast neuronal stimulation at low light levels. *Proc. Natl. Acad. Sci. U.S.A.* 108, 7595–7600. doi: 10.1073/pnas.1017210108

Bitzenhofer, S. H., Ahlbeck, J., and Hanganu-Opatz, I. L. (2017a). Methodological approach for optogenetic manipulation of neonatal neuronal networks. *Front Cell Neurosci.* 11:239. doi: 10.3389/fncel.2017.00239

Bitzenhofer, S. H., Ahlbeck, J., Wolff, A., Wiegert, J. S., Gee, C. E., Oertner, T. G., et al. (2017b). Layer-specific optogenetic activation of pyramidal neurons causes beta-gamma entrainment of neonatal networks. *Nat. Commun.* 8:14563. doi: 10.1038/ncomms14563

Boyden, E. S., Zhang, F., Bamberg, E., Nagel, G., and Deisseroth, K. (2005). Millisecond-timescale, genetically targeted optical control of neural activity. *Nat. Neurosci.* 8, 1263–1268. doi: 10.1038/nn1525

Butt, S. J., Fuccillo, M., Nery, S., Noctor, S., Kriegstein, A., Corbin, J. G., et al. (2005). The temporal and spatial origins of cortical interneurons predict their physiological subtype. *Neuron* 48, 591–604. doi: 10.1016/j.neuron.2005.09.034

Cardin, J. A., Carlén, M., Meletis, K., Knoblich, U., Zhang, F., Deisseroth, K., et al. (2010). Targeted optogenetic stimulation and recording of neurons in vivo using cell-type-specific expression of Channelrhodopsin-2. *Nat. Protoc.* 5, 247–254. doi: 10.1038/nprot.2009.228

Chen, I. W., Papagiakoumou, E., and Emiliani, V. (2018). Towards circuit optogenetics. *Curr. Opin. Neurobiol.* 50, 179–189. doi: 10.1016/j.conb.2018.03.008

Conklin, B. R., Hsiao, E. C., Claeysen, S., Dumuis, A., Srinivasan, S., Forsayeth, J. R., et al. (2008). Engineering GPCR signaling pathways with RASSLs. *Nat. Methods* 5, 673–678. doi: 10.1038/nmeth.1232

Daw, M. I., Ashby, M. C., and Isaac, J. T. (2007). Coordinated developmental recruitment of latent fast spiking interneurons in layer IV barrel cortex. *Nat. Neurosci.* 10, 453–461. doi: 10.1038/nn1866

De Lecea, L., Del Rio, J., and Soriano, E. (1995). Developmental expression of parvalbumin mRNA in the cerebral cortex and hippocampus of the rat. *Mol. Brain Res.* 32, 1–13. doi: 10.1016/0169-328X(95)00056-X

Dong, S., Rogan, S. C., and Roth, B. L. (2010). Directed molecular evolution of DREADDs: a generic approach to creating next-generation RASSLs. *Nat. Protoc.* 5, 561–573. doi: 10.1038/nprot.2009.239

Ernst, O. P., Sánchez Murcia, P. A., Daldrop, P., Tsunoda, S. P., Kateriya, S., and Hegemann, P. (2008). Photoactivation of channelrhodopsin. *J. Biol. Chem.* 283, 1637–1643. doi: 10.1074/jbc.M708039200

Gelman, D., Griveau, A., Dehorter, N., Teissier, A., Varela, C., Pla, R., et al. (2011). A wide diversity of cortical GABAergic interneurons derives from the embryonic preoptic area. *J. Neurosci.* 31, 16570–16580. doi: 10.1523/JNEUROSCI.4068-11.2011

Gibson, E. M., Purger, D., Mount, C. W., Goldstein, A. K., Lin, G. L., Wood, L. S., et al. (2014). Neuronal activity promotes oligodendrogenesis and adaptive myelination in the mammalian brain. *Science* 344:1252304. doi: 10.1126/science.1252304

Gradinaru, V., Mogri, M., Thompson, K. R., Henderson, J. M., and Deisseroth, K. (2009). Optical deconstruction of parkinsonian neural circuitry. *Science* 324, 354–359. doi: 10.1126/science.1167093

Grossman, N., Nikolic, K., Grubb, M. S., Burrone, J., Toumazou, C., and Degenaar, P. (2011). High-frequency limit of neural stimulation with ChR2. *Conf. Proc. IEEE Eng. Med .Biol. Soc.* 2011, 4167–4170. doi: 10.1109/IEMBS.2011.6091034

Gunaydin, L. A., Yizhar, O., Berndt, A., Sohal, V. S., Deisseroth, K., and Hegemann, P. (2010). Ultrafast optogenetic control. *Nat. Neurosci.* 13, 387–392. doi: 10.1038/nn.2495

Han, X., and Boyden, E. S. (2007). Multiple-color optical activation, silencing, and desynchronization of neural activity, with single-spike temporal resolution. *PLoS One* 2:e299. doi: 10.1371/journal.pone.0000299

Herman, A. M., Huang, L., Murphey, D. K., Garcia, I., and Arenkiel, B. R. (2014). Cell type-specific and time-dependent light exposure contribute to silencing in neurons expressing Channelrhodopsin-2. *Elife* 3:e01481. doi: 10.7554/eLife.01481

Hill, R. A., Patel, K. D., Goncalves, C. M., Grutzendler, J., and Nishiyama, A. (2014). Modulation of oligodendrocyte generation during a critical temporal window after NG2 cell division. *Nat. Neurosci.* 17, 1518–1527. doi: 10.1038/nn.3815

Hines, J. H., Ravanelli, A. M., Schwindt, R., Scott, E. K., and Appel, B. (2015). Neuronal activity biases axon selection for myelination in vivo. *Nat. Neurosci.* 18, 683–689. doi: 10.1038/nn.3992

Kessaris, N., Fogarty, M., Iannarelli, P., Grist, M., Wegner, M., and Richardson, W. D. (2006). Competing waves of oligodendrocytes in the forebrain and postnatal elimination of an embryonic lineage. *Nat. Neurosci.* 9, 173–179. doi: 10.1038/nn1620

Lin, J. Y., Knutsen, P. M., Muller, A., Kleinfeld, D., and Tsien, R. Y. (2013). ReaChR: a red-shifted variant of channelrhodopsin enables deep transcranial optogenetic excitation. *Nat. Neurosci.* 16, 1499–1508. doi: 10.1038/nn.3502

Lin, J. Y., Lin, M. Z., Steinbach, P., and Tsien, R. Y. (2009). Characterization of engineered channelrhodopsin variants with improved properties and kinetics. *Biophys. J.* 96, 1803–1814. doi: 10.1016/j.bpj.2008.11.034

Maldonado, P. P., and Angulo, M. C. (2015). Multiple modes of communication between neurons and oligodendrocyte precursor cells. *Neuroscientist* 21, 266–276. doi: 10.1177/1073858414530784

Maldonado, P. P., Vélez-Fort, M., and Angulo, M. C. (2011). Is neuronal communication with NG2 cells synaptic or extrasynaptic? *J. Anat.* 219, 8–17. doi: 10.1111/j.1469-7580.2011.01350.x

Marín, O. (2013). Cellular and molecular mechanisms controlling the migration of neocortical interneurons. *Eur. J. Neurosci.* 38, 2019–2029. doi: 10.1111/ejn.12225

Mensch, S., Baraban, M., Almeida, R., Czopka, T., Ausborn, J., El Manira, A., et al. (2015). Synaptic vesicle release regulates myelin sheath number of individual oligodendrocytes in vivo. *Nat. Neurosci.* 18, 628–630. doi: 10.1038/nn.3991

Nagy, B., Hovhannisyan, A., Barzan, R., Chen, T.-J., and Kukley, M. (2017). Different patterns of neuronal activity trigger distinct responses of oligodendrocyte precursor cells in the corpus callosum. *PLoS Biol.* 15:e2001993. doi: 10.1371/journal.pbio.2001993

Nery, S., Fishell, G., and Corbin, J. G. (2002). The caudal ganglionic eminence is a source of distinct cortical and subcortical cell populations. *Nat. Neurosci.* 5, 1279–1287. doi: 10.1038/nn971

Orduz, D., Maldonado, P. P., Balia, M., Vélez-Fort, M., de Sars, V., Yanagawa, Y., et al. (2015). Interneurons and oligodendrocyte progenitors form a structured synaptic network in the developing neocortex. *eLife* 22:4. doi: 10.7554/eLife.06953

Pangratz-Fuehrer, S., and Hestrin, S. (2011). Synaptogenesis of electrical and GABAergic synapses of fast-spiking inhibitory neurons in the neocortex. *J. Neurosci.* 31, 10767–10775. doi: 10.1523/JNEUROSCI.6655-10.2011

Passlick, S., Grauer, M., Schäfer, C., Jabs, R., Seifert, G., and Steinhäuser, C. (2013). Expression of the γ2-subunit distinguishes synaptic and extrasynaptic GABA(A) receptors in NG2 cells of the hippocampus. *J. Neurosci.* 33, 12030–12040. doi: 10.1523/JNEUROSCI.5562-12.2013

Rudy, B., Fishell, G., Lee, S., and Hjerling-Leffler, J. (2011). Three groups of interneurons account for nearly 100% of neocortical GABAergic neurons. *Dev. Neurobiol.* 71, 45–61. doi: 10.1002/dneu.20853

Saita, M., Pranga-Sellnau, F., Resler, T., Schlesinger, R., Heberle, J., and Lorenz-Fonfria, V. A. (2018). Photoexcitation of the P4480 state induces a secondary photocycle that potentially desensitizes channelrhodopsin-2. *J. Am. Chem. Soc.* 140, 9899–9903. doi: 10.1021/jacs.8b03931

Stedehouder, J., Brizee, D., Shpak, G., and Kushner, S. A. (2018). Activity-dependent myelination of parvalbumin interneurons mediated by axonal morphological plasticity. *J. Neurosci.* 38, 3631–3642. doi: 10.1523/JNEUROSCI.0074-18.2018

Stehfest, K., and Hegemann, P. (2010). Evolution of the channelrhodopsin photocycle model. *Chemphyschem* 11, 1120–1126. doi: 10.1002/cphc.200900980

Vélez-Fort, M., Maldonado, P. P., Butt, A. M., Audinat, E., and Angulo, M. C. (2010). Postnatal switch from synaptic to extrasynaptic transmission between interneurons and NG2 cells. *J. Neurosci.* 30, 6921–6929. doi: 10.1523/JNEUROSCI.0238-10.2010

Voronova, A., Yuzwa, S. A., Wang, B. S., Zahr, S., Syal, C., Wang, J., et al. (2017). Migrating interneurons secrete fractalkine to promote oligodendrocyte formation in the developing mammalian. *Brain Neuron* 94, 500–516. doi: 10.1016/j.neuron.2017.04.018

Wake, H., Ortiz, F. C., Woo, D. H., Lee, P. R., Angulo, M. C., and Fields, R. D. (2015). Nonsynaptic junctions on myelinating glia promote preferential myelination of electrically active axons. *Nat. Commun.* 6:7844. doi: 10.1038/ncomms8844

Wamsley, B., and Fishell, G. (2017). Genetic and activity-dependent mechanisms underlying interneuron diversity. *Nat. Rev. Neurosci.* 18, 299–309. doi: 10.1038/nrn.2017.30

Wong, F. K., Bercsenyi, K., Sreenivasan, V., Portalés, A., Fernández-Otero, M., and Marín, O. (2018). Pyramidal cell regulation of interneuron survival sculpts cortical networks. *Nature* 557, 668–673. doi: 10.1038/s41586-018-0139-6

Yizhar, O., Fenno, L. E., Davidson, T. J., Mogri, M., and Deisseroth, K. (2011). Optogenetics in neural systems. *Neuron* 71, 9–34. doi: 10.1016/j.neuron.2011.06.004

Zhang, F., Wang, L. P., Boyden, E. S., and Deisseroth, K. (2006). Channelrhodopsin-2 and optical control of excitable cells. *Nat. Methods* 3, 785–792. doi: 10.1038/nmeth936

Zhang, F., Wang, L. P., Brauner, M., Liewald, J. F., Kay, K., Watzke, N., et al. (2007). Multimodal fast optical interrogation of neural circuitry. *Nature* 446, 633–639. doi: 10.1038/nature05744

Zonouzi, M., Scafidi, J., Li, P., McEllin, B., Edwards, J., Dupree, J. L., et al. (2015). GABAergic regulation of cerebellar NG2 cell development is altered in perinatal white matter injury. *Nat. Neurosci.* 18, 674–682. doi: 10.1038/nn.3990

Conflict of Interest Statement: The authors declare that the research was conducted in the absence of any commercial or financial relationships that could be construed as a potential conflict of interest.

Article II

A. Objective

Convergent evidences pointed out a common embryonic origin and a close relationship of GABAergic INs and OPCs derived from MGE and POA derived during postnatal development. The majority of INs arise from these two embryonic regions, the 60% and 10% respectively, as well as the firstOPCs (Kessaris et al., 2006). Interestingly both progenitors express the transcription factor Nkx2.1 (Butt et al., 2008; Kessaris et al., 2006).

« Beside this common embryonic origin, GABAergic INs and OPCs are also close partners during cortical development. It has been shown that migrating INs communicate to OPCs by secreting factors that promote oligodendrogenesis. In addition, as we already mentioned before, OPCs represent the only non-neuronal cell type in the CNS that receive functional synaptic inputs from neurons and are innervated by GABAergic INs » (Orduz et al., 2019). In the mouse somatosensory cortex, the team described a peak of GABAergic synaptic activity of OPCs at PN 10, restricted to a precise temporal window and characterized by a highly sophisticated spatial organization of interneuron-OPC microcircuits (Orduz et al., 2015). « Interestingly, this connectivity occurs in parallel with the period of massive PCD of both cortical INs and OPCs» (Orduz et al., 2019). In particular, firstOPCs are believed to completely disappear at the end of cortical development while up to 40% of INs coming from the same embryonic regions are eliminated in the first postnatal week (Southwell et al., 2012; Kessaris et al., 2006).

Considering the convergence in the embryonic origin of INs and firstOPC, their concommittant death and their highly regulated transient connectivity, we hypothesized the existence of a fine-tuned balance between OPCs and their ontogenetically-related INs that might participate to cortical construction.

In order to assess the functional impact on cortical development of the strong relationship between firstOPCs and their embrionically interneuronal partners, we first focus our attention on the transient and very local arrangement of IN-firstOPC microcircuits, analyzing their spatial organization and connectivity. Second, we analyzed the fate of a surviving subpopulation of cortical firstOPCs during the second and third postnatal weeks. Finally, we

prevented the death of these two ontogenetically-related cell populations by genetically inducing the survival of cells committed to die and analyzed the consequences. We specifically inactivated the pro-apoptotic Bax in both INs and firstOPCs using the Cre *Nkx2.1^{Cre};Rosa26^{tdTomato}* line crossed to Bax$^{f/f}$;Bak$^{+/-}$ mice. Rosa26^{tdTomato} is used to label Bax knockout cells. We first evaluated the death and survival of different subtypes of INs and firstOPCs derived from a common embryonic origin to then analyze the impact of rescued INs and OPCs on cortical circuit formation, maturation and myelination. In summary, our aim was to understand how ontogenetically-related INs and OPCs interact during postnatal development.

B. Methodology

1) Transgenic Cre-Lox mice used in our study

In this study, we produced several transgenic lines. First, we used Dbx1^{Cre} , Nkx2.1^{Cre}, Rosa26^{YFP}, Rosa26^{tdTomato} lines to generate Dbx1^{Cre}/Rosa26^{YFP}, Nkx2.1^{Cre}/Rosa26^{YFP} and Nkx2.1^{Cre}/Rosa26^{tdTomato} transg enic mice which allowed us to follow cells derived from the ePOA and MGE and POA respectively (Xu et al., 2008 ; Hirata et al., 2009). « . The Dbx1^{Cre}/Rosa26^{YFP} and Nkx2.1^{Cre}/Rosa26^{YFP} mice were also crossed with the NG2^{DsRed} transgenic mouse in order to recognize the whole OPC population by the expression of the red fluorescent protein variant (DsRed.T1) expressed under the control of the mouse NG2 (*Cspg4*) promoter/enhancer (Zhu et al., 2008).

We then generated Dbx1^{Cre}/Rosa26^{YFP}/PLP^{DsRed}, triple transgenic mice in which the proteolipid protein (PLP) promoter targets the expression of DsRed , specifically in mature OLs. This mouse line allowed us to follow FirstOLs derived from Dbx1-expressing progenitors of the POA through YFP fluoresence, and OLs from all origins through DsRed (Orduz et al., 2019).

In addition, we used the Nkx2.1^{Cre} transgenic line crossed with the *Rosa26^{tdTomato}* transgenic mouse to genetically target Nkx2.1-expressing progenitors from the POA and MGE (Jax laboratories). Finally, we crossed

Nkx2.1^{Cre};Rosa26^{tdTomato} with the *Bax^{tm2Sjk};Bak$^{tm1Thsn/J}$* to induce the survival of Nkx2.1-derived FirstOPC and IN survival. Stanley J. Korsmeyer's lab (Harvard Medical School) designed this transgenic line, using a vector to flank exons 2-4 with loxP sites in Bax sequence. « When bred to Cre recombinase expressing mice, the resulting offspring will have exons 2-4 of Bax deleted in the cre-expressing tissues (determined by promoter driving cre expression) » (Jax laboratories). For Bak, Dr. Craig B. Thompson's lab (University of Pennsylvania) designed a vector to replace exons 3-6 (encoding the Bcl2 homology domains) with a neo cassette. We crossed this line with the *Bax^{tm2Sjk};Bak$^{tm1Thsn/J}$* line harboring the floxed *Bax* allele and the *Bak* knock-out allele in order to inactivate *Bax* and permanently label Nkx2.1-derived cells. Thus, we used *Nkx2.1^{Cre};Rosa26^{tdTomato};Bak$^{+/-}$;Bax$^{f/f}$* line as knockout mice.

C. Main results

In my second project, we genetically target ontogenetically-related Dbx1- and Nkx2.1-derived INs and oligodendroglia to follow the dynamic of their death and survival as well as IN-OPC microcircuits. Finally, to study the role of these two cell types in circuit formation during cortical development, we induce Nkx2.1-derived IN and firstOPC survival by using a genetic approach that inactivates Bax and Bak in these cells.

1) <u>Connectivity between Dbx1-derived INs and firstOPCs</u>

In Dbx1^{Cre};Rosa26^{YFP};NG2^{DsRed} mice, INs and firstOPCs derived from Dbx1-expressing progenitors of the POA were lineage-traced with the fluorescent reporter YFP, and OPCs from all origins with DsRed. In this line, we observed in the somatosensory cortex at PN 10, i.e. at the peak of synaptic connectivity between INs and OPCs (Orduz et al. 2015), that YFP$^+$ cells were forming small groups of cells spatially close to each other. In order to asses the presence of firstOPCs in these groups, we identified the YFP$^+$/DsRed$^+$ cells and verified their identity by co-labeling with the

oligodendroglial lineage marker Olig2. The small cell groups observed were composed of YFP^+ INs only, $YFP^+/DsRed^+$ OPCs only or YFP^+ INs and $YFP^+/DsRed^+$ OPCs simultaneously. Interestingly, we also observed that the stimulation of presynaptic YFP^+ INs elicited synaptic currents on neighbor $YFP^+/DsRed^+$ OPCs in 42.8% of tested pairs, completely abolished by $GABA_AR$ antagonist Gabazine, confirming the GABAergic nature of these synapse. On the contrary, the connection probability was significantly reduced in all IN-OPC tested pairs (23.8%) or pairs with $YFP^-/DsRed^+$ OPCs (13.5%).

This tight spatial arrangement of $YFP^+/DsRed^+$ OPCs with their ontogenetically-related INs and the preferential connectivty of YFP^+ INs with $YFP^+/DsRed^+$ OPCs suggest potential specific interactions between these two cell populations. This study identifies the common embryonic origin as a factor favoring IN-OPC connectivity.

2) Dbx1-derived INs and firstOPCs form cell clusters

In the $Dbx1^{Cre};Rosa26^{YFP}$ mice at PN 10, « using the unsupervised hierarchical cluster analysis via multi-scale bootstrap resampling, we evaluated the existence of unbiased YFP^+ cell groups clustered according to their intersomatic cell distance » (Orduz et al., 2019).

We were able to recognized clusters composed by INs only (62.4%), INs and oligodendroglia (mixed, 26.1%) or oligodendroglia only ($Olig2^+$ cells, 11.5%).

3) Surviving Dbx1-derived OPCs produce OLs in cell clusters

We analyzed the distribution and fate of Dbx1-derived oligodendroglia during development in the somatosensory cortex and observed a decrease in the density of $YFP^+/Olig2^+$ cells from PN 4 to PN 10. From PN 10 to PN 19, in contrast, we did not observe significant changes in the densities of $YFP^+/Olig2^+$ cells, and all $Olig2^+$ cells remained relatively stable. We also showed that surviving $YFP^+/Olig2^+/CC1^-$ OPCs became mature OLs mantaining the organization in cell clusters at PN 19.

4) Dbx1-derived OLs myelinate multiple axons inside the clusters

Using $Dbx1^{Cre}$;$Rosa26^{YFP}$;PLP^{DsRed} triple transgenic mice, in which PLP promoter targets the expression of DsRed specifically in mature OLs, we performed triple immunostainings against YFP to trace Dbx1-expressing progenitors, the axonal marker SMI-312 and the MBP. We observed that YFP^+/$DsRed^+$ OLs myelinate axons surrounding their YFP^+ interneuron partners. We also performed other stainings against SMI-312 and PV which revealed that PV^+ axonal segments co-localized with branches of YFP^+/$DsRed^+$ OLs in cell clusters. In addition, about a fifth of these branches were SMI-312^+/PV^+ while the others were SMI-312^+/PV^-. « Similar proportions were observed for YFP^-/$DsRed^+$ OLs derived from other origins outside YFP^+ cell clusters. Therefore, YFP^+/$DsRed^+$ OLs from the POA behave as other OLs and myelinate PV^+ and PV^- neurons without a preference for PV^+ axons, indicating that the function of these clusters is not to preferentially myelinate YFP^+ IN partners » (Orduz et al., 2019). « Finally, the branches of these YFP^+/$DsRed^+$ OLs covered relatively small areas, suggesting that they myelinate GABAergic PV^+ and glutamatergic PV^- fibers being part of the YFP^+ IN microcircuit » (Orduz et al., 2019).

5) Connectivity between Nkx2.1-derived INs and firstOPCs

We observed that Nkx2.1-derived INs showed a high connectivity with their lineage-related firstOPCs while a low connectivity with OPCs coming from other embryonic regions. These data demonstrated that firstOPCs from both MGE and POA in physiological conditions remains synaptically connected with their ontogenetically-related INs in the postnatal neocortex. On the contrary, once we induced the aberrant survival of ontogenetically-related firstOPCs and IN by inactivating Bax, we found that the cells prevented to die did not show the same high connection probability observed in physiological condition during the second postnatal

week. This suggests that the connectivity between the two populations may be a signal promoting survival.

6) Programmed cell death is key for oligodendroglia homeostasis

Interestingly, contradicting our expectations, we observed that the population of rescued tdTomato^{+}/Olig2^{+} cells was not compensated by a reduction of OPCs from other embryonic origins but, on the contrary, induced an increase in the density of the other following OPC waves tdTomato^{-}/Olig2^{+}. The PCD is thus not only a mechanism to ensure a correct IN-first OPC interactions and reach a proper excitation/inhibition balance of neuronal networks, but is also required to regulate the densities of OPCs and myelinating OLs in the cortex. We also observed a consequent increase in myelination in cortical deeper layers concordant with the increase in mature OLs density identified in LV-VI » (Orduz et al., 2019).

nature COMMUNICATIONS

ARTICLE

https://doi.org/10.1038/s41467-019-11904-4 OPEN

Developmental cell death regulates lineage-related interneuron-oligodendroglia functional clusters and oligodendrocyte homeostasis

David Orduz[1,2,5,6], Najate Benamer[1,2,3,6], Domiziana Ortolani[2,3,6], Eva Coppola[2,3,4], Lisa Vigier[2,3,4], Alessandra Pierani[2,3,4] & María Cecilia Angulo[1,2,3]

The first wave of oligodendrocyte precursor cells (firstOPCs) and most GABAergic interneurons share common embryonic origins. Cortical firstOPCs are thought to be replaced by other OPC populations shortly after birth, maintaining a consistent OPC density and making postnatal interactions between firstOPCs and ontogenetically-related interneurons unlikely. Challenging these ideas, we show that a cortical firstOPC subpopulation survives and forms functional cell clusters with lineage-related interneurons. Favored by a common embryonic origin, these clusters display unexpected preferential synaptic connectivity and are anatomically maintained after firstOPCs differentiate into myelinating oligodendrocytes. While the concomitant rescue of interneurons and firstOPCs committed to die causes an exacerbated neuronal inhibition, it abolishes interneuron-firstOPC high synaptic connectivity. Further, the number of other oligodendroglia populations increases through a non-cell-autonomous mechanism, impacting myelination. These findings demonstrate unprecedented roles of interneuron and firstOPC apoptosis in regulating lineage-related cell interactions and the homeostatic oligodendroglia density.

[1] Neurophysiology and New Microscopies laboratory, INSERM U1128, 75006 Paris, France. [2] Université de Paris, 75006 and 75013 Paris, France. [3] Institute of Psychiatry and Neuroscience of Paris (IPNP), INSERM U1266, 75014 Paris, France. [4] Imagine Institute of Genetic Diseases, 75015 Paris, France. [5] Present address: Gfi informatique, Saint-Ouen-sur-Seine, France. [6] These authors contributed equally: David Orduz, Najate Benamer, Domiziana Ortolani. Correspondence and requests for materials should be addressed to M.C.A. (email: maria-cecilia.angulo@parisdescartes.fr)

During development, oligodendrocyte precursor cells (OPCs), the obligate progenitors of myelinating oligodendrocytes (OLs) in the Central nervous system (CNS), arise from multiple restricted periventricular germinal regions. Three sequential waves of OPCs populate the cerebral cortex according to a ventro-dorsal temporal progression[1]. A first wave arises from Nkx2.1-expressing precursors of the medial ganglionic eminence (MGE) and the embryonic preoptic area (ePOA) around the embryonic day 12.5 (E12.5). A second wave is generated by E14.5 from precursors expressing the homeobox gene Gsx2 in the lateral and medial ganglionic eminences (LGE and MGE) and, finally, a third wave arises at birth from precursors expressing the homeobox gene Emx1 in the cortex[1].

Cre-loxP fate mapping in transgenic mice revealed that the first wave of OPCs (firstOPCs) from the MGE and ePOA is eliminated 10 days after birth in the mouse cerebral cortex, and replaced by OPCs produced in the second and third waves[1]. Although firstOPCs survive in other CNS regions[1,2], their massive death in the neocortex makes unlikely any role of this OPC population in cortical circuit maturation and myelination[1,3]. Furthermore, the genetic ablation of firstOPCs led to the conclusion that this cell population may play redundant functions with other OPCs since they are replaced with no drastic alterations of myelination[1,2]. In fact, OPCs tend to homeostatically maintain their cell number[4,5], and it is assumed that competition among OPC waves participates to this process during development[1].

As firstOPCs, the majority of cortical GABAergic interneurons are born from progenitors expressing the transcription factor Nkx2.1 settled in the MGE and ePOA[6]. While the MGE produces around 60% of the entire interneuron population, the ePOA contributes with ~10% (refs. [6–8]). Beyond this common embryonic origin, interneurons and OPCs are close partners during cortical development. First, migrating interneurons signal to OPCs in a paracrine fashion by secreting factors that promote oligodendrogenesis[9,10]. Furthermore, OPCs represent the only non-neuronal cell type in the CNS that receive functional synaptic inputs from neurons and are innervated by GABAergic interneurons[11–13]. In the mouse somatosensory cortex, the GABAergic synaptic activity of OPCs reaches a peak at postnatal day 10 (PN10) and then declines[12,14,15]. Restricted to a precise temporal window, OPC connectivity is characterized by a highly sophisticated spatial organization of interneuron-OPC microcircuits[15]. Interestingly, this transient connectivity occurs during the period of massive programmed cell death of both cortical interneurons and OPCs[1,12,15,16]. Indeed, the entire firstOPC population[1] and 40% of interneurons[16] are eliminated during the first two postnatal weeks. The convergence in the embryonic origin of interneurons and firstOPC, their death and their highly regulated transient interneuron-OPC connectivity suggests possible interactions between these two cell types that might participate to cortical construction.

Challenging the above-mentioned established views, our results demonstrate that not all firstOPCs die in the developing neocortex and that the surviving subpopulation displays a specific spatial distribution and a preferential synaptic connectivity with their ontogenetically-related interneurons. Furthermore, the induction of the concomitant survival of MGE- and ePOA-derived interneurons and firstOPCs committed to die causes a significant decrease of interneuron-firstOPC connection probability while generating an exacerbated neuronal inhibition. Therefore, although rescued interneurons are functional and target other neurons, they lack their preferential connectivity with firstOPCs. Finally, the prevention of interneuron and firstOPC apoptosis causes a general increase in the entire oligodendroglia population and a hypermyelination of deep cortical layers after the end of the period of massive cortical programmed cell death. Our results contradict the notion that different OPC waves play redundant roles and compensate for each other.

Results

Connectivity between Dbx1-derived interneurons and firstOPCs. The common embryonic origin of interneurons and firstOPCs may impact the transient and very local arrangement of interneuron-OPC microcircuits previously reported in the somatosensory cortex[15]. Progenitors expressing the transcription factor Dbx1 in the ePOA produce a subset of firstOPCs that begin the invasion of cortical territories by E14 (refs. [17,18]). In addition, they also give rise to a small, but very diverse population of interneurons that preferentially invades deep cortical layers[7,8,17]. To specifically follow firstOPCs and interneurons from the ePOA at postnatal stages, we produced *Dbx1^{CRE};Rosa26^{YFP};NG2^{DsRed}* triple transgenic mice. In this mouse line, interneurons and firstOPCs derived from Dbx1-expressing progenitors of the ePOA were lineage-traced with the fluorescent reporter YFP, and OPCs from all origins with DsRed[18,19]. We initially examined sections of the somatosensory cortex at PN10 when interneurons reach a peak of synaptic connectivity with OPCs[15]. As expected from previous reports[7,8,17], YFP$^+$ cells were scarce and distributed mainly in cortical layers V and VI (Fig. 1a). Interestingly, we observed that instead of appearing homogeneously distributed, a majority of them were rather prone to gather together by forming small cell groups spatially segregated from one another (Fig. 1a). To assess the presence of firstOPCs in these groups, we searched for YFP$^+$/DsRed$^+$ cells and verified their identity by co-labeling with the oligodendroglial lineage marker Olig2 (Fig. 1a). Groups of Dbx1-derived cells were composed of YFP$^+$ interneurons only, YFP$^+$/DsRed$^+$ OPCs only or YFP$^+$ interneurons and YFP$^+$/DsRed$^+$ OPCs simultaneously. This narrow spatial arrangement of YFP$^+$/DsRed$^+$ OPCs with their ontogenetically related interneurons suggests potential specific interactions between these two cell types.

OPCs synaptically interact with interneurons by forming very local microcircuits during the second postnatal week[15]. We thus compared the synaptic connection probability of presynaptic YFP$^+$ interneurons with either YFP$^+$/DsRed$^+$ OPCs (from Dbx1-expressing progenitors) or YFP$^-$/DsRed$^+$ OPCs (from other sources) using paired recordings in layers V and VI of acute somatosensory cortical slices during the second postnatal week. Patched cell pairs never exceeded intersomatic distances of 80 µm to remain in the spatial range of interneuron-OPC connections[15]. We found that the stimulation of presynaptic YFP$^+$ interneurons elicited synaptic currents on neighbor YFP$^+$/DsRed$^+$ OPCs in 42.8% of tested pairs (Fig. 1b, c). The evoked postsynaptic currents (PSCs) were completely abolished by the $GABA_A$ receptor antagonist SR95531 (Gabazine), confirming the GABAergic nature of these synapses (Fig. 1b). Interestingly, the connection probability was significantly reduced when considering all interneuron-OPC tested pairs (23.8%) or pairs with YFP$^-$/DsRed$^+$ OPCs (13.5%, Fig. 1c). The 3.2-fold higher connection probability of postsynaptic YFP$^+$/DsRed$^+$ OPCs compared to YFP$^-$/DsRed$^+$ OPCs was not accompanied by changes either in PSC amplitudes or short-term synaptic plasticity (mean amplitudes: -5.54 ± 1.23 pA vs. -5.57 ± 1.26 pA, respectively, $p = 0.98$; paired-pulse ratio: 0.45 ± 0.03 vs. 0.49 ± 0.06, respectively, $p = 0.55$, Mann–Whitney U test; data represent mean ± SEM). In addition, we observed a peak of connectivity at PN10-11 for both YFP$^+$/DsRed$^+$ OPCs and YFP$^-$/DsRed$^+$ OPCs (Fig. 1d), indicating that the connectivity of YFP$^+$ interneurons with OPCs derived from distinct origins followed the similar developmental regulation of the entire interneuron population[15].

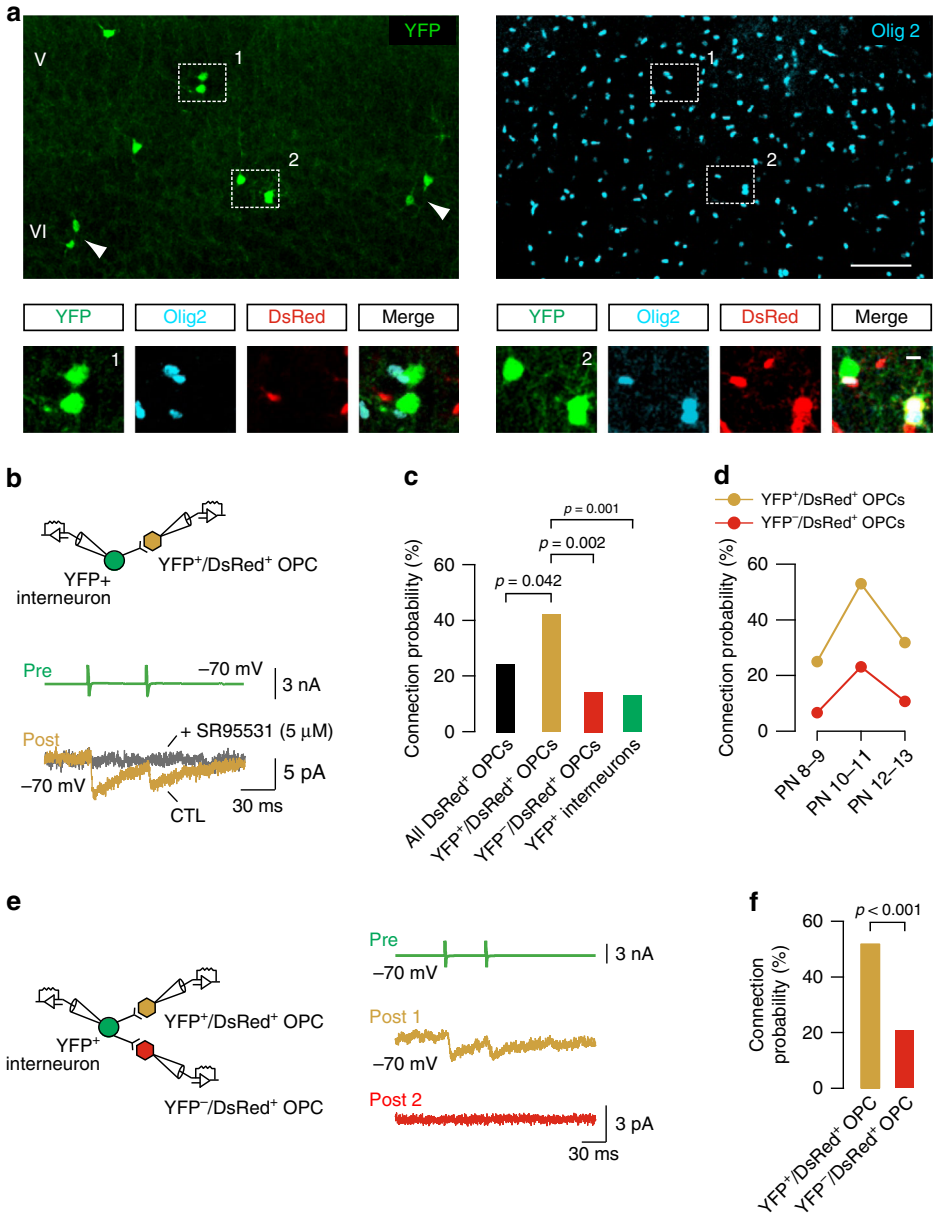

Fig. 1 Dbx1-derived interneurons preferentially target OPCs from the same lineage. **a** Confocal images of YFP$^+$ interneurons (green) and YFP$^+$/DsRed$^+$ OPCs (green and red) in layers V and VI of the somatosensory cortex in a *Dbx1^{CRE};Rosa26^{YFP};NG2^{DsRed}* mouse at PN10. Olig2 (cyan, right) immunolabeling for the same cortical field identifies oligodendroglia within these groups. White dotted squares surround two YFP$^+$ cell groups shown in insets. The first group (1) is composed of two YFP$^+$ interneurons and the second (2) of a YFP$^+$ interneuron and two YFP$^+$/DsRed$^+$/Olig2$^+$ OPCs. Arrowheads point to two other groups of YFP$^+$ interneurons. Scale bars: 100 and 10 µm. **b** Paired recording between a presynaptic YFP$^+$ interneuron and a YFP$^+$/DsRed$^+$ OPC. Action currents evoked in a YFP$^+$ interneuron (green) elicited PSCs recorded in a YFP$^+$/DsRed$^+$ OPC (yellow; average of 100 traces) that were abolished by the $GABA_A$ receptor antagonist SR95531 (5 µM, gray; $n = 5$ connected pairs). **c** Connection probabilities for all tested DsRed$^+$ OPCs (black, $n = 168$), YFP$^+$/DsRed$^+$ OPCs (yellow, $n = 56$), YFP$^-$/DsRed$^+$ OPCs (red, $n = 118$) and postsynaptic YFP$^+$ interneurons (green, $n = 72$). Note that presynaptic YFP$^+$ interneurons target preferentially YFP$^+$/DsRed$^+$ OPCs compared to YFP$^-$/DsRed$^+$ OPCs or postsynaptic YFP$^+$ interneurons (Chi-squared test; significant *p*-values are indicated). **d** Connection probabilities for YFP$^+$/DsRed$^+$ OPCs (yellow) and YFP$^-$/DsRed$^+$ OPCs (red) as a function of three postnatal stages (PN8-9, PN10-11 and PN12-13; $n = 12$, $n = 17$, $n = 6$ tested pairs for YFP$^+$/DsRed$^+$ OPCs and $n = 15$, $n = 26$, $n = 17$ tested pairs for YFP$^-$/DsRed$^+$ OPCs). **e** Sequential paired recordings between a single presynaptic YFP$^+$ interneuron (green) and two different neighbor OPCs, a YFP$^+$/DsRed$^+$ OPC (yellow) and a YFP$^-$/DsRed$^+$ OPC (red). Note that action currents evoked in the YFP$^+$ interneuron elicited PSCs in the YFP$^+$/DsRed$^+$ OPC, but not in the YFP$^-$/DsRed$^+$ OPC. **f** Connection probabilities for sequential paired recordings revealed a high connection probability for YFP$^+$/DsRed$^+$ OPCs (yellow) compared to YFP$^-$/DsRed$^+$ OPCs (red; $n = 58$ sequential paired recordings) (Chi-squared test)

The preference of YFP$^+$ interneurons to innervate YFP$^+$/DsRed$^+$ OPCs suggests that interneuron-OPC connectivity is positively influenced by the embryonic origin. However, this preferential connectivity could also result from a higher capacity of YFP$^+$ interneurons to innervate any surrounding cell when organized in YFP$^+$ cell groups. Since YFP$^+$ interneurons were also often close to each other (Fig. 1a), we tested their synaptic connectivity when their intersomatic distances were <80 µm. Despite sharing a common

origin, pairs of YFP$^+$ interneurons had a lower connection probability (13.9%) than that of their ontogenetically related YFP$^+$/DsRed$^+$ OPCs in the second postnatal week (Fig. 1c; Supplementary Fig. 1). In addition, we used sequential paired recordings between a single presynaptic YFP$^+$ interneuron and two distinct neighbor OPCs to compare, within the same YFP$^+$ cell group, the connection probability between YFP$^+$/DsRed$^+$ OPCs and YFP$^-$/DsRed$^+$ OPCs (Fig. 1e). We also observed a 2.6-fold increased connectivity onto YFP$^+$/DsRed$^+$ OPCs compared to YFP$^-$/DsRed$^+$ OPCs inside YFP$^+$ cell groups (Fig. 1e, f). Therefore, in comparison to other neighbor postsynaptic YFP$^+$ interneurons or OPCs from different origins, YFP$^+$/DsRed$^+$ OPCs constituted the preferential synaptic target of YFP$^+$ interneurons when these two YFP$^+$ cell types were spatially associated. As for the entire populations of interneurons and OPCs[15], Dbx1-derived YFP$^+$ fast-spiking interneurons (FSI) and non-fast interneurons (NFSI) innervated YFP$^+$/DsRed$^+$ OPCs and YFP$^-$/DsRed$^+$ OPCs (Supplementary Fig. 2). However, YFP$^+$ FSIs constituted a prevalent presynaptic input onto any OPC (Supplementary Fig. 2c). We concluded that, in the second postnatal week, the connectivity between interneurons and firstOPCs is favored by their embryonic origin.

Dbx1-derived interneurons and firstOPCs form cell clusters. Our functional data showed a preferential connectivity between interneurons and firstOPCs derived from the ePOA in groups of YFP$^+$ cells at postnatal stages. Therefore, these cells should form predictable YFP$^+$ cell clusters throughout layers IV and VI in *Dbx1^{CRE};Rosa26^{YFP}* mice at PN10, *i.e.* at the peak of their synaptic connectivity (Fig. 1d). To test this possibility, we used unsupervised hierarchical cluster analysis via multi-scale bootstrap resampling to evaluate the existence of unbiased YFP$^+$ cell groups clustered according to their intersomatic cell distances[20,21]. To discriminate YFP$^+$ interneurons from YFP$^+$ oligodendroglia in large field of views, we performed immunolabelings against YFP, the marker for the oligodendrocyte lineage Olig2 and the marker for mature OLs CC1 (Fig. 2a, b). We considered YFP$^+$/Olig2$^-$/CC1$^-$ cells as interneurons, YFP$^+$/Olig2$^+$/CC1$^-$ cells as firstOPCs, YFP$^+$/Olig2$^+$/CC1$^+$ cells as differentiated OLs and calculated Manhattan distances from their *x*, *y*, *z* coordinates (see Methods). Figure 2c illustrates a dendrogram showing the hierarchical relationship between identified YFP$^+$ cells, grouped according to their Manhattan distances. By randomly resampling elements of the data, the bootstrap-based approach computed *p*-values for each YFP$^+$ cell cluster at each branch of the dendrogram[20]. Only cell groups with a 95% confidence probability were considered as clusters supported by data (Fig. 2b, c, gray boxes). This statistical analysis revealed that most YFP$^+$ cells were organized in cell clusters (Fig. 2c). We found that 72.5% of detected clusters were formed by two to three cells and 93.6% of clusters contained a maximum of seven cells, indicating that a cluster size is restricted to few cells (Fig. 2d). We recognized clusters composed by interneurons only (62.4%), interneurons and oligodendroglia (mixed, 26.1%) or oligodendroglia only (Olig2$^+$ cells, 11.5%) (Fig. 2b, c, e). When considering all intersomatic distances (Euclidean) among YFP$^+$ cells in clusters, the mean distance in mixed and Olig2$^+$ cell clusters was significantly reduced with respect to that of clusters formed exclusively by YFP$^+$ interneurons (Supplementary Fig. 3a). However, when considering clusters containing only two YFP$^+$ cells, both YFP$^+$ interneuron and mixed clusters displayed similar distances (Supplementary Fig. 3b). The mean intersomatic distance of mixed clusters containing only two cells was limited to 70 ± 4 µm (Supplementary Fig. 3b). In line with the existence of predictable clusters, all connected pairs found with patch-clamp recordings occupied a very confined space with interneuron-OPC intersomatic distances <60 µm, independently of the origin of cells (Supplementary Fig. 4).

The computation analysis and distribution of OPCs in connected pairs showed that the organization of YFP$^+$ cells in cortical layers IV–VI is not random and follows a distribution where YFP$^+$ interneurons and YFP$^+$ oligodendroglia appear often close to each other. These results indicate that the preferential connectivity of interneurons and firstOPCs from the Dbx1 cell lineage can be predicted by the existence of these clusters.

Surviving Dbx1-derived OPCs produce OLs in cell clusters. It is considered that the first wave of OPCs does not play a role at postnatal stages in the neocortex because it totally disappears at around PN10 (refs. [1,3]), when the myelination process has not started yet. However, our data revealed the presence of functional lineage-related interneuron-firstOPC connections during the second postnatal week, indicating that a subpopulation of cortical firstOPCs survives. We therefore analyzed the distribution and fate of Dbx1-derived oligodendroglia during development in the somatosensory cortex (Fig. 3). We observed a seven-fold decrease in the density of YFP$^+$/Olig2$^+$ cells from PN4 to PN10 which were mainly firstOPCs at these ages (Fig. 3a, b). As expected, similar dynamics were observed for the total number of Olig2$^+$ cells and OPCs, but the decrease from PN4 to PN10 was much less pronounced (Fig. 3e, f). Together, these results indicate that firstOPCs constituted a main population of Olig2$^+$ progenitors dying during the first postnatal days. From PN10 to PN19, the densities of YFP$^+$/Olig2$^+$ cells and all Olig2$^+$ cells remained relatively stable (Fig. 3a, e). As for the whole population of OPCs and OLs (Fig. 3f, g), a reduction in the density of YFP$^+$/Olig2$^+$/CC1$^-$ OPCs at PN10 was followed by an increase in the density of YFP$^+$/Olig2$^+$/CC1$^+$ OLs at PN19 (Fig. 3b–d), indicating that surviving YFP$^+$/Olig2$^+$/CC1$^-$ OPCs became mature OLs (referred as firstOLs). At PN90, the density of YFP$^+$/Olig2$^+$ cells were not significantly different to those at PN10 and PN19 but showed a tendency to decrease (Fig. 3a–c). In fact, the entire Olig2$^+$ cell population also decreased at this age, probably because the brain reached its adult size (Fig. 3e). Interestingly, unsupervised hierarchical cluster analysis revealed that a majority of YFP$^+$ cells were still organized in cell clusters at PN19 and followed similar distributions and compositions to clusters at PN10 (Supplementary Fig. 3c–i). In particular, the mean intersomatic distance in mixed clusters formed by two cells was similar between the two developmental stages (~70 µm; Supplementary Fig. 3b, d). Finally, these clusters were also visualized in the motor and visual cortex where the dynamics of YFP$^+$ oligodendroglia followed similar trends during postnatal development (Supplementary Fig. 5).

In conclusion, YFP$^+$ interneurons and YFP$^+$ OLs keep their organization in cell clusters at later development stages, suggesting that interneurons and firstOPCs from the Dbx1 cell lineage form a functional unit that persists in the postnatal neocortex.

Dbx1-derived OLs myelinate multiple axons inside clusters. To determine the capacity of YFP$^+$ OLs to myelinate axonal fibers in the third postnatal week, we generated a *Dbx1^{CRE};Rosa26^{YFP};PLP^{DsRed}* triple transgenic mice in which the proteolipid protein (PLP) promoter targets the expression of DsRed specifically in CC1$^+$ OLs[4,22]. This mouse line allowed us to lineage-trace first-OLs derived from Dbx1-expressing progenitors of the ePOA with the fluorescent reporter YFP, and OLs from all origins with DsRed. We imaged cell clusters composed of YFP$^+$/DsRed$^+$ OLs and YFP$^+$/DsRed$^-$cells recognized as interneurons by their large somata (Fig. 4a, c) and, in some cases, by the expression of Parvalbumin (PV), a specific marker for FSI (Fig. 4d). Similar to

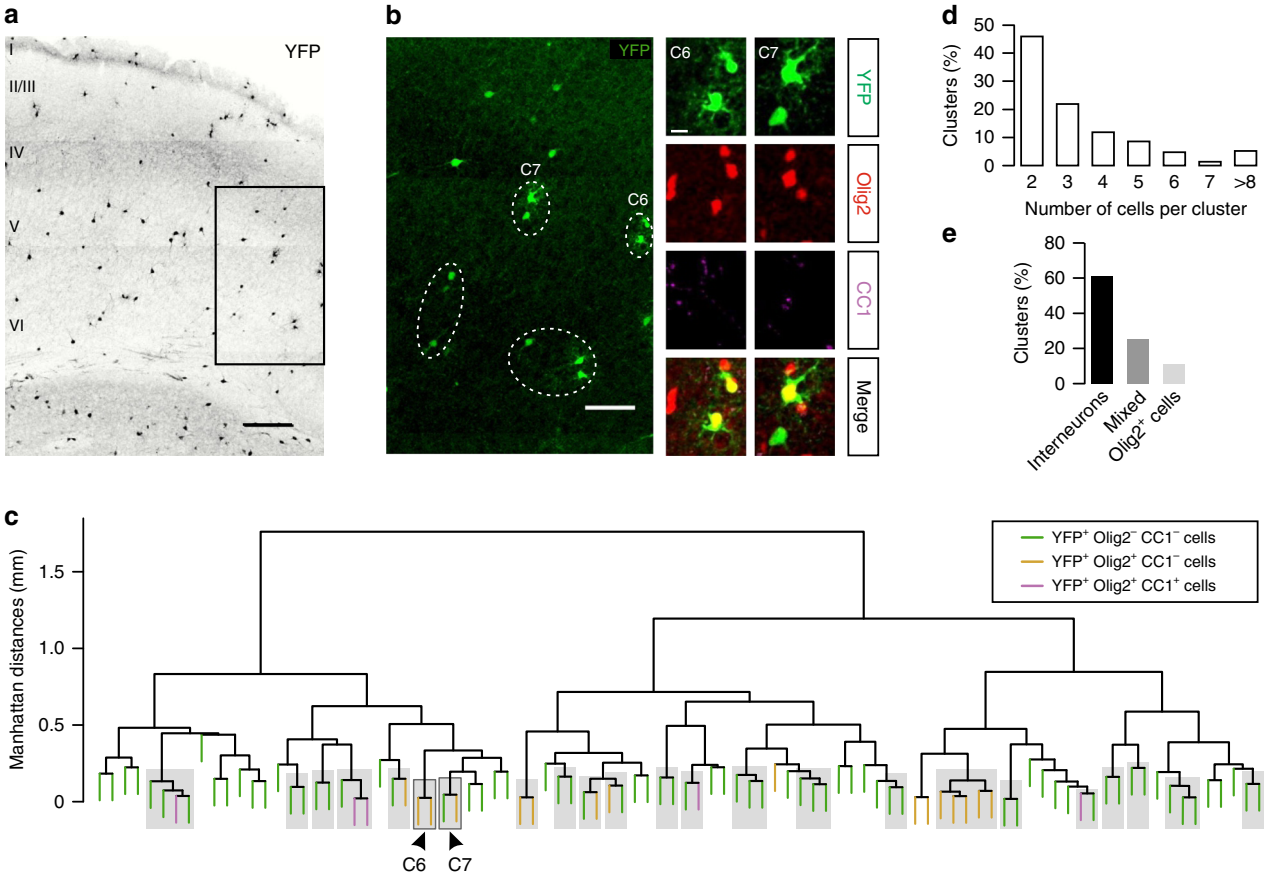

Fig. 2 Dbx1-derived interneurons and OPCs form cell clusters at PN10. **a** Confocal image of a coronal section of the somatosensory cortex from a PN10 *Dbx1*^{CRE};*Rosa26*^{YFP} mouse showing YFP$^+$ cells. Scale bar: 200 µm. **b** Magnification of the rectangle in **a** showing the unsupervised clusters of YFP$^+$ cells detected by hierarchical cluster analysis in this region (dotted ellipses). Insets: two identified clusters containing OPCs and detected with an approximately unbiased *p*-value ≥ 0.95. They are indicated by arrowheads in the dendrogram in **c**. Note that C6 is formed by two YFP$^+$/Olig2$^+$/CC1$^-$OPCs and C7 by a YFP$^+$ interneuron (negative for both Olig2 and CC1) and a YFP$^+$/Olig2$^+$/CC1$^-$OPC, showing the co-existence of different cell clusters. Mature YFP$^+$/Olig2$^+$/CC1$^+$ OLs are rarely observed at this age. Scale bars: 80 and 10 µm. **c** Hierarchical clustering dendrogram displaying the relationship between Dbx1-derived interneurons (green), OPCs (yellow) and OLs (magenta) according to their Manhattan distances in the same slice. Detected YFP$^+$ cell clusters with approximately unbiased *p* values ≥ 95% are shown in gray boxes while isolated cells are outside these boxes (72 ± 3% cells in clusters vs. 28 ± 3% isolated cells; $n = 11$ slices from 4 mice, $p < 0.0001$, Mann–Whitney *U* test). **d**, **e** Percentages of clusters according to the number of cells per cluster (**d**) and the cell composition (**e**)

PN10, YFP$^+$/DsRed$^+$ OLs at PN19 appeared confined around YFP$^+$ interneurons compared to YFP$^-$/DsRed$^+$ OLs, confirming the existence of mixed clusters formed by lineage-related interneurons and firstOLs later in development (Fig. 4e, f).

First, we performed triple immunostainings against YFP, the axonal marker SMI-312 and the myelin basic protein (MBP) (Fig. 4a, b). In 11 analyzed clusters, a large number of branches of YFP$^+$/DsRed$^+$ OLs co-localized with both SMI-312 and MBP (Fig. 4b). Hence, differentiated YFP$^+$/DsRed$^+$ OLs myelinate axons surrounding their YFP$^+$ interneuron partners (Fig. 4c). Interestingly, PV$^+$ interneurons which constitute a major input of OPCs at PN10[15] are the main myelinated GABAergic interneuron subtype in the cortex[23–25]. We thus tested whether YFP$^+$/DsRed$^+$ OLs myelinate surrounding axons of PV$^+$ interneurons. Immunostainings against SMI-312 and PV revealed that PV$^+$ axonal segments co-localized with branches of YFP$^+$/DsRed$^+$ OLs in cell clusters (Fig. 4c, d). Quantifications showed that about a fifth of these branches were SMI-312$^+$/PV$^+$ while the others were SMI-312$^+$/PV$^-$ (Fig. 4d, g). Similar proportions were observed for YFP$^-$/DsRed$^+$ OLs derived from other origins outside YFP$^+$ cell clusters (Fig. 4g). Therefore, YFP$^+$/DsRed$^+$ OLs from the ePOA behave as other OLs and myelinate PV$^+$ and PV$^-$ neurons without a preference for PV$^+$ axons, indicating that the function of these clusters is not to preferentially myelinate YFP$^+$ interneuron partners. As for the entire interneuron population[24,25], 5 out of 5 YFP$^+$ FSI were myelinated while 3 out of 4 YFP$^+$ NFSI were not (Supplementary Fig. 6). Finally, the branches of these YFP$^+$/DsRed$^+$ OLs covered relatively small areas (Fig. 4b, d), suggesting that they myelinate GABAergic (PV$^+$) and glutamatergic (PV$^-$) fibers being part of the YFP$^+$ interneuron microcircuit.

Connectivity between Nkx2.1-derived interneurons and first-OPCs. To test whether the preferential interneuron-firstOPC connectivity does not occur exclusively in the subset of Dbx1-derived firstOPCs, we generated *Nkx2.1*^{CRE};*Rosa26*^{YFP};*NG2*^{DsRed} and *Nkx2.1*^{CRE};*Rosa26*^{tdTomato} transgenic mice to label all cells derived from the MGE and ePOA with YFP or tdTomato. In the first line, OPCs from other origins also expressed the DsRed. Given the large number of Nkx2.1-derived interneurons in these mice (around 70%)[6], it was impossible to recognize a specific spatial organization in cell clusters (Fig. 5a). However, Nkx2.1-derived OPCs and OLs followed similar dynamics to those of Dbx1-derived oligodendroglia (Fig. 5b–d). While the total

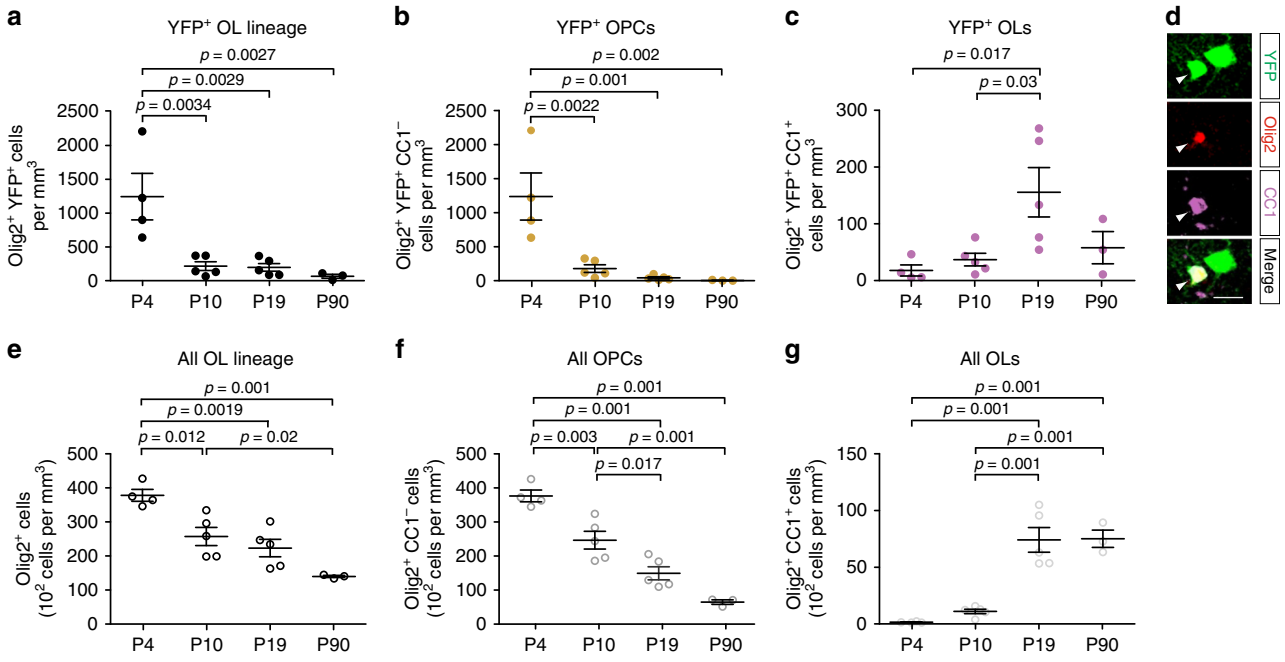

Fig. 3 Surviving Dbx1-derived OPCs become differentiated OLs. **a**–**c** Densities of YFP$^+$/Olig2$^+$ cells (**a**), YFP$^+$/Olig2$^+$/CC1$^-$OPCs (**b**) and YFP$^+$/Olig2$^+$/CC1$^+$ OLs (**c**) at PN4, PN10, PN19 and PN90 in the somatosensory cortex of *Dbx1^{CRE};Rosa26^{YFP}* mice (dots represent $n = 3$ to 5 animals per age). Note that YFP$^+$/Olig2$^+$ cell density highly decreases from PN4 to PN10 (**a**). A reduction of YFP$^+$/Olig2$^+$/CC1$^-$OPCs (**b**) is followed by an increase in YFP$^+$/Olig2$^+$/CC1$^+$ OLs (**c**) during development (one-way ANOVA test followed by a Tukey's Multiple Comparison test). **d** Confocal image of differentiated firstOLs at PN19 identified by the expression of YFP (green), Olig2 (red) and CC1 (magenta). Note the presence of a YFP$^+$/Olig2$^-$/CC1$^-$interneuron in close vicinity of this YFP$^+$/Olig2$^+$/CC1$^+$ OLs (white arrowhead). Scale bar: 20 µm. **e**–**g** Densities of total Olig2$^+$ cells (**e**), Olig2$^+$/CC1$^-$OPCs (**f**) and Olig2$^+$/CC1$^+$ OLs (**g**) at PN4, PN10, PN19 and PN90 in the somatosensory cortex of *Dbx1^{CRE};Rosa26^{YFP}* mice (dots represent $n = 3$ to 5 animals per age). Note that Olig2$^+$ cell density decreases more from PN4 to PN10 than at later stages (**e**). A reduction of Olig2$^+$/CC1$^-$ OPCs (**f**) is followed by an increase in Olig2$^+$/CC1$^+$ OLs (**g**) during development (one-way ANOVA test followed by a Tukey's Multiple Comparison test). Data are presented as mean ± SEM

population of Olig2$^+$ cells from the MGE/ePOA remained relatively stable, the OPC density decreased and OL density increased from PN10 to PN19. Then, we performed paired recordings between a fluorescent interneuron and a nearest OPC, whether from the same origin or from a different origin, during the second postnatal week (Fig. 5e, f). As for Dbx1-derived cells, Nkx2.1-derived interneurons displayed a high connection probability of 38.9% with their lineage-related firstOPCs while only of 8.3% with OPCs from distinct origins (Fig. 5h). These data show that all surviving firstOPCs from both MGE and ePOA remains functionally associated with interneurons sharing a common origin in the postnatal neocortex.

Connectivity of lineage-related cells rescued from death. Large populations of interneurons and firstOPCs are eliminated by programmed cell death in the cerebral cortex during the two first postnatal weeks[1,16]. We thus analyzed what would be their connectivity if cells committed to die survived. To examine the impact of the concomitant rescue of lineage-related interneurons and firstOPCs on interneuron-firstOPC connectivity and neuronal circuit function, we prevented their death by the conditional deletion of the pro-apoptotic Bcl2-associated X protein (*Bax*) which regulates interneuron apoptosis[16] and promotes the elimination of pre-oligodendrocytes[26]. We inactivated *Bax* function by crossing a mouse harboring floxed *Bax* alleles with *Nkx2.1^{CRE};Rosa26^{tdTomato}* mice (hereafter referred as *Bax$^{f/f}$* mice). It is noteworthy that *Dbx1^{CRE}* mice could not be used in these experiments since *Dbx1* and *Bax* alleles are on the same chromosome.

An efficient rescue of Nkx2.1-derived interneurons, firstOPCs and firstOLs occurred in *Bax$^{f/f}$* mice in all cortical layers at PN10 and PN19 (Supplementary Fig. 7; interneurons, 35.1% and 32.3% increase, firstOPCs, 59.5% and 75.1% increase and firstOLs, 61.1% and 50.5% increase at PN10 and PN19, respectively). Despite these large cell density increases, paired recordings between tdTomato$^+$ interneurons and tdTomato$^+$ OPCs revealed a significant reduction of their connection probability from 38.9% in controls to 14.3% in *Bax$^{f/f}$* mice during the second postnatal week (Fig. 5g, h). To corroborate this decrease in the connectivity, we analyzed GABAergic PSCs of tdTomato$^+$ OPCs evoked by extracellular stimulation in the presence of glutamate receptor antagonists at intensities known to activate a large number of fibers at this age[23]. Evoked GABAergic PSCs were robustly decreased in tdTomato$^+$ OPCs of *Bax$^{f/f}$* mice, confirming the reduced connectivity of rescued firstOPCs with interneurons (Fig. 5i, j). This low connectivity could result either from specific disruption of lineage-related interneuron-firstOPC interactions or a lack of capacity of rescued interneurons to form synapses and integrate neuronal networks. To distinguish between these possibilities, we used acute thalamocortical slices to analyze neuronal excitatory and inhibitory PSCs in a simple circuit motif where layer IV glutamatergic neurons receive a weak excitatory thalamic input compared to FSI which activation triggers powerful intracortical feedforward inhibition[27] (Fig. 6a). As expected in control[27], electrical thalamic stimulation induces direct small excitatory PSCs and large disynaptic inhibitory PSCs in layer IV glutamatergic neurons in the third postnatal week (Fig. 6a, b). Therefore, unlike a defect of rescued interneurons to form synapses, neuronal inhibitory currents were robustly increased in *Bax$^{f/f}$* mice, resulting in a strong decrease in the excitation/inhibition ratio (Fig. 6b, c). Furthermore, while 4 out of 8 paired recordings between FSI and glutamatergic neurons were connected in control, 7 out of 7 were

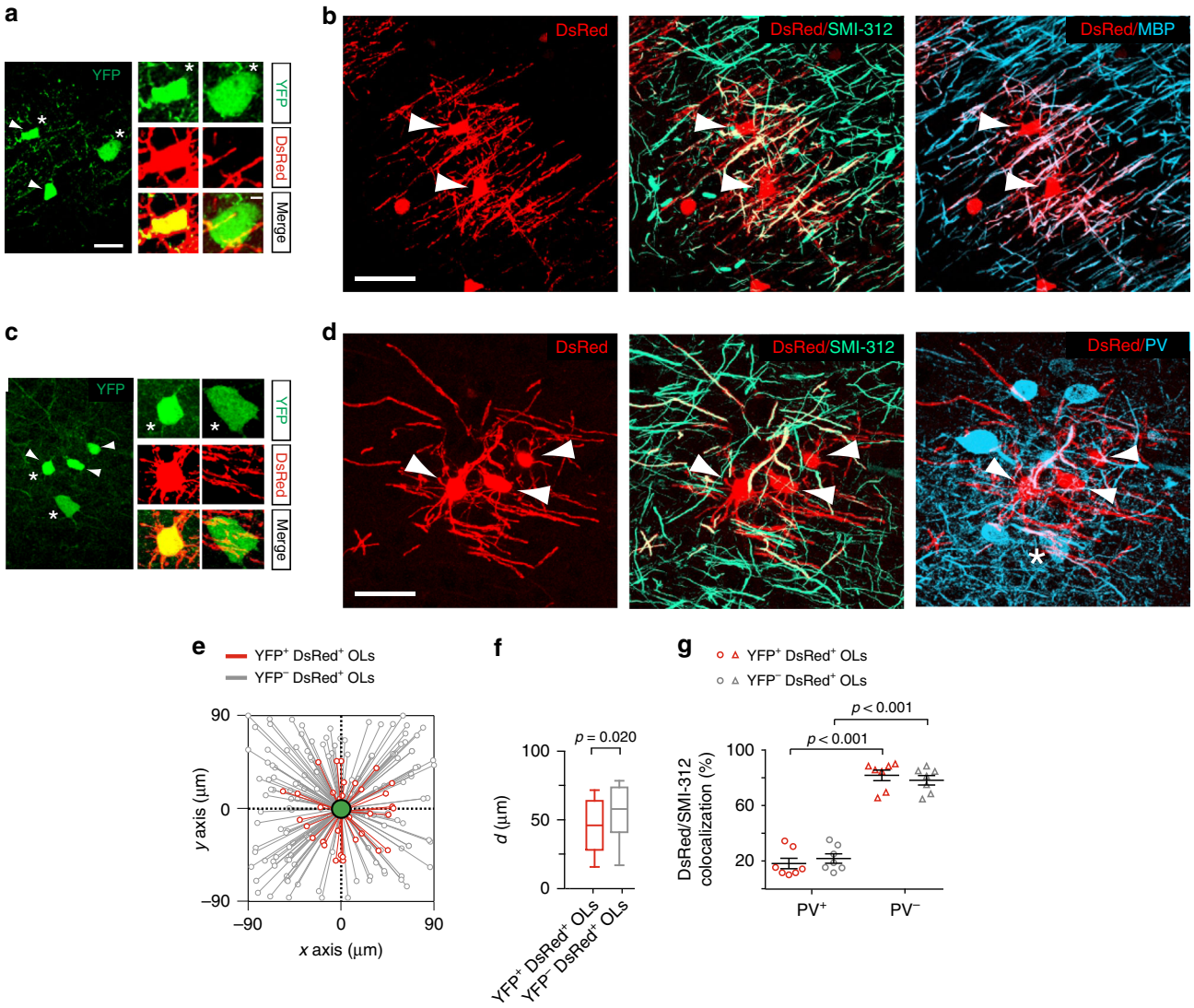

Fig. 4 Dbx1-derived OLs myelinate axons of PV$^+$ and PV$^-$ neurons in cell clusters. **a**, **c** Confocal images of two YFP$^+$ cell clusters composed of YFP$^+$/DsRed$^+$ OLs (white arrowheads) and YFP$^+$ interneurons at PN19 in the somatosensory cortex of *Dbx1^{CRE};Rosa26^{YFP};PLP^{DsRed}* mice. Insets: magnification of a YFP$^+$/DsRed$^+$ OL and a YFP$^+$ interneuron of the same clusters (asterisks). Scale bars: 25 and 5 µm. **b** The DsRed$^+$ branches of OLs belonging to the cluster in **a** (top, white arrowheads) co-localize with the axonal marker SMI-312 (middle) and MBP (bottom), confirming that these cells are myelinating cells ($n = 24$ firstOLs from $n = 3$ mice). **d** The DsRed$^+$ branches of OLs belonging to the cluster in **c** (top, white arrowheads) co-localize with the axonal marker SMI-312 (middle) and PV, the specific marker of FSI (bottom), confirming that some branches myelinate PV$^+$ interneurons. The asterisk indicates the soma of the PV$^+$/YFP$^+$ interneuron in the cluster (mean area occupied by YFP$^+$/DsRed$^+$ OL: 13419 ± 698 µm^2; mean diameter: 155.57 ± 7.88 µm; $n =$ 9 from 9 clusters). Scale bars in **b** and **d**: 50 µm. **e** Spatial distribution of YFP$^+$/DsRed$^+$ OLs (red) and YFP$^-$/DsRed$^+$ OLs (gray) with respect to YFP$^+$ interneurons (green) in YFP$^+$ cell clusters ($n = 22$ clusters). Note the shorter intersomatic distances for OLs and interneurons from the Dbx1 lineage, but the lack of a specific orientation of OLs. **f** Box plots of distances (d) of YFP$^+$/DsRed$^+$ OLs (red) and YFP$^-$/DsRed$^+$ OLs (gray) to YFP$^+$ interneurons (mean intersomatic distance: 44.2 ± 3.5 µm for $n = 33$ YFP$^+$/DsRed$^+$ OLs compared to 53.5 ± 2.1 µm for $n = 99$ YFP$^-$/DsRed$^+$ OLs, respectively, in 22 clusters; Mann–Whitney U test; significant p-value is indicated). Boxes show interquartile ranges and medians; whiskers indicate 10% and 90% percentile values. **g** Dot plots of percentages of PV$^+$ and PV$^-$ axons co-localizing with SMI-312 and DsRed$^+$ branches of YFP$^+$/DsRed$^+$ OLs (red; $n = 7$ clusters from 3 mice) and YFP$^-$/DsRed$^+$ OLs (gray; $n = 7$ clusters from 3 mice) (two-way ANOVA, F = 0.978 and DF = 1; significant p-values are indicated). Data in **g** are presented as mean ± SEM

connected in *Bax$^{f/f}$* mice (Fig. 6d, e). Connected pairs in this mouse line displayed larger inhibitory PSCs than controls without changing their short-term synaptic plasticity and thus their presynaptic release properties (Fig. 6d–f). This suggests that rescued interneurons, in addition to be supernumerary, formed more synaptic contacts into their postsynaptic glutamatergic neurons than controls. Hence, the exceeding number of interneurons in *Bax$^{f/f}$* mice caused a hyper-innervation of other neurons, enhancing the inhibitory drive of neuronal networks and leading to a drastic excitation/inhibition imbalance. In contrast, they lost their preferential innervation with their lineage-related firstOPCs. Nkx2.1-derived interneurons rescued from death were thus functional and contacted other neurons, but their survival did not promote interactions with firstOPCs.

These findings show that the connectivity between interneurons and firstOPCs sharing a common origin constitute a highly specific and regulated process that, unlike for neurons, cannot be promoted by increasing cell densities. Since forcing the survival of

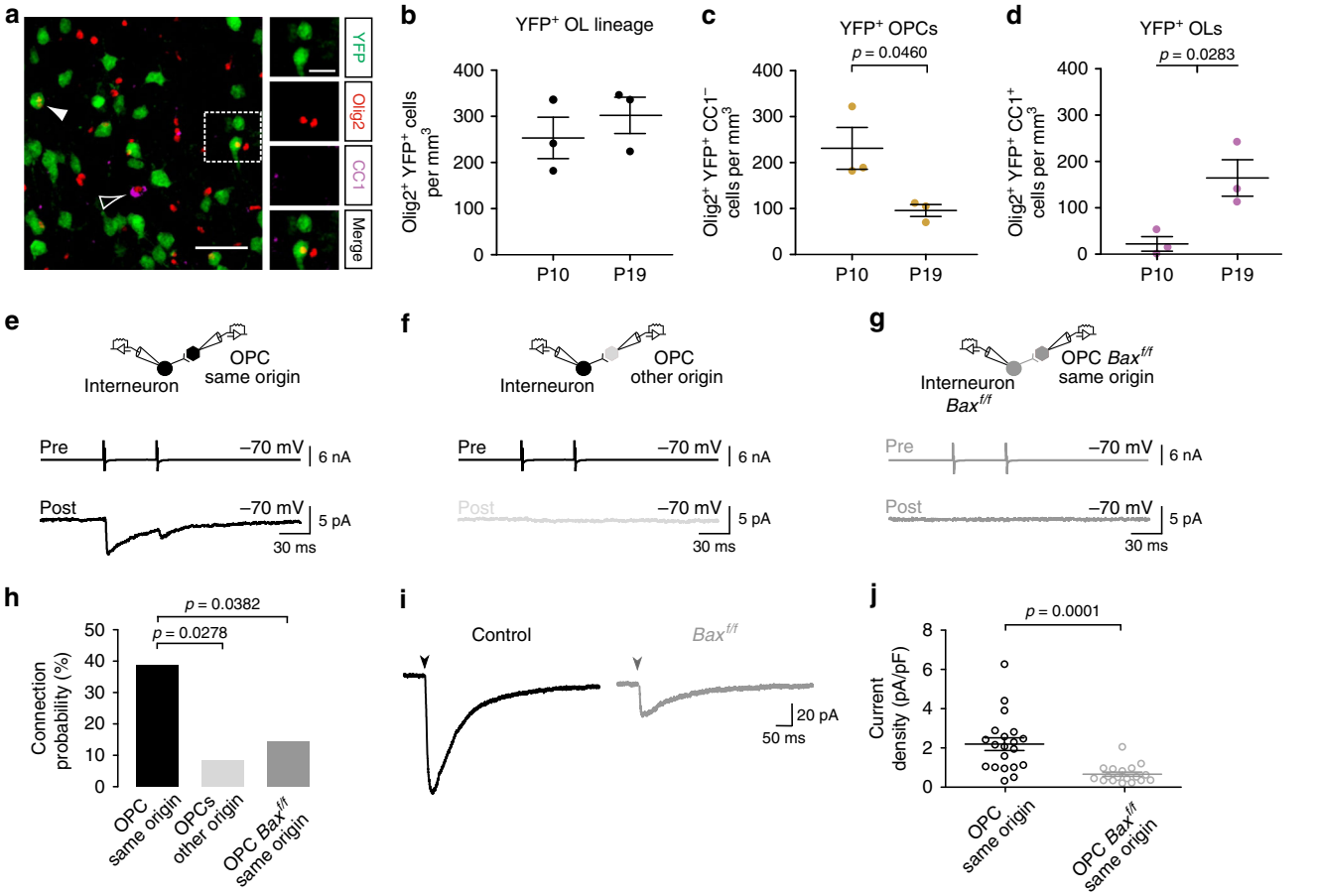

Fig. 5 The preferential interneuron-firstOPC connectivity is reduced in *Bax*$^{f/f}$ mice. **a** Confocal images of YFP$^+$ (green), Olig2$^+$ (red) and CC1$^+$ cells in layer V of the somatosensory cortex in a *Nkx2.1*^{CRE};*Rosa26*^{YFP} mouse at PN10. The white dotted square surrounds a YFP$^+$ interneuron and a YFP$^+$/Olig2$^+$/CC1$^-$ OPC shown in insets. Another YFP$^+$/Olig2$^+$/CC1$^-$ OPC (solid arrowhead) and a YFP$^-$/Olig2$^+$/CC1$^+$ OL (open arrowhead) are indicated. Scale bars: 100 and 20 µm. **b**–**d** Layer V and VI densities of YFP$^+$/Olig2$^+$ cells (**b**), YFP$^+$/Olig2$^+$/CC1$^-$OPCs (**c**) and YFP$^+$/Olig2$^+$/CC1$^+$ OLs (**d**) at PN10 and PN19 in the somatosensory cortex of *Nkx2.1*^{CRE};*Rosa26*^{YFP} mice (dots represent $n = 3$ mice per age). **e**–**g** Paired recordings between a presynaptic fluorescent interneuron and an OPC of the same origin (**e**) or a different origin (**f**) in control mice, or between a presynaptic tdTomato$^+$ interneuron and a tdTomato$^+$ OPC of the same origin in *Bax*$^{f/f}$ mice (**g**). **h** Connection probabilities for OPCs of the same origin in control (black, $n = 36$), OPCs of different origin in control (light gray, $n = 24$) and OPCs of the same origin in *Bax*$^{f/f}$ mice (dark gray, $n = 35$). Note that presynaptic interneurons target preferentially OPCs of the same origin in control (black) compared to OPCs of different origin (light gray) or OPCs of same origin but after *Bax* inactivation (dark gray; Chi-squared test; significant *p*-values are indicated). **i** GABAergic PSCs evoked by stimulation of neuronal fibers (100 µs; 20 V) in firstOPCs of control (black) and *Bax*$^{f/f}$ mice (dark gray) recorded at −70 mV in the presence of 10 µM 2,3-dioxo-6-nitro-1,2,3,4-tetrahydrobenzoquinoxaline-7-sulfonamide (NBQX) and 50 µM D-(−)-2-amino-5-phosphonopentanoic acid (D-AP5), showing a reduced mean GABAergic PSC in the *Bax*$^{f/f}$ mouse. Stimulation artefacts were blanked for visibility. The stimulation time is indicated (arrowheads). **j** Dot plots of current densities for firstOPCs in control (black; $n = 20$) and *Bax*$^{f/f}$ (dark gray; $n = 18$) mice calculated by dividing the mean amplitude of evoked PSCs by the cell capacitance. Note the decreased PSC densities in knockout mice (Mann–Whitney *U* test; significant *p*-value is indicated). Data in **b**–**d** and **j** are presented as mean ± SEM

these cell types does not promote their connectivity, our data also suggest that, in the normal postnatal neocortex, the firstOPCs that display low levels of connectivity undergo apoptosis while those highly connected survive (Fig. 7f).

Programmed cell death is key for oligodendroglia homeostasis. The genetic ablation of specific OPC waves from ventral regions does not modify the total OPC number and myelination in the postnatal cortex, suggesting that competition of OPCs from different origins compensate from one another[1]. An imbalance in the firstOPC number should therefore be compensated by a reduction of OPCs from other sources to maintain the correct cell density. To test whether the increase in firstOPCs in *Bax*$^{f/f}$ mice is counterbalanced by a reduction in OPCs from different origins, we quantified the densities of tdTomato$^-$ OPCs and tdTomato$^-$ OLs in layers I–III, VI and V–VI. At PN10, the increased density of tdTomato$^+$/Olig2$^+$ cells in *Bax*$^{f/f}$ mice was not accompanied by a reduction of non-recombinant tdTomato$^-$ OPCs and OLs in any cortical layer (Supplementary Fig. 8). Later in development, after the end of the massive programmed cell death of interneurons and firstOPCs in the cortex[28], quantifications of non-recombinant tdTomato$^-$ oligodendroglia revealed a significant increase in the density of this glial cell population in *Bax*$^{f/f}$ mice (Fig. 7; increase of 39% of tdTomato$^-$/Olig2$^+$ cells considering all layers at PN19). While tdTomato$^-$ OPCs were significantly increased in layers I–III where there is less myelin than in deep cortical layers (Fig. 7b–d; 64% increase of tdTomato$^-$ OPCs in I–III layers), tdTomato$^-$ OLs were highly increased in layers IV and V–VI of *Bax*$^{f/f}$ mice (Fig. 7b–d; 44% and 38% increase of tdTomato$^-$ OLs in layer IV and V–VI, respectively). Consequently, we observed a significant increase in myelination, detected by myelin basic protein (MBP), in layer V and VI at PN19 (Fig. 7d, e). These

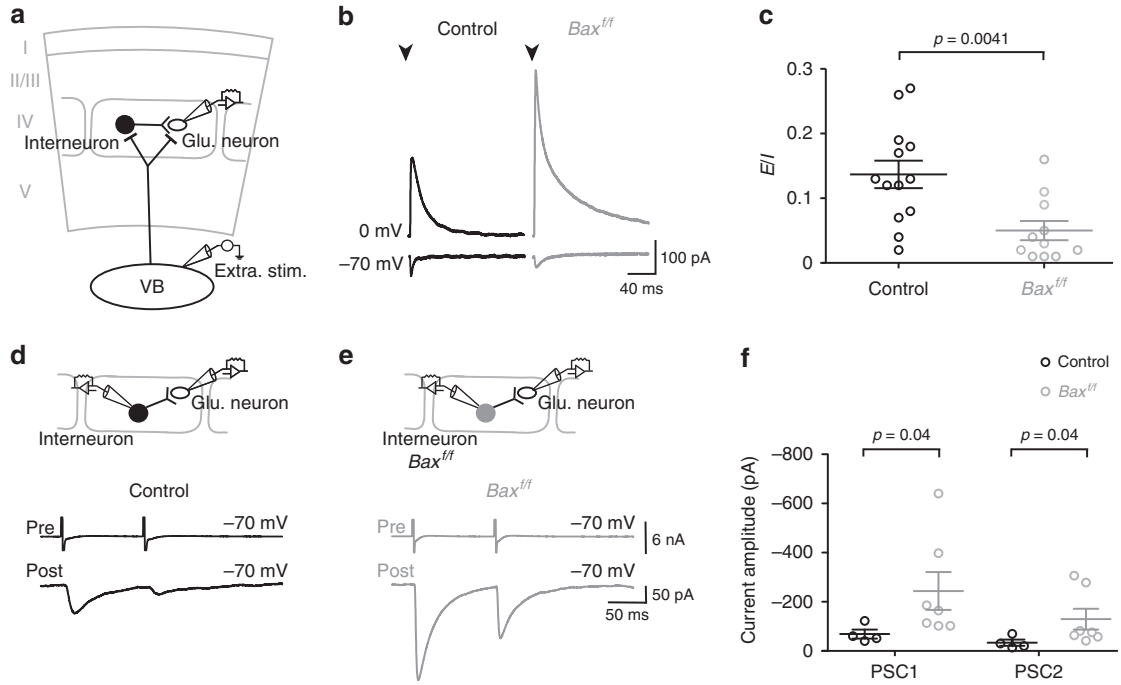

Fig. 6 An exceeding number of interneurons increases inhibition in neuronal networks. **a** Diagram representing the experimental procedure where a layer IV glutamatergic neuron recorded during the extracellular stimulation of the ventro-basal nucleus (VB) of the thalamus. In this circuit, the recorded neuron is synaptically connected by FSI which also receive thalamic input that triggers a strong disynaptic feedforward inhibition. **b** Excitatory (inward) and inhibitory (outward) PSCs evoked by thalamic stimulation in layer IV glutamatergic neurons of control (black) and $Bax^{f/f}$ mice (dark gray) recorded at −70 and 0 mV, respectively, in acute thalamocortical slices during the third postnatal week. Stimulation artifacts were blanked for visibility. The stimulation time is indicated (arrowheads). **c** Dot plots of excitation/inhibition (*E/I*) ratio obtained for glutamatergic neurons in control (black, $n = 13$) and $Bax^{f/f}$ (dark gray, $n = 10$) mice by dividing excitatory PSCs by inhibitory PSCs (Mann–Whitney *U* test; significant *p*-value is indicated). **d**, **e** Paired recordings between a presynaptic FSI and a layer IV glutamatergic neuron in control (black, **d**) and $Bax^{f/f}$ (dark gray, **e**) mice. Note that action currents evoked in FSI elicited larger PSCs in glutatamergic neurons of $Bax^{f/f}$ mice. **f** Dot plots of PSCs evoked by the first (PSC1) and second (PSC2) action current in the FSI (Mann–Whitney *U* test; significant *p*-value are indicated). The paired-pulse ratio (PPR = PSC1/PSC2) was not different between control (black, $n = 4$ out of 8 pairs connected) and $Bax^{f/f}$ (dark gray, $n = 7$ out of 7 pairs connected) mice, indicating that there were no changes in the release probability of presynaptic FSI (PPR: 0.45 ± 0.05 and 0.52 ± 0.07, respectively; $p = 0.412$, Mann–Whitney *U* test). Data are presented as mean ± SEM

results indicate that the prevention of cell death of lineage-related interneurons and firstOPCs induced a major imbalance in other oligodendroglia populations that impacted myelination at late developmental stages.

Overall, these findings show that the population of rescued tdTomato$^+$/Olig2$^+$ cells was not compensated by a reduction of OPCs from other sources. On the contrary, the concomitant persistence of lineage-related interneurons and firstOPCs committed to die induced a pronounced oligodendroglia imbalance through a non-cell-autonomous mechanism, after the period of massive cortical programmed cell death (Fig. 7g). Therefore, oligodendroglia homeostasis in the developing cortex is not solely determined by competition among different OPC waves. Apoptosis is thus not only required to properly set interneuron-firstOPC interactions and reach a correct excitation/inhibition balance of neuronal networks, but also to regulate the proper densities of OPCs and myelinating OLs across different cortical layers.

Discussion

Revealing how interneurons and OPCs interact during postnatal development is fundamental for our understanding of how these different cellular subtypes contribute to the assembly, maturation and myelination of cortical circuits. Here we shed light on a complex postnatal interplay between interneurons and firstOPCs derived from the same embryonic origin, characterized by the existence of functional cell clusters that unexpectedly display a high synaptic connectivity. Late in development, surviving firstOPCs differentiate into mature oligodendrocytes inside cell clusters where they myelinate different types of neuronal fibers in vicinity of their interneuron counterparts. Therefore, the region of birth in the embryo and the cell lineage favor postnatal cellular interactions that are tightly regulated during development. Indeed, the connectivity between lineage-related interneurons and firstOPCs is not promoted by increasing their cell densities (Fig. 7f, g). Furthermore, contrary to the idea that OPC populations from distinct embryonic origins compensate with each other to homeostatically control OPC density[1], the concomitant increase of lineage-related interneurons and firstOPCs is not translated into a decrease in other OPC populations but to a high increase in the entire oligodendroglia population via a non-cell-autonomous mechanism (Fig. 7f, g). Our findings question the idea that the different waves of OPCs compete with each other to regulate OPC density and point to unprecedented roles of developmental death of interneurons and firstOPCs in regulating their lineage-related cell interactions and the homeostasis of oligodendroglia.

Our initial hypothesis was that the common origin between interneurons and firstOPCs favors the assembly of interneuron-OPC microcircuits that display a very local arrangement[15]. Here we show that the cell lineage favors both the distribution of cells in predictable clusters and their preferential high local connectivity. Moreover, *Bax*-dependent rescue experiments indicate that interneurons and firstOPCs prevented from death induces a decrease rather than an increase in the proportion of lineage-

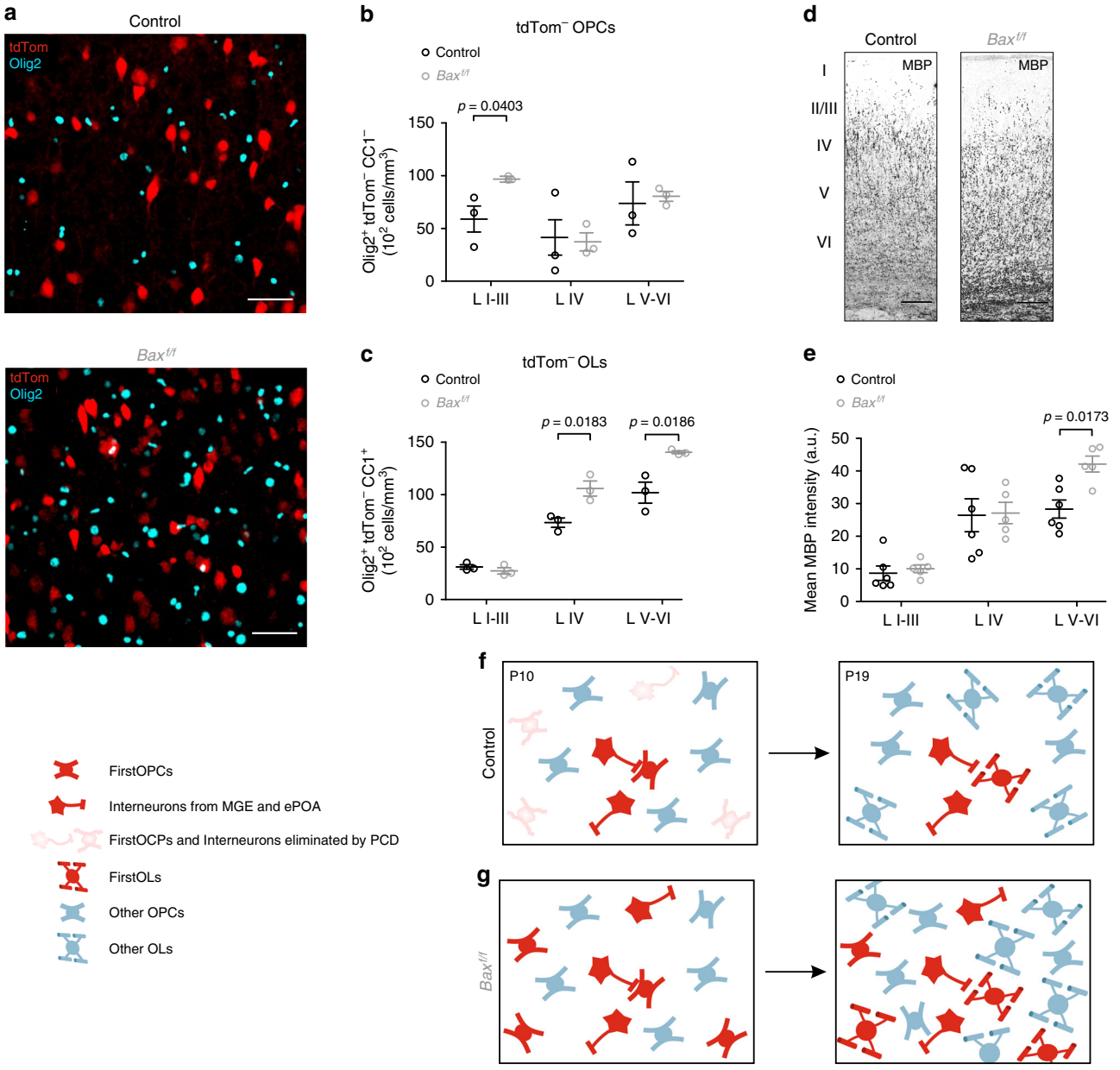

Fig. 7 Imbalance of oligodendroglia homeostasis and hypermyelination in *Bax*$^{f/f}$ mice at PN19. **a** Confocal images of tdTomato^{+} (red) and Olig2^{+} (cyan) cells of layers V and VI of the somatosensory cortex in control (left) and *Bax*$^{f/f}$ (right) mice at PN19. Note the large increase in the number of non-recombinant tdTomato^{-}/Olig2^{+} oligodendroglia in *Bax*$^{f/f}$ mice. Scale bar: 50 µm. **b**, **c** Densities of non-recombinant tdTomato^{-}/Olig2^{+}/CC1^{-}OPCs (**b**) and tdTomato^{-}/Olig2^{+}/CC1^{+} OLs (**c**) in layers I–III, IV and V–VI of the somatosensory cortex in control (left) and *Bax*$^{f/f}$ (right) mice at PN19 (dots represent $n = 3$ animals per condition; Mann–Whitney *U* test; significant *p*-values are indicated). **d** Confocal images of MBP in the somatosensory cortex of control (left) and *Bax*$^{f/f}$ (right) mice at PN19. The characteristic gradient of increasing myelination from superficial to deep cortical layers occurs in both controls and *Bax*$^{f/f}$ mice. Note the increased myelination of deep layers in the *Bax*$^{f/f}$ mouse. Scale bar: 200 µm. **e** Dot plots of mean MBP fluorescence intensities in layers I–III, IV and V–VI of the somatosensory cortex in control ($n = 6$ slices from 2 animals) and *Bax*$^{f/f}$ ($n = 5$ slices from 2 animals) mice at PN19 (Mann–Whitney *U* test; significant *p*-value is indicated). Data are presented as mean ± SEM. **f**, **g** Schematic diagram illustrating postnatal functional clusters between interneurons and oligodendroglia derived from the MGE and ePOA (red), same cell types already eliminated by programmed cell death (PCD, pink) and oligodendroglia from other sources (blue) in control (**f**) and *Bax*$^{f/f}$ (**g**) mice during postnatal development. Note the decreased connection probability of firstOPCs in *Bax*$^{f/f}$ mice with respect to controls at PN10 and the increase in both recombinant (red) and non-recombinant (blue) oligodendroglia in *Bax*$^{f/f}$ mice (**g**) with respect to controls (**f**) at PN19. A non-cell-autonomous mechanism impacts the number of non-recombinant oligodendroglia as these cells are not targeted in *Bax*$^{f/f}$ mice at PN19

related interneuron-firstOPC synaptic connections. Since Bax-dependent rescue of firstOPCs circumvents synaptic activity, our results suggest that those firstOPCs that display low levels of connectivity undergo apoptosis in normal conditions (Fig. 7f, g). This is in line with a role of these neuron-glia synapses in OPC survival[23]. Interestingly, a recent report demonstrates that interneuron survival depends on their high levels of connectivity by pyramidal neurons during the period of interneuron programmed cell death[29]. Synaptic activity seems therefore to be a crucial factor favoring both neuron and OPC survival. The sophisticated organization in small clusters formed by interneurons and firstOPCs establishing functional interactions also

recall previous reports describing a delicate anatomical and functional interplay between clonal pyramidal neurons in the network[30]. Nevertheless, reports on how cortical GABAergic interneurons are organized in the cortex remain contradictory. While interneurons labeled at the clonal level tend to distribute into local clusters of few neurons[31,32], findings using barcoded retrovirus libraries for large-scale analyses of specific identified clonal cells show that interneurons disperse broadly in the neocortex[33,34]. A more recent report shows that spatially clustered interneurons from the MGE and ePOA obtained by low-titer retrovirus-injected radial glia in the embryo develop electrical but not chemical synapses after PN14[35]. Although the non-random allocation of interneurons derived from MGE/ePOA seems acknowledged by all authors, restricted clustering of sibling interneurons is still a matter of debate. In this report, interneurons and firstOPCs inside cell clusters are unlikely to be clonal since the massive interneuron production occurs two days before that of firstOPCs: E10.5 for Nkx2.1-derived interneurons[36] and E12.5 for firstOPCs[1]. However, this point as well as the molecular and cellular factors allowing for the joint positioning of these two cell types in deep cortical layers will need further investigation.

Recent reports show that 5–15% of myelinated deep-layer axons belong to GABAergic PV$^+$ FSI[23–25]. In addition, the protein composition of myelin enwrapping non-GABAergic and GABAergic axons differ, the latter expressing 20% more MBP[24]. Considering the recently established OL heterogeneity[37], we could speculate that pyramidal cells and interneurons are myelinated by distinct OLs endowed with the ability to produce different myelin. However, our data show that individual OLs, derived or not from the ePOA, myelinate similar proportions of PV$^+$ and PV$^-$axons and thus neurons of different nature and origins. Whether a single OL has the ability to produce myelin segments with distinct molecular composition according to the neuronal subtype remains unknown. Moreover, the lack of preference of firstOLs for PV$^+$ axons in YFP$^+$ cell clusters suggests that interactions between lineage-related interneurons and firstOLs do not guide the firstOL to preferentially myelinate the axon of its interneuron partner. Thus, activity-dependent myelination by firstOLs probably does not follow a predetermined ontogenetic program. Nevertheless, firstOLs remain close to their lineage-related interneurons and their processes project towards different directions covering a whole distance of around 150 µm which ensures the myelination of multiple axons in proximity of their interneuron counterparts. Therefore, the proximity of firstOLs to Dbx1-derived interneurons might substantially contribute to myelination and maturation of specific local circuits by facilitating action potential propagation and synchronization of glutamatergic and GABAergic neurons within a restricted space. In line with this, neuronal circuits formed by interneurons onto pyramidal cells are confined with a high connection probability at intersomatic distances < 200 µm[38].

Although OPCs are highly motile[4,5], it is more likely that these progenitors stay in the same cluster rather than move from a cluster to another during postnatal development. In fact, cultured OPCs derived from ventral regions, which includes firstOPCs, have less inherent migration capabilities than OPCs from dorsal regions[39]. Furthermore, in adult demyelinating lesions, OPCs derived from ventral regions display a reduced capacity to proliferate and differentiate into mature OLs compared to those of dorsal regions[39]. Although RNA-sequencing did not reveal differences in the gene expression profile among OPC populations[2], unappreciated functional differences of OPCs from distinct origins are emerging, underlying the importance of functional analyses of specific cell types.

Oligodendroglia are over-generated during development and subsequently eliminated by programmed cell death during the first two postnatal weeks[1,40,41]. It was recently showed that the transcription factor EB (TFEB) promotes the death of pre-myelinating OLs in a *Bax*-dependent manner, a mechanism controlling the spatial and temporal specificity of brain myelination[26]. In the neocortex, the three waves of OPCs are thought to contribute to the homeostatic regulation of these progenitors by competition[1]. In fact, cortical OPCs have an incredible capacity to regulate their own density throughout life. In the developing somatosensory cortex, a sensory (whisker) deprivation causes an increased death of newly-formed OLs that is accompanied by an enhanced OPC proliferation[4]. OPC differentiation or ablation also triggers OPC migration and proliferation in the adult, a process that rapidly restore cell density[5]. OPCs react to any change in the oligodendroglia population to compensate for its loss and ensure the correct myelination of neuronal circuits. Only severe pathological conditions such as chronic hypoxia in the young[13] or progressive Multiple Sclerosis in the adult[42] perturb the OPC capacity to preserve the homeostasis of its pool. However, a potential impact of neuron-glia interactions on oligodendroglia homeostasis had not been previously explored. Challenging previous views, our findings show that the rescue of lineage-related interneurons and firstOPCs committed to die induces an unexpected global increase in oligodendroglia density (Fig. 7f, g). These findings reveal a new role of programmed cell death during cortical development in controlling the oligodendroglia number via a non-cell-autonomous mechanism.

The mammalian cortex is unique as it is the only structure in the CNS that hosts different transient cell populations that almost completely disappear at early postnatal stages: Cajal Retzius neurons, subplate neurons, cortical plate transient neurons and firstOPCs[28]. In addition, glutamatergic projection neurons and GABAergic interneurons also undergo a significant cell death that induces 30–40% reduction of their initial population[28]. The precise functions of this previously underestimated cellular death are still unknown, but they are probably not restricted to a simple elimination of supernumerary cells. Interestingly, recent data show that pyramidal neuron apoptosis is critical to regulate interneuron survival and stabilize excitatory–inhibitory ratios of cortical networks[29]. Beyond these findings, our study shows that the death/survival balance of interacting neurons and glia is key to build their long-term interactions and ensures the proper myelination and construction of cortical circuits after the phase of massive cell death in the cortex.

Methods

Transgenic mice. The experiments of the present study followed European Union and institutional guidelines for the care and use of laboratory animals and were approved by the French ethical committee for animal care of the University Paris Descartes (Committee N°CEEA34) and the Ministry of National Education and Research (Project No: 13094-2017081712355709). Several transgenic lines were produced. First, Cre lines driven by the Dbx1 and Nkx2.1 promoter were used as heterozygous to generate *Dbx1^{CRE};Rosa26^{YFP}*, *Nkx2.1^{CRE};Rosa26^{YFP}* and *Nkx2.1^{CRE};Rosa26^{tdTomato}* transgenic mice and lineage-trace cells derived from the ePOA[18] and MGE and ePOA[1]. *Dbx1^{CRE};Rosa26^{YFP}* and *Nkx2.1^{CRE};Rosa26^{YFP}* mice were also crossed with the *NG2^{DsRed}* heterozygous transgenic line which allowed us to recognize the whole OPC population by the expression of DsRed[19]. In another set of experiments, the *Dbx1^{CRE};Rosa26^{YFP}* mice was bred with the *PLP^{DsRed}* mice[22] which allowed us to recognize the OL population by the expression of DsRed. Finally, the *Bax^{tm2Sjk};Bak1$^{tm1Thsn/J}$* line[43] harboring the floxed *Bax* allele and the *Bak* knock-out allele (stock N°006329; Jackson Laboratories) was crossed with the *Nkx2.1^{CRE};Rosa26^{tdTomato}* line to inactivate *Bax* and permanently label Nkx2.1-derived cells. We used *Nkx2.1^{CRE};Rosa26^{tdTomato};Bak$^{+/-}$;Bax$^{f/f}$* line as knockout (*Bax$^{f/f}$*) mice. For electrophysiological experiments, we used as controls *Nkx2.1^{CRE};Rosa26^{tdTomato}* line when recorded OPCs needed to be identified by fluorescence, otherwise Cre negative *Nkx2.1^{CRE};Rosa26^{tdTomato};Bak$^{+/-}$;Bax1$^{f/f}$* mice from the same littermates of *Bax$^{f/f}$* mice were used. For cell countings, we used as controls *Nkx2.1^{CRE};Rosa26^{tdTomato};Bak$^{+/-}$;Bax$^{f/+}$* animals from the same littermates of *Bax$^{f/f}$* mice. *Dbx1*-expressing progenitors of the ePOA generate interneurons in deep cortical layers and firstOPCs in all layers; other Dbx1-derived neuronal types such as layer I Cajal Retzius neurons and cortical plate transient neurons in upper layers are not generated from the ePOA and were not considered in this study[7,8,17,18,28]. No other Dbx1-derived neuron or glial cell types have been reported in the cerebral cortex[17]. Animals were genotyped by PCR using primers specific for the different alleles and maintained in the animal

facility under 12 h light/dark cycle with ad libitum access to food and water. Both female and male were indiscriminately used.

Acute slice preparation. Most experiments were performed using 300-µm-thick acute parasagittal slices of the barrel cortex from transgenic mouse with an angle of 10° to the sagittal plane[12,15]. In experiments aiming to analyze the *E*/*I* ratio of layer IV glutamatergic neurons we performed 350-µm-thick tangential thalamocortical slices. An Olympus BX51 microscope equipped with a ×40 fluorescent water-immersion objective allowed us to visualize YFP and DsRed fluorescent proteins by means of excitation beams supplied by Blue and Green Optoleds (Optoled Light Sources, Cairn Research, UK). Two sets of excitation/emission filters were used (470 and 525 nm filters for YFP, and 560 and 620 nm filters for DsRed) and images were collected and acquired with an iXon+ 14-bit digital camera (Andor Technology, UK) and with Imaging Workbench 6.0 software (Indec Biosystems, USA), respectively.

Paired recordings and extracellular stimulation. Electrophysiological experiments were performed at RT using an extracellular solution containing (in mM): 126 NaCl, 2.5 KCl, 1.25 NaH_2PO_4, 26 $NaHCO_3$, 20 glucose, 5 pyruvate, 3 $CaCl_2$, and 1 $MgCl_2$ (95% O_2, 5% CO_2). During paired recordings, presynaptic interneurons were recorded with an intracellular solution containing (in mM): 130 K-gluconate (KGlu), 10 GABA, 0.1 EGTA, 0.5 $CaCl_2$, 2 $MgCl_2$, 10 HEPES, 2 Na_2-ATP, 0.2 Na-GTP, and 10 Na_2-phosphocreatine (pH ≈ 7.3), and postsynaptic cells (OPCs, interneurons and layer IV glutamatergic neurons) with an intracellular solutions containing (in mM): 130 CsCl, 5 4-aminopyridine, 10 tetraethylammonium chloride, 0.2 EGTA, 0.5 $CaCl_2$, 2 $MgCl_2$, 10 HEPES, 2 Na_2-ATP, 0.2 Na-GTP, and 10 Na_2-phosphocreatine (pH ≈ 7.3). During extracellular stimulation, layer IV glutamatergic neurons were recorded with a similar intracellular solution but containing 125 mM $CsCH_3SO_3H$ (CsMeS) instead of CsCl (pH ≈ 7.3). Extracellular stimulations were obtained using either a monopolar electrode (glass pipette) placed in layers V and VI near the OPC recorded with a CsCl-based intracellular solution or a bipolar concentric electrode placed in the thalamic nucleus while recording layer IV glutamatergic neurons in CsMeS-based intracellular solution (100 ms pulse, 5–40 V; Iso-Stim 01D, npi electronic GmbH, Tamm, Germany). Potentials were corrected for a junction potential of −10 mV when using KGlu- and CsMeS-based intracellular solution.

Whole-cell recordings were performed with a Multiclamp 700B and signals filtered at digitized at 4 kHz and 20 kHz respectively. Off-line analysis of digitized data was performed using pClamp10.1 software (Molecular Devices) and Neuromatic package within IGOR Pro 6.0 environment (Wavemetrics, USA)[44]. A paired recording was considered as connected when the average of PSCs recorded in the postsynaptic cells was 2-fold larger than the standard deviation of the noise. Paired-pulse ratios were calculated as PSC2/PSC1[15]. The *E*/*I* of ratio of layer IV glutamatergic neurons was calculated as EPSCs/IPSCs.

The spatial *x*–*y* coordinates of connected and unconnected YFP^+ interneurons and OPCs were extracted from DIC images. The recorded slice was oriented to fix the *y* axis as the shorter imaginary line from the soma of the YFP^+ interneuron, considered at position 0, to the cortical surface (Supplementary Fig. 4a). The *x* axis was parallel to the cortical surface. After obtaining the *x*–*y* position of each recorded OPC with respect to the presynaptic YFP^+ interneuron, we calculated the intersomatic interneuron-OPC distance (*d*), and the angle α with respect to the *y* axis (Supplementary Fig. 4a).

Immunostainings and cell countings. Immunostanings were performed on perfused mice at different ages ($n = 3$–5 animals per age)[23]. Animals were perfused with phosphate buffer saline (PBS) followed by 4% paraformaldehyde (PFA). Brains were postfixed during 1 h in PFA and stored in PBS at 4 °C. For immunostainings against Olig2, CC1, YFP and MBP, coronal vibratome slices (100 µm) were prepared in PBS ice-cold solution (4 °C), permeabilized with 0.2% triton X-100 and 4% Normal Goat Serum (NGS) for 1 h and incubated one night with antibodies diluted in a 0.2% triton X-100 solution and 5% NGS. For immunostainings against PV, SMI-312 and MBP, slices were permeabilized with 1% triton X-100 and 10% NGS overnight and incubated four nights with primary antibodies diluted in a 1% triton X-100 solution and 10% NGS. Different immunostainings were performed by using rabbit anti-Olig2 (1:400; ref. AB9610, Millipore), mouse monoclonal anti-CC1 (1:100; ref. OP80, Calbiochem), chicken anti-GFP (for detection of YFP; 1:1000; ref. A10262, ThermoFisher Scientific), rat monoclonal anti-MBP (1:100; ref. AB7349, Abcam), rabbit anti-PV (1:1000; ref. PV-27, Swant) and mouse anti-SMI-312 (1:1000; ref. 837901, Eurogentec) antibodies. All primary antibodies were washed three times in PBS and incubated in secondary antibodies coupled to Alexa-405, Alexa-488, Alexa-546 or Alexa-633 at room temperature for 2 h for immunostainings against Olig2, CC1, GFP and MBP (1:500) and for 2 days for immunostainings against PV, SMI-312 and MBP (1:200; Life Technologies). Confocal images were acquired using a ×20 water objective or ×63 oil objective with LSM-710 confocal microscope or a ×20 and ×63 oil objectives with a SP8 Leica confocal microscope. Images were processed and analyzed using NIH ImageJ and Imaris softwares.

For cell countings, YFP^+ or $TdTomato^+$ cells were identified as co-localized or not with $Olig2^+$ and $CC1^+$ (at least $n = 3$ mouse per age; for each mouse, we counted $n = 4$ slices). To prevent border effects in countings, cells that were at the boundaries of the analyzed volume were not considered in three of the six sides of the cube if their $Olig2^+$ nucleus was not fully inside. To estimate the percentage of myelinated PV^+ and PV^- axon segments per $DsRed^+$ OLs, we first determine the number of $DsRed^+$ OLs branches co-localizing with SMI-312 and then determine the number of PV^+ and PV^- branches. For MBP fluorescent intensities, images were acquired with a ×63 oil objective and submitted to a background subtraction measured in layer I. Then, the mean intensity values were directly measured with NIH ImageJ using rectangle selection tool to delineate different layers.

Unsupervised cluster analysis of YFP^+ cells from the ePOA. The unbiased identification of YFP^+ cell clusters was assessed by applying an unsupervised agglomerative cluster analysis via multi-scale bootstrap resampling[20,21]. First, we extracted *x*, *y*, *z* positions of layers IV–VI $YFP^+/Olig2^+/CC1^-$OPCs, $YFP^+/Olig2^+/CC1^+$ OLs and $YFP^+/Olig2^-/CC1^-$ interneurons in the confocal sections used for cell countings at PN10 and PN19 (3–4 slices per mouse; $n = 4$ mouse per age). To display the hierarchical relationship of identified YFP^+ cells according to their spatial proximity, we computed Manhattan intersomatic distances to produce a distance matrix and build a hierarchical dendrogram using the package *hclust* under the R environment[21]. It is noteworthy that Manhattan distances were used for building the dendrogram because, based in absolute distances, they are less influenced by outliers than Euclidean distances. Instead, the proximity of cells was evaluated with Euclidean distances. In the dendrogram, each identified YFP^+ cell is considered as a single object which repeatedly merges into higher-level clusters to its closest objects until forming a hierarchical tree. To determine whether unbiased clusters of YFP^+ cells were supported by data, we assessed the uncertainty of clusters at each branch of the dendrogram with the *Pvclust* package under the R environment[20]. This package computes 10,000 bootstrap samples generated by randomly resampling our experimental data and by performing bootstrap replications of the dendrogram. By computing both bootstrap probability values and approximately unbiased probability values for each cluster in the dendrogram, we inferred whether the distribution of cell clusters was random or not. If the probability of a given cluster is too low, the cluster does not exist, but if the probability is >95%, we considered that the cluster is strongly supported by the data[20]. Finally, once objective cell clusters were detected, we determined the number of cells per cluster, the cell composition of each cluster, and the Euclidean intersomatic distances among all cells in a cluster.

Statistics. All data are expressed as mean ± SEM from *n* pairs, cells or animals. GraphPad InStat software version 3.06 was used for statistical comparisons. The nonparametric two-tailed Mann–Whitney *U* test for independent samples was used to determine statistical differences between two means. When comparisons within single pairs were required, the two-way Wilcoxon signed-rank test for related samples was used. For comparisons of cell densities, we used a one-way ANOVA test followed by a Tukey's multiple comparison post hoc test. In the case of comparisons of myelinated PV^+ and PV^- axons by $DsRed^+$ and $DsReD^-$ OLs, we used a two-way ANOVA test followed by a multiple comparison Bonferroni's multiple comparison post hoc test. For comparisons of cluster composition and cell distances generated by hierarchical cluster analysis, each group of data was subjected to D'Agostino–Pearson normality test. Since data were not normally distributed, we used one-way Kruskal–Wallis test followed by a Dunn's multiple comparison post hoc test. Cumulative distributions were compared using Kolmogorov–Smirnov test. Correlations were tested with a Pearson *r* test and differences were considered significant when $p < 0.05$.

Reporting summary. Further information on research design is available in the Nature Research Reporting Summary linked to this article.

Data availability

The data that support the findings of this study are available from the corresponding author upon reasonable request.

Received: 28 June 2019 Accepted: 4 August 2019
Published online: 18 September 2019

References

1. Kessaris, N. et al. Competing waves of oligodendrocytes in the forebrain and postnatal elimination of an embryonic lineage. *Nat. Neurosci.* **9**, 173–179 (2006).
2. Marques, S. et al. Transcriptional convergence of oligodendrocyte lineage progenitors during development. *Dev. Cell* **46**, 504–517.e7 (2018).
3. Minocha, S. et al. NG2 glia are required for vessel network formation during embryonic development. *eLife* **4**, pii: e09102 (2015).
4. Hill, R. A., Patel, K. D., Goncalves, C. M., Grutzendler, J. & Nishiyama, A. Modulation of oligodendrocyte generation during a critical temporal window after NG2 cell division. *Nat. Neurosci.* **17**, 1518–1527 (2014).

5. Hughes, E. G., Kang, S. H., Fukaya, M. & Bergles, D. E. Oligodendrocyte progenitors balance growth with self-repulsion to achieve homeostasis in the adult brain. *Nat. Neurosci.* **16**, 668–676 (2013).
6. Wamsley, B. & Fishell, G. Genetic and activity-dependent mechanisms underlying interneuron diversity. *Nat. Rev. Neurosci.* **18**, 299–309 (2017).
7. Gelman, D. et al. A wide diversity of cortical GABAergic interneurons derives from the embryonic preoptic area. *J. Neurosci.* **31**, 16570–16580 (2011).
8. Gelman, D. M. et al. The embryonic preoptic area is a novel source of cortical GABAergic interneurons. *J. Neurosci.* **29**, 9380–9389 (2009).
9. Voronova, A. et al. Migrating interneurons secrete fractalkine to promote oligodendrocyte formation in the developing mammalian brain. *Neuron* **94**, 500–516.e9 (2017).
10. Winkler, C. C. et al. The dorsal wave of neocortical oligodendrogenesis begins embryonically and requires multiple sources of sonic hedgehog. *J. Neurosci.* **38**, 5237–5250 (2018).
11. Lin, S. C. & Bergles, D. E. Synaptic signaling between GABAergic interneurons and oligodendrocyte precursor cells in the hippocampus. *Nat. Neurosci.* **7**, 24–32 (2004).
12. Vélez-Fort, M., Maldonado, P. P., Butt, A. M., Audinat, E. & Angulo, M. C. Postnatal switch from synaptic to extrasynaptic transmission between interneurons and NG2 cells. *J. Neurosci.* **30**, 6921–6929 (2010).
13. Zonouzi, M. et al. GABAergic regulation of cerebellar NG2 cell development is altered in perinatal white matter injury. *Nat. Neurosci.* **18**, 674–682 (2015).
14. Balia, M. et al. Postnatal down-regulation of the GABAA receptor gamma2 subunit in neocortical NG2 cells accompanies synaptic-to-extrasynaptic switch in the GABAergic transmission mode. *Cereb. Cortex* **25**, 1114–1123 (2015).
15. Orduz, D. et al. Interneurons and oligodendrocyte progenitors form a structured synaptic network in the developing neocortex. *eLife* **4**, e06953 (2015).
16. Southwell, D. G. et al. Intrinsically determined cell death of developing cortical interneurons. *Nature* **491**, 109–113 (2012).
17. Teissier, A. et al. A novel transient glutamatergic population migrating from the pallial-subpallial boundary contributes to neocortical development. *J. Neurosci.* **30**, 10563–10574 (2010).
18. Bielle, F. et al. Multiple origins of Cajal-Retzius cells at the borders of the developing pallium. *Nat. Neurosci.* **8**, 1002–1012 (2005).
19. Ziskin, J. L., Nishiyama, A., Rubio, M., Fukaya, M. & Bergles, D. E. Vesicular release of glutamate from unmyelinated axons in white matter. *Nat. Neurosci.* **10**, 321–330 (2007).
20. Suzuki, R. & Shimodaira, H. Pvclust: an R package for assessing the uncertainty in hierarchical clustering. *Bioinformatics* **22**, 1540–1542 (2006).
21. R Core Team.*R: A Language and Environment for Statistical Computing*. R Foundation for Statistical Computing (R Development Core Team, Vienna, Austria, 2014).
22. Hirrlinger, P. G. et al. Expression of reef coral fluorescent proteins in the central nervous system of transgenic mice. *Mol. Cell Neurosci.* **30**, 291–303 (2005).
23. Balia, M., Benamer, N. & Angulo, M. C. A specific GABAergic synapse onto oligodendrocyte precursors does not regulate cortical oligodendrogenesis. *Glia* **65**, 1821–1832 (2017).
24. Micheva, K. D. et al. A large fraction of neocortical myelin ensheathes axons of local inhibitory neurons. *Elife* **5**, e15784 (2016).
25. Stedehouder, J. et al. Fast-spiking parvalbumin interneurons are frequently myelinated in the cerebral cortex of mice and humans. *Cereb. Cortex* **27**, 5001–5013 (2017).
26. Sun, L. O. et al. Spatiotemporal control of CNS myelination by oligodendrocyte programmed cell death through the TFEB-PUMA axis. *Cell* **175**, 1811–1826.e21 (2018).
27. Cruikshank, S. J., Lewis, T. J. & Connors, B. W. Synaptic basis for intense thalamocortical activation of feedforward inhibitory cells in neocortex. *Nat. Neurosci.* **10**, 462–468 (2007).
28. Causeret, F., Coppola, E. & Pierani, A. Cortical developmental death: selected to survive or fated to die. *Curr. Opin. Neurobiol.* **53**, 35–42 (2018).
29. Wong, F. K. et al. Pyramidal cell regulation of interneuron survival sculpts cortical networks. *Nature* **557**, 668–673 (2018).
30. Yu, Y.-C., Bultje, R. S., Wang, X. & Shi, S.-H. Specific synapses develop preferentially among sister excitatory neurons in the neocortex. *Nature* **458**, 501 (2009).
31. Brown, K. N. et al. Clonal production and organization of inhibitory interneurons in the neocortex. *Science* **334**, 480–486 (2011).
32. Ciceri, G. et al. Lineage-specific laminar organization of cortical GABAergic interneurons. *Nat. Neurosci.* **16**, 1199–1210 (2013).
33. Harwell, C. C. et al. Wide dispersion and diversity of clonally related inhibitory interneurons. *Neuron* **87**, 999–1007 (2015).
34. Mayer, C. et al. Clonally related forebrain interneurons disperse broadly across both functional areas and structural boundaries. *Neuron* **87**, 989–998 (2015).
35. Zhang, X.-J. et al. Precise inhibitory microcircuit assembly of developmentally related neocortical interneurons in clusters. *Nat. Commun.* **8**, 16091 (2017).
36. Butt, S. J. B. et al. The requirement of Nkx2-1 in the temporal specification of cortical interneuron subtypes. *Neuron* **59**, 722–732 (2008).
37. Marques, S. et al. Oligodendrocyte heterogeneity in the mouse juvenile and adult central nervous system. *Science* **352**, 1326–1329 (2016).
38. Fino, E. & Yuste, R. Dense inhibitory connectivity in neocortex. *Neuron* **69**, 1188–1203 (2011).
39. Crawford, A. H., Tripathi, R. B., Richardson, W. D. & Franklin, R. J. M. Developmental origin of oligodendrocyte lineage cells determines response to demyelination and susceptibility to age-associated functional decline. *Cell Rep.* **15**, 761–773 (2016).
40. Raff, M. C. et al. Programmed cell death and the control of cell survival: lessons from the nervous system. *Science* **262**, 695–700 (1993).
41. Trapp, B. D., Nishiyama, A., Cheng, D. & Macklin, W. Differentiation and death of premyelinating oligodendrocytes in developing rodent brain. *J. Cell Biol.* **137**, 459–468 (1997).
42. Franklin, R. J. M. & Ffrench-Constant, C. Regenerating CNS myelin - from mechanisms to experimental medicines. *Nat. Rev. Neurosci.* **18**, 753–769 (2017).
43. Takeuchi, O. et al. Essential role of BAX,BAK in B cell homeostasis and prevention of autoimmune disease. *Proc. Natl Acad. Sci. USA* **102**, 11272–11277 (2005).
44. Rothman, J. S. & Silver, R. A. NeuroMatic: an integrated open-source software toolkit for acquisition, analysis and simulation of electrophysiological data. *Front. Neuroinform.* **12**, 14 (2018).

Acknowledgements

This work was supported by grants from Fondation pour la Recherche Médicale (FRM, «Equipe FRM DEQ20150331681»), Agence Nationale de la Recherche (ANR, ANR-14-CE13-0023), Fondation pour l'aide à la recherche sur la Sclérose en Plaques (ARSEP), ANR under the frame of Neuron Cofund (Era-Net Neuron; project No. R19068KK) and a subaward agreement from the University of Connecticut with funds provided by Grant No. RG-1612-26501 from National Multiple Sclerosis Society (NMSS) (to M.C.A.), from IDEX-Paris Cité Sorbonne (TransGABA) (to M.C.A. and A.P.) and from FRM («Equipe FRM DEQ20130326521») (to A.P.). D. Ort. is recipient of an INSPIRE PhD fellowship from Marie Skłodowska-Curie Action (European Union's Horizon 2020) and Université de Paris (grant agreement: 665850). M.C.A. and A.P. are CNRS (Centre National de la Recherche Scientifique) investigators and teams of the ENP−Ile-de-France network.

Author contributions

D.Ord., N.B. and D.Ort. conducted electrophysiological experiments, immunostainings and analysis of data. L.V. helped with animal maintenance. M.C.A. performed hierarchical cluster analysis. D.Ord., N.B., D.Ort., E.C., A.P. and M.C.A. designed experiments, and A.P. and M.C.A. supervised the project. D.Ord., N.B., D.Ort., E.C., A.P. and M.C.A. wrote the manuscript.

Additional information

Supplementary Information accompanies this paper at https://doi.org/10.1038/s41467-019-11904-4.

Competing interests: The authors declare no competing interests.

Reprints and permission information is available online at http://npg.nature.com/reprintsandpermissions/

Peer review information *Nature Communications* thanks Akiko Nishiyama, and the other, anonymous, reviewer(s) for their contribution to the peer review of this work. Peer reviewer reports are available.

Publisher's note Springer Nature remains neutral with regard to jurisdictional claims in published maps and institutional affiliations.

Discussion

In the CNS, neuronal myelination is ensured by OLs, a process that is higly regulated and depending on the generation, proliferation and differentiation of OPCs during development and throughout life. Interestingly, many evidences in the litterature have shown that oligodendroglia dynamics and homeostasis is mainly influenced by neuron-oligodendrocyte lineage communcation which occurs through many different mechanisms, regulating multiple stages of OL maturation. Nowadays, it is well known that both OPCs and OLs can sense environmental signals through a large diversity of receptors for growth factors, signaling molecules, neurotransmitters and neuromodulators (Thornton and Hughes, 2020). Moreover, in addition of non-synaptic communication, it has been shown that OPCs are the only glial cells receiving *bona fide* synapses from neurons. All neuron-oligodendroglia communication modes influence oligodendroglia function and myelination in order to ensure brain function (Habermacher et al., 2019).

Since the last 15 years, it has been demonstrated that OPCs receive a major synaptic input from GABAergic INs that disappears after the second postnatal week (Lin and bergles 2004; Vélez-Fort et al., 2010; Balia et al., 2015). Interestingly, previous studies in the team demonstrated that, in the somatosensrory cortex, OPCs form a transient and highly organized network with GABAergic INs, characterized by a peak of synaptic connectivity at PN 10 (Orduz et al., 2015). In addition, PV FSIs represents a preferential synaptic input of OPC (Orduz et al., 2015, 2019). Nowadays, we have many evidences in litterature pointing out a strong relationship between cortical INs and OPCs during both, embryonic and postnatal development. It has been shown that these two populations share a common embryonic origin deriving from the MGE and POA from progenitors expressing the same transcription factors such as Nkx2.1 (Butt et al., 2008). Interestingly, beyond the common origin both cell types are also initially over-produced to then significantly die during the first PN week (Kessaris et al., 2006 ; Southwell et al., 2012). In additions, PV INs represent the largest proportion of myelinated GABAergic axons in mice and human cortex (Micheva et al., 2016 ; Stedehouder et al., 2017). Finally, Voronova et al. (2017) showed that migrating INs release Fraktalkine, paracrine factors promoting OPC differentiation. Even if several evidences suggest a crucial role of IN-OPC interactions for the development and correct

function of neuronal circuitry, many questions are still unresolved. Acquiring more knowledge about how INs and OPCs interact during embryonic and postnatal development is of crucial importance to understand how these two populations contribute to the assembly, maturation and myelination of cortical circuits.

In the first project, we followed a previous study in the team, focusing our attention on the transient synaptic input that OPCs receive from INs at the begining of the massive OPC differentiation, to potentially identify the implication of interneuron activity on OPC maturation. Using an optogenetic approach, we set up an experimental procedure to selectively activate cortical GABAergic INs *in vivo* in PN 10 mice. This specific age corresponds to the peak of interneuron-OPC synaptic activity.
As a first step, we identified Nkx2.1^{Cre} mice as a more suitable mouse model than PV^{Cre} mice to obtain an efficient ChR2 expression and photoactivation of cortical INs at PN 10. Thus, combining optogenetics, whole cell patch-clamp recordings in brain slices and extracellular recordings *in vivo*, we determined a photostimulation protocol to ensure an efficient photoactivation of targeted cells. We also set up a surgical procedure to implant a mini-optic fiber in the neonatal mouse brain in order to photoactivate cortical INs in awake pups. Finally, we analyzed the effect of INs photoactivation protocol on the oligodendroglia population in the neonatal neocortex.

In the last 10 years, optogenetics has been considered one of the most groundbreaking innovations in the field of neuroscience since it largely contributed to our understanding of mature nervous system circuits, allowing for the observation and modulation of cellular activities. However, not many studies have been performed in neonatal brain due to many techniqual limitations and efforts for the implementation of this technique in mouse pups (Bitzenhofer et al., 2017; Ahlbeck et al., 2018).

The first prerequisite to obtain a selective and reliable optogenetic activation of targeted cells is to reach a good level of opsin expression. This is more challenging in mouse pups since protein expression during early PN stages is lower and more viarable compared to later developmental periods. In our study, we first drove the ChR2 expression using PV promoter, Ca^{2+}-binding protein major marker of FSIs and expressed during the first PN week. However

we found that the ChR2 expression was very low in FSIs of PV-Cre:ChR2-YFP$^{flox/flox}$ mice. As a consequence, FSI were not able to trigger action potentials. However, immunostainings performed later in the development on PV-Cre mouse slices revealed a simulataneous increase of PV expression in concomitance with an increased of ChR2 expression in the same neurons. Cortical INs expressing both ChR2 (YFP^{+}) and PV^{+} displayed a more extensive and brighter membrane expression of the channel at PN 26 compared to the faintly cytoplasmatic expression observed at PN 10. Indeed, patch clamp recordings at PN 26 revealed that photoactivation-induced responses. Our results are in line with previous studies showing a weakly PV mRNAexpression at PN 10 in layer V of the somatosensory cortex compared to PN 16, i.e. where it has been observed a mature levels of PV mRNA expression (De Lecea et al., 1995). We thus identified PV-Cre transgenic mouse line as not suitable for our study at PN 10. We finally chose Nkx2.1-Cre:ChR2-YFP$^{flox/+}$ mice for the earlier expression of Nkx2.1 transcription factor during cortical development compared to PV, which ensured a consistent ChR2 expression with a reliable IN photoactivation at so early developmental stages (Marín, 2013; Wamsley and Fishell, 2017). In addition Butt and colleagues (2005), using a fate-mapping approach, followed Nkx2.1-derived IN development demostrating that they were already invading the mouse somatosensory barrel cortex during the first postnatal week. Therefore the first and crucial condition to take into account in optogenetics studies is the choice of the appropriate Cre transgenic mouse line to obtain a sufficient ChR2 expression in the age of your interest.

Once ensured the light sensitive channel expression, another key aspect to take into account when using an optogenetic approach is the kinetics response of the channels after photostimulation. It has been shown that the stimulation dynamics can be limited by both, light pulse duration and high frequency photostimulation. Although ChR2 is a depolarizing channel, studies conducted by Herman and colleagues (2014) demonstrated that ChR2 might silence rather than activate certain types of neurons. This effect is due to a long-lasting ChR2 photostimulation which leads to a mechannism of « depolarization block », a state characterized by an excessive cation influx followed by a difficult membrane repolarization and following the inability to trigger action potentials. In particular, increasing pulse duration and keeping moderate frequency of light stimulation induce a transient activation of regular-spiking INs followed by a period of inability to trigger action potentials. On the contrary,

excitatory PNs and subsets of fast-spiking neuronal populations are less sensitive to this block width pulse dependent. In any case, it has been shown that light pulse duration has a treshold over which neurons expressing ChR2 fail to trigger action potentials and get silenced (Herman et al., 2014). As mentioned, increasing the frequency of photocativation can also trigger the depolarization block. This effect is due to a decrease in membrane re-polarization between consecutive spikes which reduces the ionic driving force to restore the conditionf for a spiking event. This effect is dependent on the repolarizing rate of ion channels expressed in the cell type. It has been shown indeed that some neuronal populations are more sensitive to depolarization block, as it has been demonstrated in vitro by Mattis et al. (2011) where the use of ultrafast microbial opsins showed a greater tendency of excitatory neurons to enter depolarization block compared to FSIs.

Based on previous reports, we tested different frequencies and we finally decided to use for our project short-width light pulses (10 ms light pulses) delivered at 10–20 Hz to photostimulate ChR2-expressing INs of Nkx2.1-Cre:ChR2-YFP$^{flox/+}$ mice at PN 10. This frequency was the most reliable to trigger action potential discharges during 30 s. Interestingly, we observed that at the higher used photostimulation frequency (50 Hz), the INs response was characterized by action potential failures while current injections delivered at the same frequency were able to induce action potentials in these same cells. Different from the effects described before, depending on INs intrinsic membrane properties, these results indicate that the failures observed in IN responses were due to ChR2 expression levels and channel gated properties. It has been described that ChR2 opening and closing kinetics is slower than those of voltage-gated Na^+ and K^+ channels. In addition, it has been described many photocycle models to explain the ChR2 photocurrent decay under both continuous illumination and high frequency trains of light pulses. The most convincing is characterized by four-state, two open states (O_1– O_2) and two non-conductive “D” sub-states with a slow recovery (from 10 s to 20 s) after a dark period (Ernst et al., 2008; Stehfest and Hegemann, 2010; Saita et al., 2018). This long-lasting recovery time needed to restore ChR2 activation could explain the failures observed in IN responses (Ernst et al., 2008; Grossman et al., 2011). In addition, according to the model, O_1 and O_2 are usually at equilibrium but sustained illumination increases O_2/O_1 ratio. O_2 state is characterized by ~10 to 20 fold lower conductance compared to O_1, which could explain the reduced ChR2 response to

sustained photostimulation (Saita et al., 2018). Moreover, Grossman et al. (2011) found that, after photostimulation at 50 Hz of ChR2-expressing hippocampal neurons, the 63% of the responsive ChR2 were closed in the inter-pulse interval compared to 99% when stimulated at 10 Hz, preventing membrane repolarization and inducing the already introduced depolarization block (Grossman et al., 2011). This weak response obtained when applying high frequency light pulses due to ChR2 slow kinetics could be attenuated by a strong level of protein expression. Indeed, we observed that FSI response in PV-Cre:ChR2-YFP$^{flox/flox}$ mice recorded during the fourth postnatal week was less efficient than the one observed in Nkx2.1-Cre:ChR2-YFP$^{flox/+}$ mice recorded in earlier developmental stages.

Another aspect to take into account when using optical stimulation *in vivo* is the limited light penetration in the tissue due to its absorption and scattering. This effect decreases light intensity propagation and avoid a porper excitation in deep cortical layers. Indeed, previous reports showed that light intensity measured immediately below the fiber is the highest and then drops exponentially when penetrating in the brain tissue (Al-Juboori et al., 2013; Miyamoto and Murayama, 2015). Looking at previous *in vivo* studies, it has been shown that, using light pulses of 11.6 mW/mm^2, produced by a blue miniature light emitting diode (LED; 470 nm) placed at the surface of the brain was enough to trigger repsonses in ChR2-GFP-expressing layer 2/3 neurons (Huber et al., 2008). In another study, the stimulation at a higher light power (100 mW/mm^2) with an optic fiber placed on a small-window craniotomy while recording with extracellular electrodes was able to allow for the detection of neuronal firing responses in deep layer V of the primary motor cortex (Arenkiel et al., 2007). These evidences show that a huge increase in the photostimulus intensity is required to trigger action potentials from the surface in deep layers. In our in vivo study, we implanted a cannulae accomodating a mini-optic fiber on the cranial bone (Gradinaru et al., 2009; Yizhar et al., 2011), in order to trigger action potentials in a large number of layer V ChR2-expressing INs in pups. We chose this region because most of IN-OPC interactions have been described in that region, early in postnatal development (Vélez-Fort et al., 2010; Balia et al., 2015-2017; Orduz et al., 2015). We first tested whether photostimulation was able to elicit LFPs in acute cortical slices. In addition, using a pharmacological approach, we confirmed that recorded light-evoked LFPs in slices resulted from the direct generation of action potentials by multiple nearby ChR2-expressing INs . Indeed, the observed responses were

less sensitive to glutamatergic and GABAergic receptor antagonists than to the Na^+-channel blocker TTX which abolishes action potential generation. After these preliminary results in slices, we moved *in vivo*. Taking into account the light limitations due to scattering tissue, we first implanted both, the optic fiber and a wire electrode to record evoked LFPs in layer V upon photostimulation. We tested different Led powers from 1.5 mW to 4 mW. We obtained LFP responses using a low power stimulation, probably for the short distance light needed to travel to deep layers and the less myelinated cortex in pups compared to adult mice. We thus established the best protocol and ensure layer V IN activation *in vivo*.

All these evidences highlight the multiple aspects that must be taken into account when using an optogenetic approach. In particular, it is needed to establish the suitable light pulse duration, frequency and power to illuminate neurons avoiding undesirable effects. We thus set our photostimulation parameters taking in account all the limitations due to ChR2 expression at so early postnatal developmental stages and both, IN and ChR2 intrinsic properties.

Other limit we had to consider for our experimental design was the placement of a cannulae that accomodates a mini-optic fiber, directly fixed on the mouse skull for the photostuimulation *in vivo* (Gradinaru et al., 2009; Yizhar et al., 2011). This procedure is more difficult to apply in mouse pups, since their cranial bones are still too soft to stably mantain the implant. This issue has probably precluded the use of optogenetics to study developing circuits, privileging pharmacogenetics (Kozorovitskiy et. al 2012 ; Wong et al., 2018), a versatile but less precise technique in time and space. We found a solution by artificially hardening the bones with a double layer of glue just before to stereotaxically drill the hole where the implant will be placed.

Finally, we analyzed how the increase of interneuron activity in Nkx2.1-Cre:ChR2-$YFP^{flox/+}$ mouse *in vivo* could impact OPC proliferation at PN 10, a critical developmental stage for oligodednrogenesis and haracterized by a peak of IN-OPC connectivity in the somatosensory cortex (Orduz et al.,2015 Hill et al., 2014; Balia et al., 2017). « We found that the activity of GABAergic INs did not change either OPC proliferation or the number of OPCs and OLs in response to a 3 h photostimulation session » (Ortolani et al., 2018). Our result

support a previous study in the team in which the inactivation of IN-OPC synapses at PN 10 had not impact on OPC proliferation (Balia et al., 2017). However, Gibson et al., (2014) had previously shown that long-lasting photostimulation session of cortical glutamatergic neurons (30 min) in juvenile weaned mice promote OPC proliferation. Another study in the team used the the 3h photostimulation protocol to stimulate glutamatergic neurons in demyelinated lesions of adult mice, also observing an increase in OPC proliferation and differentiation (Ortiz et al., 2019). Unlike glutamatergic neurons, our results suggest that GABAergic INs might have different roles in controlling OPC function in the neocortex. Another possibility is the need to test different stimulation paradigms to reproduce with high fidelity IN activation, using more efficient variants of ChR2 enabling higher frequency firings, closer to that of INs, in particular that of FSIs. Indeed, OPCs respond in a different manner to different stimulation paradigms (Nagy et al., 2017). Thus, it would be interesting to test for example ChR2 E123T/T159C or the ChETA variant that displays a faster kinetics and 80% of success when using up to 200 Hz as photostimulation frequency respectively (Berndt et al., 2011 ; Gunaydin et al., 2010). Another possibility would be to explore the involvement of metabotropic GABAR activation, like the $GABA_BR$, abundantly expressed in and downregulated during the differentiation process as for $GABA_AR$ (Charles, Deuchars, Davies, & Pangalos, 2003; Luyt et al., 2007).

While in this first project we investigated the effect of GABAergic INs activity on OPCs proliferation and differentiation in the early neocortex (Vélez-Fort et al., 2010; Balia et al., 2015; Orduz et al., 2015), in the second report, we focused our attention on the common embryonic origin of these two cell populations derived from the MGE and POA (Kessaris et al., 2006; Fishell et al., 2017). Interestingly, we discovered that a proportion of firstOPCs, subpopulation believed to completely disappear during postnatal development, survives and forms functional cell clusters with lineage-related INs. In addition, these cells showed a high synaptic connectivity within these cell clusters. We also demonstrated that this ratio of surviving firstOPCs differentiate into mature OLs, myelinating different types of neuronal fibers nearby their interneuron counterparts, with any preference for their lineage-related INs . These results reveal that the same embrionic region favors cellular interactions later in the development that are tightly regulated and crucial for a correct organization and function of neuronal circuits. Finally, after inducing the aberrant survival of firstOPCs

committed to die by genetic manipulation, we did not observe any increase in the connectivity with interneuronal related partners and, surprisingly, any compensation in the total number of OPCs to homeostatically control and mantain OPC density. On the contrary, the aberrant survival of lineage-related INs and firstOPCs promotes an increase in the entire oligodendroglia population, probably through a non-cell-autonomous mechanism. This is in contradiction with Kessaris et al. work (2006), showing that following OPC waves compete with each other to regulate OPC density. In summary, we identified a new role for interneuron and firsOPC cell death in regulating their lineage-related cell communcation and the oligodendroglia population homeostasis during postnatal development.

This study is in continuity with previous studies of the team (Orduz et al., 2015), but following the idea that INs and firstOPCs common embryonic origin could favor the preferential IN-OPC synaptic connectivity , and promote a local arrangement of these two populations in the somatosensory cortex. In this report, after genetically targeting Dbx1-derived INs and firstOPCs, we confirmed a high connection probability, positively influenced by the common embryonic origin. In addition, we investigated the role of firstOPCs and INs PCD through Bax-dependent rescue experiments. First, the surviving cells rescued from death do not show the same high connectivity observed in physiological conditions. This missing communication between INs and rescued firstOPCs suggest that, in normal conditions, the survival of firstOPCs could be influenced by the connectivity with their interneuronal partners. On the contrary, the cells displaying low levels of connectivity are the ones supposed to die. Previous *in vitro* and *in vivo* studies demonstrated that, depending on the cell population, neuronal activity modulate both, cell survival or death (Ghosh et al., 1994; Golbs et al., 2011; Murase et al., 2011; Blanqui et al. 2017). In addition, a recent report demonstrated that the prevention of PN death induces the MGE/POA-derived INs rescue from PCD through an activity-dependent mechanism (Wong et al., 2018). This process has probably the role to appropriately balance the ratio of excitatory and inhibitory inputs in the cerebral cortex. From these evidences, it is possible that, as described for PNs and INs, IN activity favors OPC survival.

The IN and OPC spatial organization in clusters recalls several reports describing the synaptic connectivity in the neocortex to be highly specific (Yu et al., 2009). For example, it has been

described in LV from the mouse primary visual cortex that corticotectal PNs and the position of partner synaptically connected was determined across different species, revealing a precisely organized cortical microcircuits (Kozloski et la., 2001). Another example is described in Yu et al. (2009) where excitatory neurons coming from the same mother cell form a highly specific microcircuit during cortical development. Differently from PN organization, little is known about the spatial arrangement of neocortical inhibitory INs. Nevertheless, Ueno et al., (2017) described how temporal cortex subregions develop following different developmental programs compared to other cortical regions, with different developmental stages for GABAergic INs not following the same described in the primary sensory cortex. These results suggest the existence of a substantial difference in the developmental program in the somatosensory and visual cortex which specifies the organization of the two regions. This reveal how different cortical regions could have region-specific characteristics and organization during cortical development. Another study, labelling clonally related INs, identified their spatial organization in individual clonal clusters containing different IN subtypes (Brown et al., 2011 ; Sultan et al. ; 2016). Interestingly, a recent study found that cortical INs organized in clusters form electrical, but not chemical, synapses with each other at PN 14 (Zhang et al., 2017). Although all these evidences suggest that the common embryonic origin plays a crucial role in the organization and circuit formation of inhibitory INs in the neocortex, a highly organized distribution in functional clusters is still under discussion. Here we described how INs and firstOPCs, both MGE and POA derived, are organized in functional cell clusters. Despite this result, the molecular and cellular mechanisms responsible for their highly regulated localization in deep cortical layers need to be elucidated.

We also investigated whether MGE/POA-derived IN and FirstOPC organization in clusters, with IN-OPC intersomatic distances limited to 70 ± 4 µm, favor the preferential axon myelination of embrionically-related interneuronal partners. Previous reports showed that a substantial fraction of myelin in the cortex and hippocampus ensheathes axons of GABAergic INs, in particular of PV INs, in both mice and humans (Micheva et al., 2016 ; Stedehouder et al., 2017). In addition, Stedehouder et al. (2018) described how chemogenetic activation of neocortical PV INs was followed by an increase in their myelination, mostly mediated by a more elaborated axonal morphology. Interestingly, Micheva et al. (2016) also found a

significantly different protein composition in GABAergic axon myelin compared to that of excitatory axons, the first expressing 20% more MBP. This difference in protein composition might suggest that PNs and INs are myelinated by distinct OLs since it has been already shown that different regions of CNS are populated by diverse mature OL with some populations present throughout the brain and others enriched in specific regions (Marques et al., 2016). Indeed, in line with recent studies (Marisca et al., 2020 ; Marques et al., 2016), Zonouzi et al., (2019) suggests the existence of different OPC and OL populations in the neocortex. However, our data did not show any tendency of POA-derived OL in myelinating INs from the same origin, observing similar proportions of PV^+ and PV^- myelinated axons. This lack of preference of firstOLs for PV^+ axons in YFP^+ cell clusters suggests that interactions between lineage-related INs and firstOLs do not guide the firstOL to preferentially myelinate the axon of its IN partner. We can thus conclude that activity-dependent myelination by firstOLs is not guided by a predetermined ontogenetic program (Orduz et al., 2019). It is possible, however, that firstOLs confined in a so small space with their lineage-related INs could contribute to myelination and maturation of specific local circuits, facilitating synchronization and propagation of action potentials of both, glutamatergic and GABAergic neurons, within a restricted space (Orduz et al., 2019).

It has been described in many reports how OPC are over-produced during development, in three sequential waves to then be eliminated by PCD in order to adjust their final number during the first two postnatal weeks (Kessaris et al., 2006; Raff et al., 1993). As we already introduced before, Southwell and colleagues (2012) shown that the 40% of cortical INs are eliminated through a Bax-dependent mechanism in concomitance with firstOPC death. Interestingly it has been recently shown the TFEB promotes the death of pre-myelinating OLs in a Bax-dependent manner, mechanism to ensure a correct spatial and temporal specification of brain myelination (Sun et al., 2018). Initally, it was thought that the three waves of OPCs were in competition between each other in order to ensure a correct balance in OL lineage homeostasis (Kessaris et al., 2006). Previous studies in the optic nerve indeed decsribed that 50% of OLs die in early development by competition for limited amounts of survival signals (Barres et al., 1992). It has been also demontrsated in recent reports the incredible plasticity of Oligodendglia lineage in regulating their cell number during development, in adult life and also in pathological conditions.

It has been shown that cortical OPCs are highly dynamic and explore the surrounding enviroment through motile filopodia (Hughes et al., 2013). Since this continous monitoring, a decrease in OPC cell number through death, differentiation or injury is rapidly detected and followed by local migration and proliferation in order to mantain their homeostasis (Hughes et al., 2013). Other example of oligodendroglia plasticity has been described in the developing somatosensory cortex, where whisker deprivation was followed by an increase of newly-formed OLs death, accompanied to an enhancing in OPC proliferation (Hill et al., 2014). All these evidences show how OPCs react to environmental changes to compensate for its loss and preserve their homeostasis in order to ensure a correct myelination and function of neuronal circuits. However, a potential impact of IN-glia interactions on oligodendroglia homeostasis had not been previously explored. Our groundbreaking results are in contrast with previous studies. Indeed, the impact of lineage-related INs and firstOPCs rescued from PCD on the entire oligodendroglial population induces a significant increase of their density. Our findings reveal a new role of PCD during cortical development in controlling the oligodendroglia number via a non-cell-autonomous mechanism (Orduz et al., 2019).

Conclusions

Nowadays, it is recognized that GABAergic INs , over the interplay with PNs, adjust excitation/inhibition balance for a healthy brain activity. Our study shows that INs also constitute true partners of oligodendroglia during cortical embryonic and postnatal development. It is thus very likely that the proper functioning of these two different cell populations has an impact on each other, at least during the early phases of circuit formation and maturation.

In our first report, we investigated how interneuron activity affects OPCs at PN 10 in the somatosensory cortex, prior to their differentiation by describing a step-by-step experimental protocol for the optogenetic interrogation of this neuron-oligodendroglia interaction in mouse pups *in vivo*. Increasing the activity of Nkx2.1 INs we did not observe any difference in the density of proliferating OPCs, suggesting a limited effect of interneuron activity on OPC proliferation at this age. This result supports and complements our previous findings showing that the GABAergic synaptic activity of OPCs does not play a role in

oligodendrogenesis (Balia et al., 2017). It would be interesting analyze whether GABAergic activity promotes oligodendroglia migration, mightly related with GABAB receptors activation, (Luyt et al., 2007) by inspecting the cell density in different cortical layers after *in vivo* stimulation. Furthermore, this methodology could be useful to study other cellular interactions in the developing brain to get new insights on the role of glial cells *in vivo* during neuronal circuit formation and maturation. In the second report, we analysed interneuron-first OPCs common embryonic origin. We shed light on a complex postnatal interplay between the two distinct populations that is favor by the same embryonic origin of the cells. In addition, we found unexpectedly a new role for firstOPCs and interneuron PCD, previously underestimated and restricted to an adjustment of the overproduced cell number. In line with recent studies, showing how pyramidal cells number is crucial to regulate interneuron survival and stabilize excitation/inhibition balance (ref), our study identified in INs and firstOPCs death/survival balance a crucial role to ensure oligondendroglia homeostasis and a proper myelination.

Several evidences in litterature suggest that GABA communcation of neurons with OL lineage cells may constitute a major mechanisms of building and modulating the cortical networks. INs -OL lineage interactions have to be thus further investigated to shed light on the mechanisms behind this communication and deeply understand this complex and highly sophisticated interplay which fine-tunes cortical circuitry during embryonic development and throughout life.

Bibliography

Achilles, K., Okabe, A., Ikeda, M., Shimizu-Okabe, C., Yamada, J., Fukuda, A., Luhmann, H.J., Kilb, W., 2007. Kinetic properties of Cl uptake mediated by Na+-dependent K+-2Cl cotransport in immature rat neocortical neurons. J. Neurosci. 27, 8616–8627. https://doi.org/10.1523/JNEUROSCI.5041-06.2007

Agresti, C., Meomartini, M.E., Amadio, S., Ambrosini, E., Volonté, C., Aloisi, F., Visentin, S., 2005. ATP regulates oligodendrocyte progenitor migration, proliferation, and differentiation: involvement of metabotropic P2 receptors. Brain Res. Brain Res. Rev. 48, 157–165. https://doi.org/10.1016/j.brainresrev.2004.12.005

Ahlbeck, J., Song, L., Chini, M., Bitzenhofer, S.H., Hanganu-Opatz, I.L., 2018. Glutamatergic drive along the septo-temporal axis of hippocampus boosts prelimbic oscillations in the neonatal mouse. Elife 7. https://doi.org/10.7554/eLife.33158

Alfano, C., Studer, M., 2013. Neocortical arealization: evolution, mechanisms, and open questions. Dev Neurobiol 73, 411–447. https://doi.org/10.1002/dneu.22067

Al-Juboori, S.I., Dondzillo, A., Stubblefield, E.A., Felsen, G., Lei, T.C., Klug, A., 2013. Light scattering properties vary across different regions of the adult mouse brain. PLoS ONE 8, e67626. https://doi.org/10.1371/journal.pone.0067626

Anastasiades, P.G., Marques-Smith, A., Lyngholm, D., Lickiss, T., Raffiq, S., Kätzel, D., Miesenböck, G., Butt, S.J.B., 2016. GABAergic INs form transient layer-specific circuits in early postnatal neocortex. Nat Commun 7, 10584. https://doi.org/10.1038/ncomms10584

Anderson, D.J., Groves, A., Lo, L., Ma, Q., Rao, M., Shah, N.M., Sommer, L., 1997. Cell lineage determination and the control of neuronal identity in the neural crest. Cold Spring Harb. Symp. Quant. Biol. 62, 493–504.

Andriezen, W.L., 1893. The Neuroglia Elements in the Human Brain. Br Med J 2, 227–230. https://doi.org/10.1136/bmj.2.1700.227

Angulo, M.C., Le Meur, K., Kozlov, A.S., Charpak, S., Audinat, E., 2008. GABA, a forgotten gliotransmitter. Prog. Neurobiol. 86, 297–303. https://doi.org/10.1016/j.pneurobio.2008.08.002

Arellano, R.O., Sánchez-Gómez, M.V., Alberdi, E., Canedo-Antelo, M., Chara, J.C., Palomino, A., Pérez-Samartín, A., Matute, C., 2016. Axon-to-Glia Interaction Regulates GABAA Receptor Expression in Oligodendrocytes. Mol. Pharmacol. 89, 63–74. https://doi.org/10.1124/mol.115.100594

Arenkiel, B.R., Peca, J., Davison, I.G., Feliciano, C., Deisseroth, K., Augustine, G.J., Ehlers, M.D., Feng, G., 2007. In vivo light-induced activation of neural circuitry in transgenic mice expressing channelrhodopsin-2. Neuron 54, 205–218. https://doi.org/10.1016/j.neuron.2007.03.005

Arminjon M, 2009. EspacesTemps.net. L'homoncule de Penfield.

Bacmeister, C.M., Barr, H.J., McClain, C.R., Thornton, M.A., Nettles, D., Welle, C.G., Hughes, E.G., 2020. Motor learning promotes remyelination via new and surviving oligodendrocytes. Nat. Neurosci. https://doi.org/10.1038/s41593-020-0637-3

Balia, M., Benamer, N., Angulo, M.C., 2017. A specific GABAergic synapse onto oligodendrocyte precursors does not regulate cortical oligodendrogenesis. Glia 65, 1821–1832. https://doi.org/10.1002/glia.23197

Balia, M., Vélez-Fort, M., Passlick, S., Schäfer, C., Audinat, E., Steinhäuser, C., Seifert, G., Angulo, M.C., 2015. Postnatal down-regulation of the GABAA receptor γ2 subunit in neocortical NG2 cells accompanies synaptic-to-extrasynaptic switch in the GABAergic transmission mode. Cereb. Cortex 25, 1114–1123. https://doi.org/10.1093/cercor/bht309

Baraban, M., Koudelka, S., Lyons, D.A., 2018. Ca 2+ activity signatures of myelin sheath formation and growth in vivo. Nat. Neurosci. 21, 19–23. https://doi.org/10.1038/s41593-017-0040-x

Baron, W., Colognato, H., ffrench-Constant, C., Ffrench-Constant, C., 2005. Integrin-growth factor interactions as regulators of oligodendroglial development and function. Glia 49, 467–479. https://doi.org/10.1002/glia.20132

Barres, B.A., Hart, I.K., Coles, H.S., Burne, J.F., Voyvodic, J.T., Richardson, W.D., Raff, M.C., 1992. Cell death and control of cell survival in the oligodendrocyte lineage. Cell 70, 31–46. https://doi.org/10.1016/0092-8674(92)90531-g

Barres, B.A., Jacobson, M.D., Schmid, R., Sendtner, M., Raff, M.C., 1993. Does oligodendrocyte survival depend on axons? Curr. Biol. 3, 489–497. https://doi.org/10.1016/0960-9822(93)90039-q

Barres, B.A., Raff, M.C., 1993. Proliferation of oligodendrocyte precursor cells depends on electrical activity in axons. Nature 361, 258–260. https://doi.org/10.1038/361258a0

Bartolini, G., Sánchez-Alcañiz, J.A., Osório, C., Valiente, M., García-Frigola, C., Marín, O., 2017. Neuregulin 3 Mediates Cortical Plate Invasion and Laminar Allocation of GABAergic INs . Cell Rep 18, 1157–1170. https://doi.org/10.1016/j.celrep.2016.12.089

Battefeld, A., Popovic, M.A., de Vries, S.I., Kole, M.H.P., 2019. High-Frequency Microdomain Ca2+ Transients and Waves during Early Myelin Internode Remodeling. Cell Rep 26, 182-191.e5. https://doi.org/10.1016/j.celrep.2018.12.039

Baude, A., Nusser, Z., Roberts, J.D., Mulvihill, E., McIlhinney, R.A., Somogyi, P., 1993. The metabotropic glutamate receptor (mGluR1 alpha) is concentrated at perisynaptic membrane of neuronal subpopulations as detected by immunogold reaction. Neuron 11, 771–787. https://doi.org/10.1016/0896-6273(93)90086-7

Beck, T.W., Magnuson, N.S., Rapp, U.R., 1995. Growth factor regulation of cell cycle progression and cell fate determination. Curr. Top. Microbiol. Immunol. 194, 291–303. https://doi.org/10.1007/978-3-642-79275-5_34

Benamer, N., Vidal, M., Angulo, M.C., 2020. The cerebral cortex is a substrate of multiple interactions between GABAergic INs and oligodendrocyte lineage cells. Neurosci. Lett. 715, 134615. https://doi.org/10.1016/j.neulet.2019.134615

Bennett, M.V.L., Zukin, R.S., 2004. Electrical coupling and neuronal synchronization in the Mammalian brain. Neuron 41, 495–511. https://doi.org/10.1016/s0896-6273(04)00043-1

Bergles, D.E., Richardson, W.D., 2015. Oligodendrocyte Development and Plasticity. Cold Spring Harb Perspect Biol 8, a020453. https://doi.org/10.1101/cshperspect.a020453

Bergles, D.E., Roberts, J.D., Somogyi, P., Jahr, C.E., 2000. Glutamatergic synapses on oligodendrocyte precursor cells in the hippocampus. Nature 405, 187–191. https://doi.org/10.1038/35012083

Berndt, A., Schoenenberger, P., Mattis, J., Tye, K.M., Deisseroth, K., Hegemann, P., Oertner, T.G., 2011. High-efficiency channelrhodopsins for fast neuronal stimulation at low light levels. Proc. Natl. Acad. Sci. U.S.A. 108, 7595–7600. https://doi.org/10.1073/pnas.1017210108

Bitzenhofer, S.H., Ahlbeck, J., Hanganu-Opatz, I.L., 2017. Methodological Approach for Optogenetic Manipulation of Neonatal Neuronal Networks. Front Cell Neurosci 11, 239. https://doi.org/10.3389/fncel.2017.00239

Blanquie, O., Kilb, W., Sinning, A., Luhmann, H.J., 2017. Homeostatic interplay between electrical activity and neuronal apoptosis in the developing neocortex. Neuroscience 358, 190–200. https://doi.org/10.1016/j.neuroscience.2017.06.030

Blaschke, A.J., Staley, K., Chun, J., 1996. Widespread programmed cell death in proliferative and postmitotic regions of the fetal cerebral cortex. Development 122, 1165–1174.

Bortone, D.S., Olsen, S.R., Scanziani, M., 2014. Translaminar inhibitory cells recruited by layer 6 corticothalamic neurons suppress visual cortex. Neuron 82, 474–485. https://doi.org/10.1016/j.neuron.2014.02.021

Brody, B.A., Kinney, H.C., Kloman, A.S., Gilles, F.H., 1987. Sequence of central nervous system myelination in human infancy. I. An autopsy study of myelination. J. Neuropathol. Exp. Neurol. 46, 283–301. https://doi.org/10.1097/00005072-198705000-00005

Brown, K.N., Chen, S., Han, Z., Lu, C.-H., Tan, X., Zhang, X.-J., Ding, L., Lopez-Cruz, A., Saur, D., Anderson, S.A., Huang, K., Shi, S.-H., 2011. Clonal production and organization of inhibitory INs in the neocortex. Science 334, 480–486. https://doi.org/10.1126/science.1208884

Brunet, A., Bonni, A., Zigmond, M.J., Lin, M.Z., Juo, P., Hu, L.S., Anderson, M.J., Arden, K.C., Blenis, J., Greenberg, M.E., 1999. Akt promotes cell survival by phosphorylating and inhibiting a Forkhead transcription factor. Cell 96, 857–868. https://doi.org/10.1016/s0092-8674(00)80595-4

Butt, F., S, N., A, K., Jg, C., G, F., 2005. The Temporal and Spatial Origins of Cortical INs Predict Their Physiological Subtype [WWW Document]. Neuron. https://doi.org/10.1016/j.neuron.2005.09.034

Butt, S.J.B., Sousa, V.H., Fuccillo, M.V., Hjerling-Leffler, J., Miyoshi, G., Kimura, S., Fishell, G., 2008. The requirement of Nkx2-1 in the temporal specification of cortical interneuron subtypes. Neuron 59, 722–732. https://doi.org/10.1016/j.neuron.2008.07.031

Cahoy, J.D., Emery, B., Kaushal, A., Foo, L.C., Zamanian, J.L., Christopherson, K.S., Xing, Y., Lubischer, J.L., Krieg, P.A., Krupenko, S.A., Thompson, W.J., Barres, B.A., 2008. A transcriptome database for astrocytes, neurons, and oligodendrocytes: a new

resource for understanding brain development and function. J. Neurosci. 28, 264–278. https://doi.org/10.1523/JNEUROSCI.4178-07.2008

Causeret, F., Coppola, E., Pierani, A., 2018. Cortical developmental death: selected to survive or fated to die. Curr. Opin. Neurobiol. 53, 35–42. https://doi.org/10.1016/j.conb.2018.04.022

Charles, K.J., Deuchars, J., Davies, C.H., Pangalos, M.N., 2003. GABA B receptor subunit expression in glia. Mol. Cell. Neurosci. 24, 214–223. https://doi.org/10.1016/s1044-7431(03)00162-3

Chen, T.-J., Kula, B., Nagy, B., Barzan, R., Gall, A., Ehrlich, I., Kukley, M., 2018a. In Vivo Regulation of Oligodendrocyte Precursor Cell Proliferation and Differentiation by the AMPA-Receptor Subunit GluA2. Cell Rep 25, 852-861.e7. https://doi.org/10.1016/j.celrep.2018.09.066

Chen, T.-J., Kula, B., Nagy, B., Barzan, R., Gall, A., Ehrlich, I., Kukley, M., 2018b. In Vivo Regulation of Oligodendrocyte Precursor Cell Proliferation and Differentiation by the AMPA-Receptor Subunit GluA2. Cell Rep 25, 852-861.e7. https://doi.org/10.1016/j.celrep.2018.09.066

Chowdhury, T.G., Jimenez, J.C., Bomar, J.M., Cruz-Martin, A., Cantle, J.P., Portera-Cailliau, C., 2010. Fate of cajal-retzius neurons in the postnatal mouse neocortex. Front Neuroanat 4, 10. https://doi.org/10.3389/neuro.05.010.2010

Clarke, L.E., Young, K.M., Hamilton, N.B., Li, H., Richardson, W.D., Attwell, D., 2012. Properties and fate of oligodendrocyte progenitor cells in the corpus callosum, motor cortex, and piriform cortex of the mouse. J. Neurosci. 32, 8173–8185. https://doi.org/10.1523/JNEUROSCI.0928-12.2012

Clarke, P.G., 1992. Neuron death in the developing avian isthmo-optic nucleus, and its relation to the establishment of functional circuitry. J. Neurobiol. 23, 1140–1158. https://doi.org/10.1002/neu.480230907

Colgin, L.L., Denninger, T., Fyhn, M., Hafting, T., Bonnevie, T., Jensen, O., Moser, M.-B., Moser, E.I., 2009. Frequency of gamma oscillations routes flow of information in the hippocampus. Nature 462, 353–357. https://doi.org/10.1038/nature08573

Colgin, L.L., Moser, E.I., 2010. Gamma Oscillations in the Hippocampus. Physiology 25, 319–329. https://doi.org/10.1152/physiol.00021.2010

Crawley, J.N., Belknap, J.K., Collins, A., Crabbe, J.C., Frankel, W., Henderson, N., Hitzemann, R.J., Maxson, S.C., Miner, L.L., Silva, A.J., Wehner, J.M., Wynshaw-Boris, A., Paylor, R., 1997. Behavioral phenotypes of inbred mouse strains: implications and recommendations for molecular studies. Psychopharmacology (Berl.) 132, 107–124. https://doi.org/10.1007/s002130050327

Daw, M.I., Ashby, M.C., Isaac, J.T.R., 2007. Coordinated developmental recruitment of latent fast spiking INs in layer IV barrel cortex. Nat. Neurosci. 10, 453–461. https://doi.org/10.1038/nn1866

De Biase, L.M., Nishiyama, A., Bergles, D.E., 2010. Excitability and synaptic communication within the oligodendrocyte lineage. J. Neurosci. 30, 3600–3611. https://doi.org/10.1523/JNEUROSCI.6000-09.2010

de Lecea, L., del Río, J.A., Soriano, E., 1995. Developmental expression of parvalbumin mRNA in the cerebral cortex and hippocampus of the rat. Brain Res. Mol. Brain Res. 32, 1–13. https://doi.org/10.1016/0169-328x(95)00056-x

DeFelipe, J., Hendry, S.H., Jones, E.G., 1986. A correlative electron microscopic study of basket cells and large GABAergic neurons in the monkey sensory-motor cortex. Neuroscience 17, 991–1009. https://doi.org/10.1016/0306-4522(86)90075-8

Dekkers, M.P.J., Nikoletopoulou, V., Barde, Y.-A., 2013. Cell biology in neuroscience: Death of developing neurons: new insights and implications for connectivity. J. Cell Biol. 203, 385–393. https://doi.org/10.1083/jcb.201306136

Demerens, C., Stankoff, B., Logak, M., Anglade, P., Allinquant, B., Couraud, F., Zalc, B., Lubetzki, C., 1996. Induction of myelination in the central nervous system by electrical activity. Proc. Natl. Acad. Sci. U.S.A. 93, 9887–9892. https://doi.org/10.1073/pnas.93.18.9887

DiGregorio, D.A., Nusser, Z., Silver, R.A., 2002. Spillover of glutamate onto synaptic AMPA receptors enhances fast transmission at a cerebellar synapse. Neuron 35, 521–533. https://doi.org/10.1016/s0896-6273(02)00787-0

Dimou, L., Simon, C., Kirchhoff, F., Takebayashi, H., Götz, M., 2008. Progeny of Olig2-expressing progenitors in the gray and white matter of the adult mouse cerebral cortex. J. Neurosci. 28, 10434–10442. https://doi.org/10.1523/JNEUROSCI.2831-08.2008

Dingledine, R., Hume, R.I., Heinemann, S.F., 1992. Structural determinants of barium permeation and rectification in non-NMDA glutamate receptor channels. J. Neurosci. 12, 4080–4087.

Doischer, D., Hosp, J.A., Yanagawa, Y., Obata, K., Jonas, P., Vida, I., Bartos, M., 2008. Postnatal differentiation of basket cells from slow to fast signaling devices. J. Neurosci. 28, 12956–12968. https://doi.org/10.1523/JNEUROSCI.2890-08.2008

Du, J., Zhang, L., Weiser, M., Rudy, B., McBain, C.J., 1996. Developmental expression and functional characterization of the potassium-channel subunit Kv3.1b in parvalbumin-containing INs of the rat hippocampus. J. Neurosci. 16, 506–518.

Du, T., Xu, Q., Ocbina, P.J., Anderson, S.A., 2008. NKX2.1 specifies cortical interneuron fate by activating Lhx6. Development 135, 1559–1567. https://doi.org/10.1242/dev.015123

Duebel, J., Marazova, K., Sahel, J.-A., 2015. Optogenetics. Curr Opin Ophthalmol 26, 226–232. https://doi.org/10.1097/ICU.0000000000000140

Dugas, J.C., Cuellar, T.L., Scholze, A., Ason, B., Ibrahim, A., Emery, B., Zamanian, J.L., Foo, L.C., McManus, M.T., Barres, B.A., 2010. Dicer1 and miR-219 Are required for normal oligodendrocyte differentiation and myelination. Neuron 65, 597–611. https://doi.org/10.1016/j.neuron.2010.01.027

Duque, A., Krsnik, Z., Kostović, I., Rakic, P., 2016. Secondary expansion of the transient subplate zone in the developing cerebrum of human and nonhuman primates. Proc. Natl. Acad. Sci. U.S.A. 113, 9892–9897. https://doi.org/10.1073/pnas.1610078113

Ellis, R.E., Yuan, J.Y., Horvitz, H.R., 1991. Mechanisms and functions of cell death. Annu. Rev. Cell Biol. 7, 663–698. https://doi.org/10.1146/annurev.cb.07.110191.003311

Emery, B., Agalliu, D., Cahoy, J.D., Watkins, T.A., Dugas, J.C., Mulinyawe, S.B., Ibrahim, A., Ligon, K.L., Rowitch, D.H., Barres, B.A., 2009. Myelin gene regulatory factor is a critical transcriptional regulator required for CNS myelination. Cell 138, 172–185. https://doi.org/10.1016/j.cell.2009.04.031

Ernst, O.P., Sánchez Murcia, P.A., Daldrop, P., Tsunoda, S.P., Kateriya, S., Hegemann, P., 2008. Photoactivation of channelrhodopsin. J. Biol. Chem. 283, 1637–1643. https://doi.org/10.1074/jbc.M708039200

Fairén, A., Peters, A., Saldanha, J., 1977. A new procedure for examining Golgi impregnated neurons by light and electron microscopy. J. Neurocytol. 6, 311–337. https://doi.org/10.1007/BF01175194

Fan, X., Agid, Y., 2018. At the Origin of the History of Glia. Neuroscience 385, 255–271. https://doi.org/10.1016/j.neuroscience.2018.05.050

Fannon, J., Tarmier, W., Fulton, D., 2015. Neuronal activity and AMPA-type glutamate receptor activation regulates the morphological development of oligodendrocyte precursor cells. Glia 63, 1021–1035. https://doi.org/10.1002/glia.22799

Farrant, M., Nusser, Z., 2005. Variations on an inhibitory theme: phasic and tonic activation of GABA(A) receptors. Nat. Rev. Neurosci. 6, 215–229. https://doi.org/10.1038/nrn1625

Fernandez, P.A., Tang, D.G., Cheng, L., Prochiantz, A., Mudge, A.W., Raff, M.C., 2000. Evidence that axon-derived neuregulin promotes oligodendrocyte survival in the developing rat optic nerve. Neuron 28, 81–90. https://doi.org/10.1016/s0896-6273(00)00087-8

Ferrer, I., Bernet, E., Soriano, E., del Rio, T., Fonseca, M., 1990. Naturally occurring cell death in the cerebral cortex of the rat and removal of dead cells by transitory phagocytes. Neuroscience 39, 451–458. https://doi.org/10.1016/0306-4522(90)90281-8

Finlay, B.L., Slattery, M., 1983. Local differences in the amount of early cell death in neocortex predict adult local specializations. Science 219, 1349–1351. https://doi.org/10.1126/science.6828866

Flames, N., Pla, R., Gelman, D.M., Rubenstein, J.L.R., Puelles, L., Marín, O., 2007. Delineation of multiple subpallial progenitor domains by the combinatorial expression of transcriptional codes. J. Neurosci. 27, 9682–9695. https://doi.org/10.1523/JNEUROSCI.2750-07.2007

Fogarty, C.E., Bergmann, A., 2015. The Sound of Silence: Signaling by Apoptotic Cells. Curr. Top. Dev. Biol. 114, 241–265. https://doi.org/10.1016/bs.ctdb.2015.07.013

Fogarty, M., Grist, M., Gelman, D., Marín, O., Pachnis, V., Kessaris, N., 2007. Spatial genetic patterning of the embryonic neuroepithelium generates GABAergic interneuron diversity in the adult cortex. J. Neurosci. 27, 10935–10946. https://doi.org/10.1523/JNEUROSCI.1629-07.2007

Fulton, D., Paez, P.M., Campagnoni, A.T., 2010. The multiple roles of myelin protein genes during the development of the oligodendrocyte. ASN Neuro 2. https://doi.org/10.1042/AN20090051

Galarreta, M., Hestrin, S., 1999. A network of fast-spiking cells in the neocortex connected by electrical synapses. Nature 402, 72–75. https://doi.org/10.1038/47029

Gallo, V., Mangin, J.-M., Kukley, M., Dietrich, D., 2008. Synapses on NG2-expressing progenitors in the brain: multiple functions? J. Physiol. (Lond.) 586, 3767–3781. https://doi.org/10.1113/jphysiol.2008.158436

Gallo, V., Zhou, J.M., McBain, C.J., Wright, P., Knutson, P.L., Armstrong, R.C., 1996. Oligodendrocyte progenitor cell proliferation and lineage progression are regulated by glutamate receptor-mediated K+ channel block. J. Neurosci. 16, 2659–2670.

Galluzzi, L., Vitale, I., Aaronson, S.A., Abrams, J.M., Adam, D., Agostinis, P., Alnemri, E.S., Altucci, L., Amelio, I., Andrews, D.W., Annicchiarico-Petruzzelli, M., Antonov, A.V., Arama, E., Baehrecke, E.H., Barlev, N.A., Bazan, N.G., Bernassola, F., Bertrand, M.J.M., Bianchi, K., Blagosklonny, M.V., Blomgren, K., Borner, C., Boya, P., Brenner, C., Campanella, M., Candi, E., Carmona-Gutierrez, D., Cecconi, F., Chan, F.K.-M., Chandel, N.S., Cheng, E.H., Chipuk, J.E., Cidlowski, J.A., Ciechanover, A., Cohen, G.M., Conrad, M., Cubillos-Ruiz, J.R., Czabotar, P.E., D'Angiolella, V., Dawson, T.M., Dawson, V.L., De Laurenzi, V., De Maria, R., Debatin, K.-M., DeBerardinis, R.J., Deshmukh, M., Di Daniele, N., Di Virgilio, F., Dixit, V.M., Dixon, S.J., Duckett, C.S., Dynlacht, B.D., El-Deiry, W.S., Elrod, J.W., Fimia, G.M., Fulda, S., García-Sáez, A.J., Garg, A.D., Garrido, C., Gavathiotis, E., Golstein, P., Gottlieb, E., Green, D.R., Greene, L.A., Gronemeyer, H., Gross, A., Hajnoczky, G., Hardwick, J.M., Harris, I.S., Hengartner, M.O., Hetz, C., Ichijo, H., Jäättelä, M., Joseph, B., Jost, P.J., Juin, P.P., Kaiser, W.J., Karin, M., Kaufmann, T., Kepp, O., Kimchi, A., Kitsis, R.N., Klionsky, D.J., Knight, R.A., Kumar, S., Lee, S.W., Lemasters, J.J., Levine, B., Linkermann, A., Lipton, S.A., Lockshin, R.A., López-Otín, C., Lowe, S.W., Luedde, T., Lugli, E., MacFarlane, M., Madeo, F., Malewicz, M., Malorni, W., Manic, G., Marine, J.-C., Martin, S.J., Martinou, J.-C., Medema, J.P., Mehlen, P., Meier, P., Melino, S., Miao, E.A., Molkentin, J.D., Moll, U.M., Muñoz-Pinedo, C., Nagata, S., Nuñez, G., Oberst, A., Oren, M., Overholtzer, M., Pagano, M., Panaretakis, T., Pasparakis, M., Penninger, J.M., Pereira, D.M., Pervaiz, S., Peter, M.E., Piacentini, M., Pinton, P., Prehn, J.H.M., Puthalakath, H., Rabinovich, G.A., Rehm, M.,

Rizzuto, R., Rodrigues, C.M.P., Rubinsztein, D.C., Rudel, T., Ryan, K.M., Sayan, E., Scorrano, L., Shao, F., Shi, Y., Silke, J., Simon, H.-U., Sistigu, A., Stockwell, B.R., Strasser, A., Szabadkai, G., Tait, S.W.G., Tang, D., Tavernarakis, N., Thorburn, A., Tsujimoto, Y., Turk, B., Vanden Berghe, T., Vandenabeele, P., Vander Heiden, M.G., Villunger, A., Virgin, H.W., Vousden, K.H., Vucic, D., Wagner, E.F., Walczak, H., Wallach, D., Wang, Y., Wells, J.A., Wood, W., Yuan, J., Zakeri, Z., Zhivotovsky, B., Zitvogel, L., Melino, G., Kroemer, G., 2018. Molecular mechanisms of cell death: recommendations of the Nomenclature Committee on Cell Death 2018. Cell Death Differ. 25, 486–541. https://doi.org/10.1038/s41418-017-0012-4

Gelman, D., Griveau, A., Dehorter, N., Teissier, A., Varela, C., Pla, R., Pierani, A., Marín, O., 2011. A wide diversity of cortical GABAergic INs derives from the embryonic preoptic area. J. Neurosci. 31, 16570–16580. https://doi.org/10.1523/JNEUROSCI.4068-11.2011

Gelman, D.M., Marín, O., 2010. Generation of interneuron diversity in the mouse cerebral cortex. Eur. J. Neurosci. 31, 2136–2141. https://doi.org/10.1111/j.1460-9568.2010.07267.x

Gelman, D.M., Martini, F.J., Nóbrega-Pereira, S., Pierani, A., Kessaris, N., Marín, O., 2009. The embryonic preoptic area is a novel source of cortical GABAergic INs . J. Neurosci. 29, 9380–9389. https://doi.org/10.1523/JNEUROSCI.0604-09.2009

Ghosh, A., Carnahan, J., Greenberg, M.E., 1994. Requirement for BDNF in activity-dependent survival of cortical neurons. Science 263, 1618–1623. https://doi.org/10.1126/science.7907431

Gibson, J.R., Beierlein, M., Connors, B.W., 1999. Two networks of electrically coupled inhibitory neurons in neocortex. Nature 402, 75–79. https://doi.org/10.1038/47035

Gilbert, P., Kettenmann, H., Schachner, M., 1984. gamma-Aminobutyric acid directly depolarizes cultured oligodendrocytes. J. Neurosci. 4, 561–569.

Glucksmann, A., 1951. Cell deaths in normal vertebrate ontogeny. Biol Rev Camb Philos Soc 26, 59–86. https://doi.org/10.1111/j.1469-185x.1951.tb00774.x

Goebbels, S., Wieser, G.L., Pieper, A., Spitzer, S., Weege, B., Yan, K., Edgar, J.M., Yagensky, O., Wichert, S.P., Agarwal, A., Karram, K., Renier, N., Tessier-Lavigne, M., Rossner, M.J., Káradóttir, R.T., Nave, K.-A., 2017. A neuronal PI(3,4,5)P3-dependent program

of oligodendrocyte precursor recruitment and myelination. Nat. Neurosci. 20, 10–15. https://doi.org/10.1038/nn.4425

Golbs, A., Nimmervoll, B., Sun, J.-J., Sava, I.E., Luhmann, H.J., 2011. Control of programmed cell death by distinct electrical activity patterns. Cereb. Cortex 21, 1192–1202. https://doi.org/10.1093/cercor/bhq200

Goldschneider, D., Mehlen, P., 2010. Dependence receptors: a new paradigm in cell signaling and cancer therapy. Oncogene 29, 1865–1882. https://doi.org/10.1038/onc.2010.13

Götz, M., Huttner, W.B., 2005. The cell biology of neurogenesis. Nat. Rev. Mol. Cell Biol. 6, 777–788. https://doi.org/10.1038/nrm1739

Gradinaru, V., Mogri, M., Thompson, K.R., Henderson, J.M., Deisseroth, K., 2009. Optical deconstruction of parkinsonian neural circuitry. Science 324, 354–359. https://doi.org/10.1126/science.1167093

Grossman, N., Nikolic, K., Grubb, M.S., Burrone, J., Toumazou, C., Degenaar, P., 2011. High-frequency limit of neural stimulation with ChR2. Conf Proc IEEE Eng Med Biol Soc 2011, 4167–4170. https://doi.org/10.1109/IEMBS.2011.6091034

Gunaydin, L.A., Yizhar, O., Berndt, A., Sohal, V.S., Deisseroth, K., Hegemann, P., 2010. Ultrafast optogenetic control. Nat. Neurosci. 13, 387–392. https://doi.org/10.1038/nn.2495

Guo, F., Maeda, Y., Ma, J., Xu, J., Horiuchi, M., Miers, L., Vaccarino, F., Pleasure, D., 2010. Pyramidal neurons are generated from oligodendroglial progenitor cells in adult piriform cortex. J. Neurosci. 30, 12036–12049. https://doi.org/10.1523/JNEUROSCI.1360-10.2010

Gupta, A., Tsai, L.-H., Wynshaw-Boris, A., 2002. Life is a journey: a genetic look at neocortical development. Nat. Rev. Genet. 3, 342–355. https://doi.org/10.1038/nrg799

Haberlandt, C., Derouiche, A., Wyczynski, A., Haseleu, J., Pohle, J., Karram, K., Trotter, J., Seifert, G., Frotscher, M., Steinhäuser, C., Jabs, R., 2011. Gray matter NG2 cells display multiple Ca2+-signaling pathways and highly motile processes. PLoS ONE 6, e17575. https://doi.org/10.1371/journal.pone.0017575

Habermacher, C., Angulo, M.C., Benamer, N., 2019. Glutamate versus GABA in neuron-oligodendroglia communication. Glia 67, 2092–2106. https://doi.org/10.1002/glia.23618

Hamilton, N., Vayro, S., Wigley, R., Butt, A.M., 2010. Axons and astrocytes release ATP and glutamate to evoke calcium signals in NG2-glia. Glia 58, 66–79. https://doi.org/10.1002/glia.20902

Hamilton, N.B., Clarke, L.E., Arancibia-Carcamo, I.L., Kougioumtzidou, E., Matthey, M., Káradóttir, R., Whiteley, L., Bergersen, L.H., Richardson, W.D., Attwell, D., 2017. Endogenous GABA controls oligodendrocyte lineage cell number, myelination, and CNS internode length. Glia 65, 309–321. https://doi.org/10.1002/glia.23093

Hansen, D.V., Lui, J.H., Flandin, P., Yoshikawa, K., Rubenstein, J.L., Alvarez-Buylla, A., Kriegstein, A.R., 2013. Non-epithelial stem cells and cortical interneuron production in the human ganglionic eminences. Nat. Neurosci. 16, 1576–1587. https://doi.org/10.1038/nn.3541

Hatch, R.J., Mendis, G.D.C., Kaila, K., Reid, C.A., Petrou, S., 2017. Gap Junctions Link Regular-Spiking and Fast-Spiking INs in Layer 5 Somatosensory Cortex. Front Cell Neurosci 11, 204. https://doi.org/10.3389/fncel.2017.00204

Haydar, T.F., Kuan, C.Y., Flavell, R.A., Rakic, P., 1999. The role of cell death in regulating the size and shape of the mammalian forebrain. Cereb. Cortex 9, 621–626. https://doi.org/10.1093/cercor/9.6.621

He, L., Lu, Q.R., 2013. Coordinated control of oligodendrocyte development by extrinsic and intrinsic signaling cues. Neurosci Bull 29, 129–143. https://doi.org/10.1007/s12264-013-1318-y

He, M., Tucciarone, J., Lee, S., Nigro, M.J., Kim, Y., Levine, J.M., Kelly, S.M., Krugikov, I., Wu, P., Chen, Y., Gong, L., Hou, Y., Osten, P., Rudy, B., Huang, Z.J., 2016. Strategies and Tools for Combinatorial Targeting of GABAergic Neurons in Mouse Cerebral Cortex. Neuron 92, 555. https://doi.org/10.1016/j.neuron.2016.10.009

Henley, J.M., 2003. Proteins interactions implicated in AMPA receptor trafficking: a clear destination and an improving route map. Neurosci. Res. 45, 243–254. https://doi.org/10.1016/s0168-0102(02)00229-8

Herman, A.M., Huang, L., Murphey, D.K., Garcia, I., Arenkiel, B.R., 2014. Cell type-specific and time-dependent light exposure contribute to silencing in neurons expressing Channelrhodopsin-2. Elife 3, e01481. https://doi.org/10.7554/eLife.01481

Hildebrand, C., Remahl, S., Persson, H., Bjartmar, C., 1993. Myelinated nerve fibres in the CNS. Prog. Neurobiol. 40, 319–384. https://doi.org/10.1016/0301-0082(93)90015-k

Hill, R.A., Patel, K.D., Goncalves, C.M., Grutzendler, J., Nishiyama, A., 2014. Modulation of oligodendrocyte generation during a critical temporal window after NG2 cell division. Nat. Neurosci. 17, 1518–1527. https://doi.org/10.1038/nn.3815

Hines, J.H., Ravanelli, A.M., Schwindt, R., Scott, E.K., Appel, B., 2015. Neuronal activity biases axon selection for myelination in vivo. Nat. Neurosci. 18, 683–689. https://doi.org/10.1038/nn.3992

Hippenmeyer, S., Vrieseling, E., Sigrist, M., Portmann, T., Laengle, C., Ladle, D.R., Arber, S., 2005. A developmental switch in the response of DRG neurons to ETS transcription factor signaling. PLoS Biol. 3, e159. https://doi.org/10.1371/journal.pbio.0030159

Hirata, T., Li, P., Lanuza, G.M., Cocas, L.A., Huntsman, M.M., Corbin, J.G., 2009. Identification of distinct telencephalic progenitor pools for neuronal diversity in the amygdala. Nat. Neurosci. 12, 141–149. https://doi.org/10.1038/nn.2241

Hoerder-Suabedissen, A., Molnár, Z., 2015. Development, evolution and pathology of neocortical subplate neurons. Nat. Rev. Neurosci. 16, 133–146. https://doi.org/10.1038/nrn3915

Horton, J.C., Adams, D.L., 2005. The cortical column: a structure without a function. Philos. Trans. R. Soc. Lond., B, Biol. Sci. 360, 837–862. https://doi.org/10.1098/rstb.2005.1623

Huber, D., Petreanu, L., Ghitani, N., Ranade, S., Hromádka, T., Mainen, Z., Svoboda, K., 2008. Sparse optical microstimulation in barrel cortex drives learned behaviour in freely moving mice. Nature 451, 61–64. https://doi.org/10.1038/nature06445

Hughes, E.G., Kang, S.H., Fukaya, M., Bergles, D.E., 2013. Oligodendrocyte progenitors balance growth with self-repulsion to achieve homeostasis in the adult brain. Nat. Neurosci. 16, 668–676. https://doi.org/10.1038/nn.3390

Hughes, E.G., Orthmann-Murphy, J.L., Langseth, A.J., Bergles, D.E., 2018. Myelin remodeling through experience-dependent oligodendrogenesis in the adult

somatosensory cortex. Nat. Neurosci. 21, 696–706. https://doi.org/10.1038/s41593-018-0121-5

Hume, R.I., Dingledine, R., Heinemann, S.F., 1991. Identification of a site in glutamate receptor subunits that controls calcium permeability. Science 253, 1028–1031. https://doi.org/10.1126/science.1653450

Inan, M., Welagen, J., Anderson, S.A., 2012. Spatial and temporal bias in the mitotic origins of somatostatin- and parvalbumin-expressing interneuron subgroups and the chandelier subtype in the medial ganglionic eminence. Cereb. Cortex 22, 820–827. https://doi.org/10.1093/cercor/bhr148

Jacob, C., Lebrun-Julien, F., Suter, U., 2011. How histone deacetylases control myelination. Mol. Neurobiol. 44, 303–312. https://doi.org/10.1007/s12035-011-8198-9

Jacobson, M.D., Weil, M., Raff, M.C., 1997. Programmed cell death in animal development. Cell 88, 347–354. https://doi.org/10.1016/s0092-8674(00)81873-5

Jiang, X., Shen, S., Cadwell, C.R., Berens, P., Sinz, F., Ecker, A.S., Patel, S., Tolias, A.S., 2015. Principles of connectivity among morphologically defined cell types in adult neocortex. Science 350, aac9462. https://doi.org/10.1126/science.aac9462

Julien, O., Wells, J.A., 2017. Caspases and their substrates. Cell Death Differ. 24, 1380–1389. https://doi.org/10.1038/cdd.2017.44

Kale, J., Liu, Q., Leber, B., Andrews, D.W., 2012. Shedding light on apoptosis at subcellular membranes. Cell 151, 1179–1184. https://doi.org/10.1016/j.cell.2012.11.013

Kanatani, S., Yozu, M., Tabata, H., Nakajima, K., 2008. COUP-TFII Is Preferentially Expressed in the Caudal Ganglionic Eminence and Is Involved in the Caudal Migratory Stream. J. Neurosci. 28, 13582–13591. https://doi.org/10.1523/JNEUROSCI.2132-08.2008

Kang, S.H., Fukaya, M., Yang, J.K., Rothstein, J.D., Bergles, D.E., 2010. NG2+ CNS glial progenitors remain committed to the oligodendrocyte lineage in postnatal life and following neurodegeneration. Neuron 68, 668–681. https://doi.org/10.1016/j.neuron.2010.09.009

Káradóttir, R., Attwell, D., 2007a. Neurotransmitter receptors in the life and death of oligodendrocytes. Neuroscience 145, 1426–1438. https://doi.org/10.1016/j.neuroscience.2006.08.070

Káradóttir, R., Attwell, D., 2007b. Neurotransmitter receptors in the life and death of oligodendrocytes. Neuroscience 145, 1426–1438. https://doi.org/10.1016/j.neuroscience.2006.08.070

Káradóttir, R., Cavelier, P., Bergersen, L.H., Attwell, D., 2005. NMDA receptors are expressed in oligodendrocytes and activated in ischaemia. Nature 438, 1162–1166. https://doi.org/10.1038/nature04302

Káradóttir, R.T., Kuo, C.T., 2018. Neuronal Activity-Dependent Control of Postnatal Neurogenesis and Gliogenesis. Annu. Rev. Neurosci. 41, 139–161. https://doi.org/10.1146/annurev-neuro-072116-031054

Kawaguchi, Y., Katsumaru, H., Kosaka, T., Heizmann, C.W., Hama, K., 1987. Fast spiking cells in rat hippocampus (CA1 region) contain the calcium-binding protein parvalbumin. Brain Res. 416, 369–374. https://doi.org/10.1016/0006-8993(87)90921-8

Kerr, J.F., Wyllie, A.H., Currie, A.R., 1972. Apoptosis: a basic biological phenomenon with wide-ranging implications in tissue kinetics. Br. J. Cancer 26, 239–257. https://doi.org/10.1038/bjc.1972.33

Kessaris, N., Fogarty, M., Iannarelli, P., Grist, M., Wegner, M., Richardson, W.D., 2006. Competing waves of oligodendrocytes in the forebrain and postnatal elimination of an embryonic lineage. Nat. Neurosci. 9, 173–179. https://doi.org/10.1038/nn1620

Kiecker, C., Lumsden, A., 2012. The role of organizers in patterning the nervous system. Annu. Rev. Neurosci. 35, 347–367. https://doi.org/10.1146/annurev-neuro-062111-150543

Kostovic, I., Rakic, P., 1980. Cytology and time of origin of interstitial neurons in the white matter in infant and adult human and monkey telencephalon. J. Neurocytol. 9, 219–242. https://doi.org/10.1007/BF01205159

Kougioumtzidou, E., Shimizu, T., Hamilton, N.B., Tohyama, K., Sprengel, R., Monyer, H., Attwell, D., Richardson, W.D., 2017. Signalling through AMPA receptors on oligodendrocyte precursors promotes myelination by enhancing oligodendrocyte survival. Elife 6. https://doi.org/10.7554/eLife.28080

Kozloski, J., Hamzei-Sichani, F., Yuste, R., 2001. Stereotyped position of local synaptic targets in neocortex. Science 293, 868–872. https://doi.org/10.1126/science.293.5531.868

Krasnow, A.M., Ford, M.C., Valdivia, L.E., Wilson, S.W., Attwell, D., 2018. Regulation of developing myelin sheath elongation by oligodendrocyte calcium transients in vivo. Nat. Neurosci. 21, 24–28. https://doi.org/10.1038/s41593-017-0031-y

Kukley, M., Capetillo-Zarate, E., Dietrich, D., 2007. Vesicular glutamate release from axons in white matter. Nat. Neurosci. 10, 311–320. https://doi.org/10.1038/nn1850

Kukley, M., Kiladze, M., Tognatta, R., Hans, M., Swandulla, D., Schramm, J., Dietrich, D., 2008. Glial cells are born with synapses. FASEB J. 22, 2957–2969. https://doi.org/10.1096/fj.07-090985

Kukley, M., Nishiyama, A., Dietrich, D., 2010. The fate of synaptic input to NG2 glial cells: neurons specifically downregulate transmitter release onto differentiating oligodendroglial cells. J. Neurosci. 30, 8320–8331. https://doi.org/10.1523/JNEUROSCI.0854-10.2010

Kvansakul, M., Hinds, M.G., 2015. The Bcl-2 family: structures, interactions and targets for drug discovery. Apoptosis 20, 136–150. https://doi.org/10.1007/s10495-014-1051-7

Larson, V.A., Zhang, Y., Bergles, D.E., 2016. Electrophysiological properties of NG2(+) cells: Matching physiological studies with gene expression profiles. Brain Res. 1638, 138–160. https://doi.org/10.1016/j.brainres.2015.09.010

Ledonne, F., Orduz, D., Mercier, J., Vigier, L., Grove, E.A., Tissir, F., Angulo, M.C., Pierani, A., Coppola, E., 2016. Targeted Inactivation of Bax Reveals a Subtype-Specific Mechanism of Cajal-Retzius Neuron Death in the Postnatal Cerebral Cortex. Cell Rep 17, 3133–3141. https://doi.org/10.1016/j.celrep.2016.11.074

Lee, S., Hjerling-Leffler, J., Zagha, E., Fishell, G., Rudy, B., 2010. The largest group of superficial neocortical GABAergic INs expresses ionotropic serotonin receptors. J. Neurosci. 30, 16796–16808. https://doi.org/10.1523/JNEUROSCI.1869-10.2010

Lee, S., Leach, M.K., Redmond, S.A., Chong, S.Y.C., Mellon, S.H., Tuck, S.J., Feng, Z.-Q., Corey, J.M., Chan, J.R., 2012. A culture system to study oligodendrocyte myelination processes using engineered nanofibers. Nat. Methods 9, 917–922. https://doi.org/10.1038/nmeth.2105

Li, P., Nijhawan, D., Budihardjo, I., Srinivasula, S.M., Ahmad, M., Alnemri, E.S., Wang, X., 1997. Cytochrome c and dATP-dependent formation of Apaf-1/caspase-9 complex initiates an apoptotic protease cascade. Cell 91, 479–489. https://doi.org/10.1016/s0092-8674(00)80434-1

Li, Q., Brus-Ramer, M., Martin, J.H., McDonald, J.W., 2010. Electrical stimulation of the medullary pyramid promotes proliferation and differentiation of oligodendrocyte progenitor cells in the corticospinal tract of the adult rat. Neurosci. Lett. 479, 128–133. https://doi.org/10.1016/j.neulet.2010.05.043

Lin, J.Y., 2011. A user's guide to channelrhodopsin variants: features, limitations and future developments. Exp. Physiol. 96, 19–25. https://doi.org/10.1113/expphysiol.2009.051961

Lin, S., Bergles, D.E., 2004. Synaptic signaling between GABAergic INs and oligodendrocyte precursor cells in the hippocampus. Nat. Neurosci. 7, 24–32. https://doi.org/10.1038/nn1162

Liodis, P., Denaxa, M., Grigoriou, M., Akufo-Addo, C., Yanagawa, Y., Pachnis, V., 2007. Lhx6 activity is required for the normal migration and specification of cortical interneuron subtypes. J. Neurosci. 27, 3078–3089. https://doi.org/10.1523/JNEUROSCI.3055-06.2007

Liu, J., Dietz, K., DeLoyht, J.M., Pedre, X., Kelkar, D., Kaur, J., Vialou, V., Lobo, M.K., Dietz, D.M., Nestler, E.J., Dupree, J., Casaccia, P., 2012. Impaired adult myelination in the prefrontal cortex of socially isolated mice. Nat. Neurosci. 15, 1621–1623. https://doi.org/10.1038/nn.3263

Lodato, S., Shetty, A.S., Arlotta, P., 2015. Cerebral cortex assembly: generating and reprogramming projection neuron diversity. Trends Neurosci. 38, 117–125. https://doi.org/10.1016/j.tins.2014.11.003

Long, J.E., Cobos, I., Potter, G.B., Rubenstein, J.L.R., 2009. Dlx1&2 and Mash1 Transcription Factors Control MGE and CGE Patterning and Differentiation through Parallel and Overlapping Pathways. Cereb Cortex 19, i96–i106. https://doi.org/10.1093/cercor/bhp045

Luyt, K., Slade, T.P., Dorward, J.J., Durant, C.F., Wu, Y., Shigemoto, R., Mundell, S.J., Váradi, A., Molnár, E., 2007. Developing oligodendrocytes express functional GABA(B) receptors that stimulate cell proliferation and migration. J. Neurochem. 100, 822–840. https://doi.org/10.1111/j.1471-4159.2006.04255.x

Luyt, K., Váradi, A., Durant, C.F., Molnár, E., 2006. Oligodendroglial metabotropic glutamate receptors are developmentally regulated and involved in the prevention of apoptosis. J. Neurochem. 99, 641–656. https://doi.org/10.1111/j.1471-4159.2006.04103.x

Luyt, K., Varadi, A., Molnar, E., 2003. Functional metabotropic glutamate receptors are expressed in oligodendrocyte progenitor cells. J. Neurochem. 84, 1452–1464. https://doi.org/10.1046/j.1471-4159.2003.01661.x

Ma, Y., Hu, H., Berrebi, A.S., Mathers, P.H., Agmon, A., 2006. Distinct Subtypes of Somatostatin-Containing Neocortical INs Revealed in Transgenic Mice. J. Neurosci. 26, 5069–5082. https://doi.org/10.1523/JNEUROSCI.0661-06.2006

Mably, A.J., Colgin, L.L., 2018. Gamma oscillations in cognitive disorders. Curr. Opin. Neurobiol. 52, 182–187. https://doi.org/10.1016/j.conb.2018.07.009

Makinodan, M., Rosen, K.M., Ito, S., Corfas, G., 2012. A critical period for social experience-dependent oligodendrocyte maturation and myelination. Science 337, 1357–1360. https://doi.org/10.1126/science.1220845

Maldonado, P.P., Angulo, M.C., 2015. Multiple Modes of Communication between Neurons and Oligodendrocyte Precursor Cells. Neuroscientist 21, 266–276. https://doi.org/10.1177/1073858414530784

Maldonado, P.P., Vélez-Fort, M., Levavasseur, F., Angulo, M.C., 2013. Oligodendrocyte precursor cells are accurate sensors of local K+ in mature gray matter. J. Neurosci. 33, 2432–2442. https://doi.org/10.1523/JNEUROSCI.1961-12.2013

Mandl, R.C.W., Schnack, H.G., Luigjes, J., van den Heuvel, M.P., Cahn, W., Kahn, R.S., Hulshoff Pol, H.E., 2010. Tract-based analysis of magnetization transfer ratio and diffusion tensor imaging of the frontal and frontotemporal connections in schizophrenia. Schizophr Bull 36, 778–787. https://doi.org/10.1093/schbul/sbn161

Mangin, J.-M., Gallo, V., 2011. The curious case of NG2 cells: transient trend or game changer? ASN Neuro 3, e00052. https://doi.org/10.1042/AN20110001

Mangin, J.-M., Kunze, A., Chittajallu, R., Gallo, V., 2008. Satellite NG2 progenitor cells share common glutamatergic inputs with associated INs in the mouse dentate gyrus. J. Neurosci. 28, 7610–7623. https://doi.org/10.1523/JNEUROSCI.1355-08.2008

Mangin, J.-M., Li, P., Scafidi, J., Gallo, V., 2012. Experience-dependent regulation of NG2 progenitors in the developing barrel cortex. Nat. Neurosci. 15, 1192–1194. https://doi.org/10.1038/nn.3190

Maricich, S.M., Gilmore, E.C., Herrup, K., 2001. The role of tangential migration in the establishment of mammalian cortex. Neuron 31, 175–178. https://doi.org/10.1016/s0896-6273(01)00370-1

Marin-Husstege, M., Muggironi, M., Liu, A., Casaccia-Bonnefil, P., 2002. Histone deacetylase activity is necessary for oligodendrocyte lineage progression. J. Neurosci. 22, 10333–10345.

Marisca, R., Hoche, T., Agirre, E., Hoodless, L.J., Barkey, W., Auer, F., Castelo-Branco, G., Czopka, T., 2020. Functionally distinct subgroups of oligodendrocyte precursor cells integrate neural activity and execute myelin formation. Nat. Neurosci. 23, 363–374. https://doi.org/10.1038/s41593-019-0581-2

Marques, S., van Bruggen, D., Vanichkina, D.P., Floriddia, E.M., Munguba, H., Väremo, L., Giacomello, S., Falcão, A.M., Meijer, M., Björklund, Å.K., Hjerling-Leffler, J., Taft, R.J., Castelo-Branco, G., 2018a. Transcriptional Convergence of Oligodendrocyte Lineage Progenitors during Development. Dev. Cell 46, 504-517.e7. https://doi.org/10.1016/j.devcel.2018.07.005

Marques, S., van Bruggen, D., Vanichkina, D.P., Floriddia, E.M., Munguba, H., Väremo, L., Giacomello, S., Falcão, A.M., Meijer, M., Björklund, Å.K., Hjerling-Leffler, J., Taft, R.J., Castelo-Branco, G., 2018b. Transcriptional Convergence of Oligodendrocyte Lineage Progenitors during Development. Dev. Cell 46, 504-517.e7. https://doi.org/10.1016/j.devcel.2018.07.005

Marques, S., Zeisel, A., Codeluppi, S., van Bruggen, D., Mendanha Falcão, A., Xiao, L., Li, H., Häring, M., Hochgerner, H., Romanov, R.A., Gyllborg, D., Muñoz Manchado, A., La Manno, G., Lönnerberg, P., Floriddia, E.M., Rezayee, F., Ernfors, P., Arenas, E., Hjerling-Leffler, J., Harkany, T., Richardson, W.D., Linnarsson, S., Castelo-Branco, G., 2016. Oligodendrocyte heterogeneity in the mouse juvenile and adult central nervous system. Science 352, 1326–1329. https://doi.org/10.1126/science.aaf6463

Marx, M., Qi, G., Hanganu-Opatz, I.L., Kilb, W., Luhmann, H.J., Feldmeyer, D., 2017. Neocortical Layer 6B as a Remnant of the Subplate - A Morphological Comparison. Cereb. Cortex 27, 1011–1026. https://doi.org/10.1093/cercor/bhv279

Masahira, N., Takebayashi, H., Ono, K., Watanabe, K., Ding, L., Furusho, M., Ogawa, Y., Nabeshima, Y., Alvarez-Buylla, A., Shimizu, K., Ikenaka, K., 2006. Olig2-positive progenitors in the embryonic spinal cord give rise not only to motoneurons and oligodendrocytes, but also to a subset of astrocytes and ependymal cells. Dev. Biol. 293, 358–369. https://doi.org/10.1016/j.ydbio.2006.02.029

Mateos, J.M., Benítez, R., Elezgarai, I., Azkue, J.J., Lázaro, E., Osorio, A., Bilbao, A., Doñate, F., Sarría, R., Conquet, F., Ferraguti, F., Kuhn, R., Knöpfel, T., Grandes, P., 2000. Immunolocalization of the mGluR1b splice variant of the metabotropic glutamate receptor 1 at parallel fiber-Purkinje cell synapses in the rat cerebellar cortex. J. Neurochem. 74, 1301–1309. https://doi.org/10.1046/j.1471-4159.2000.741301.x

Matsui, K., Jahr, C.E., 2003. Ectopic release of synaptic vesicles. Neuron 40, 1173–1183. https://doi.org/10.1016/s0896-6273(03)00788-8

Mattis, J., Tye, K.M., Ferenczi, E.A., Ramakrishnan, C., O'Shea, D.J., Prakash, R., Gunaydin, L.A., Hyun, M., Fenno, L.E., Gradinaru, V., Yizhar, O., Deisseroth, K., 2012. Principles for applying optogenetic tools derived from direct comparative analysis of microbial opsins. Nature Methods 9, 159–172. https://doi.org/10.1038/nmeth.1808

Mazzola, L., Isnard, J., Peyron, R., Mauguière, F., 2012. Stimulation of the human cortex and the experience of pain: Wilder Penfield's observations revisited. Brain 135, 631–640. https://doi.org/10.1093/brain/awr265

McKenzie, I.A., Ohayon, D., Li, H., de Faria, J.P., Emery, B., Tohyama, K., Richardson, W.D., 2014. Motor skill learning requires active central myelination. Science 346, 318–322. https://doi.org/10.1126/science.1254960

Mensch, S., Baraban, M., Almeida, R., Czopka, T., Ausborn, J., El Manira, A., Lyons, D.A., 2015. Synaptic vesicle release regulates myelin sheath number of individual oligodendrocytes in vivo. Nat. Neurosci. 18, 628–630. https://doi.org/10.1038/nn.3991

Micheva, K.D., Chang, E.F., Nana, A.L., Seeley, W.W., Ting, J.T., Cobbs, C., Lein, E., Smith, S.J., Weinberg, R.J., Madison, D.V., 2018. Distinctive Structural and Molecular Features of Myelinated Inhibitory Axons in Human Neocortex. eNeuro 5. https://doi.org/10.1523/ENEURO.0297-18.2018

Micheva, K.D., Wolman, D., Mensh, B.D., Pax, E., Buchanan, J., Smith, S.J., Bock, D.D., 2016a. A large fraction of neocortical myelin ensheathes axons of local inhibitory neurons. Elife 5. https://doi.org/10.7554/eLife.15784

Micheva, K.D., Wolman, D., Mensh, B.D., Pax, E., Buchanan, J., Smith, S.J., Bock, D.D., 2016b. A large fraction of neocortical myelin ensheathes axons of local inhibitory neurons. Elife 5. https://doi.org/10.7554/eLife.15784

Minocha, S., Valloton, D., Brunet, I., Eichmann, A., Hornung, J.-P., Lebrand, C., 2015. NG2 glia are required for vessel network formation during embryonic development. Elife 4. https://doi.org/10.7554/eLife.09102

Mitew, S., Gobius, I., Fenlon, L.R., McDougall, S.J., Hawkes, D., Xing, Y.L., Bujalka, H., Gundlach, A.L., Richards, L.J., Kilpatrick, T.J., Merson, T.D., Emery, B., 2018. Pharmacogenetic stimulation of neuronal activity increases myelination in an axon-specific manner. Nat Commun 9, 306. https://doi.org/10.1038/s41467-017-02719-2

Miyamoto, D., Murayama, M., 2016. The fiber-optic imaging and manipulation of neural activity during animal behavior. Neurosci. Res. 103, 1–9. https://doi.org/10.1016/j.neures.2015.09.004

Moshrefi-Ravasdjani, B., Dublin, P., Seifert, G., Jennissen, K., Steinhäuser, C., Kafitz, K.W., Rose, C.R., 2017. Changes in the proliferative capacity of NG2 cell subpopulations during postnatal development of the mouse hippocampus. Brain Struct Funct 222, 831–847. https://doi.org/10.1007/s00429-016-1249-2

Mountcastle, V.B., 1957. Modality and topographic properties of single neurons of cat's somatic sensory cortex. J. Neurophysiol. 20, 408–434. https://doi.org/10.1152/jn.1957.20.4.408

Murase, S., Owens, D.F., McKay, R.D., 2011a. In the Newborn Hippocampus, Neurotrophin-Dependent Survival Requires Spontaneous Activity and Integrin Signaling. J. Neurosci. 31, 7791–7800. https://doi.org/10.1523/JNEUROSCI.0202-11.2011

Murase, S., Owens, D.F., McKay, R.D., 2011b. In the newborn hippocampus, neurotrophin-dependent survival requires spontaneous activity and integrin signaling. J. Neurosci. 31, 7791–7800. https://doi.org/10.1523/JNEUROSCI.0202-11.2011

Nagel, G., Ollig, D., Fuhrmann, M., Kateriya, S., Musti, A.M., Bamberg, E., Hegemann, P., 2002. Channelrhodopsin-1: a light-gated proton channel in green algae. Science 296, 2395–2398. https://doi.org/10.1126/science.1072068

Nagy, B., Hovhannisyan, A., Barzan, R., Chen, T.-J., Kukley, M., 2017. Different patterns of neuronal activity trigger distinct responses of oligodendrocyte precursor cells in the corpus callosum. PLoS Biol. 15, e2001993. https://doi.org/10.1371/journal.pbio.2001993

Naka, A., Adesnik, H., 2016. Inhibitory Circuits in Cortical Layer 5. Front Neural Circuits 10, 35. https://doi.org/10.3389/fncir.2016.00035

Nave, K.-A., 2010. Myelination and support of axonal integrity by glia. Nature 468, 244–252. https://doi.org/10.1038/nature09614

Nery, S., Wichterle, H., Fishell, G., 2001. Sonic hedgehog contributes to oligodendrocyte specification in the mammalian forebrain. Development 128, 527–540.

Nigro, M.J., Hashikawa-Yamasaki, Y., Rudy, B., 2018. Diversity and Connectivity of Layer 5 Somatostatin-Expressing INs in the Mouse Barrel Cortex. J. Neurosci. 38, 1622–1633. https://doi.org/10.1523/JNEUROSCI.2415-17.2017

Nikodemova, M., Kimyon, R.S., De, I., Small, A.L., Collier, L.S., Watters, J.J., 2015. Microglial numbers attain adult levels after undergoing a rapid decrease in cell number in the third postnatal week. J. Neuroimmunol. 278, 280–288. https://doi.org/10.1016/j.jneuroim.2014.11.018

Nishiyama, A., Komitova, M., Suzuki, R., Zhu, X., 2009. Polydendrocytes (NG2 cells): multifunctional cells with lineage plasticity. Nat. Rev. Neurosci. 10, 9–22. https://doi.org/10.1038/nrn2495

Nishiyama, A., Lin, X.H., Giese, N., Heldin, C.H., Stallcup, W.B., 1996a. Interaction between NG2 proteoglycan and PDGF alpha-receptor on O2A progenitor cells is required for optimal response to PDGF. J. Neurosci. Res. 43, 315–330. https://doi.org/10.1002/(SICI)1097-4547(19960201)43:3<315::AID-JNR6>3.0.CO;2-M

Nishiyama, A., Lin, X.H., Giese, N., Heldin, C.H., Stallcup, W.B., 1996b. Interaction between NG2 proteoglycan and PDGF alpha-receptor on O2A progenitor cells is required for optimal response to PDGF. J. Neurosci. Res. 43, 315–330. https://doi.org/10.1002/(SICI)1097-4547(19960201)43:3<315::AID-JNR6>3.0.CO;2-M

Nishiyama, A., Watanabe, M., Yang, Z., Bu, J., 2002. Identity, distribution, and development of polydendrocytes: NG2-expressing glial cells. J. Neurocytol. 31, 437–455. https://doi.org/10.1023/a:1025783412651

Noble, M., Murray, K., Stroobant, P., Waterfield, M.D., Riddle, P., 1988. Platelet-derived growth factor promotes division and motility and inhibits premature differentiation of the oligodendrocyte/type-2 astrocyte progenitor cell. Nature 333, 560–562. https://doi.org/10.1038/333560a0

Nykjaer, A., Willnow, T.E., Petersen, C.M., 2005. p75NTR--live or let die. Curr. Opin. Neurobiol. 15, 49–57. https://doi.org/10.1016/j.conb.2005.01.004

Oesterhelt, D., Stoeckenius, W., 1971. Rhodopsin-like protein from the purple membrane of Halobacterium halobium. Nature New Biol. 233, 149–152. https://doi.org/10.1038/newbio233149a0

Oppenheim, R.W., 1991. Cell death during development of the nervous system. Annu. Rev. Neurosci. 14, 453–501. https://doi.org/10.1146/annurev.ne.14.030191.002321

Oppenheim, R.W., 1989. The neurotrophic theory and naturally occurring motoneuron death. Trends Neurosci. 12, 252–255. https://doi.org/10.1016/0166-2236(89)90021-0

Orduz, D., Benamer, N., Ortolani, D., Coppola, E., Vigier, L., Pierani, A., Angulo, M.C., 2019. Developmental cell death regulates lineage-related interneuron-oligodendroglia functional clusters and oligodendrocyte homeostasis. Nat Commun 10, 4249. https://doi.org/10.1038/s41467-019-11904-4

Orduz, D., Maldonado, P.P., Balia, M., Vélez-Fort, M., de Sars, V., Yanagawa, Y., Emiliani, V., Angulo, M.C., 2015. INs and oligodendrocyte progenitors form a structured synaptic network in the developing neocortex. Elife 4. https://doi.org/10.7554/eLife.06953

Ortiz, F.C., Habermacher, C., Graciarena, M., Houry, P.-Y., Nishiyama, A., Nait Oumesmar, B., Angulo, M.C., 2019. Neuronal activity in vivo enhances functional myelin repair. JCI Insight 5. https://doi.org/10.1172/jci.insight.123434

Ortolani, D., Manot-Saillet, B., Orduz, D., Ortiz, F.C., Angulo, M.C., 2018. In vivo Optogenetic Approach to Study Neuron-Oligodendroglia Interactions in Mouse Pups. Front Cell Neurosci 12, 477. https://doi.org/10.3389/fncel.2018.00477

Passlick, S., Grauer, M., Schäfer, C., Jabs, R., Seifert, G., Steinhäuser, C., 2013. Expression of the γ2-subunit distinguishes synaptic and extrasynaptic GABA(A) receptors in NG2 cells of the hippocampus. J. Neurosci. 33, 12030–12040. https://doi.org/10.1523/JNEUROSCI.5562-12.2013

Pérez-Cerdá, F., Sánchez-Gómez, M.V., Matute, C., 2015. Pío del Río Hortega and the discovery of the oligodendrocytes. Front Neuroanat 9, 92. https://doi.org/10.3389/fnana.2015.00092

Petersen, C.C.H., 2019. Sensorimotor processing in the rodent barrel cortex. Nat. Rev. Neurosci. 20, 533–546. https://doi.org/10.1038/s41583-019-0200-y

Petryniak, M.A., Potter, G.B., Rowitch, D.H., Rubenstein, J.L.R., 2007. Dlx1 and Dlx2 control neuronal versus oligodendroglial cell fate acquisition in the developing forebrain. Neuron 55, 417–433. https://doi.org/10.1016/j.neuron.2007.06.036

Pierani, A., Moran-Rivard, L., Sunshine, M.J., Littman, D.R., Goulding, M., Jessell, T.M., 2001. Control of interneuron fate in the developing spinal cord by the progenitor homeodomain protein Dbx1. Neuron 29, 367–384. https://doi.org/10.1016/s0896-6273(01)00212-4

Pilaz, L.-J., McMahon, J.J., Miller, E.E., Lennox, A.L., Suzuki, A., Salmon, E., Silver, D.L., 2016. Prolonged mitosis of neural progenitors alters cell fate in the developing brain. Neuron 89, 83–99. https://doi.org/10.1016/j.neuron.2015.12.007

Pla, R., Stanco, A., Howard, M.A., Rubin, A.N., Vogt, D., Mortimer, N., Cobos, I., Potter, G.B., Lindtner, S., Price, J.D., Nord, A.S., Visel, A., Schreiner, C.E., Baraban, S.C., Rowitch, D.H., Rubenstein, J.L.R., 2018. Dlx1 and Dlx2 Promote Interneuron GABA Synthesis, Synaptogenesis, and Dendritogenesis. Cereb. Cortex 28, 3797–3815. https://doi.org/10.1093/cercor/bhx241

Pozas, E., Paco, S., Soriano, E., Aguado, F., 2008. Cajal-Retzius cells fail to trigger the developmental expression of the Cl- extruding co-transporter KCC2. Brain Res. 1239, 85–91. https://doi.org/10.1016/j.brainres.2008.08.058

Price, D.J., Aslam, S., Tasker, L., Gillies, K., 1997. Fates of the earliest generated cells in the developing murine neocortex. J. Comp. Neurol. 377, 414–422.

Prönneke, A., Scheuer, B., Wagener, R.J., Möck, M., Witte, M., Staiger, J.F., 2015. Characterizing VIP Neurons in the Barrel Cortex of VIPcre/tdTomato Mice Reveals Layer-Specific Differences. Cereb. Cortex 25, 4854–4868. https://doi.org/10.1093/cercor/bhv202

Raff, M.C., Barres, B.A., Burne, J.F., Coles, H.S., Ishizaki, Y., Jacobson, M.D., 1993. Programmed cell death and the control of cell survival: lessons from the nervous system. Science 262, 695–700. https://doi.org/10.1126/science.8235590

Rheims, S., Minlebaev, M., Ivanov, A., Represa, A., Khazipov, R., Holmes, G.L., Ben-Ari, Y., Zilberter, Y., 2008. Excitatory GABA in rodent developing neocortex in vitro. J. Neurophysiol. 100, 609–619. https://doi.org/10.1152/jn.90402.2008

Richardson, W.D., Pringle, N., Mosley, M.J., Westermark, B., Dubois-Dalcq, M., 1988. A role for platelet-derived growth factor in normal gliogenesis in the central nervous system. Cell 53, 309–319. https://doi.org/10.1016/0092-8674(88)90392-3

Rivers, L.E., Young, K.M., Rizzi, M., Jamen, F., Psachoulia, K., Wade, A., Kessaris, N., Richardson, W.D., 2008. PDGFRA/NG2 glia generate myelinating oligodendrocytes

and piriform projection neurons in adult mice. Nat. Neurosci. 11, 1392–1401. https://doi.org/10.1038/nn.2220

Rudy, B., Fishell, G., Lee, S., Hjerling-Leffler, J., 2011. Three groups of INs account for nearly 100% of neocortical GABAergic neurons. Dev Neurobiol 71, 45–61. https://doi.org/10.1002/dneu.20853

Rudy, B., McBain, C.J., 2001. Kv3 channels: voltage-gated K+ channels designed for high-frequency repetitive firing. Trends Neurosci. 24, 517–526. https://doi.org/10.1016/s0166-2236(00)01892-0

Ruijter, J.M., Baker, R.E., De Jong, B.M., Romijn, H.J., 1991. Chronic blockade of bioelectric activity in neonatal rat cortex grown in vitro: morphological effects. Int. J. Dev. Neurosci. 9, 331–338. https://doi.org/10.1016/0736-5748(91)90054-p

Saelens, X., Festjens, N., Vande Walle, L., van Gurp, M., van Loo, G., Vandenabeele, P., 2004. Toxic proteins released from mitochondria in cell death. Oncogene 23, 2861–2874. https://doi.org/10.1038/sj.onc.1207523

Saita, M., Pranga-Sellnau, F., Resler, T., Schlesinger, R., Heberle, J., Lorenz-Fonfria, V.A., 2018. Photoexcitation of the P4480 State Induces a Secondary Photocycle That Potentially Desensitizes Channelrhodopsin-2. J. Am. Chem. Soc. 140, 9899–9903. https://doi.org/10.1021/jacs.8b03931

Shi, S., Hayashi, Y., Esteban, J.A., Malinow, R., 2001. Subunit-specific rules governing AMPA receptor trafficking to synapses in hippocampal pyramidal neurons. Cell 105, 331–343. https://doi.org/10.1016/s0092-8674(01)00321-x

Silberberg, G., Markram, H., 2007. Disynaptic inhibition between neocortical pyramidal cells mediated by Martinotti cells. Neuron 53, 735–746. https://doi.org/10.1016/j.neuron.2007.02.012

Somjen, G.G., 1988. Nervenkitt: notes on the history of the concept of neuroglia. Glia 1, 2–9. https://doi.org/10.1002/glia.440010103

Somogyi, P., Soltész, I., 1986. Immunogold demonstration of GABA in synaptic terminals of intracellularly recorded, horseradish peroxidase-filled basket cells and clutch cells in the cat's visual cortex. Neuroscience 19, 1051–1065. https://doi.org/10.1016/0306-4522(86)90122-3

Southwell, D.G., Paredes, M.F., Galvao, R.P., Jones, D.L., Froemke, R.C., Sebe, J.Y., Alfaro-Cervello, C., Tang, Y., Garcia-Verdugo, J.M., Rubenstein, J.L., Baraban, S.C., Alvarez-

Buylla, A., 2012. Intrinsically determined cell death of developing cortical INs . Nature 491, 109–113. https://doi.org/10.1038/nature11523

Spitzer, S.O., Sitnikov, S., Kamen, Y., Evans, K.A., Kronenberg-Versteeg, D., Dietmann, S., de Faria, O., Agathou, S., Káradóttir, R.T., 2019. Oligodendrocyte Progenitor Cells Become Regionally Diverse and Heterogeneous with Age. Neuron 101, 459-471.e5. https://doi.org/10.1016/j.neuron.2018.12.020

Stedehouder, J., Brizee, D., Shpak, G., Kushner, S.A., 2018. Activity-Dependent Myelination of Parvalbumin INs Mediated by Axonal Morphological Plasticity. J. Neurosci. 38, 3631–3642. https://doi.org/10.1523/JNEUROSCI.0074-18.2018

Stedehouder, J., Couey, J.J., Brizee, D., Hosseini, B., Slotman, J.A., Dirven, C.M.F., Shpak, G., Houtsmuller, A.B., Kushner, S.A., 2017. Fast-spiking Parvalbumin INs are Frequently Myelinated in the Cerebral Cortex of Mice and Humans. Cereb. Cortex 27, 5001–5013. https://doi.org/10.1093/cercor/bhx203

Stedehouder, J., Kushner, S.A., 2017a. Myelination of parvalbumin INs : a parsimonious locus of pathophysiological convergence in schizophrenia. Mol. Psychiatry 22, 4–12. https://doi.org/10.1038/mp.2016.147

Stedehouder, J., Kushner, S.A., 2017b. Myelination of parvalbumin INs : a parsimonious locus of pathophysiological convergence in schizophrenia. Mol. Psychiatry 22, 4–12. https://doi.org/10.1038/mp.2016.147

Stehfest, K., Hegemann, P., 2010a. Evolution of the channelrhodopsin photocycle model. Chemphyschem 11, 1120–1126. https://doi.org/10.1002/cphc.200900980

Stehfest, K., Hegemann, P., 2010b. Evolution of the channelrhodopsin photocycle model. Chemphyschem 11, 1120–1126. https://doi.org/10.1002/cphc.200900980

Sugiyama, Y., Mukohata, Y., 1984. Isolation and characterization of halorhodopsin from Halobacterium halobium. J. Biochem. 96, 413–420. https://doi.org/10.1093/oxfordjournals.jbchem.a134852

Sultan, K.T., Han, Z., Zhang, X.-J., Xianyu, A., Li, Z., Huang, K., Shi, S.-H., 2016. Clonally Related GABAergic INs Do Not Randomly Disperse But Frequently Form Local Clusters in the Forebrain. Neuron 92, 31–44. https://doi.org/10.1016/j.neuron.2016.09.033

Sun, L.O., Mulinyawe, S.B., Collins, H.Y., Ibrahim, A., Li, Q., Simon, D.J., Tessier-Lavigne, M., Barres, B.A., 2018. Spatiotemporal Control of CNS Myelination by Oligodendrocyte

Programmed Cell Death through the TFEB-PUMA Axis. Cell 175, 1811-1826.e21. https://doi.org/10.1016/j.cell.2018.10.044

Sun, Q.-Q., Huguenard, J.R., Prince, D.A., 2006. Barrel cortex microcircuits: thalamocortical feedforward inhibition in spiny stellate cells is mediated by a small number of fast-spiking INs . J. Neurosci. 26, 1219–1230. https://doi.org/10.1523/JNEUROSCI.4727-04.2006

Suzuki, N., Sekimoto, K., Hayashi, C., Mabuchi, Y., Nakamura, T., Akazawa, C., 2017. Differentiation of Oligodendrocyte Precursor Cells from Sox10-Venus Mice to Oligodendrocytes and Astrocytes. Sci Rep 7, 14133. https://doi.org/10.1038/s41598-017-14207-0

Tanaka, Y., Tozuka, Y., Takata, T., Shimazu, N., Matsumura, N., Ohta, A., Hisatsune, T., 2009. Excitatory GABAergic Activation of Cortical Dividing Glial Cells. Cereb Cortex 19, 2181–2195. https://doi.org/10.1093/cercor/bhn238

Tansey, E.P., Chow, A., Rudy, B., McBain, C.J., 2002. Developmental expression of potassium-channel subunit Kv3.2 within subpopulations of mouse hippocampal inhibitory INs . Hippocampus 12, 137–148. https://doi.org/10.1002/hipo.1104

Tekki-Kessaris, N., Woodruff, R., Hall, A.C., Gaffield, W., Kimura, S., Stiles, C.D., Rowitch, D.H., Richardson, W.D., 2001. Hedgehog-dependent oligodendrocyte lineage specification in the telencephalon. Development 128, 2545–2554.

Temple, S., Raff, M.C., 1986. Clonal analysis of oligodendrocyte development in culture: evidence for a developmental clock that counts cell divisions. Cell 44, 773–779. https://doi.org/10.1016/0092-8674(86)90843-3

Thomaidou, D., Mione, M.C., Cavanagh, J.F., Parnavelas, J.G., 1997. Apoptosis and its relation to the cell cycle in the developing cerebral cortex. J. Neurosci. 17, 1075–1085.

Thornton, M.A., Hughes, E.G., 2020. Neuron-oligodendroglia interactions: Activity-dependent regulation of cellular signaling. Neuroscience Letters 727, 134916. https://doi.org/10.1016/j.neulet.2020.134916

Tomassy, G.S., Berger, D.R., Chen, H.-H., Kasthuri, N., Hayworth, K.J., Vercelli, A., Seung, H.S., Lichtman, J.W., Arlotta, P., 2014. Distinct profiles of myelin distribution along single axons of pyramidal neurons in the neocortex. Science 344, 319–324. https://doi.org/10.1126/science.1249766

Tong, X., Li, X., Zhou, B., Shen, W., Zhang, Z., Xu, T., Duan, S., 2009. Ca(2+) signaling evoked by activation of Na(+) channels and Na(+)/Ca(2+) exchangers is required for GABA-induced NG2 cell migration. J. Cell Biol. 186, 113–128. https://doi.org/10.1083/jcb.200811071

Torigoe, M., Yamauchi, K., Kimura, T., Uemura, Y., Murakami, F., 2016. Evidence That the Laminar Fate of LGE/CGE-Derived Neocortical INs Is Dependent on Their Progenitor Domains. J. Neurosci. 36, 2044–2056. https://doi.org/10.1523/JNEUROSCI.3550-15.2016

Trapp, B.D., Nishiyama, A., Cheng, D., Macklin, W., 1997. Differentiation and death of premyelinating oligodendrocytes in developing rodent brain. J. Cell Biol. 137, 459–468. https://doi.org/10.1083/jcb.137.2.459

Tremblay, R., Lee, S., Rudy, B., 2016. GABAergic INs in the Neocortex: From Cellular Properties to Circuits. Neuron 91, 260–292. https://doi.org/10.1016/j.neuron.2016.06.033

Tsai, H.-H., Niu, J., Munji, R., Davalos, D., Chang, J., Zhang, H., Tien, A.-C., Kuo, C.J., Chan, J.R., Daneman, R., Fancy, S.P.J., 2016. Oligodendrocyte precursors migrate along vasculature in the developing nervous system. Science 351, 379–384. https://doi.org/10.1126/science.aad3839

Tsoa, R.W., Coskun, V., Ho, C.K., de Vellis, J., Sun, Y.E., 2014. Spatiotemporally different origins of NG2 progenitors produce cortical INs versus glia in the mammalian forebrain. Proc. Natl. Acad. Sci. U.S.A. 111, 7444–7449. https://doi.org/10.1073/pnas.1400422111

Ueno, H., Suemitsu, S., Murakami, S., Kitamura, N., Wani, K., Okamoto, M., Aoki, S., Ishihara, T., 2017. Postnatal development of GABAergic INs and perineuronal nets in mouse temporal cortex subregions. Int. J. Dev. Neurosci. 63, 27–37. https://doi.org/10.1016/j.ijdevneu.2017.08.003

Veinante, P., Deschênes, M., 1999. Single- and multi-whisker channels in the ascending projections from the principal trigeminal nucleus in the rat. J. Neurosci. 19, 5085–5095.

Vélez-Fort, M., Audinat, E., Angulo, M.C., 2012. Central role of GABA in neuron-glia interactions. Neuroscientist 18, 237–250. https://doi.org/10.1177/1073858411403317

Vélez-Fort, M., Maldonado, P.P., Butt, A.M., Audinat, E., Angulo, M.C., 2010. Postnatal switch from synaptic to extrasynaptic transmission between INs and NG2 cells. J. Neurosci. 30, 6921–6929. https://doi.org/10.1523/JNEUROSCI.0238-10.2010

Verney, C., Takahashi, T., Bhide, P.G., Nowakowski, R.S., Caviness, V.S., 2000. Independent controls for neocortical neuron production and histogenetic cell death. Dev. Neurosci. 22, 125–138. https://doi.org/10.1159/000017434

Viganò, F., Möbius, W., Götz, M., Dimou, L., 2013. Transplantation reveals regional differences in oligodendrocyte differentiation in the adult brain. Nat. Neurosci. 16, 1370–1372. https://doi.org/10.1038/nn.3503

Vitali, I., Jabaudon, D., 2014. Synaptic biology of barrel cortex circuit assembly. Semin. Cell Dev. Biol. 35, 156–164. https://doi.org/10.1016/j.semcdb.2014.07.009

Vogt, D., Hunt, R.F., Mandal, S., Sandberg, M., Silberberg, S.N., Nagasawa, T., Yang, Z., Baraban, S.C., Rubenstein, J.L.R., 2014. Lhx6 directly regulates Arx and CXCR7 to determine cortical interneuron fate and laminar position. Neuron 82, 350–364. https://doi.org/10.1016/j.neuron.2014.02.030

von Blankenfeld, G., Kettenmann, H., 1991. Glutamate and GABA receptors in vertebrate glial cells. Mol. Neurobiol. 5, 31–43. https://doi.org/10.1007/BF02935611

Von Blankenfeld, G., Trotter, J., Kettenmann, H., 1991. Expression and Developmental Regulation of a GABAA Receptor in Cultured Murine Cells of the Oligodendrocyte Lineage. Eur. J. Neurosci. 3, 310–316. https://doi.org/10.1111/j.1460-9568.1991.tb00817.x

Voronova, A., Yuzwa, S.A., Wang, B.S., Zahr, S., Syal, C., Wang, J., Kaplan, D.R., Miller, F.D., 2017. Migrating INs Secrete Fractalkine to Promote Oligodendrocyte Formation in the Developing Mammalian Brain. Neuron 94, 500-516.e9. https://doi.org/10.1016/j.neuron.2017.04.018

Wake, H., Ortiz, F.C., Woo, D.H., Lee, P.R., Angulo, M.C., Fields, R.D., 2015. Nonsynaptic junctions on myelinating glia promote preferential myelination of electrically active axons. Nat Commun 6, 7844. https://doi.org/10.1038/ncomms8844

Wamsley, B., Fishell, G., 2017a. Genetic and activity-dependent mechanisms underlying interneuron diversity. Nat. Rev. Neurosci. 18, 299–309. https://doi.org/10.1038/nrn.2017.30

Wamsley, B., Fishell, G., 2017b. Genetic and activity-dependent mechanisms underlying interneuron diversity. Nat. Rev. Neurosci. 18, 299–309. https://doi.org/10.1038/nrn.2017.30

Wang, B., Long, J.E., Flandin, P., Pla, R., Waclaw, R.R., Campbell, K., Rubenstein, J.L.R., 2013. Loss of Gsx1 and Gsx2 function rescues distinct phenotypes in Dlx1/2 mutants. J. Comp. Neurol. 521, 1561–1584. https://doi.org/10.1002/cne.23242

Wang, Y., Dye, C.A., Sohal, V., Long, J.E., Estrada, R.C., Roztocil, T., Lufkin, T., Deisseroth, K., Baraban, S.C., Rubenstein, J.L.R., 2010. Dlx5 and Dlx6 regulate the development of parvalbumin-expressing cortical INs . J. Neurosci. 30, 5334–5345. https://doi.org/10.1523/JNEUROSCI.5963-09.2010

Weider, M., Starost, L.J., Groll, K., Küspert, M., Sock, E., Wedel, M., Fröb, F., Schmitt, C., Baroti, T., Hartwig, A.C., Hillgärtner, S., Piefke, S., Fadler, T., Ehrlich, M., Ehlert, C., Stehling, M., Albrecht, S., Jabali, A., Schöler, H.R., Winkler, J., Kuhlmann, T., Wegner, M., 2018. Nfat/calcineurin signaling promotes oligodendrocyte differentiation and myelination by transcription factor network tuning. Nat Commun 9, 899. https://doi.org/10.1038/s41467-018-03336-3

Wheeler, N.A., Fuss, B., 2016. Extracellular cues influencing oligodendrocyte differentiation and (re)myelination. Exp. Neurol. 283, 512–530. https://doi.org/10.1016/j.expneurol.2016.03.019

Williamson, A.V., Mellor, J.R., Grant, A.L., Randall, A.D., 1998. Properties of GABA(A) receptors in cultured rat oligodendrocyte progenitor cells. Neuropharmacology 37, 859–873. https://doi.org/10.1016/s0028-3908(98)00016-1

Wonders, C.P., Anderson, S.A., 2006. The origin and specification of cortical INs . Nat. Rev. Neurosci. 7, 687–696. https://doi.org/10.1038/nrn1954

Wong, F.K., Bercsenyi, K., Sreenivasan, V., Portalés, A., Fernández-Otero, M., Marín, O., 2018. Pyramidal cell regulation of interneuron survival sculpts cortical networks. Nature 557, 668–673. https://doi.org/10.1038/s41586-018-0139-6

Woolsey, T.A., Van der Loos, H., 1970. The structural organization of layer IV in the somatosensory region (SI) of mouse cerebral cortex. The description of a cortical field composed of discrete cytoarchitectonic units. Brain Res. 17, 205–242. https://doi.org/10.1016/0006-8993(70)90079-x

Xiao, L., Ohayon, D., McKenzie, I.A., Sinclair-Wilson, A., Wright, J.L., Fudge, A.D., Emery, B., Li, H., Richardson, W.D., 2016. Rapid production of new oligodendrocytes is required in the earliest stages of motor-skill learning. Nature Neuroscience 19, 1210–1217. https://doi.org/10.1038/nn.4351

Xu, H., Jeong, H.-Y., Tremblay, R., Rudy, B., 2013a. Neocortical somatostatin-expressing GABAergic INs disinhibit the thalamorecipient layer 4. Neuron 77, 155–167. https://doi.org/10.1016/j.neuron.2012.11.004

Xu, H., Jeong, H.-Y., Tremblay, R., Rudy, B., 2013b. Neocortical somatostatin-expressing GABAergic INs disinhibit the thalamorecipient layer 4. Neuron 77, 155–167. https://doi.org/10.1016/j.neuron.2012.11.004

Xu, Q., Tam, M., Anderson, S.A., 2008. Fate mapping Nkx2.1-lineage cells in the mouse telencephalon. J. Comp. Neurol. 506, 16–29. https://doi.org/10.1002/cne.21529

Xu, X., Roby, K.D., Callaway, E.M., 2006. Mouse cortical inhibitory neuron type that coexpresses somatostatin and calretinin. J. Comp. Neurol. 499, 144–160. https://doi.org/10.1002/cne.21101

Yamaguchi, Y., Miura, M., 2015. Programmed cell death in neurodevelopment. Dev. Cell 32, 478–490. https://doi.org/10.1016/j.devcel.2015.01.019

Yamawaki, N., Borges, K., Suter, B.A., Harris, K.D., Shepherd, G.M.G., 2014. A genuine layer 4 in motor cortex with prototypical synaptic circuit connectivity. Elife 3, e05422. https://doi.org/10.7554/eLife.05422

Ye, Z., Mostajo-Radji, M.A., Brown, J.R., Rouaux, C., Tomassy, G.S., Hensch, T.K., Arlotta, P., 2015. Instructing Perisomatic Inhibition by Direct Lineage Reprogramming of Neocortical Projection Neurons. Neuron 88, 475–483. https://doi.org/10.1016/j.neuron.2015.10.006

Young, K.M., Psachoulia, K., Tripathi, R.B., Dunn, S.-J., Cossell, L., Attwell, D., Tohyama, K., Richardson, W.D., 2013. Oligodendrocyte dynamics in the healthy adult CNS: evidence for myelin remodeling. Neuron 77, 873–885. https://doi.org/10.1016/j.neuron.2013.01.006

Yu, Y.-C., Bultje, R.S., Wang, X., Shi, S.-H., 2009. Specific synapses develop preferentially among sister excitatory neurons in the neocortex. Nature 458, 501–504. https://doi.org/10.1038/nature07722

Zhang, X.-J., Li, Z., Han, Z., Sultan, K.T., Huang, K., Shi, S.-H., 2017. Precise inhibitory microcircuit assembly of developmentally related neocortical INs in clusters. Nat Commun 8. https://doi.org/10.1038/ncomms16091

Zhang, Y., Chen, K., Sloan, S.A., Bennett, M.L., Scholze, A.R., O'Keeffe, S., Phatnani, H.P., Guarnieri, P., Caneda, C., Ruderisch, N., Deng, S., Liddelow, S.A., Zhang, C., Daneman, R., Maniatis, T., Barres, B.A., Wu, J.Q., 2014. An RNA-sequencing transcriptome and splicing database of glia, neurons, and vascular cells of the cerebral cortex. J. Neurosci. 34, 11929–11947. https://doi.org/10.1523/JNEUROSCI.1860-14.2014

Zhao, X., He, X., Han, X., Yu, Y., Ye, F., Chen, Y., Hoang, T., Xu, X., Mi, Q.-S., Xin, M., Wang, F., Appel, B., Lu, Q.R., 2010. MicroRNA-mediated control of oligodendrocyte differentiation. Neuron 65, 612–626. https://doi.org/10.1016/j.neuron.2010.02.018

Zhou, L., Shao, C.-Y., Xie, Y.-J., Wang, N., Xu, S.-M., Luo, B.-Y., Wu, Z.-Y., Ke, Y.H., Qiu, M., Shen, Y., 2020. Gab1 mediates PDGF signaling and is essential to oligodendrocyte differentiation and CNS myelination. Elife 9. https://doi.org/10.7554/eLife.52056

Zhu, X., Bergles, D.E., Nishiyama, A., 2008. NG2 cells generate both oligodendrocytes and gray matter astrocytes. Development 135, 145–157. https://doi.org/10.1242/dev.004895

Ziskin, J.L., Nishiyama, A., Rubio, M., Fukaya, M., Bergles, D.E., 2007. Vesicular release of glutamate from unmyelinated axons in white matter. Nat. Neurosci. 10, 321–330. https://doi.org/10.1038/nn1854

Zonouzi, M., Berger, D., Jokhi, V., Kedaigle, A., Lichtman, J., Arlotta, P., 2019. Individual Oligodendrocytes Show Bias for Inhibitory Axons in the Neocortex. Cell Rep 27, 2799-2808.e3. https://doi.org/10.1016/j.celrep.2019.05.018

Zonouzi, M., Renzi, M., Farrant, M., Cull-Candy, S.G., 2011. Bidirectional plasticity of calcium-permeable AMPA receptors in oligodendrocyte lineage cells. Nat. Neurosci. 14, 1430–1438. https://doi.org/10.1038/nn.2942

Zonouzi, M., Scafidi, J., Li, P., McEllin, B., Edwards, J., Dupree, J.L., Harvey, L., Sun, D., Hübner, C.A., Cull-Candy, S.G., Farrant, M., Gallo, V., 2015. GABAergic regulation of cerebellar NG2 cell development is altered in perinatal white matter injury. Nat. Neurosci. 18, 674–682. https://doi.org/10.1038/nn.3990